

AD-A211 462

REPORT DOCUMENTATION PAGE

Form Approved
OMB No. 0704-0188

Public reporting burden for this collection of information is estimated to average 1 hour per response, including the time for reviewing instructions, searching existing data sources, gathering and maintaining the data needed, and reviewing the collection of information. Send comments regarding this burden estimate or any other aspect of this collection of information, including suggestions for reducing this burden, to Washington Headquarters Services, Directorate for Information Operations and Reports, 1215 Jefferson Davis Highway, Suite 1204, Arlington, VA 22202-4302, and to the Office of Information and Regulatory Affairs, Office of Management and Budget, Washington, DC 20503.

1. AGENCY USE ONLY (Leave Blank)		2. REPORT DATE May 1989	3. REPORT TYPE AND DATES COVERED Final June 1988-May 1989
4. TITLE AND SUBTITLE A Hydrothermal Study of Lochusett Reservoir with Considerations of Water Quality Management		5. FUNDING NUMBERS DTIC ELECTE S AUG 15 1989 DCS D	
6. AUTHOR(S) Robert R Rooney		8. PERFORMING ORGANIZATION REPORT NUMBER N/A	
7. PERFORMING ORGANIZATION NAME(S) AND ADDRESS(ES) United States Army Corps of Engineers Massachusetts Institute of Technology, Cambridge, MA 02139 (Masters Thesis in Dept of Civil Engineering)		10. SPONSORING/MONITORING AGENCY REPORT NUMBER	
9. SPONSORING/MONITORING AGENCY NAME(S) AND ADDRESS(ES) Dept of Army, Corps of Engineers 200 Stennis St (A-10-2) Alexandria, VA		11. SUPPLEMENTARY NOTES Masters Thesis prepared at MIT, Parsons Laboratory for Water Resources, Dept of Civil Engr, Cambridge, MA	
12a. DISTRIBUTION/AVAILABILITY STATEMENT No Limitations (UL)		12b. DISTRIBUTION CODE DISTRIBUTION STATEMENT A Approved for public release Distribution Unlimited	
13. ABSTRACT (Maximum 200 words) Water quality modelling in reservoirs is integrally linked to the thermal stratification regime. Thus, modelling the temporal and spatial variability of temperature within a reservoir is a first step toward modelling various water quality parameters. This study focuses on Lochusett Reservoir which provides approximately forty percent of the water supply to the Boston metropolitan area and serves as a connecting link for the other sixty percent. The model selected for application - MIEM, which is a one dimensional (vertical) hydrothermal model which accounts for surface heat fluxes, entrance mixing, variable withdrawal elevation, internal absorption of solar radiation, effects of wind mixing and an option for temporally and spatially variable diffusivity. The temperature model was calibrated using 1987 field data and verified using data from 1988. Model theory and sensitivity to different model parameters are presented and the computer code and typical input data files are included. Alternative reservoir management strategies and a water quality monitoring plan are discussed.			
14. SUBJECT TERMS Hydrothermal Model, Water Quality Management		15. NUMBER OF PAGES 225	
17. SECURITY CLASSIFICATION OF REPORT UNCLASSIFIED		18. SECURITY CLASSIFICATION OF THIS PAGE UNCLASSIFIED	
19. SECURITY CLASSIFICATION OF ABSTRACT UNCLASSIFIED		20. LIMITATION OF ABSTRACT UL	

A HYDROTHERMAL STUDY OF WACHUSETT RESERVOIR
WITH CONSIDERATIONS OF WATER QUALITY MANAGEMENT

by

Robert R. Rooney

B.S. 1979, Syracuse University
Syracuse, New York

B.S. 1979, State University of New York
College of Environmental Science and Forestry at Syracuse
Syracuse, New York

Submitted to

Ralph M. Parsons Laboratory for Water Resources and Hydrodynamics
Department of Civil Engineering
Massachusetts Institute of Technology
Cambridge, MA

in Partial Fulfillment of the Requirements
of the Degree of
Master of Science in Civil Engineering

May 1989

© Robert R. Rooney 1989

The author hereby grants to Massachusetts Institute of
Technology permission to reproduce and to distribute
copies of this thesis document in whole or in part.

Signature of Author

Robert R. Rooney

Department of Engineering
May 19, 1989

Certified by

Donald R. F. Harleman

Donald R. F. Harleman
Ford Professor of Engineering
Thesis Supervisor

Accepted by

Ole S. Madsen

Ole S. Madsen
Chairman, Department Committee on Graduate Students

89 8 15 025

A HYDROTHERMAL STUDY OF WACHUSETT RESERVOIR WITH CONSIDERATIONS OF WATER QUALITY MANAGEMENT

by

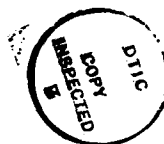
Robert R. Rooney

Submitted to the Department of Civil Engineering
on May 19, 1989 in partial fulfillment
of the requirements for the degree of
Master of Science in Civil Engineering

ABSTRACT

Continual assessment of surface water impoundments is necessary to implement timely decisions with regard to water quality management. The use of mathematical models plays an increasing role as a management tool to quantify the impacts of various management strategies. Nutrient and phytoplankton dynamics are integrally linked to the thermal stratification regime in a reservoir. Thus, modeling the temporal and spatial variability of temperature within a reservoir is a first step toward modeling various water quality kinetics. This study focuses on Wachusett Reservoir which provides approximately forty percent of the water supply to the Boston metropolitan area and serves as a connecting link for the other sixty percent. The model selected for application is MITEMP, which is a one-dimensional (vertical) hydrothermal model which accounts for surface heat fluxes, entrance mixing, variable withdrawal elevation, internal absorption of solar radiation, effects of wind mixing, and an option for temporally and spatially variable diffusivity. The temperature model was calibrated using 1987 field data and verified using data from 1988. Model theory and sensitivity to different model parameters are presented and the computer code and a typical input data file are included. Alternative management strategies to include selective withdrawal for the reservoir, land use planning in the watershed, and a water quality monitoring plan are discussed.

Thesis Supervisor: Donald R. F. Harleman
Title: Ford Professor of Engineering



Accession For	
NTIS	CRA&I <input checked="" type="checkbox"/>
DTIC	IAB <input type="checkbox"/>
Unannounced	<input type="checkbox"/>
Justification	
By	
Distribution /	
Availability Codes	
Dist	Acquired / or Special
A-1	

Acknowledgements

If a diploma were divisible, I would be compelled to pass it out to the many people that have made it possible for me to make it to graduation day! Well, maybe I would keep a small piece for myself ⁰. But certainly, much of the learning takes place this way; among peers, after class, asking questions to the point where a working knowledge is developed. After ten years away from academia, I probably had a bit more of this learning to catch up on than most. I'm very grateful to fellow students and faculty who availed themselves to answer my seemingly endless stream of questions.

I am especially grateful to Claire, who humanized the mathematical theory and whose interest in her work is contagious. Certainly her encouragement and survival advice were invaluable. She taught me the art and science of library building which will stand me in good stead for years to come. Thanks also to Emmet who was often the target of my 'theory' questions; only because he did such a good job of explaining them— so as a reward I'd bring him another question. To Lani, whose wry sense of humor put things in perspective and was a welcomed relief any hour of the day. Without her help coming down the home stretch who knows what class I'd be celebrating reunions with! And yes, many thanks to John for the opportunity beat him at nerf hoops once a nite, and to whom I'm bequeathing the hoop (as we all know he needs the practice!). With it are hopes that he writes a paper finally that has something to do with anything but fish! To Shawn, who replaces me as the 'old man' in the office and who impresses me with his sense of priorities from which we all can gain.... Who else would go on a cruise to Bermuda a week before finals?!

Special thanks to my parents and family, always giving me full support in my endeavors even if it means not seeing or hearing from me in ages.... maybe *that's why* they encourage me to do it! To my Aunt Joan who at 93 years, has revitalized me on numerous occasions with a refreshing perspective that can only be gotten from a full life of living. To my advisor, who's patience in my zig zag progress and who together with his dear wife Marty, shed a different light on the MIT experience making it much more personable and really a family affair.

There's space here that I've saved for mention of a truly special person who has given so freely of her time and energies, while she's had more than a full work load herself; whose unfaltering loyalty and unselfishness has been an inspiration to me. If it's true that by giving of yourself you will get three-fold in return, then I am forever indebted to you, Tracey. Your efforts are to be commended! I would very much like you to wear your nametag from the graduate dinner. ♣.

Finally, to all the taxpayers in the country who so willingly contributed part of their income for my education and to make this study possible, I hope you are satisfied that it was put to good use. To the U.S. Army Corps of Engineers who allowed me the time in my career to pursue this educational goal and who sponsored me throughout the entire period, I am grateful for such an opportunity.

I think when it comes to education, judgement should not be passed solely as to the level to which one has attained, but rather by how far one has progressed to get there. Certainly, in this sense, my study at MIT has been a tremendous success!

CONTENTS

	page
List of Tables and Figures	7
Chapter 1 Introduction and Overview	10
1.1 Motivation for the study	10
1.2 Study objectives	12
1.3 Description of Wachusett Reservoir	13
1.3.1 Brief history	13
1.3.2 Basin morphology	16
1.3.3 Intake geometry	23
1.3.4 Other characteristics	26
Chapter 2 Model Evaluation and Selection	27
2.1 Purpose of Modeling	27
2.2 Characteristics of generic models	28
2.3 Distinctions among hydrothermal models	29
2.3.1 Dimensionality considerations	29
2.3.2 Time and length scales	31
2.3.3 Model representation of reservoirs	32
2.3.4 Determination of E_z	34
2.3.5 Modifications to the mixed-layer model	35
2.4 Appropriate Model for Wachusett Reservoir	36
2.5 Examination of CE-THERM-R1 (Corps of Engineers' Model)	39
2.5.1 Reservoir schematization	39
2.5.2 Characterization of inflows and outflows	40
2.5.3 Vertical turbulent diffusivity	44
2.5.4 Wind mixing	44
2.5.5 Other features of COE model	45

Chapter 3 Model Theory (MITEMP)	46
3.1 Heat transfer in lakes and reservoirs - basic concepts	46
3.2 Thermal cycle in lakes and reservoirs	50
3.3 Hydrothermal model (MITEMP)	51
3.3.1 Assumptions of the model	51
3.3.2 Model schematization of the reservoir	52
3.3.3 Heat transport equation	55
3.3.4 Input data	59
3.4 Calculations conducted iteratively in the model	59
3.4.1 Entrance mixing	60
3.4.2 Calculation of withdrawal layer thickness	63
3.4.3 Computation of diffusivity	66
3.4.4 Numerical stability criteria	71
3.4.5 Wind effects on mixing in the epilimnion	72
Chapter 4 Calibration and Verification	76
4.1 Presentation of input data	76
4.1.1 Schematization of basin	77
4.1.2 Climatological data	79
4.1.3 Inflow, outflow, and surface elevations	87
4.1.4 Diffusivity and extinction coefficient	90
4.2 Calibration of the hydrothermal model	93
4.3 Verification of the hydrothermal model	100
4.4 Sensitivity of parameters	100
4.4.1 Intake elevation	103
4.4.2 Sensitivity to magnitude of diffusion term	103
4.4.3 Sensitivity of other model parameters	106
4.5 Timing of the spring overturn	107

Chapter 5 Evaluation of Water Quality Management Techniques	108
5.1 Current operational management techniques	108
5.2 Copper toxicity and considerations for algicide treatment	112
5.3 Problems with copper sulfate application	115
5.4 Alternative management techniques	116
5.5 In-Reservoir chemical treatment alternatives	118
5.5.1 Deep water application of copper sulfate	118
5.5.2 Alum precipitation	119
5.5.3 Potassium permanganate	119
5.5.4 Ozone	120
5.6 Physical treatment techniques	121
5.6.1 Selective withdrawal	121
5.6.2 Activated carbon treatment	123
5.6.3 Destratification	124
5.7 Development of a management plan	125
5.7.1 Coordination between MDC/MWRA	125
5.7.2 Plan objectives	126
5.7.3 Land use planning	127
5.7.4 Water quality monitoring plan	129
Chapter 6 Conclusion and Recommendations	134
6.1 Reservoir water quality status	134
6.2 Conclusions of the hydrothermal study	136
Appendix A Julian Calendar	145
Appendix B MITEMP Input Data File	146
Appendix C MITEMP Hydrothermal Model Computer Code	152
Bibliography	221

LIST OF TABLES

	page
Table 1.1 Morphometric properties of Wachusett Reservoir.	19
Table 4.1 Annually averaged water inputs to Wachusett Reservoir.	88
Table 4.2 Annually averaged water losses to Wachusett Reservoir.	88
Table 4.3 Calibrated parameters for model calibration and verification	96
Table 4.4 Additional input parameters in the hydrothermal model	96
Table 5.1 Land use in Wachusett Watershed.	126

LIST OF FIGURES

Fig 1.1 Map of Boston water supply system and contributing watersheds.	11
Fig 1.2 Map of Wachusett Reservoir illustrating original river channel.	17
Fig 1.3 Effect of reservoir inflow temperature on retention time.	18
Fig 1.4 Wachusett Reservoir cross-sections: a. longitudinal; b. width.	21
Fig 1.5 Wachusett Reservoir morphometry: a. depth-area curve; b. depth-volume curve.	22
Fig 1.6 Cosgrove intake geometry: a. plan view; b. elevation view.	24
 Fig 2.1 One-box model.	 32
Fig 2.2 Two-box model.	32
Fig 2.3 Mixed-layer model.	33
Fig 2.4 Variability and diffusivity with depth (field study determination).	34
Fig 2.5 Comparative temperature profiles for Wachusett Reservoir, 1987.	38
Fig 2.6 Lagrangian (variable layer) vs. Eulerian (fixed layer) models.	40
Fig 2.7 Physical representation of outflow parameters for Corps of Engineers' model, CE-THERM-R1.	42

Fig 3.1	Density of water as a function of temperature.	47
Fig 3.2	Relative comparison of potential energy for a stratified and a fully mixed column.	48
Fig 3.3	Molecular diffusion relative to bulk advective motion.	49
Fig 3.4	a. Idealized reservoir basin schematization; b. control volume for maintaining continuity in model.	53
Fig 3.5	Illustration of near-field entrance mixing in relation to layer outflow velocity.	61
Fig 3.6	Effect of varying the number of outflow standard deviations contained within the withdrawal layer.	65
Fig 3.7	Relative effect of basin morphology on potential energy of stratification.	69
Fig 3.8	Evaluation of control volume with regards to maintaining numerical stability.	72
Fig 4.1	a. Finite difference schematization; b. Area-volume scheme.	78
Fig 4.2	Wind velocity for Wachusett Reservoir 1987 & 1988.	80
Fig 4.3	Air temperatures for Wachusett Reservoir 1987 & 1988.	81
Fig 4.4	Humidity for Wachusett Reservoir 1987 & 1988.	82
Fig 4.5	Cloud cover for Wachusett Reservoir 1987 & 1988.	83
Fig 4.6	Inflow and outflow 1987 & 1988.	84
Fig 4.7	Surface elevation 1987 & 1988.	85
Fig 4.8	Insolation - 100% clear sky compared to net available at the water surface.	86
Fig 4.9	Water temperature at intake depth temperature at Quabbin Reservoir 1987 & 1988	91
Fig 4.10	Water surface elevation calculated and measured (1988).	92
Fig 4.11	Model calibration temperature profile 1987.	97
Fig 4.12	Model calibration bottom/surface temperature 1987.	98
Fig 4.13	Model calibration outflow temperature comparison 1987.	99

Fig 4.14	Model verification temperature profile 1988.	101
Fig 4.15	Model verification surface & bottom temperature 1988.	102
Fig 4.16	Comparative withdrawal elevations vs. temperature.	104
Fig 4.17	Comparative diffusion rates vs. temperature profile.	105
Fig 5.1	Map of Wachusett Reservoir monitoring stations, traffic routes, and towns.	107
Fig 5.2	Copper sulfate applications on Wachusett Reservoir (Fall 1987).	109
Fig 5.3	Hierarchy of eutrophication problem.	115
Fig 5.4	Blockage grates used to effect selective withdrawal.	120
Fig 5.5	Destratification effects on algae in the photic zone.	122
Fig 6.1	Concentration of algae types throughout the year (1987).	139
Fig 6.2	Dissolved oxygen profile, 1987 (measured vs. saturated).	140
Fig 6.3	Dissolved oxygen profile, 1988 (measured vs. saturated).	141
Fig 6.4	Phosphate concentration (surface & deep samples), 1987.	142
Fig 6.5	Nitrate/nitrite concentration (surface & deep samples), 1987.	143
Fig 6.6	Ammonia concentration (surface & deep samples), 1987.	144

Chapter 1 Introduction and Overview

1.1 Motivation For The Study

The Massachusetts agencies responsible for public water service have a long history of providing sufficient quantity and superior quality of water to the city of Boston. Today those agencies are the Metropolitan District Commission (MDC) and the Massachusetts Water Resources Authority (MWRA) whose responsibilities range from protection of water sources through management of watersheds to maintenance of the delivery network to the 46 communities and over 2 million people in the Boston metropolitan area (see Figure 1.1). Basically, the MDC is responsible for the watershed management while the MWRA provides the means of delivery to its customers. Both agencies are concerned with the water quality in the reservoir. The smooth interfacing of these two agencies is critical for effective management of this resource and will be examined further in Chapter 5.

To date, the water coming into the city has not needed any treatment other than routine pH adjustment (NaOH), disinfection (chloramine) and fluoridation prior to distribution. Increased environmental stresses in the vicinity of Wachusett Reservoir, however, have raised concerns about the insurance of future water quality. Increasingly, the MWRA receives customer complaints with regard to the taste and odor. Odors described as "cucumber" or "fishy" and tastes that are "bitter" are suspected to be the result of increased algae concentrations of species notorious for offensive odors at relatively low concentrations.

In 1988 the MDC and the MWRA commissioned a joint Odor and Taste Task Force to investigate the source of the water quality complaints and recommend courses of action that the agencies could implement to assure better water quality through the control of nuisance algal blooms in the reservoir. The taste and odor

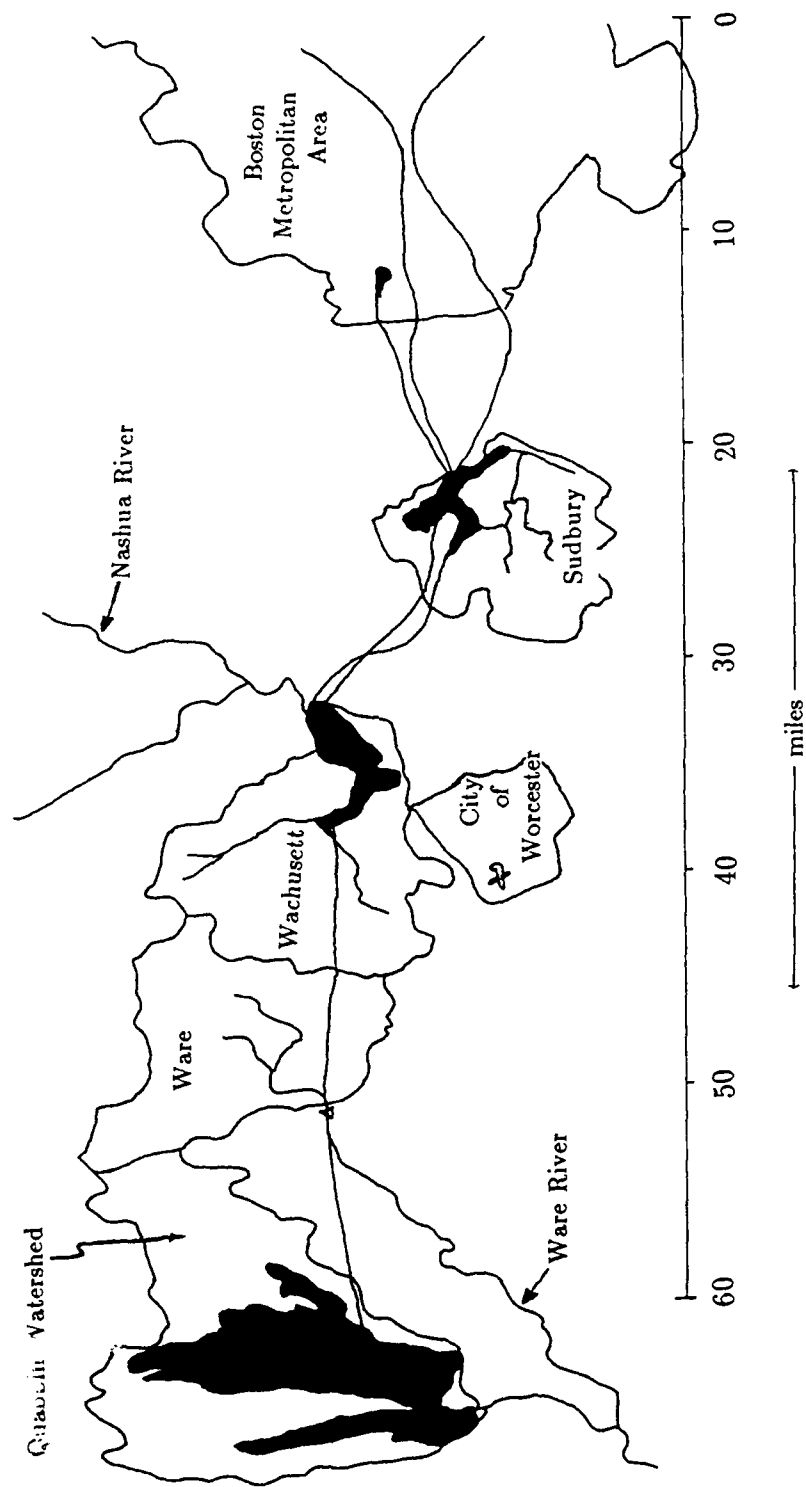


Figure 1.1 Boston water supply system and contributing watersheds.

problems in 1987/88 stemmed from the growth of a flagellated golden-brown algae, *Synura*, in Wachusett Reservoir. This colonial algae can produce a discernable odor with as little as 10 colonies per milliliter. However in other years, high concentrations of the blue-green algae *Anabaena*, the diatomaceous algae *Asterionella*, and other flagellates *Volvox* and *Dinobryon* have posed water quality problems but to a lesser extent than *Synura*. Control measures in the past involved the application of copper sulfate to the epilimnion of the reservoir. This has had little success in reducing the concentrations of the algae for longer than a few days. In fact, in the fall of 1986 and 1987, applications were made on a weekly basis until ice cover made it impossible [MWRA/MDC, 1988].

In their final report, the Odor and Taste Task Force recommended a study of the circulation dynamics in the reservoir in order to better understand the seasonal mixing and nutrient distribution. This would provide insight into more effective algal control strategies before more expensive conventional water treatment becomes necessary. It is in light of this scenario that the present study evolved.

1.2 Study Objectives

Nutrient and various phytoplankton dynamics are integrally linked to the thermal stratification regime in a reservoir. The same processes of advection, convection and diffusion, which affect the movement and ultimate distribution of these constituents, are responsible for the distribution of heat within the water column. Furthermore, it is well known that biological growth rates and the rate of chemical interaction are driven by temperature. Therefore, modeling the temporal and spatial variability of temperature within the reservoir is a first step in modeling various water quality kinetics (e.g., algae distribution, nutrient concentrations, dissolved oxygen).

Thus, with the understanding of this dependency on the hydrothermal characteristics of the water column, a model was sought that could be adapted, calibrated, and verified with field data from the Wachusett Reservoir. Later, a water quality model could be coupled to this hydrothermal model to predict various water quality constituents. Once this is accomplished, the model can be used as a predictive tool to evaluate the ramifications of various management techniques on the quality of water delivered to the City of Boston.

It is the purpose of this study to: (1) select an appropriate hydrothermal model, (2) collect and compile the necessary data to run the model, (3) accomplish the model's calibration and verification, and (4) present some insight into the water quality management challenges currently experienced at the Wachusett Reservoir. The field data for calibration was chosen from year 1987 and, for verification, from 1988.

1.3 Description of Wachusett Reservoir

1.3.1 Brief History

At the time of its completion in 1906, Wachusett Reservoir was acclaimed as the largest reservoir in the world. Today, the water is completely gravity fed about 40 miles to Boston through 14 foot aqueducts at an average rate of 345 million gallons per day (mgd) at depths reaching 438 feet below the ground surface. The story of the development of the water system to the level of service enjoyed today is a fascinating one and is briefly described here.

Boston lays claim to one of the oldest public conveyances of fresh water in the country, dating back to 1652, when trenches carried water to large cisterns [French, 1986]. In 1796, the first pipe conduits were made from logs with four-inch holes bored down the center providing service from Jamaica Pond to approximately 20,000

customers in the South End of Boston. The service involved about 15 miles of this type of "piping" which sufficed for about 35 years. By 1825, poor water quality and the additional strain on the available quantity mandated an expansion of the supplies. Sources under consideration included the Charles River, the Mystic Lakes and Long Pond. After over 20 years of debate on the water supply issue for Boston, Long Pond in Natick (subsequently named Lake Cochituate) was chosen in 1846 to provide water to the city with a yield of 18 mgd. The significance of this time period was the creation of a city Water Board comprised of technical experts, which ceased to make water an issue of politics, but rather one of factual necessity [Nesson, 1983].

By the 1850s, the wood distribution system had been almost entirely replaced by ten-inch cast iron pipes. With demand continuing to outpace the supply, the Water Board for the first time recommended to the Mayor of Boston that metering of water should be implemented and conservation exercised by consumers. Indeed, at that time, faucets were routinely left open in the winter to prevent pipes from freezing!

After adding the Sudbury Reservoir in 1872 to Boston's water supply inventory, exponential population growth of the city forced another major decision as to the future supply in 1895. In an extensive study, which considered supply alternatives as far away as Lake Winnepesaukee in New Hampshire, the conclusions supported a westward expansion employing a gravity flow system and calling for the first regional solution to water supply. Upon acceptance of the report's recommendation, the city appointed Frederick Stearns as Chief Engineer for the construction of the Wachusett Reservoir, which involved damming the South Fork of the Nashua River, inundating much of the town of West Boylston. The rubble masonry dam completed in 1906 was 944 feet long, 207 feet high, with a 452 foot spillway. At that time water would be provided to almost one million people in 29 municipalities.

In 1919 the Metropolitan Water Board became the Water Division of the Metropolitan District Commission (MDC). At that time they were charged with the task of recommending yet again a new source of water for an ever increasing demand. By 1927, flow from the Ware River was added through an aqueduct intake. Additionally, construction of the Quabbin Reservoir was begun in 1931, completed in 1941 and filled by 1948. As with past searches for new water sources, a common thread of thinking was that the water should necessarily be from clean sources not requiring treatment, and be distributed using a gravity flow system.

Quabbin Reservoir completed the supply configuration as it exists today (Figure 1.1). The addition of Quabbin increased the safe yield (the guaranteed delivery rate) to 300 mgd; almost double the yield of the Wachusett system. In 1965, the Sudbury aqueduct and reservoir were abandoned due to the deteriorating water quality and the completion of the Wachusett aqueduct. However, in times of emergency it could still be used. In 1969, for the first time since Quabbin was added to the system, the demand exceeded the 300 mgd safe yield and today outflows average 345 mgd; 15% above the calculated safe yield [Vogel, 1988].

Up to this time, the MDC's Water Division was a state agency. By 1985, it was recognized that a separate water and sewer authority, independent of state government, could better manage the water quality and distribution. As a result, the Massachusetts Water Resources Authority (MWRA) was created. However, the MDC retained the Division of Watershed Management which continues to manage the reservoir and the watershed.

In summary, there were four major expansions in Boston's water supply history:

- * 1848 — System expanded to include Lake Cochituate in Natick
- * 1872 — Sudbury Reservoir added to the supply

* 1906 – Wachusett Reservoir construction completed

* 1939 – Quabbin Reservoir attained present day yield

Many less significant additions and deletions of smaller water supplies also occurred between these dates.

Today, as has occurred every 30 to 40 years in Boston's history of water supply, additional sources of water are needed to meet ever higher demands. Water quality management has taken on eminent importance since no longer can we afford to *replace* supplies as they become undrinkable (e.g., Jamaica Pond, Mystic Lake, Sudbury Reservoir) but rather new sources must be *added to* existing sources. Hence, the understanding of the hydrodynamic properties and their impact on water quality are key to maintaining the high grade of drinking water that exists today.

1.3.2 Basin Morphology

The Wachusett Reservoir is situated about 10 miles north of Worcester, Massachusetts in a geologic area formed some 15,000 years ago with the retreat of the last ice age. Before inundation for the reservoir, the South Fork of the Nashua River had carved out a distinct river channel in what is largely glacial outwash. This channel is illustrated in Figure 1.2 with respect to the reservoir as roughly transposed from the original construction survey sheets. This channel will have an impact on the flow patterns through the reservoir and could alter the retention time of some of the inflow water. The retention time is the reservoir volume divided by the average outflow rate and is on the order of six months. A summary of other morphometric data is provided in Table 1.1 .

Many of the physical processes of interest in the reservoir are identical to that of a lake with regard to the influences of morphometry. The basic difference between the two is the elevation of the outflow, which is usually lower in the reservoir. This

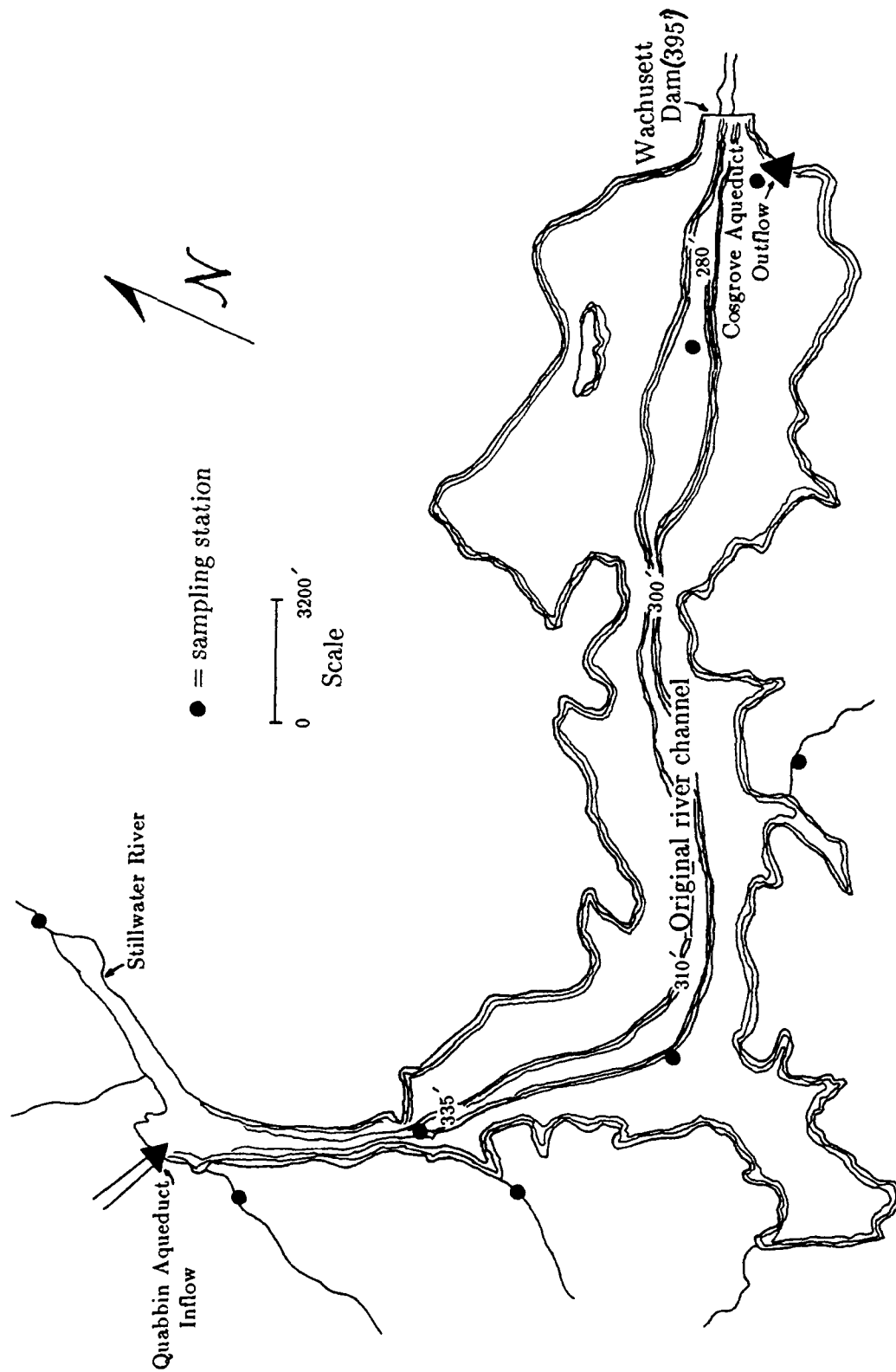


Figure 1.2 Wachusett reservoir. Original river channel has significant impact on basin morphology.

results in the dominance of advection over diffusion by a few orders of magnitude with respect to the mass transport of constituents. By changing the level of the outlet, the thermal distribution in the water column can be significantly altered, especially in regard to the depth of the mixed layer, thus affecting the retention time and the distribution of water quality constituents.

This concept of relating thermal stratification to retention time and water quality takes on added significance when changes in water quality by the implementation of different reservoir operational policies are considered. As water enters the reservoir in the spring, it is largely the result of snow-melt and is colder than the reservoir water. Due to its higher density, it will sink until it has reached a level of equal density. Should this inflow water be colder than the hypolimnetic waters, it will flow along the bottom and possibly remain there for most of the season (Figure 1.3). In this case, the retention time could be a few months longer than originally calculated.

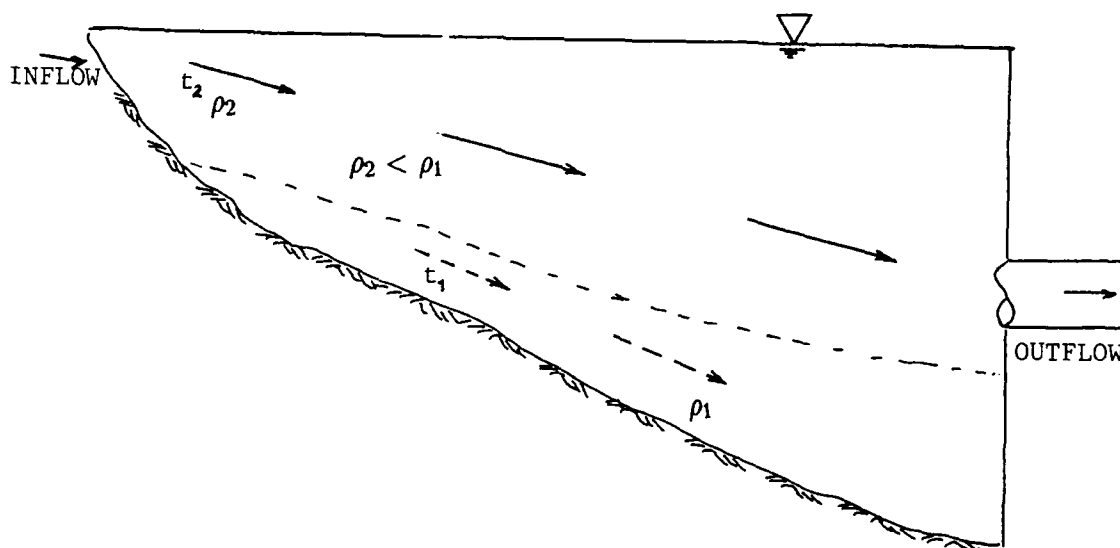


Figure 1.3 Effects of reservoir inflow temperature on retention time. Warmer water tends to flow over colder, denser water.

As the inflow water becomes warmer over the next few weeks, it will continue to flow over this colder denser water at the bottom. Thus, as the earlier water becomes "trapped" at the bottom, later warmer water may "short-circuit" through the reservoir and have a retention time on the order of weeks. Additionally, Wachusett has a relatively large fetch (approximately 5.0 miles) defined as the straight line distance with exposure to the wind. The reservoir alignment to the direction of the prevailing winds will tend to aid in this short-circuiting [Culp, 1986].

TABLE 1.1

Morphometric properties of Wachusett Reservoir

Volume Capacity (at elev 395')	65 billion gals ($2.46 \times 10^8 \text{ m}^3$)
Length	8.5 miles (13683 m)
Surface Area (A_o)	6.1 miles ² ($1.58 \times 10^7 \text{ m}^2$)
Max Width	1.1 miles (1770m)
Mean Width (A_o/L)	0.7 miles (1155m)
Maximum depth (at dam)	128 ft (39m)
Mean depth (V/A_o)	49 ft (15m)
Retention Time (V/Q)	0.5 yr
Watershed area	114 mi ² ($2.95 \times 10^8 \text{ m}^2$)
Normal operating range (above datum)*	387-392 ft (118-119.5m)
Average outflow	345 mgd ($15.1 \text{ m}^3/\text{s}$)
Range of outflow	255-370 mgd ($11.2\text{-}16.2 \text{ m}^3/\text{s}$)
Intake elevations (above datum)*	364 & 345 ft (111m & 105m)

*datum used throughout this study is Boston City Base
(or 5.65' lower than USGS 1929 datum used for
topo mapping)

The maximum depth (z_m) of the reservoir is located at the Wachusett Dam and measures 39 meters while the mean depth (\bar{z}) is defined by:

$$\bar{z} = \frac{V}{A_o}$$

where

$$\begin{aligned} V &= \text{volume of reservoir} \\ A_o &= \text{surface area} \end{aligned}$$

The ratio $z_m : \bar{z}$ is similar to the volume development of a basin. Equal to .33 for a basin of a perfect cone, most basins in easily eroded rock would have values typically between .33 and .5 [Wetzel, 1983]. For Wachusett, it is equal to .36 .

The actual reservoir cross-sections in Figure 1.4 illustrate the basin non-uniformity and the relative location of the intakes. Location of the intake shafts are also shown on the hypsographic curve (depth-area curve) as well as on the depth-volume curve in Figure 1.5 . Due to the level of the intakes, a considerable volume of water is retained as the minimum pool (unavailable water).

Wachusett Reservoir is classified as a dimictic, mesotrophic water body [CDM, 1988]. This describes the fact that it experiences a freely circulating water column twice each year (in April and in late October), has low productivity, and is similarly low in nutrient concentration (phosphorus and nitrogen). Since phosphorus is most often the limiting nutrient (the nutrient in least supply and thus controls growth) trophic level predictions can be based on the in-reservoir phosphorus concentrations [Vollenweider, 1968]. Phosphorus concentrations for oligotrophic reservoirs would be less than 10 $\mu\text{gP/l}$, and greater than 20 $\mu\text{gP/l}$ for eutrophic reservoirs. Concentrations in Wachusett generally range between 6 and 13 $\mu\text{gP/l}$. Other predictions of trophic level, based on net oxygen depletion, likewise characterize Wachusett as between oligotrophic and mesotrophic [Tighe and Bond, 1987].

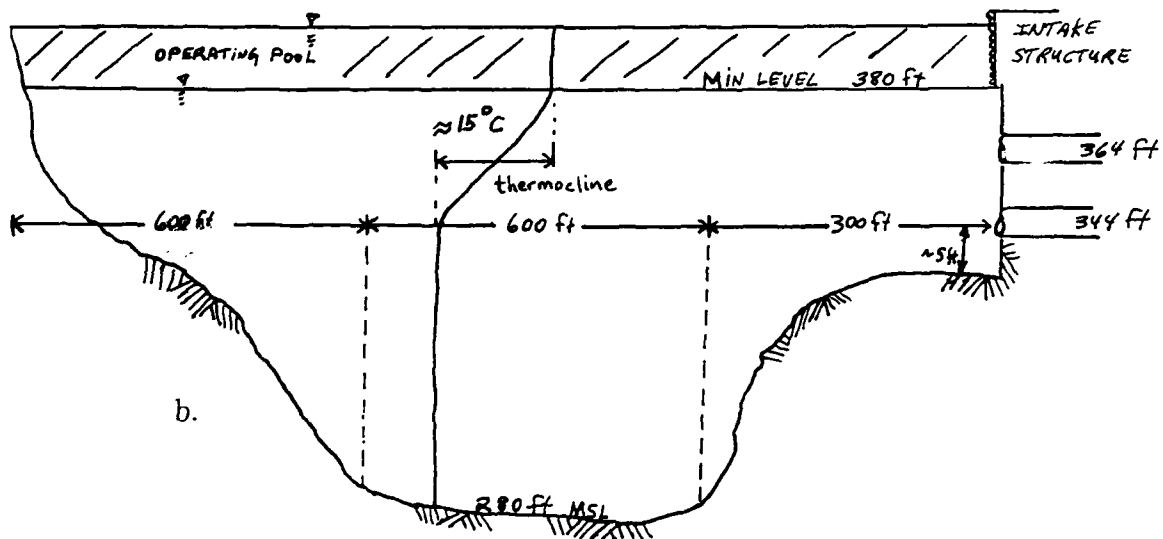
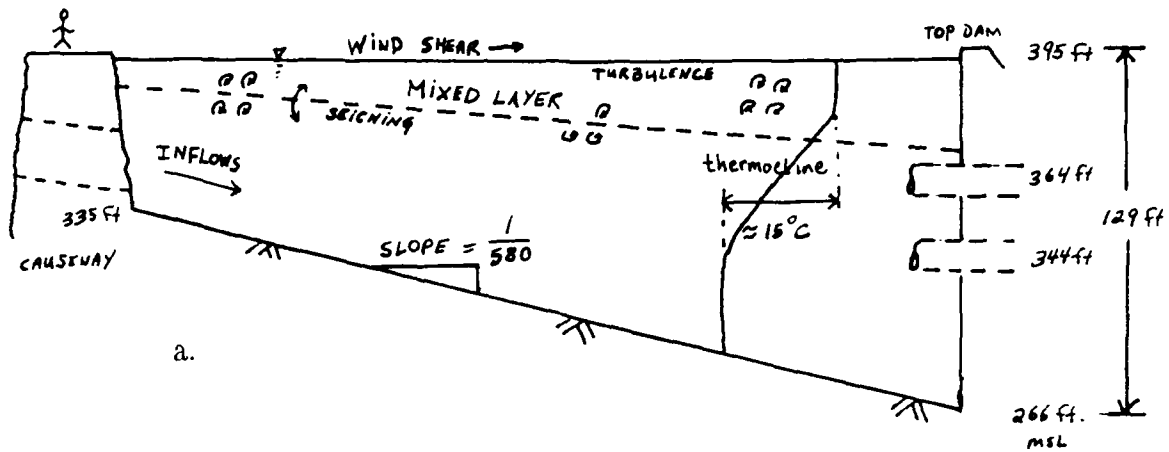


Figure 1.4 Wachusett reservoir cross sections: a. longitudinal, b. width.

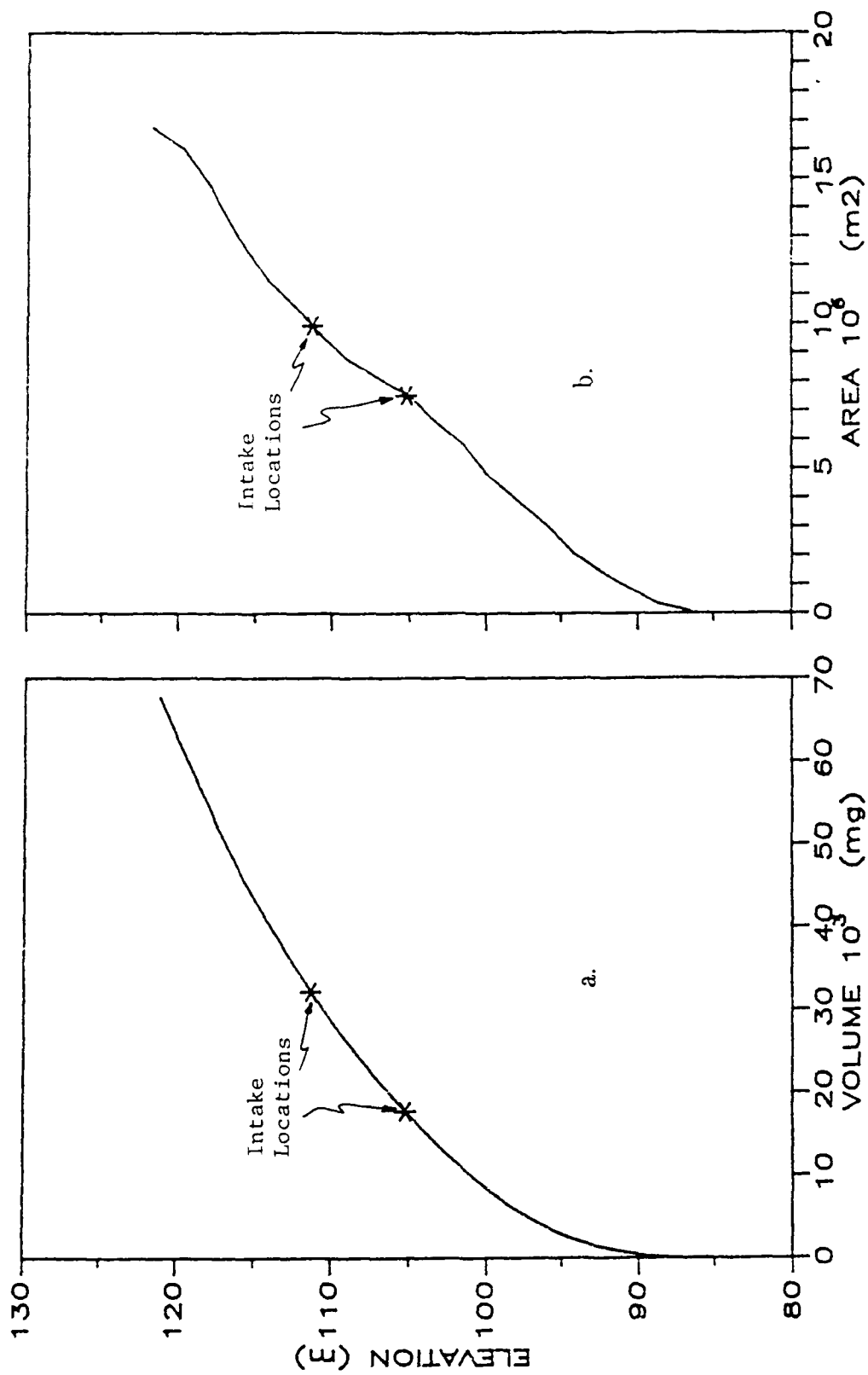


Figure 1.5 Wachusett reservoir morphometry: a. depth-volume curve, b. depth-area curve.

During summer months, Wachusett Reservoir develops a strong thermal stratification with surface temperatures reaching 27°C while the hypolimnion remains about 10°C . In the location of the thermocline (plane of greatest temperature gradient), there is a 14°C change over a 10 meter depth which is shown relative to the basin morphology and intake locations in Figure 1.3 . A strong temperature gradient such as this reduces vertical mixing in the water column. Hence, nutrients and phytoplankton that are largely dependent on convection for transport will be restricted in their distribution due to the thermocline.

Orientation of the reservoir in the direction of the prevailing summer winds maximizes the wind energy imparted to the water surface. If substantial wind velocities continue for a period of time, this continued force will tend to push the water to one end, causing it to pile up in what is called *denivellation* or *set-up*. Once the wind stops, the resulting momentum of the water trying to establish equilibrium causes an oscillation known as a *seiche*. Both denivellation and seiches will contribute to water to a degree very much dependent on the morphology.

1.3.3 Intake Geometry

The geometry of the intake can have an effect on the localized velocity distribution of the outflowing water. Additionally, a strong thermocline located near the level of the intake may restrict the thickness of the withdrawal layer. This restriction is due to the greater energy required to move a particle of water against a thermal gradient, as opposed to a particle located in a volume of uniform density. (See Section 3.1 .)

The intake geometry shown in Figure 1.6 depicts two series of 4 ft by 6 ft intake shafts with six shafts at each level. For modeling purposes their arrangement in the horizontal direction best illustrates a line sink at that level. Maximum outflow

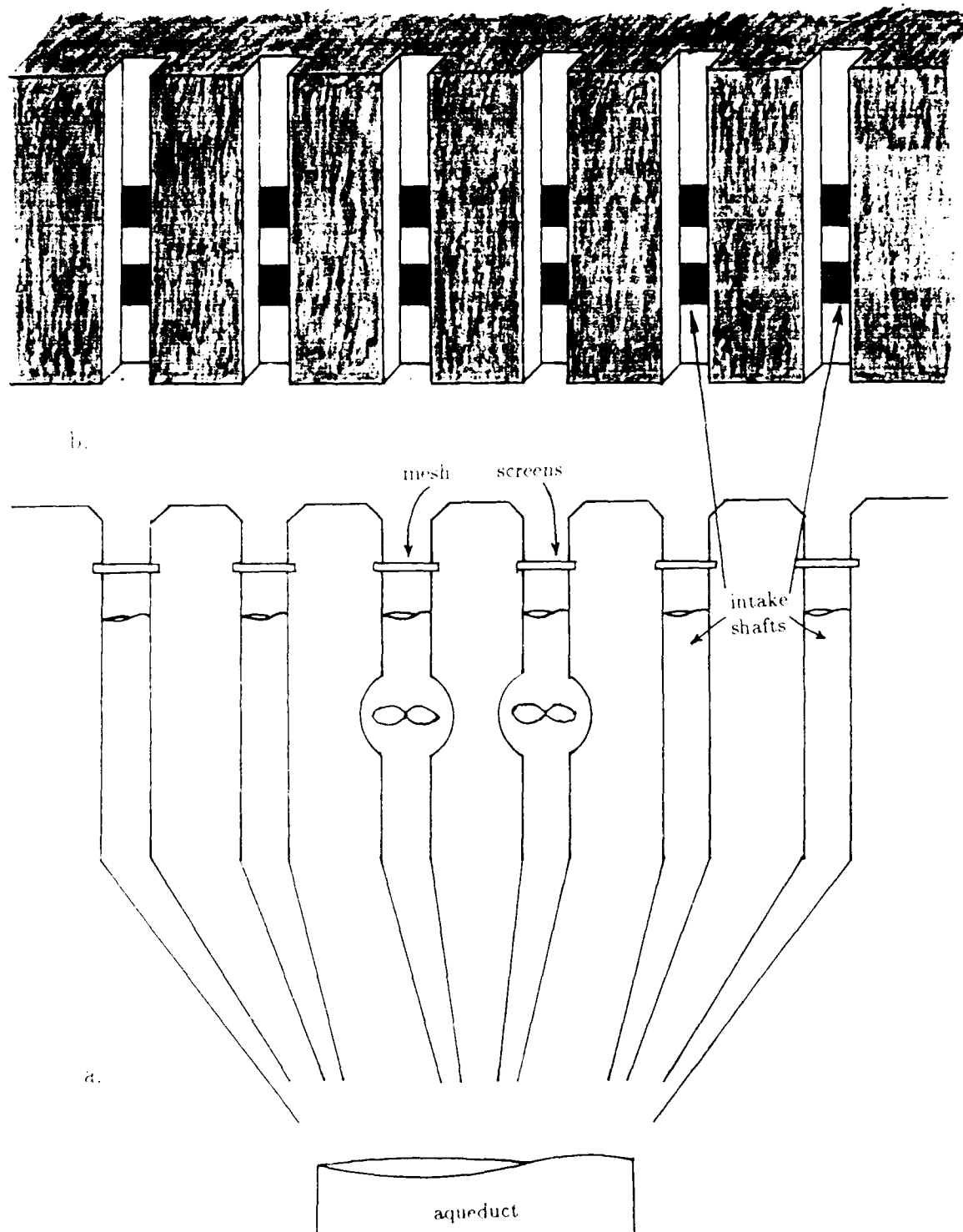


Figure 1.6 Cosgrove intake geometry: a. plan view showing cut out channels and placement of mesh screens, b. elevation view depicting a double row of intakes.

capacity of the intake is approximately 390 mgd, but normally only five of the twelve shafts are operational at any one time. The other seven shafts are closed until such time as the water quality, maintenance, or the build-up of frazil ice on the mesh screens requires the utilization of alternative intake shafts. Currently, no documentation exists in MDC or MWRA records as to which shafts are operational and for what length of time. As discussed in Section 4.4.1, alternate elevations will have a profound impact on the amount of heat advected out of the reservoir and will have a large impact on model simulation results.

The plan view of the intake shafts (Figure 1.6b) reveals a channel that runs vertically 72 feet in front of the actual shaft openings. This channel is used for two sets of stainless steel mesh screens which block the entrainment of large, suspended matter into the turbines or directly into the aqueduct. To effect a water stoppage for the purpose of access to the shaft openings (e.g., cleaning the screens), blocking gates are used which slide down this channel and cut off water flow throughout the entire depth of the channel. This presents an interesting possibility for selective withdrawal experimentation, as the blocking gates could be interchanged with the screens to allow water entry at selected levels. More will be said of this potential in Chapter 5.

One last observation is that the lower intake is located just 1.5 meters above the local bottom (see Reservoir Cross-Section, Figure 1.4b), which ends as a ledge some 90 meters before dropping off to the true bottom elevation (at 87 meters). This may have an effect on the intake velocity distribution since an assumed Gaussian distribution may be better represented as a truncated half-Gaussian or a skewed-upward distribution. (See Section 3.4.2.)

1.3.4 Other Characteristics

Wachusett Reservoir provides approximately 40% of the water supplied to the Boston metropolitan area, with the other 60% coming from the Quabbin Reservoir about 25 miles to the west. The importance of Quabbin in a study of Wachusett is underscored in terms of the water constituents flowing into the reservoir. Currently, near pristine quality water originating at Quabbin Reservoir flows via underground or enclosed aqueducts to Boston with only one connecting surface impoundment; that being Wachusett Reservoir. The reservoir is arguably the weak link in any management plan to ensure delivery of the cleanest possible water. This is due to the proximity to land development around Wachusett and the reservoir's vulnerability to increased environmental stresses as an open water body.

The reason for Wachusett's vulnerability lies in the amount of its watershed that is owned and controlled by the state. Although the MDC owns approximately 65% of the land comprising the Quabbin watershed, it owns less than 10% of the land that makes up the surrounding watershed to Wachusett Reservoir. This has significant implications for the future control of the water's quality as it flows through the reservoir.

Chapter 2 Model Evaluation and Selection

2.1 Purpose of Modeling

With continued interest to quantify the impacts that environmental stress has placed on surface water impoundments, the use of mathematical models plays an increasing role in the management of these resources. The plethora of surface water models available today vary as much in their specific objectives as the waters which they describe. But in general, the aim of modeling is either to provide evaluation of parameters in a diagnostic sense, or to carry out system simulation in a predictive mode.

If chosen carefully, a good model can quantitatively simulate various management alternatives with regard to water quality constituents quickly, accurately, and at a modest cost when compared to conducting field scale experimentation. This is not to infer that modeling should be carried out to the exclusion of experimentation, but rather that modeling be used in concert with field testing to narrow the range of attractive alternatives and provide insight into impacts to be expected. Only through an iterative process involving modeling, collecting data, and refining the model, can the best quantitative solution be arrived at.

How modeling interfaces with management and the political infrastructure is the topic of Chapter 6. In this chapter, the important considerations of generic models are examined, followed by a classification in the development of hydrothermal models, and a selection of an appropriate model for application to Wachusett Reservoir. Finally, an examination of CE-THERM-R1, a widely used US Army Corps of Engineer hydrothermal reservoir model, is presented. This chapter will provide a perspective for specific model theory of the MIT Temperature Model presented in Chapter 3.

2.2 Characteristics of Generic Models

A mathematical model of a surface water body attempts to represent dominant physical, biological, or chemical processes as accurately as possible. This is accomplished by mathematically describing the interrelationships of these processes based on theoretical understanding. The most complex models are gross simplifications of the dynamic and non-linear processes that occur in nature.

To successfully model a water body is to capture the spatial and temporal variability of the internal processes thereby supporting the theory of the principles involved. Thus, the stronger the theoretical basis for particular processes, the more likely is success in their quantification. However, in most instances of modeling, trade-offs must be made between simplifying the expressions of complex interrelationships and the resultant accuracy of the simulation. Before employing a model to serve a particular end, an evaluation of its assumptions and theory is important.

As presented by Adams et al. (1987), a basic consideration for evaluation of any model is the question of whether dominant processes in the physical system are properly represented in the model. For instance, the major distinction between a lake and a reservoir is the relative importance of vertical advection over diffusion. This is because most reservoirs have much greater inflows and outflows in proportion to their volume, and the outflow is usually at depth; as opposed to smaller flows and a surface outlet in lakes. Thus, to properly model transport processes in reservoirs, inclusion of an advection term is imperative. Similarly, in order to properly model the thermal processes in a water body, major heat fluxes through the water surface must be critically evaluated. All significant features must be represented either as input to the model or by the model generating values internally.

Models vary widely in the number of parameters they invoke to describe characteristic processes. However, a model with a large number of parameters is not necessarily more accurate or better suited for use in a given purpose. The accuracy of the model can only be as good as the understanding of the process it describes. A model using empirical parameters to make up for a deficiency in scientific information is usually not reliable in predicting changes as a consequence of man's intervention.

Documentation of model components and clarity of model formulations is an important consideration when searching for an appropriate model. By this is meant, to what degree the model is "user friendly"? Well documented models reduce misinterpretation of input/output requirements and define limitations of the model with changing environmental conditions. Furthermore, any documentation of previous successful applications of the model will be helpful in deciding the appropriateness of the model for the problem at hand.

Finally, it is important to have a clear statement of the problem to be studied. Only then can one find (or develop) a model that meets the needs as well as the constraints imposed.

2.3 Distinctions Among Hydrothermal Models

2.3.1 Dimensionality Considerations

A number of hydrothermal reservoir models are in use. When choosing a model for a particular application, a description of its basic characteristics is needed. The transport of heat (and mass) is a dynamic process occurring in three-dimensional space within a water body. Due to the complexity of formulation, the burden on mathematical computations, the volume of data required to run a three-dimensional model, it is useful to seek simplifying assumptions that can reduce the dimensionality of the problem. Evaluation of a water body may reveal properties which generally

allow the decoupling of horizontal advection from vertical transport [Harleman, 1982]. Basically, deep reservoirs (>15m) with relatively small inflows compared to the reservoir volume (about a factor of 10) will achieve stratification during the summer period and could possibly be simplified to a one-dimensional (vertical) model for the simulation of most biological and physical processes. Orlob (1983) presents a reservoir stratification criterion based on a densimetric Froude number

$$F_r = \frac{LQ}{Vd} \left[\frac{d}{\beta g (T_s - T_b)} \right]^{1/2}$$

where

L = reservoir length

d = mean depth of reservoir

V = reservoir volume

Q = through-flow of reservoir

g = acceleration due to gravity

T_s = surface temperature

T_b = bottom temperature

β = coefficient of thermal expansion

When F_r is $< 1/\pi$, stratification of the reservoir is expected and the assumption of horizontal homogeneity is appropriate. Additionally, Ford and Thorton (1979) suggest that a one-dimensional (area-averaged) schematization is appropriate for reservoirs with a length scale less than 10 km.

An unstratified shallow reservoir with a high rate of inflow relative to the total volume may be modelled as a river with evaluation of the longitudinal direction only. In this case, values for all parameters will be averaged across the width and depth,

inferring that for all practical purposes variability in these directions is insignificant. Therefore, thermal rates of change will only be modelled as longitudinally and temporally variable. Alternately, if particular parameters of interest exhibit variability across both the length and depth (long, deep reservoirs), and it is of interest to capture these gradients, perhaps a two-dimensional laterally-averaged model would be appropriate.

Multi-dimensional hydrothermal models have significantly larger data requirements, most notably with regard to wind direction, duration, and velocity. However, it is important to recognize the limitations for application of a one-dimensional model.

2.3.2 Time and Length Scales

To fully capture the dynamics of a process, it is necessary to observe it at intervals consistent with its natural variability. Time and length scales appropriate for use in a simulation are a function of the problem definition. For instance, since dissolved oxygen concentration in the photic zone responds to a diurnal cycle, a time scale on the order of hours is appropriate for modeling if these fluctuations are to be captured. Alternatively, seasonal variation in algae concentrations could be modelled with a time scale of one day.

Compatibility of time scales with inherent spatial scale of an observed process must be maintained. For example, to model algae exhibiting wide spatial variability in a reservoir, with a time scale of 3 hours and an area-averaged spatial scale would not be reasonable. Ford and Thorton (1979) found that spatial and temporal scales were intrinsically coupled. Furthermore, they detected errors in model results when the scales were inconsistent. Thus, initial evaluation of monitoring data should indicate to what scale modeling should be carried out.

2.3.3 Model Representation of Reservoirs

In addition to the question of model dimensionality, hydrothermal models differ in the way they characterize the reservoir. An excellent review of models is presented by Wang (1982).

A reservoir which is considered fully mixed and averaged over all three directions is a zero-dimensional model or a "one-box model," as illustrated in Figure 2.1 .

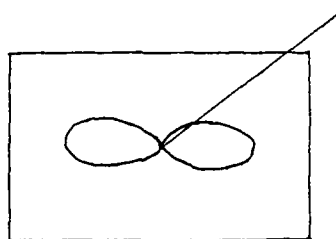


Figure 2.1 One-box model

The limitations of this model are severe since all gradients of temperature and concentration are neglected. Significant processes such as differential absorption of heat with depth in the water column is impossible. The primary application for this one-box model is in small, shallow (<5m) lakes.

The two-box model shown in Figure 2.2, differentiates between a fully mixed epilimnion and hypolimnion (separated by a fixed thermocline).

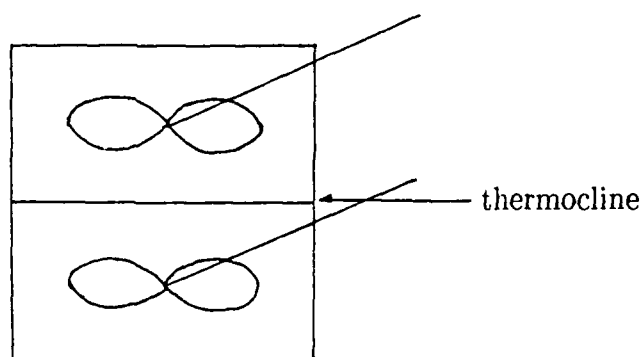


Figure 2.2 Two-box model

This model over-simplifies advective and diffusive transport phenomena by means of a fixed exchange coefficient describing transport between the two layers. The fixed thermocline does not represent temperate lakes very well since they characteristically exhibit high variability in the depth of the mixed layer throughout the year. The fully mixed hypolimnion is incapable of describing concentration (or density) gradients which are critical for evaluation of the exchange processes between sediments and overlying water.

Further evolution of the box model brought about a multi-layered hypolimnion underneath a fully-mixed epilimnion as shown in Figure 2.3, subsequently referred to as a mixed-layer model in this study.

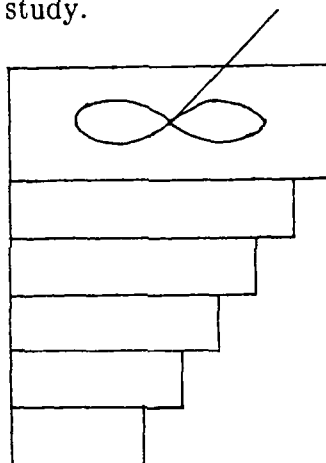


Figure 2.3 Mixed-layer model

In this model, the thermocline (the depth of the mixed layer) moves up and down in the water column over time and vertical advection due to inflows and outflows is computed. The upper mixed layer is fully mixed due to environmentally induced turbulence (e.g., wind) and accounts for absorption of solar radiation with depth. In more sophisticated models, additional coefficients require the assignment of values for parameters such as extinction rates and wind mixing effects on the entrainment of lower waters into the mixed layer. A mixed-layer model [Bloss and Harleman, 1979] was chosen for application to Wachusett Reservoir, and is discussed in Chapter 3.

2.3.4 Determination of E_z

One of the most difficult parameters to quantify in a water body is the degree of transport by the means of turbulent diffusion. Various modelers have proposed methods for determining a value of the diffusion term as a function of depth, time, temperature gradients, wind, and inflows/outflows.

Evaluation of the vertical eddy diffusivity would be significant in the analysis of any model. Field studies using tracers such as dye, temperature, phosphorus, radon, or tritium show distinct variability of diffusion with depth as depicted in Figure 2.4 [COE, 1986]. Since wind will dominate mixing processes in the epilimnion, the importance of hypolimnetic mixing by this diffusion coefficient is exemplified below.

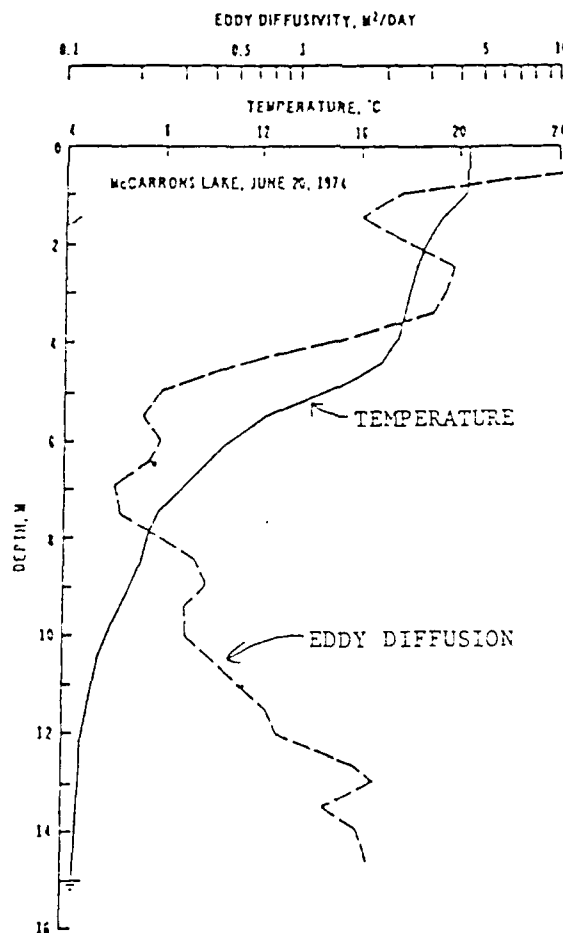


Figure 2.4 Variability of diffusivity with depth
[taken from COE (1986)]

The mixed layer is not sensitive to E_z because there is no temperature gradient. Similarly, below the mixed layer, if heat transport is dominated by advection the correct description of E_z may not be significant. This condition of advection domination is the basic distinction between a lake and a reservoir since the latter typically has large inflows and outflows. A dimensionless ratio ($\frac{A_d E}{dQ}$) proposed by Octavio et al. (1977) is proportional to the ratio between the rate of vertical heat transport by diffusion to the transport by vertical advection. As defined, A_d is the horizontal area at outlet depth d , E is the vertical turbulent diffusivity, and Q is the average inflow/outflow rate. If this ratio is small compared to unity, advection dominates diffusion. If the ratio is large, diffusion dominates.

2.3.5 Modifications to the Mixed-layer Model

Variations of the mixed-layer model have evolved by conceptual improvements that are added to the model for use in specific circumstances. However, the basic model formulation has not changed. For instance, improvements in wind mixing routines, entrainment functions, and evaluation of longitudinal variability in the mixed layer have occurred.

A recent improvement that has been applied to one-dimensional models is an algorithm for selective withdrawal from a stratified water body which allows for the use of longer time steps without numerical instability [Hocking et al., 1988]. This has the impact of significantly reducing computer time for long term simulation in reservoirs with large withdrawals. Additionally, simulations using this algorithm seem to indicate greater definition of the mixed layer.

Some thermal models use a fixed layer schematization (Eulerian models) which provides for a vertical advective transport term to maintain continuity between layers of constant volume [Bloss and Harleman, 1979]. An alternative is provided by

a Lagrangian or variable layer scheme model where the vertical advection term is eliminated and layers are allowed to expand or contract with variations in inflow and outflows [COE, 1986]. This latter model reduces the excessive mixing which is experienced in middle layers with the fixed layer models. Thus, better accuracy is achieved in the area of the thermocline with the variable layer model.

Many one-dimensional hydrothermal models are coupled to water quality models. Although this is not a modification to the mixed layer model, it underscores the applicability of the models and the importance of the thermal processes with regards to distribution of water quality constituents. Thus, a reliable water quality model must necessarily first solve the heat transport equation (see Section 3.3.3) to determine the distribution of heat and then couple results with conservation of mass principles. Mass distribution in turn will affect the temperature and density gradients due to its heat absorbing characteristics. But the influence of mass on temperature distribution is not as great as the temperature influence on mass distribution [Harleman, 1982].

This discussion illustrates the need for a concise problem statement to best choose between the capabilities of different models and to obtain an adequate model for the desired needs, with a minimum of input data required.

2.4 Appropriate Model for Wachusett Reservoir

The MIT Temperature Model [Bloss and Harleman, 1979], was selected for this study on Wachusett reservoir and it meets all the criteria for a reasonable analysis of the stratification cycle. From the discussion above, several points should be considered when selecting a model to simulate thermal distributions in a reservoir.

First, with regard to dimensionality appropriate for the reservoir, Wachusett is a reservoir of medium size (<10 km in length) and calculation of the Froude number using the equation in Section 2.3.1 yields:

$$F_r = \frac{LQ}{\sqrt{d}} \left[\frac{d}{\beta g (T_s - T_b)} \right]^{1/2}$$

$$= \frac{(9800\text{m})(15\text{ m}^3/\text{s})}{(2.46 \times 10^8 \text{ m}^3)(15\text{m})} \left[\frac{15\text{m}}{(2 \times 10^{-4}/^\circ\text{C})(9.8 \text{ m}/\text{sec}^2)(10^\circ\text{C})} \right]^{1/2} = .001 \quad (<1/\pi)$$

Thus, based on guidance presented in Section 2.3, Wachusett would qualify for a one-dimensional study. Additionally, field data compiled from two monitoring stations at nearly opposite ends of the reservoir (Stations 3412 & 3417) reveal practically identical temperature profiles throughout the monitored period as shown in Figure 2.5. This correlation of temperatures lends support to the assumption that horizontal uniformity exists.

Greater than 85% of the inflows enter the reservoir from one end and flows can vary from 20 to over 700 mgd on any given day. Therefore, the model must be able to handle variable flow rates and surface elevations in the simulations. Since the objective of the thermal simulations is to accurately predict the seasonal variations of temperature in the reservoir, a time step of one day is appropriate. Local meteorological data is available as daily averaged values so that consistency can be maintained with respect to the input data.

The MIT Temperature model is compatible with all these constraints, and accounts for wind effects in the upper mixed layer and variable diffusion options ranging from molecular diffusion to a turbulent eddy diffusivity dependent on depth and wind.

The MIT model has been coupled to a water quality model [Serrahima, 1987] which would be a likely follow-on study upon completion of verification of the

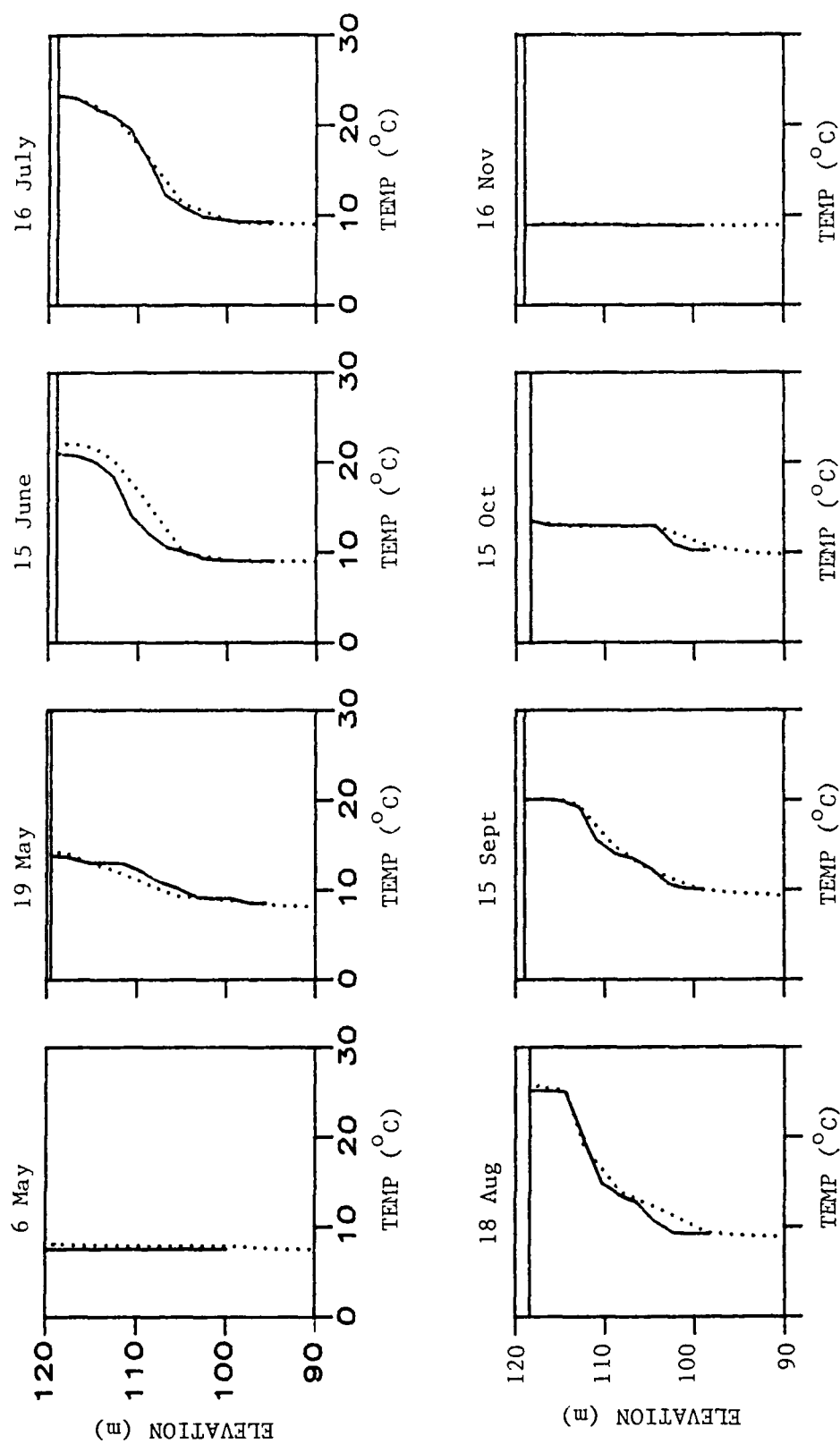


Figure 2.5 Comparative profile for two stations illustrating horizontal isotherms. (Solid line is Station 3412, dotted line Station 3417.)

thermal model as presented here. The MIT model has been in use since the early 1970's and has been subjected to rigorous testing by the EPA and the US Army Corps of Engineers [EPA, 1975]. Applications in previous years include a voluminous list of lakes and reservoirs from large regional water supplies (e.g., Sau Reservoir in Spain) to major TVA reservoirs such as Fontana Reservoir, as well as Lake L227 in the Experimental Lakes Area in Manitoba, Canada. This model is well suited for application to Wachusett Reservoir.

2.5 Examination of CE-THERM-R1 (Corps of Engineers' Model)

A one-dimensional hydrothermal model widely used for reservoir studies is CE-THERM-R1, developed by the U.S. Army Corps of Engineers [COE, 1986]. Many characteristics of this model are similar to the MIT temperature model, and comparative references should be made to Chapter 3. In this section, differences pertinent to calculations of the heat transport in the reservoir are presented. In comparison to MITEMP, CE-THERM-R1 has a different theoretical basis for calculation of vertical turbulent diffusivity, inflows, outflows, and reservoir schematization. The model theory for solar absorption below the water surface, and surface layer mixing is similar to MITEMP, although parameter values used are somewhat different and are noted below. Most of the following discussion in reference to CE-THERM-R1 comes from the model's user manual [COE, 1986].

2.5.1 Reservoir Schematization

CE-THERM-R1 uses a variable layer thickness (Lagrangian model) in the representation of the water column as depicted in Figure 2.6 . This infers that each layer can expand or contract to account for water flowing into or out of each layer. As a result, there is no vertical vertical advection between adjacent vertical layers.

These vertical flows (characteristic of fixed layer models) contribute to mixing through numerical dispersion. The Lagrangian model has the advantage of decreasing the numerical mixing between layers, thus refining the degree of mixing in the region of the thermocline.

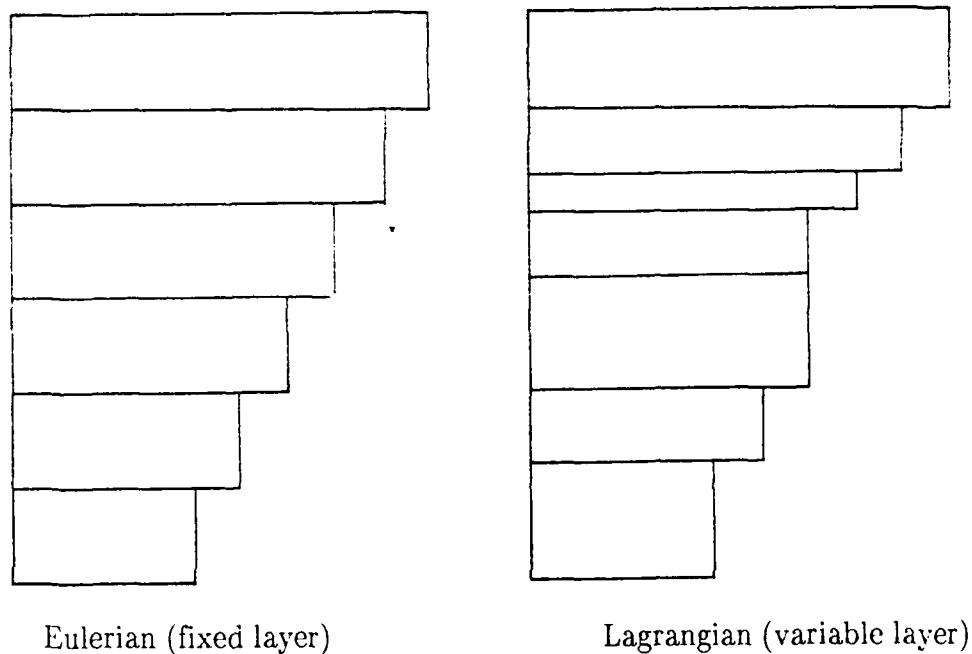


Figure 2.6 Lagrangian vs. Eulerian (fixed layer) models

2.5.2 Characterization of Inflows and Outflows

As water enters the stratified reservoir, the centerline of the inflow zone is at the reservoir layer with a density that most closely matches the inflow density. In the event that the inflow density is less than or greater than any reservoir layer density, the inflow will enter at the surface or the bottom of the reservoir respectively.

The thickness of the inflow zone is determined by a formula related to the densimetric Froude number given by:

$$d = 1.35 \left[\frac{QL}{A} \frac{1}{\sqrt{g \frac{\Delta \rho}{\rho_o}}} \right]^{2/3}$$

where

d = one-half thickness of inflow zone (m)

Q = inflow rate ($m^{3/5}$)

L = reservoir length (m)

A = lower horizontal surface area of inflow layer (m^2)

g = acceleration due to gravity (m/sec^2)

$\Delta \rho$ = difference in density between inflow layer and boundary layer

ρ_o = density of inflow layer (kg/m^3)

If no density gradient exists in the reservoir, the inflow is distributed over the entire pool depth. Otherwise, the inflow is distributed based on a volume-weighting scheme where both the volume and the velocity into each reservoir layer is proportional to the volume of the layer within the inflow zone. For instance, if each reservoir layer in the inflow zone was of equal volume, the inflow would be evenly distributed among each layer.

Outflow zones and flow distribution are calculated by a very different method than inflows. First, the withdrawal zone is calculated for each intake, through an iterative process and solving for the equation:

$$Q - Z^2 \left(\frac{\Delta \rho}{\rho} g z \right)^{1/2} = 0$$

where

Q = discharge rate (m^3/hr)

Z = distance from intake to zone boundary (m)

$\Delta\rho$ = density difference between intake and zone boundary (kg/m^3)

ρ = water density at intake (kg/m^3)

g = acceleration due to gravity (m/hr^2)

The discharge zone may not be symmetric about the intake, and while representing the outflow velocities by a parabolic distribution, the maximum velocity may not be centered on the intake (see Figure 2.7).

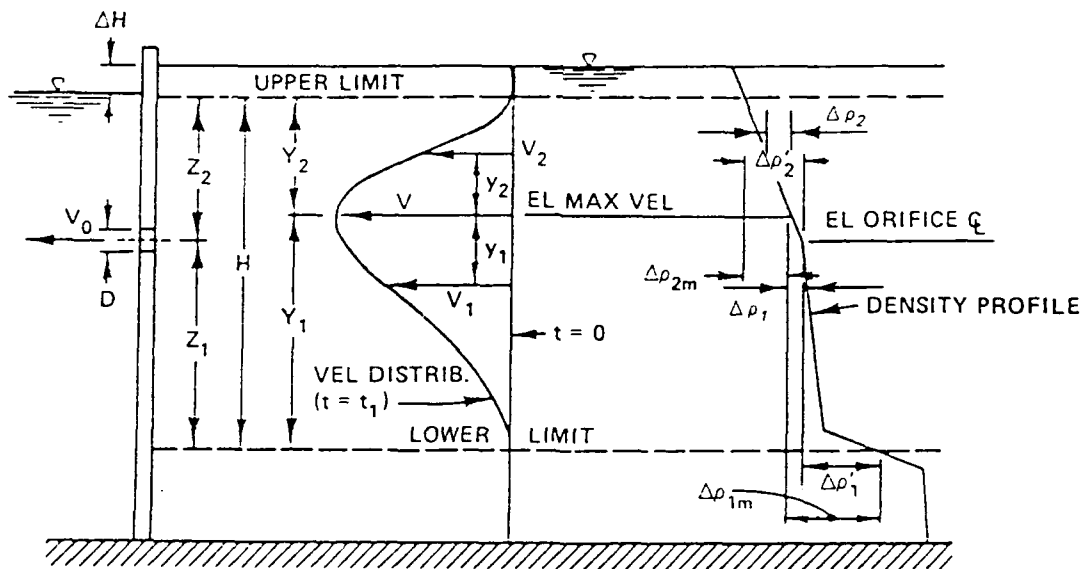


Figure 2.7 Physical representation of outflow parameters
[taken from COE, 1986]

This calculation outflow distribution is a significantly different formulation from MITEMP, where outflow velocities are represented by a Gaussian distribution

centered on the intake. MITEMP allows for designation of the volume of flow coming from the withdrawal layer (see Section 3.5.1) whereas in CE-THERM-R1, the velocity distribution is predetermined from the equation

$$U = U_m \left(1 - \frac{y \Delta \rho}{Y \Delta \rho_m} \right)^2$$

where

y = distance from elevation of velocity being computed to the maximum velocity elevation

Y = distance from the elevation of maximum velocity to zone boundary

$\Delta \rho$ = density difference between elevation of velocity being computed to maximum velocity

ρ_m = density difference between elevation of maximum velocity to zone boundary

and

U_m = maximum velocity (m/s) located by the equation

$$\frac{Y_1}{H} = \sin^2 \left(\frac{\pi}{2} \cdot \frac{Z_1}{H} \right)$$

where

Y_1 = distance from lower withdrawal limit to elevation of maximum velocity

H = total vertical distance of withdrawal zone

Z_1 = distance from lower withdrawal limit to the intake

Refer to Figure 2.7 for the physical meaning of these parameters just defined.

2.5.3 Vertical Turbulent Diffusivity

The vertical eddy diffusivity used in CE-THERM-R1 is proportional to the dissipation turbulent kinetic energy computed as a result of inflows, outflows, and wind. The diffusivity is computed at each layer using a Richardson number containing a local density gradient, a densimetric Froude number, and a time scale. The minimum value allowed for any layer is molecular diffusion (.0124 m²/day) while the maximum diffusivity allowed can be as high as 480 m²/day. An option exists which assigns a constant value of .1853 m²/day to each layer, eliminating the need for any calibration of this parameter.

2.5.4 Wind Mixing

The effect of wind on the upper mixed layer is computed in the same manner as MITEMP and taken from Bloss and Harleman (1979). However, the work available from wind forces on the water surface given by

$$\tau_o = \rho_a C_d w^2$$

where

τ_o = surface shear stress due to wind

ρ_a = density of air

w = wind velocity

C_d = drag coefficient at water surface equal to

$$.0005 \sqrt{w} \text{ for } w < 15 \text{ m/s or } .0026 \text{ for } w > 15 \text{ m/s}$$

This differs from MITEMP as discussed in Section 3.7.2 . Furthermore, solar radiation absorbed below the water surface, as in MITEMP, decreases at an exponential rate, however this decrease starts at 0.6m below the surface as given by

$$\phi_z = (1 - \beta) \phi_{sn} e^{-\eta z}$$

where

z = depth below water surface starting at 0.6m below the surface

β = fraction energy absorbed within 0.6m of surface

ϕ_z = flux of solar radiation at depth z

ϕ_{sn} = net incident solar radiation

η = extinction coefficient

2.5.5 Other Features of COE Model

CE-THERM-R1 has features extraneous to the calculation of thermal transport which expand its usefulness from an operational standpoint. For instance, the model includes a pumpback option which simulates pumping water from the outflow back into the reservoir from an afterbay during periods of off-peak power demand, in the case of use for a hydro-electric facility. Furthermore, the model can be operated in a prescriptive mode, when the input specifies a set discharge temperature, the model will determine the level of withdrawal throughout the simulation period that is required to meet this criteria. This has obvious advantages for cooling water discharges which are limited by environmental concerns. In comparison, MITEMP operates on the premise that given an operating elevation, the discharge temperature is calculated.

Chapter 3 Model Theory (MITEMP)

The MIT Temperature Model (MITEMP) has undergone several revisions toward expanding capability and upgrading accuracy since its inception by Huber and Harleman (1968). Expansion of the model to include the coupling of a water quality model for reservoirs by Markofsky and Harleman (1971) and application to cooling ponds was made by Ryan and Harleman (1973). A subsequent wind mixing model was added by Octavio and Harleman (1977) with refinements made by Bloss and Harleman (1979). Calgano (1979) developed a dissolved oxygen model using the wind mixing model and Serrahima (1987) extended it to include other water quality parameters such as nutrients, biological oxygen demand, and three types of algae. Addition of a variable diffusion coefficient, which is important in hypolimnetic mixing and is dependent on power imparted by the wind, was made by Aldama et al. (1988). This last version was adapted for this study.

Before discussing the specifics of the thermal model, it is important to review first some fundamental processes of water bodies and in the process to lay down some operational definitions.

3.1 Heat Transfer in Lakes and Reservoirs - Basic Concepts

The distribution of heat and chemical pollutants in surface water impoundments has been of widespread interest due to their implications for localized ecosystems as well as the direct correlation to the quality of water released for consumption. The method of transport throughout a water column is the key to understanding the resultant distribution of heat and mass which is forced by three major processes; advection, convection and diffusion. Methodologies used in attempts to quantify the

relative importance of these transport mechanisms are the basis for model selection and subsequent application to a specific water body (see Chapter 2).

The fundamental processes that comprise the characteristic hydrodynamics of a body of water are inflows and outflows, local meteorology, and the properties of water itself. Most importantly, transport processes are influenced by the temperature regime of the water column. The density of water is related to temperature in a non-linear fashion, as shown in Figure 3.1.

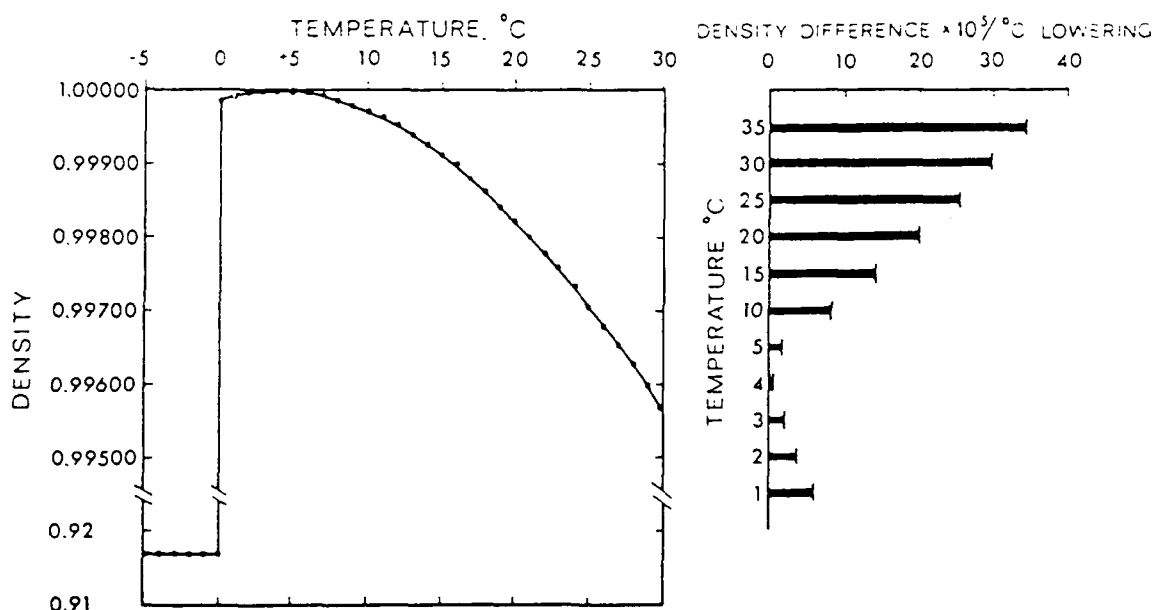


Figure 3.1 Density of water (g/ml) as a function of temperature. The right hand portion is the density difference per °C lowering at various temperatures. [From Wetzel, 1983]

Due to gravitational forces, a vertical column of water of different density will stabilize with the densest water at the bottom and the least dense at the top. For water above 4°C, this simply infers that warmer water will lie above cold water under relatively quiescent conditions (known as stratification). Below 4°C the

reverse is true (reverse stratification). Should environmental conditions result in more dense water lying on top of less dense water (from inflows or heat loss due to radiation) then the unstable buoyancy forces will initiate *convective mixing* to redistribute the densities into a more stable configuration.

The potential energy of a stratified column (Figure 3.2a) can be shown to be less than that of a fully mixed column of the same mean density (Figure 3.2b) as calculated by summing the moments about a reference point:

$$PE = \sum V \rho l g$$

where

V = volume of layer of uniform density

ρ = density of water at that layer

l = distance to center of mass from plane of reference

g = acceleration due to gravity

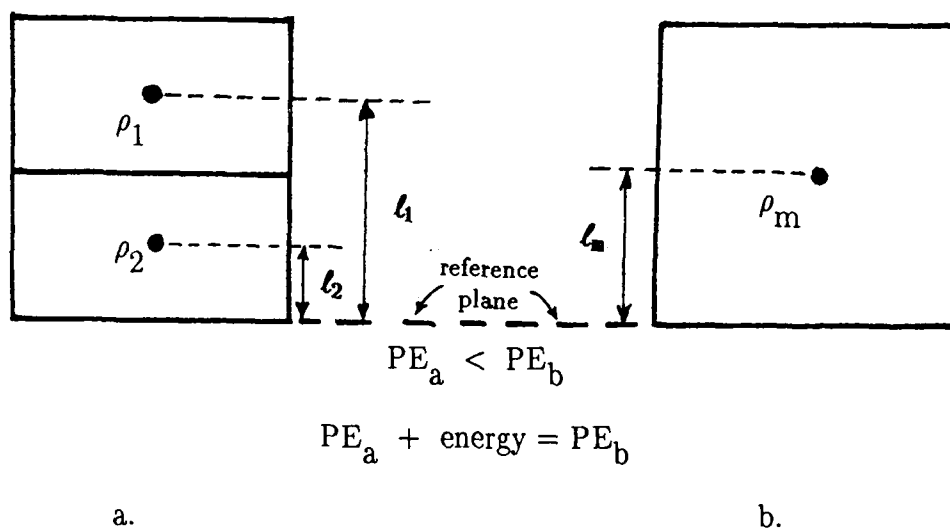


Figure 3.2 Comparison of potential energy for a stratified water column vs. a fully mixed column. (ρ_m = mixed density weighted by volumes.)

From this principle, it follows that for a stratified column of water to become mixed, the input of energy is necessary. The greater the density gradient ($d\rho/dz$), the greater the energy required to overcome this stratification. For lakes and reservoirs, the source of this energy comes overwhelmingly from the wind. Thus, knowing the density gradient and wind velocities, the amount of mixing due to the wind can be calculated. Equations as used in the MITEMP wind mixing routine are presented in Section 3.4.5.

The processes of diffusion and advection in their most simplified form can be explained by reference to Figure 3.3. The *diffusive flux* of a constituent on a molecular level occurs in the direction of a decreasing concentration gradient within a carrier fluid (e.g., water). It represents the movement of individual particles relative to a center of mass whose coordinates may move in space. Density gradients of the carrier fluid may tend to inhibit this diffusive transport.

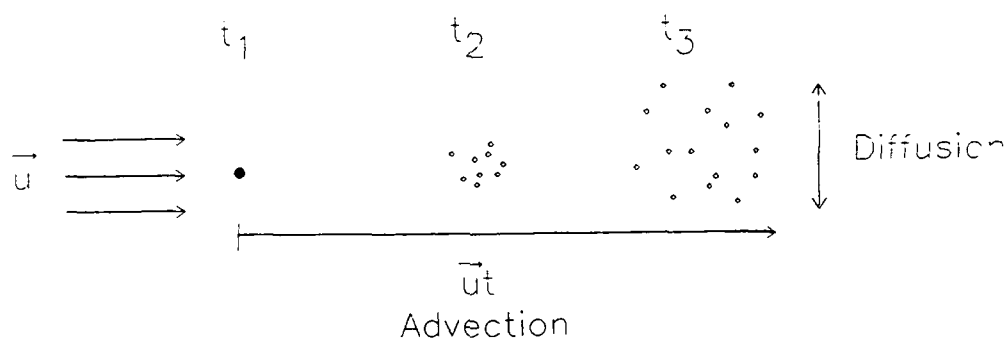


Figure 3.3 Molecular diffusion relative to bulk advective motion [Harleman, 1988].

Advection on the other hand, occurs in response to shear or pressure gradients and results in mass transport due to bulk motion (\vec{u}). It is referenced to a fixed point with respect to the particles. The purpose of this explanation is to underscore the coupled relationships of temperature, potential energy, and mixing which drive the

mass transport processes and result in the distribution of constituents in a water body.

3.2 Thermal Cycle in Lakes and Reservoirs

Dimictic water bodies in temperate regions undergo a very characteristic annual cycle which strongly influences the distribution of temperature, nutrients, and planktonic organisms. Beginning with ice melt in early spring, nearly isothermal conditions prevail with mixing occurring throughout the entire water column (spring overturn). Heat energy absorbed from solar fluxes increases dramatically in the upper layers compared to periods of ice cover. Depending upon water clarity, meteorological conditions, and turbulent mixing processes, this differential heating of the upper layers will set up a thermal stratification which will resist further mixing. With clear skies (maximum solar energy absorption) and low wind velocities (minimum mixing forces), this can occur on the order of several days after ice melt [Wetzel, 1983]. At this point the lake or reservoir is divided into a distinguishable upper mixed layer (epilimnion), a region of high temperature gradient (thermocline), and a colder bottom region (hypolimnion) isolated from surface heat fluxes.

Total daily solar insolation decreases as summer wanes, and as air temperatures drop, net heat losses result in cooler surface waters overlying warmer, less dense water creating an unstable condition. Convective mixing helps stabilize this condition through deepening of the mixed layer and erosion of the thermocline. This continues through the fall until sufficient heat has been lost to result in isothermal conditions again. As with spring overturn, the water temperature, nutrients, and plankton are uniformly distributed over the entire depth (fall overturn). This is essential to many biological phenomenon which depend on this redistribution of constituents.

The cooling process continues until temperatures of maximum density (4°C) exist throughout the water column, at which time continued heat loss causes upper layers to become colder and less dense (see Figure 3.1) than lower waters. This condition of reverse stratification remains throughout the ice covered period until spring when the cycle begins again. It should be noted that the interaction of wind forces and solar radiation with the water are significantly muted during times of ice cover and are much less coupled during this period. It is the goal of the hydrothermal model to capture this annual stratification cycle.

3.3 Hydrothermal Model (MITEMP)

MITEMP is a one-dimensional (vertical) hydrothermal reservoir model which uses an explicit finite difference scheme to numerically solve simultaneous differential equations describing the reservoir transport processes. It is a mixed layer model with variable-sized arrays and matrices to handle simulation periods ranging from 3 hours to a year. The version of the model as used in this study includes the modification by Aldama et al. (1988) and accounts for surface heat fluxes, entrance mixing, multiple outflows, variable withdrawal elevations, variable surface elevation, temporally and spatially variable diffusion, effects of wind mixing and internal absorption of incoming solar radiation. All of these capabilities will be discussed in the sequence they are used in the model. This model may be used in either the verification mode or, once calibrated, in the predictive mode using synthesized operational and meteorological conditions.

3.3.1 Assumptions of the Model

A major assumption of the model is that the isotherms (elevations of constant temperature) are horizontal throughout the reservoir. This was deemed appropriate

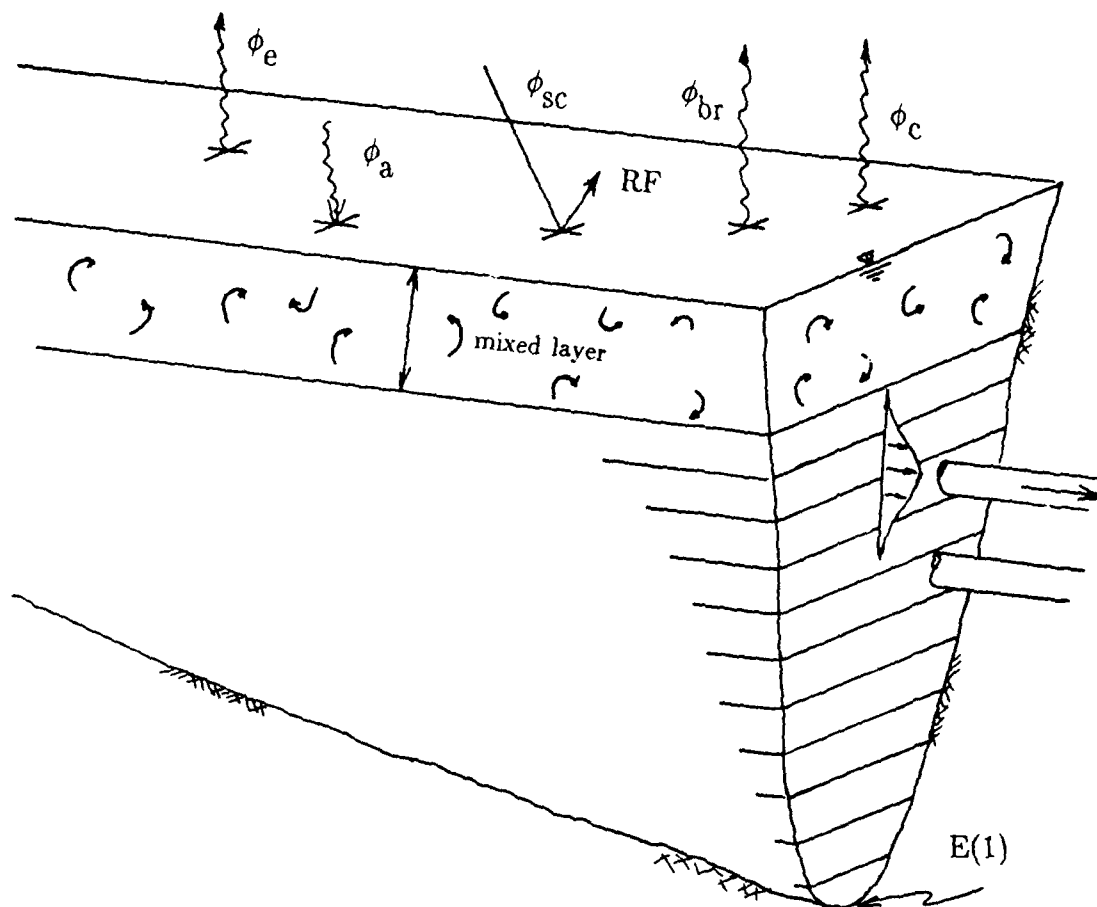
after consideration of the low discharge to volume ratio, reservoir Froude number (Section 2.4), and evaluation of monitoring data at nearly opposite ends of the reservoir which demonstrate similar vertical temperature profiles throughout the year (Figure 2.5).

A second assumption is that the bottom and sides of the reservoir are insulated as a no-flux boundary for the passage of heat. This is reasonable unless there were considerable decomposition of organic matter (heat source) or significant groundwater infiltration, which is unlikely given the large volume of the reservoir.

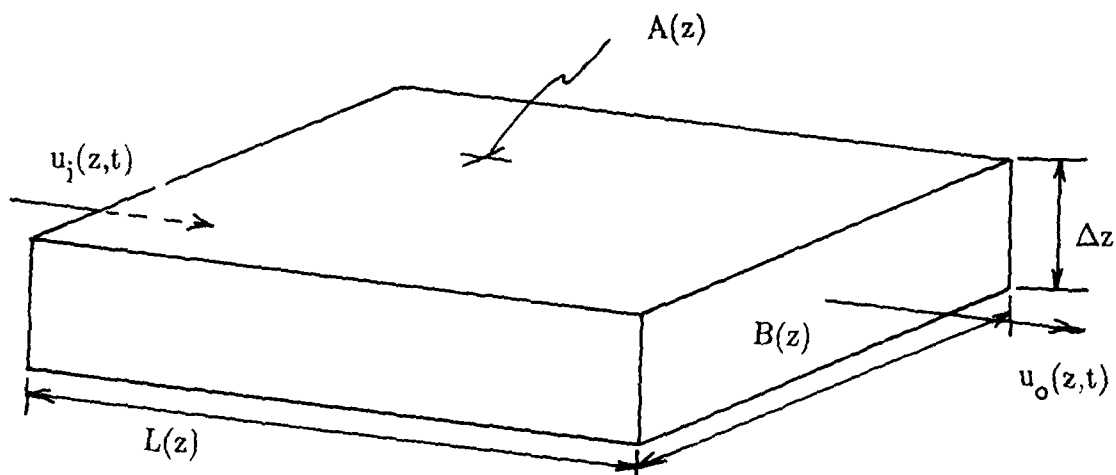
Additionally, water loss through evaporation and water gain from precipitation are neglected in the water balance. This is also an appropriate assumption for reservoirs in temperate climates since annual precipitation is very nearly offset by losses through evaporation. Density between layers is only a function of temperature and does not account for salinity gradients, but should not be of significance in this reservoir.

3.3.2 Model Schematization of the Reservoir

The model assumes that the variation of area with depth is known and uses a fixed layer grid (Eulerian model) of thickness Δz as shown in Figure 3.4a. All layers are the same thickness except for the bottom layer which is $.5 \Delta z$ and the surface layer which varies from $.25 \Delta z$ to $1.25 \Delta z$ to account for variation in surface elevation. Each layer is a control volume (with area $A(z)$, and width $B(z)$, and length $L(z)$) and inflows $u_i(z,t)$ enter at one end and outflows $u_o(z,t)$ exit through the other end (Figure 3.4b). Solution of the continuity equation and conservation of heat equations is executed for each layer at every time step. It can be readily seen how choosing the appropriate time step and grid resolution is important in reducing the number of calculations and optimizing computer time. With Δt of one day, and Δz



(a) Idealized reservoir basin schematization.



(b) Control volume used in maintaining continuity.

Figure 3.4

of two meters, a simulation of 200 time steps (about 6 months) requires approximately 1 minute of cpu time on a Microvax computer.

The above description of basin schematization refers to the finite difference grid used in all model computations. However, a length-area schematization must be input initially describing the basin morphology. The discretized interval (Δz) can be any value, since this grid will be transposed to the finite difference grid and needed values are interpolated.

The bottom most horizontal area $A(1)$ in the finite difference scheme also has an associated width $B(1)$ computed from:

$$B(1) = \frac{A(1)}{L(1)}$$

where

$A(1)$ = horizontal area at grid (1)

$L(1)$ = length at grid (1)

Thus, to avoid computation errors, $A(1)$ and $L(1)$ must take on some finite value greater than zero. This can be achieved in one of two ways:

- * Begin the length-area schematization equal to zero at an elevation slightly lower than the bottom $E(1)$ used in the finite difference scheme, or;
- * Begin the length-area schematization at the same elevation as the finite difference scheme $E(1)$, however insure that the values for length and area are slightly greater than zero.

3.3.3 Heat Transport Equation

The continuity equation and conservation of heat equation are used to derive the basic heat transport equation for an internal control volume which is expressed as:

$$\frac{\partial T}{\partial t} + \frac{1}{A} \left[\frac{\partial}{\partial z} (Q_v T) \right] = \frac{1}{A} \frac{\partial}{\partial z} (A E_z \frac{\partial T}{\partial z}) + \frac{B u_i T_i}{A} - \frac{B u_o T}{A} - \frac{1}{A \rho c} \frac{\partial (\phi_z A)}{\partial z}$$

where

- T = temperature of water at depth z
- A = horizontal area of control volume
- Q_v = vertical flow rate
- u_i = inflow velocity
- u_o = outflow velocity
- E_z = vertical turbulent diffusion
- T_i = temperature of inflow
- B = width of control volume
- ρ = density of water
- c = heat capacity of water
- t = time

and

- ϕ_z = solar radiation at depth z as given by Dake and Harleman (1966)
- $\phi_z = \phi_{sn} (1-\beta) e^{-\eta(z_s - z)}$

where

- β = fraction of incident radiation absorbed at the surface ($\cong 0.5$)
- z = elevation under consideration

z_s = surface water elevation

ϕ_{sn} = net incident short wave solar radiation.

η = extinction coefficient from the Secchi disc depth, SD (in meters)
given by

$$\eta = 1.7/SD$$

The continuity equation asserts that the volume of each layer must be conserved as described by:

$$Q_v = B \int_0^z u_i(z,t) dz - B \int_0^z u_o(z,t) dz$$

There are two boundary conditions and an initial condition imposed for solution of the heat transport equation. The first is a no heat flux condition at the bottom (therefore no solar radiation reaches the bottom). The second is a surface layer which accounts for all heat fluxes between the air and the water surface. (See Figure 3.4a.)

$$\phi_N = \phi_{sn} + \phi_a - \phi_{br} - \phi_e - \phi_c$$

where

ϕ_N = net heat flux at water surface

ϕ_a = atmospheric radiation (long wave)

ϕ_b = back radiation from water to air

ϕ_e = evaporative heat flux

ϕ_c = conductive heat flux

and

$$\phi_{sn} = \phi_{sc} (1 - RF) (1 - .65 CLC^2)$$

where

ϕ_{sc} = 100% sunshine curve [Hamon et al., 1954]

RF = reflectivity at the water surface

CLC = cloud cover as a fraction of clear sky

If measured solar radiation is not available, net incident short wave radiation can be calculated within the model based on latitude, elevation, reflectivity, and dust depletion factor. The model also provides an option for the input of measured atmospheric radiation or calculating it as a function of cloud cover, air temperature, and vapor pressure. If internally calculated, two formulae for atmospheric radiation (ϕ_a) are available:

(1) Swinbank's formula is given by

$$\phi_a = 1.06 \times 10^{-11} (T_a + 273)^6 (1.0 + .17 CLC^2)$$

(2) Brutsaert's formula is given by

$$\phi_a = 1.24 \left[\frac{\epsilon_a}{T_a + 273} \right]^{1/6} (1.14 \times 10^{-6}) (T_a + 273)^4$$

where

T_a = air temperature ($^{\circ}C$)

CLC = cloud cover as a fraction of clear sky

ϵ_a = water vapor pressure at air temperature

Evaporation and conductive fluxes can be calculated using either Kohler, Rohwer, or the Lake Hefner equations as given by Markofsky (1971):

Kohler equation:

$$\phi_e = [H(DE) + HCAP(DE) T_s] [.000135(P)W]$$

$$\phi_c = (\rho) (.000135)(W)(372)(T_s - T_a)$$

Rohwer equation:

$$\phi_e = \rho (EVP)(DE) [H + HCAP(T_s)] [.0308 + .01 W]$$

$$\phi_c = \rho (EVP) (269) [T_s - T_a] [.0308 + .01 W]$$

Lake Hefner equation:

$$\phi_e = 46.1 (DE) (W)$$

$$\phi_c = 47.3 (T_s - T_a) (W)$$

where

W = wind velocity (measured 2m above the surface in Kohler and L. Hefner equation; 6 inches above surface in Rohwer equation)

EVP = evaporation constant (~.01)

HCAP = specific heat of water (~.998 kcal/kg)

T_s/T_a = surface/air temperature

ρ = density of water (~997 kg/m³)

DE = difference between saturated water vapor present at water surface temperature and water vapor pressure at ambient air temperature

H = heat of vaporization (Kcal/kg)

From these equations, the important interrelationship of wind velocity, air temperature, and vapor pressure in these calculations is apparent.

3.3.4 Input Data

Meteorological data should be representative of environmental conditions at the reservoir and averaged over an appropriate time scale based on the time step used in the model. Hence, with a time step of one day, daily averaged data would be appropriate. All data input at intervals greater than one day will be linearly interpolated to a daily average. Interpolation can miss capturing large perturbations from the mean and should be avoided where possible. Alternately, there is no advantage to using meteorological data averaged less than one day unless the time step for the simulation is reduced as well. Typical meteorological data required include air temperatures, wind velocities, humidity, and cloud cover.

Reservoir lengths and areas of a control volume as a function of depth describe the morphometry of the basin and are specified as input for a constant interval (Δz). Additionally, inflow rates, outflow rates, measured surface elevations, and initial temperatures of the water column are required input. Surface elevations are calculated in the model based on the water balance and actual measured values are used for comparison only.

3.4 Calculations Conducted Iteratively in the Model

Using Euler's method, at each time step (Δt), a new thermal distribution (T_{n+1}) comes directly from the current distribution (T_n) after applying all transport processes and meteorological inputs. Restated:

$$T_{n+1} = T_n + \Delta t f(t_n, T_n)$$

Thus with each time step, iterative calculations update existing conditions (T_n) with (T_{n+1}), and continue with the next time step. The following topics are part of the iterative calculations.

3.4.1 Entrance Mixing

The degree of nearfield entrance mixing is determined by the dilution factor (R_m) and the number of layers to be mixed (MIXED). R_m specifies the number of parts of reservoir water to be mixed with one part of inflow water which determines the final mixed temperature (T_m) by:

$$T_m = \frac{T_i + T_r (R_m)}{1.0 + R_m}$$

where

T_i = temperature of inflow

$$T_r = \frac{\sum_{n=2}^{1+MIXED} T(1) + T(n)}{1.0 + MIXED}$$

where

$T(n)$ = the temperature of the n^{th} grid layer from the surface (see Figure 3.5).

The values of R_m and MIXED are calibrated parameters but as a starting point, MIXED should approximate the depth of the inflow. Values of R_m equal to 1.0 have been recommended [Markofsky, 1971] and are used in other model applications [Serrahima, 1987] as well as for model testing on other reservoirs [EPA, 1975].

Entrance mixing essentially pulls water out of the layers defined by MIXED and moves it to lower layers with an equivalent density. Continuity is maintained by accounting for this loss as an outflow defined by:

$$u_{om} = \frac{Q' (R_m)}{1.0 + \text{MIXED}}$$

where

u_{om} = outflow velocity due to mixing

Q' = flow per unit cross-sectional area

R_m = dilution factor

MIXED = number of layers involved in mixing

The outflow velocity from the layer due to mixing is added to the outflow velocity due to water entering the intake in Section 3.4.2, to realize a total outflow from each respective layer.

The new inflow temperature after mixing (T_m) then enters the reservoir at a level where density of the water column equals the inflow density as shown in Figure 3.5 .

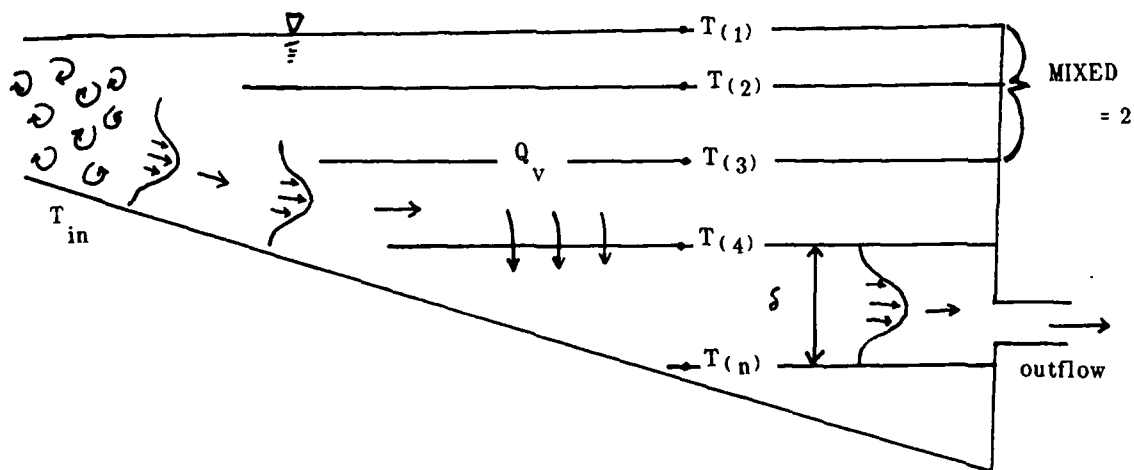


Figure 3.5 Illustration of near-field entrance mixing in relation to layer outflow velocity.

The inflow velocity distribution as shown above is assumed to be Gaussian and is computed by:

$$u_i = u_{i \max} \exp \left[\frac{-[z - z_{in}(t)]^2}{2 \sigma_{in}^2} \right]$$

where

σ_{in} = inflow standard deviation

$z_{in}(t)$ = elevation of inflow at time t

z = surface elevation

$u_{i \max}$ = maximum inflow velocity at time t , as computed by:

$$u_{i \max} = \frac{Q_{in}}{\int_0^{h_{in}} \exp \left[\frac{-[z - z_{in}(t)]^2}{2 \sigma_{in}^2} \right] B \, dz}$$

where

h_{in} = depth of inflow

B = width of each control volume

Q_{in} = rate of inflow

Since the inflow is known, the only parameter to be specified is the inflow standard deviation (σ_{in}). Intuitively, as an initial guide, $\pm 2\sigma_{in}$ should approximately equal the inflow depth.

3.4.2 Calculation of Withdrawal Layer Thickness

For each outlet modelled, the withdrawal layer thickness (δ) is calculated as a function of the density gradient centered about the outlet. There are two conditions for which the withdrawal thickness calculation differs.

1. Existence of sharp gradient at the outlet:

If the temperature gradient (dT/dz) $> .01^\circ\text{C}/\text{m}$ at the outlet elevation, the withdrawal layer thickness (δ) is calculated using either the KOH equation or the KAO equation.

KAO equation:

$$\delta = 4.8 \left[\frac{q^2}{g \cdot \epsilon} \right]^{1/4}$$

where

q = outflow rate per unit width

g = gravitational constant (m/day^2)

ϵ = normalized density gradient $= 1/\rho (d\rho/dz)$

ϵ is derived by using the chain rule, $\frac{d\rho}{dz} = \left(\frac{d\rho}{dT}\right) \left(\frac{dT}{dz}\right)$, for temperatures in the range $4^\circ\text{C} - 26^\circ\text{C}$ and produces a least squares fit to Figure 3.1 [Markofsky, 1971] which results in $\rho = 1.0 - 6.63 \times 10^{-6}(T-4)^2$. Thus

$$\epsilon = \frac{1}{\rho} \left(\frac{d\rho}{dT}\right) \left(\frac{dT}{dz}\right) = \frac{2(T-4)}{151000 - (T-4)^2} \frac{dT}{dz} (\text{cm}^{-1})$$

Solving for half the withdrawal thickness in this formulation and using the gravitational constant of $7.315 \times 10^{10} \text{ m/day}^2$, requires the input of a constant $\text{DELCON} = .005$.

KOH equation:

$$\delta = \frac{7.14 (x)^{1/3}}{\left[\frac{\epsilon g}{D \nabla} \right]^{1/6}}$$

2. Temperature gradient at the outlet ($< .01^\circ\text{C/m}$):

The withdrawal layer is calculated based on a cutoff gradient of $.05^\circ\text{C/m}$ (thermocline) and will again center the withdrawal layer about the outlet. Under isothermal conditions, the withdrawal layer thickness is the full depth of the water column. The thickness is also bound by a minimum value in this case, of two grid layers ($\cong 4$ meters).

Whichever condition is used to determine the withdrawal thickness, the outflow standard deviation is then found by using the half withdrawal thickness ($\delta/2$) as defined by:

$$\sigma_o = \frac{\delta/2}{\text{SPREAD}}$$

where

SPREAD = specified input as the number of standard deviations to capture a desired percent of the outflow water within the withdrawal layer.

Since the outflow is assumed to be a Gaussian distribution about the outlet, varying the number of standard deviations in the withdrawal layer will determine the

amount of flow contained within this layer as shown in Figure 3.6 . For example, if it is desired that 68% of the outflow comes from the withdrawal layer, then with $\text{SPREAD} = 1.0$ it infers that $\pm 1.0\sigma_o$ will be captured within the layer boundaries. For most applications, $\text{SPREAD} = 1.96$ and 95% of the outflow from within the withdrawal layer is assumed.

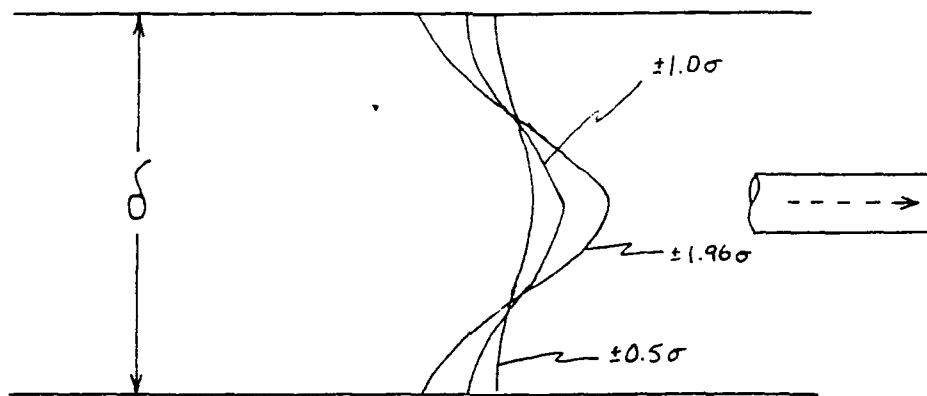


Figure 3.6 Effect of varying the number of outflow standard deviations contained within the withdrawal layer (parameter SPREAD).

As with inflow, the outflow velocity distribution is computed by:

$$u_o = u(t)_o \max \exp \left[\frac{-(z - z_o)^2}{2\sigma_o^2} \right]$$

where

σ_o = outflow standard deviation

z_o = elevation of outlet centerline

and

$u(t)_{o \max}$ = maximum outflow velocity

$$u(t)_{o \max} = \frac{Q_o}{\int_0^{h_o} \exp \left[\frac{-[z - (t)_o]^2}{2 \sigma_o^2} \right] B \, dz}$$

Truncation of the velocity distribution occurs at boundary surfaces and for multiple outlet elevations the outflow velocities are superimposed on one another. Total outflow velocity (u_{ot}) for each layer is then the sum of the outflow velocity to the intake (u_o) and that due to entrance mixing (u_{om}) (from Section 3.4.1):

$$u_{ot} = u_o + u_{om}$$

3.4.3 Computation of Diffusivity

There are four options available in the model to compute diffusivity:

- I. Molecular diffusion α_o , (constant)
- II. Turbulent diffusion $\alpha_z(z)$, dependent on stability (depth)
- III. Turbulent diffusion $\alpha_z(t)$, dependent on wind (independent of depth)
- IV. Turbulent diffusion $\alpha_z(z,t)$, dependent on stability (depth) and wind (temporally variable)

Distinctions between the options are provided.

Option I: α_o

Diffusivity is a constant at all depths for all time.

Option II: $\alpha_z(z)$

This option uses molecular diffusion as a minimum value and calculates the "effective diffusion" as a function of the local water column stability factor S_L defined by:

$$\alpha(z) = \frac{\alpha_o}{S_L(z)}$$

where

$$S_L(z) = \frac{H_S}{\Delta\rho} \frac{d\rho}{dz}$$

and

H_S = maximum depth of reservoir

$\Delta\rho$ = difference between the maximum and minimum density

Depth dependency states that the diffusivity is inversely proportional to a local stability factor which takes into account density differences between two adjacent layers, thereby calculating a local "effective diffusivity" which will vary with depth. A strong stratification (thermocline) infers a large stability factor, reducing the effective diffusivity. Alternatively, in regions where temperatures (and densities) are uniform, S_L will be small, resulting in a large effective diffusivity. Local diffusion rates can vary in the range from molecular (.0124 m²/day) to 8.64 m²/day depending on the density differences between layers. The cap used on the vertical diffusivity is the same maximum value observed in field studies by Imboden and Emerson (1978).

Option III: $\alpha_z(t)$

Time-varying diffusivity is calculated as directly proportional to the power input by the wind as derived by Aldama et al. (1988) and is composed of the sum of both

molecular diffusion (α_o) and a turbulent eddy diffusivity (α_t):

$$\alpha_z = \alpha_o + \alpha_t$$

and

$$\alpha_t = C_\alpha \rho_o \frac{u_*^3 A_s H_s^2}{P_s}$$

where

C_α = dimensionless parameter which depends on basin shape and stratification

u_* = water friction velocity at free surface

ρ_o = density of water at 4°

H_s = maximum depth of reservoir

A_s = surface area of reservoir

and

P_s is the depth averaged potential energy of stratification as defined by:

$$P_s = \int_0^{H_s} (\bar{\rho} - \rho) g A z dz$$

where

$\bar{\rho}$ = the volumetric mean density of the water in the reservoir

A = surface area of control volume at elevation z

z = elevation of control volume under evaluation

g = acceleration due to gravity (9.8 m/s²)

The potential energy of stratification is a function of the area as it varies with depth $A(z)$, and the volumetric mean density of the water in the reservoir. As such, it will be very much influenced by basin morphology. For instance, given two basins as shown in Figures 3.7a and 3.7b, with identical depth, surface area, and stratification profile, but different volume developments (actual volume/volume of cone with same surface area and depth), the potential energy of stratification will be larger for the more bowl-shaped basin (Figure 3.7b). So all other factors being constant ($A(z), H_s, C_{\alpha}, u_*$), the morphology can influence the magnitude of the diffusivity.

As the water column reaches isothermal conditions ($\Delta\rho \rightarrow 0$), $P_s \rightarrow 0$ and $\alpha_t \rightarrow \infty$. Thus, the diffusivity is capped at a maximum value determined from tracer tests in the field [Imboden and Emerson, 1978], resulting in a range from molecular (.0124 m^2/day) to a maximum of 8.64 m^2/day .

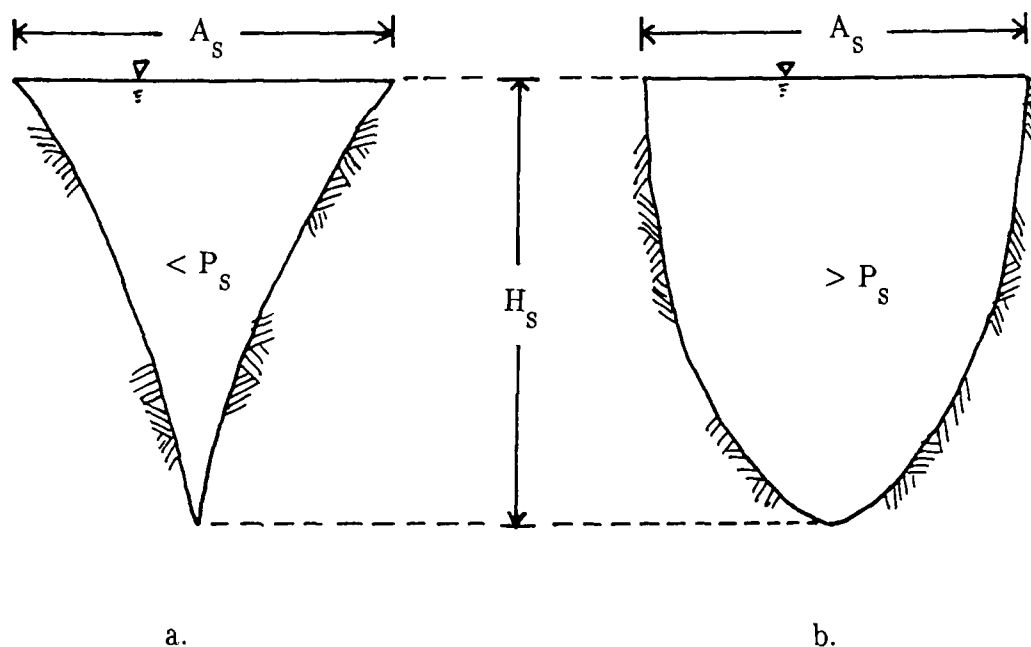


Figure 3.7 Relative effect of basin morphology on potential energy of stratification.

The water friction velocity (u_*) is computed from the shear stress imparted to the water surface (τ_o) by the wind, where:

$$\tau_o = \rho_a C_d W^2 = \rho_o u_*^2$$

where

τ_o = surface shear stress due to wind

ρ_a = density of air

W = wind velocity

C_d = drag coefficient at water surface

with assigned values:

.0005 for $W < 1$ m/s
 .0012 for $W < 3$ m/s
 .0026 for $W > 12$ m/s

so that

$$u_* = \tau_o / \rho_o^{\frac{1}{2}}$$

Option IV: $\alpha_z(z,t)$

With this option the diffusivity is calculated as in Option III; however local stability is accounted for as in Option II and the effective diffusion is calculated as a function of depth. Limits to the values result in a range at any particular level from molecular to 8.64 m²/day (as in Options II and III).

3.4.4 Numerical Stability Criteria

Due to the explicit scheme used in the model, numerical stability must be met with regard to two conditions:

$$1. \quad E_z \frac{\Delta t}{(\Delta z)^2} < \frac{1}{2}$$

$$2. \quad \frac{Q_v}{A(z)} \frac{\Delta t}{\Delta z} < 1$$

where

E_z = vertical eddy diffusivity

$Q_v/A(z)$ = vertical velocity

For Condition 2 above, the constraint prevents the outflow from removing all the water from a given layer during one time step. This can be evaluated by Figure 3.8 where a control volume is depicted with outflow Q_o and inflow Q_{in} at the top surface. Evaluating the control volume, the constraint states:

$$\frac{Q_v(\Delta t)}{A(z)(\Delta z)} < 1.0$$

where

$A(z)(\Delta z)$ = Volume

then

$$\Delta t \leq \frac{\text{Volume}}{Q_v} \leq \text{Detention time}$$

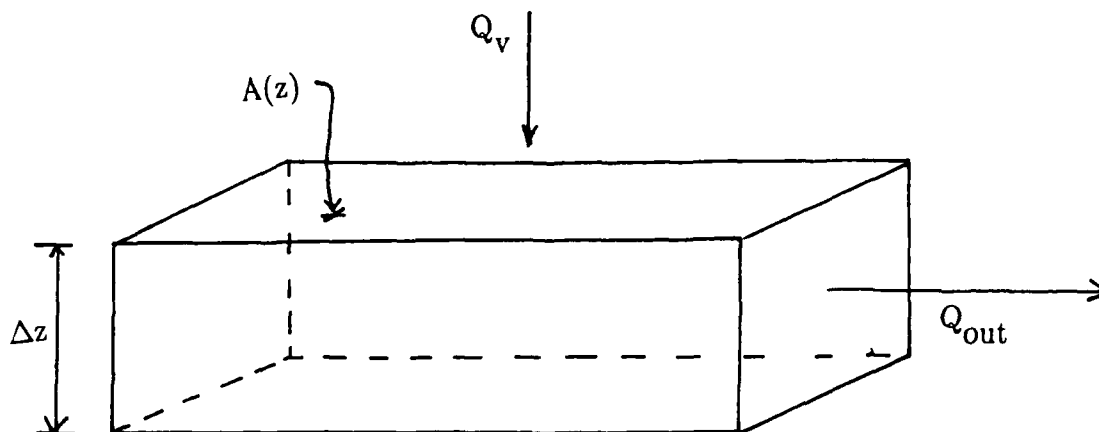


Figure 3.8 Evaluation of control volume with regard to maintaining numerical stability.

As stated, the time step must be smaller than the detention time to avoid emptying the control volume. If the conditions are not met, the time step will be automatically sub-divided until stability requirements are met.

3.4.5 Wind Effects on Mixing in the Epilimnion

The depth of the mixed layer is dependent on the energy available for mixing as well as the degree of stratification. The most prominent source of energy in lakes and reservoirs is that of the wind, referred to as turbulent kinetic energy (TKE). Another source of energy is from turbulence generated due to buoyancy fluxes. Turbulence generated in the epilimnion will generate shear forces at the thermocline which tend to entrain hypolimnetic water. This process satisfies the principle discussed in Section 3.1 whereby the water column stores potential energy in the form of a deeper mixed layer.

The rate of increase in the depth of the mixed layer (dh/dt) is referred to as the entrainment velocity and can be related to the change of potential energy or the amount of TKE which goes into a "storage" term given by Zeman and Tennekes (1977) as:

$$\frac{dk}{dt} = C_t \frac{\sigma^2}{h} \frac{dh}{dt}$$

where

$\frac{dk}{dt}$ = rate of conversion to potential energy

C_t = empirical parameter

h = depth of mixed layer

σ = turbulent velocity scale which combines effects of wind and buoyancy generated turbulence and is defined as:

$$\sigma = \frac{(C_w u_*^3 + CCON w_*^3)^{1/3}}{C_c}$$

where:

u_* = water friction velocity due to wind shear

w_* = buoyancy scale as defined by Zenman and Tennekes (1977)

C_c = efficiency of converting input energy to TKE

C_w = wind mixing coefficient specified as input

$CCON$ = penetrative convective mixing coefficient specified as input

Aldama et al. (1988) calibrated the coefficients C_w and $CCON$ for Lake Valencia and determined $C_w = 4.0$ and $CCON = .5$. These same values were used for the Wachusett model.

If the total power input is defined by:

$$\frac{dE}{dt} = \rho_o \sigma^3 A_s$$

where

ρ_o = reference density

A_s = surface area of reservoir

then the power available can be compared to the required energy of mixing to calculate the depth over which mixing will occur. Of course, not all the TKE is converted to potential energy but will be dissipated by viscosity or radiated through the generation of internal waves. This is termed *energy leakage* and is proportional to the magnitude of the gradient through:

$$\epsilon_{iw} = C_D a^2 N^3$$

where

ϵ_{iw} = leakage of energy to internal waves

a = characteristic amplitude of interface deflection

N = Brunt-Vaisala frequency

C_D = empirical parameter

With these terms defined, final derivation of the entrainment law is provided by Aldama et al. (1988) which states:

$$\frac{dh}{dt} = \frac{1 - C_D' R_s}{C_T' + R_i}$$

where

R_i = bulk Richardson number

R_s = dimensionless number

C'_D, C'_T = entrainment coefficients specified as input

Values used by Aldama et al. (1988) in the Lake Valencia model were $C'_D = 0.4$ and $C'_T = 5.6$. These same values were used for the Wachusett model.

The Richardson number describes whether available kinetic energy will overcome stratification forces to produce turbulent mixing. When R_i is large, the flow is relatively stable and a small amount of mixing will take place. For small values of R_i , density differences are overcome by kinetic energy and turbulent mixing occurs. Thus, the available energy imparted by the wind at the water surface either will be dissipated or will contribute toward mixing the epilimnion (or a fraction thereof) as well as the entrainment of deeper water at the thermocline.

Chapter 4 Calibration and Verification

The first step after having described the thermal processes in terms of a mathematical model is to use data collected in the field to calibrate the model parameters. This is an iterative process whereby the coefficients of parameters (e.g., entrance mixing, wind mixing, withdrawal layer thickness, and diffusion) are determined. These values are site specific, very often dependent on the morphology, and can be adjusted until they yield results that closely represent field measurements. Once the agreement is made, the model is considered calibrated.

The unchanged parameter values from the calibration are then applied to another data set with the expectation of producing results that are representative of that year's measured values. If the results are again favorable, the model is said to be verified. This gives some assurance that applications to other years will produce reasonably accurate results when there are *no* measured profiles for comparison.

4.1 Presentation of Input Data

Data was compiled from the MDC, the MWRA, and the National Oceanic and Atmospheric Administration (NOAA). Availability of consistent data (same parameters, same method of measurement) from year to year is important if trends and relative comparisons are to be made.

In addition to the physical basin schematization (which probably will not change from year to year), data for daily changing events such as air temperatures, wind velocity, humidity, cloud cover, and solar radiation as well as the inflows, outflows, Secchi disc, and the elevation of outflows, is required. Because the goal is to capture the long term (seasonal) dynamics of the reservoir, a time step of one day was used.

This way, daily averaged variability can be captured by simulations generated for any selected day throughout the modeling period.

4.1.1 Schematization of Basin

The actual basin morphology described in Chapter 1 must be generalized into a discretized form that represents the basin without sacrificing accuracy. In other words, generalization should not exclude information that will have a significant impact on the results, yet it should reduce computation time and improve manageability of the data as much as possible. Since the model chosen solves the continuity and conservation of energy equation in vertical direction only, then the schematization should represent a length- and width- averaged basin.

The Wachusett Reservoir finite difference schematization for computation of heat and mass fluxes is a one-dimensional grid with 18 layers and Δz equal to 2 meters. Each layer, as shown in Figure 4.1a, is considered a control volume which must obey the conservation of heat and mass. For a reservoir of this depth, a 2 meter node spacing is probably about the maximum that should be used to sufficiently reflect the dynamics of the hydrothermal processes. The closer the spacing the more refined the simulation output. However, the trade-off is the additional computer time required to perform the repetitive calculations on each additional layer.

The volume is discretized by length-area data at an interval of 1.52 m (5 feet) as shown in Figure 4.1b. Note that the initial length and area equal zero, .1 m below the bottom discretization in 4.1a. This is to satisfy computational requirements where $A(1)$ must have a positive value other than zero at the reservoir bottom (87 m) when transposed to the finite difference grid. (See Section 3.3.2 for further explanation.) The maximum length was measured from the causeway (Station 3410, Figure 1.3) to the dam face. For modeling purposes, the reservoir begins at the

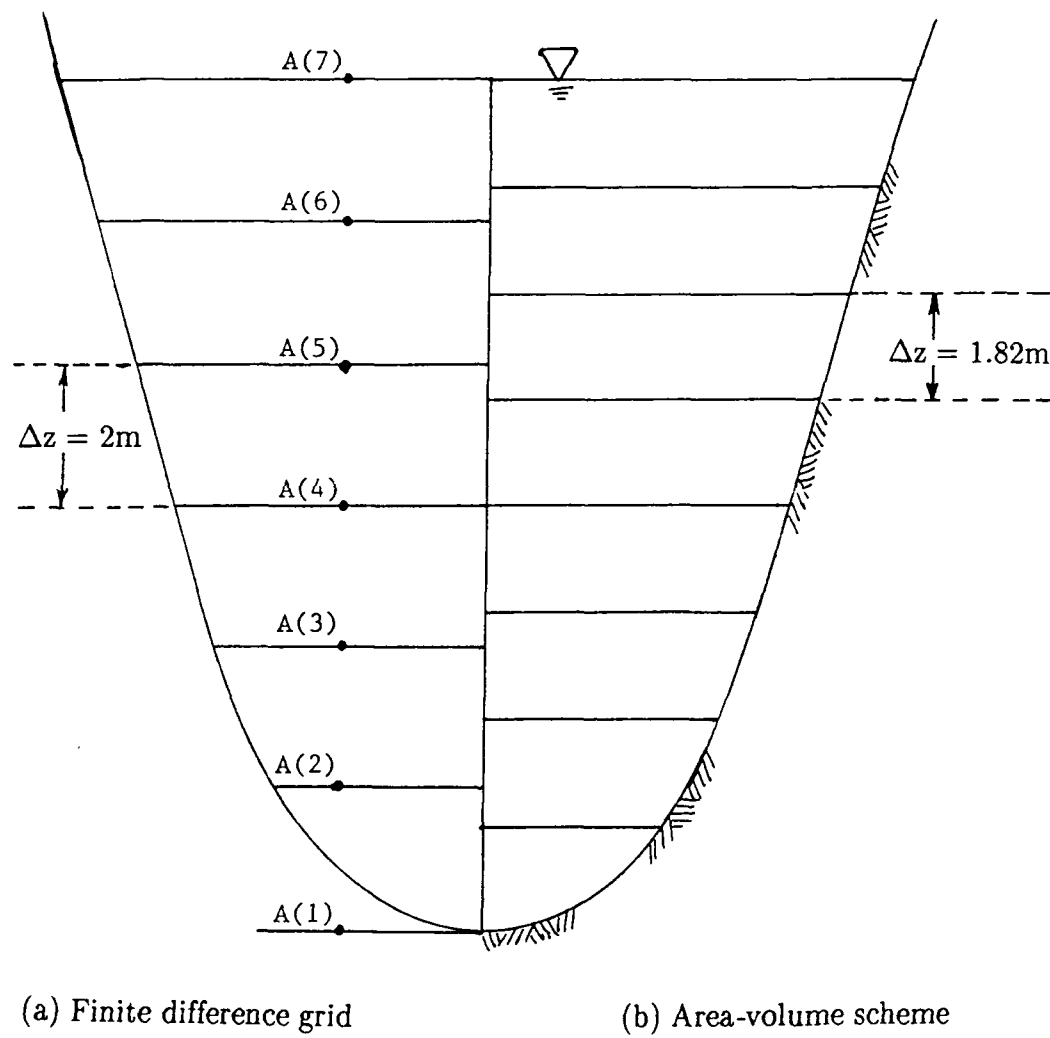


Figure 4.1 Superposition of area-volume schematization on the finite difference.

causeway since all tributary inflows upstream from this point must pass through a 50 ft wide constriction, which best represents a single point source.

The maximum reservoir depth used for model schematization is 33 meters (110 feet) measured from a maximum surface elevation (top of dam) of 120 meters (395 feet). All elevations in this study are referenced to Boston City base, which is 5.65 feet lower than the 1929 USGS datum used in topo mapping. This depth is consistent with the MDC depth-volume tables as well as maximum sampling depths (Station 3417), but is somewhat less than the maximum depth at the dam face.

4.1.2 Climatological Data

Climatological data (air temperatures, wind velocity, humidity, cloud cover, and solar radiation) as well as inflows, outflows and surface elevation of the reservoir for 1987 and 1988 are shown graphically in Figures 4.2 thru 4.8 . The source of the climatological data is the NOAA station located at the Worcester Municipal Airport, which is approximately ten miles south of the reservoir and almost 700 feet higher in elevation. Despite this variation in topography, no alterations have been made to the data in either the calibration or the verification of the model. All data input represents daily averaged values.

Short wave solar radiation either can be measured by pyrheliometer or calculated from clear sky solar radiation by an empirical formula:

$$\begin{aligned}\phi_{sn} &= \phi_{sc}(1 - RF)(1 - .65 CLC^2) \\ &= .94 \phi_{sc} (1 - .65 CLC^2)\end{aligned}$$

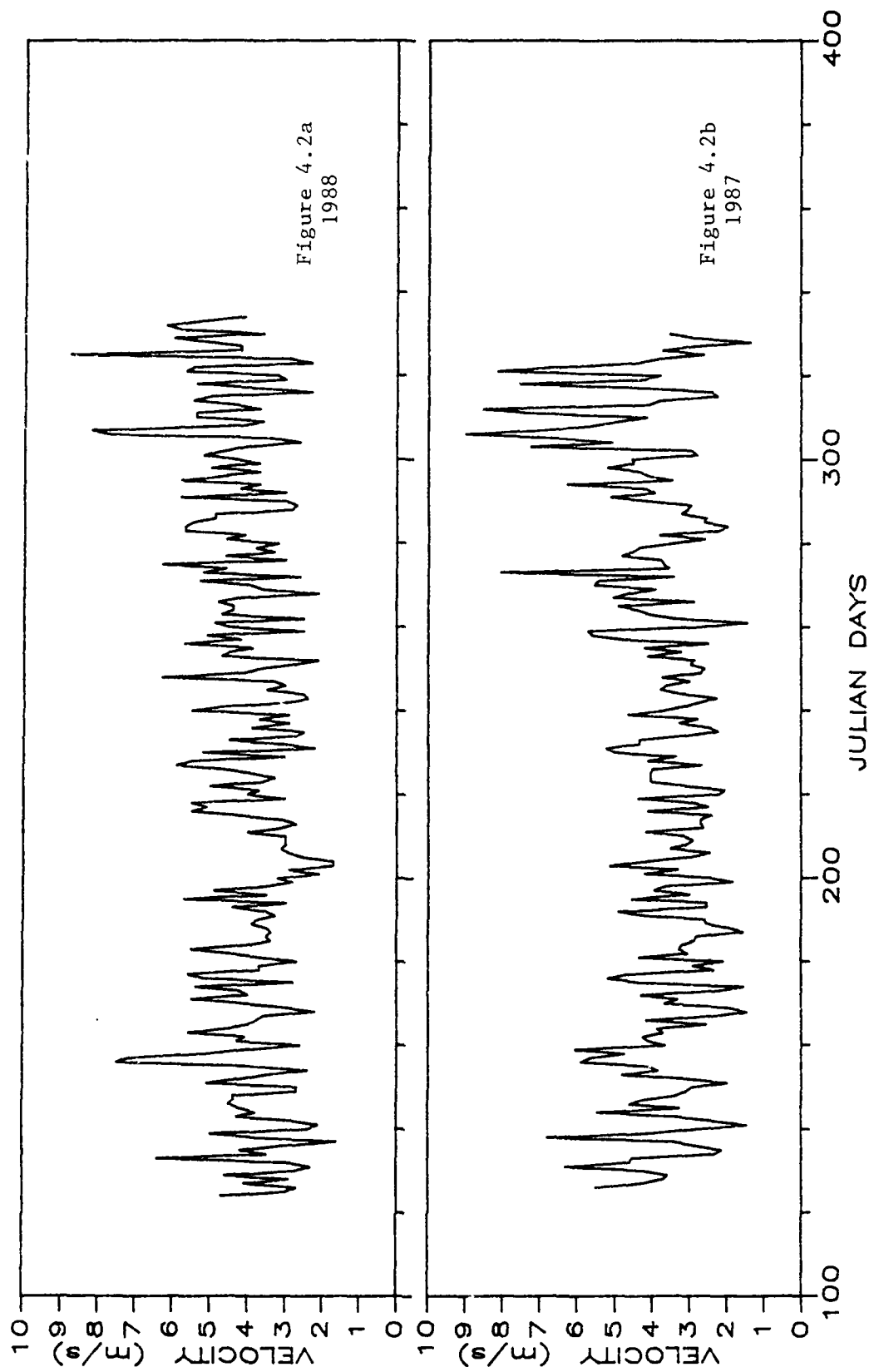


Figure 4.2 Wind velocity for Wachusett Reservoir (daily averaged).

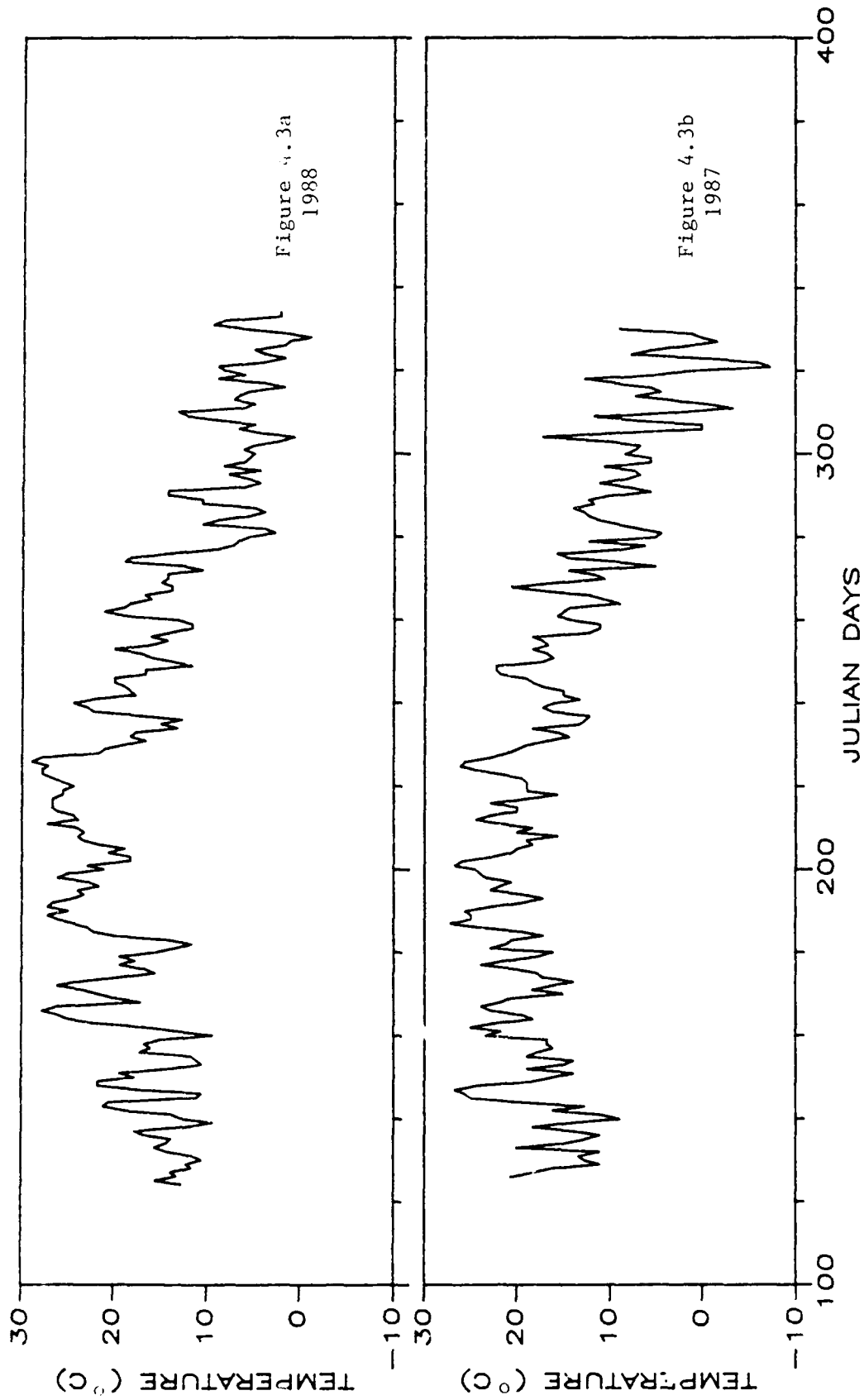


Figure 4.3 Air temperature for Wachusett Reservoir (daily averaged).

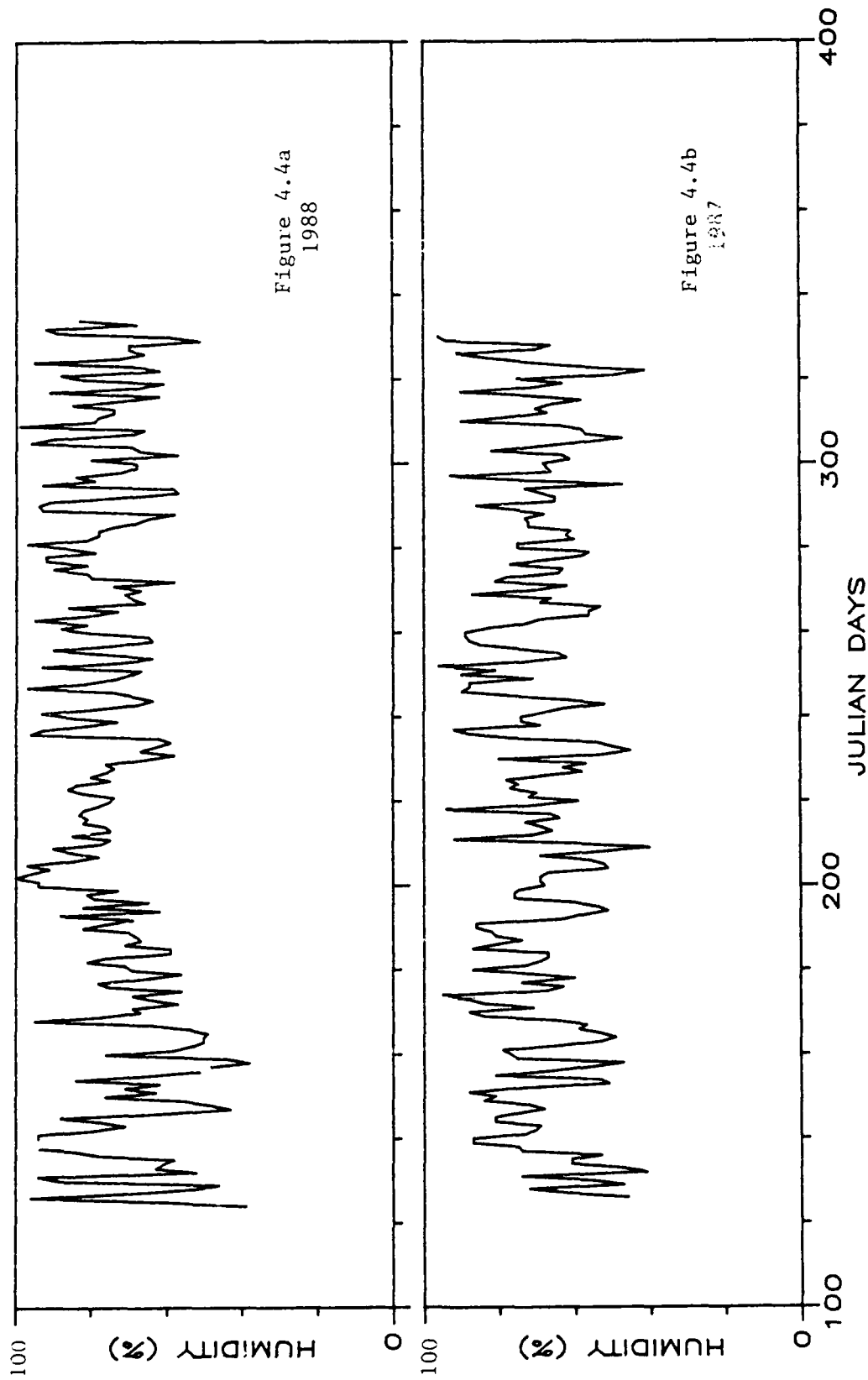


Figure 4.4 Humidity for Wachusett Reservoir (daily averaged).

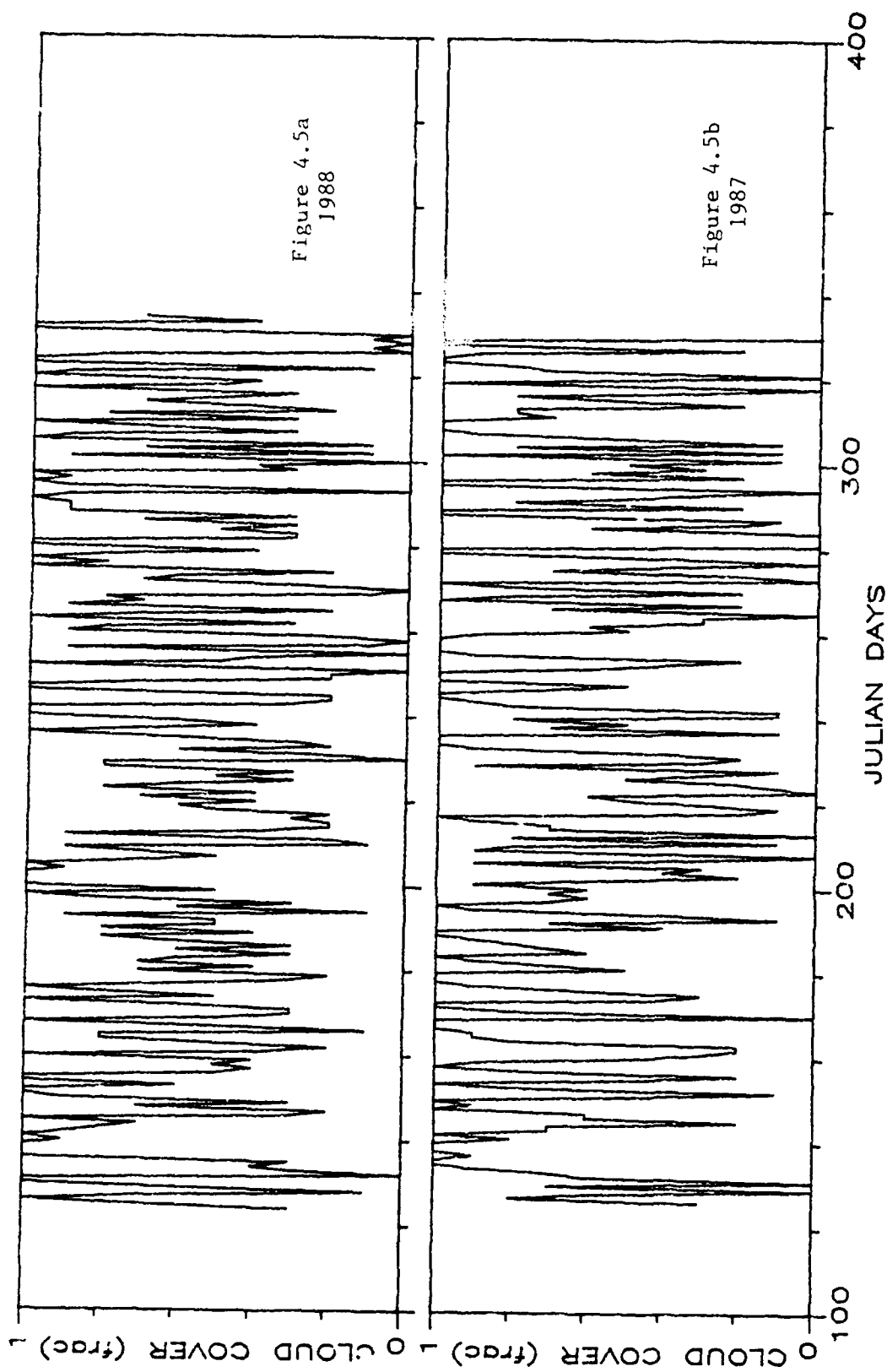


Figure 4.5 Cloud cover for Wachusett Reservoir (daily averaged).

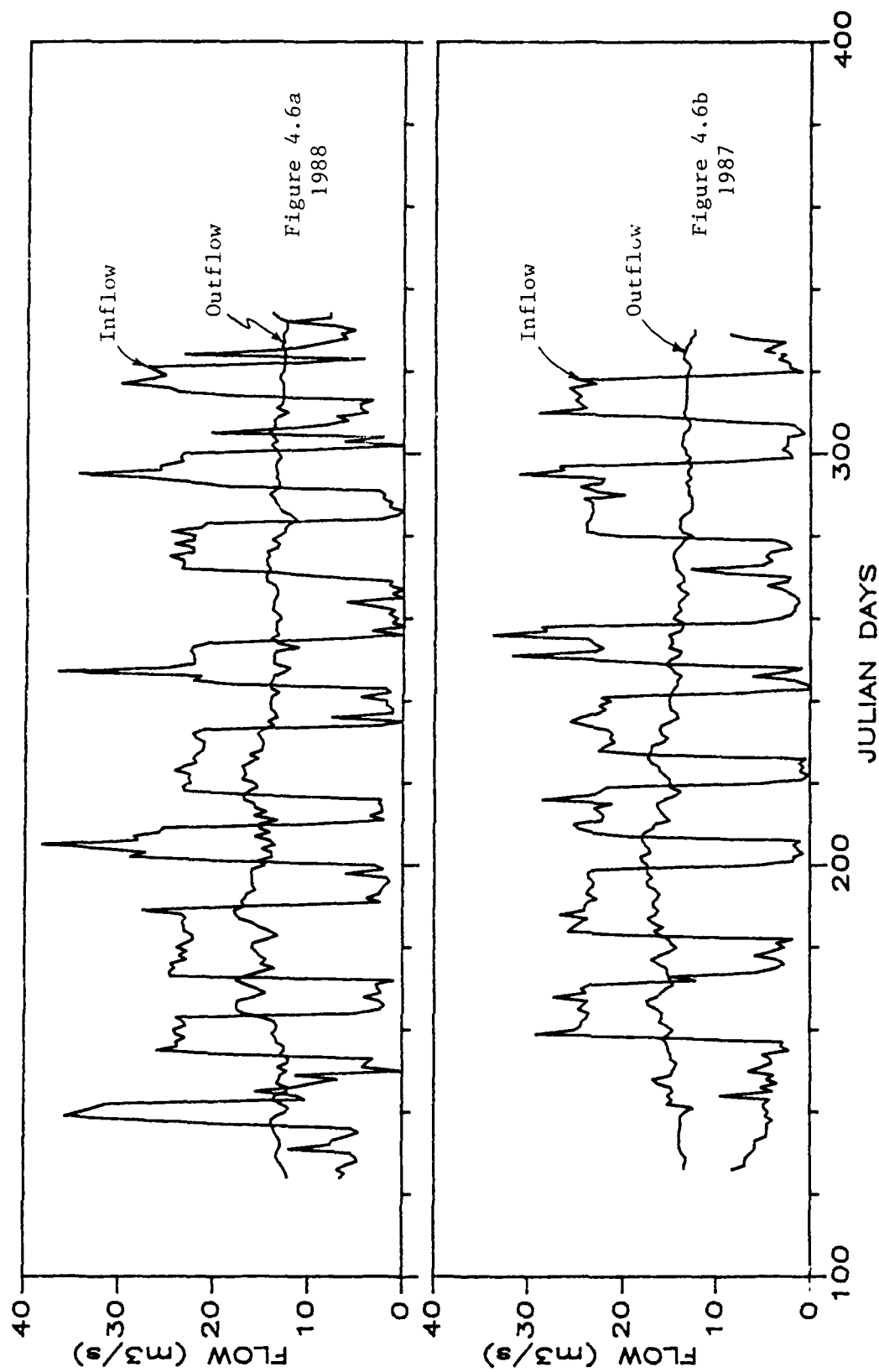


Figure 4.6 Reservoir inflows and outflows.

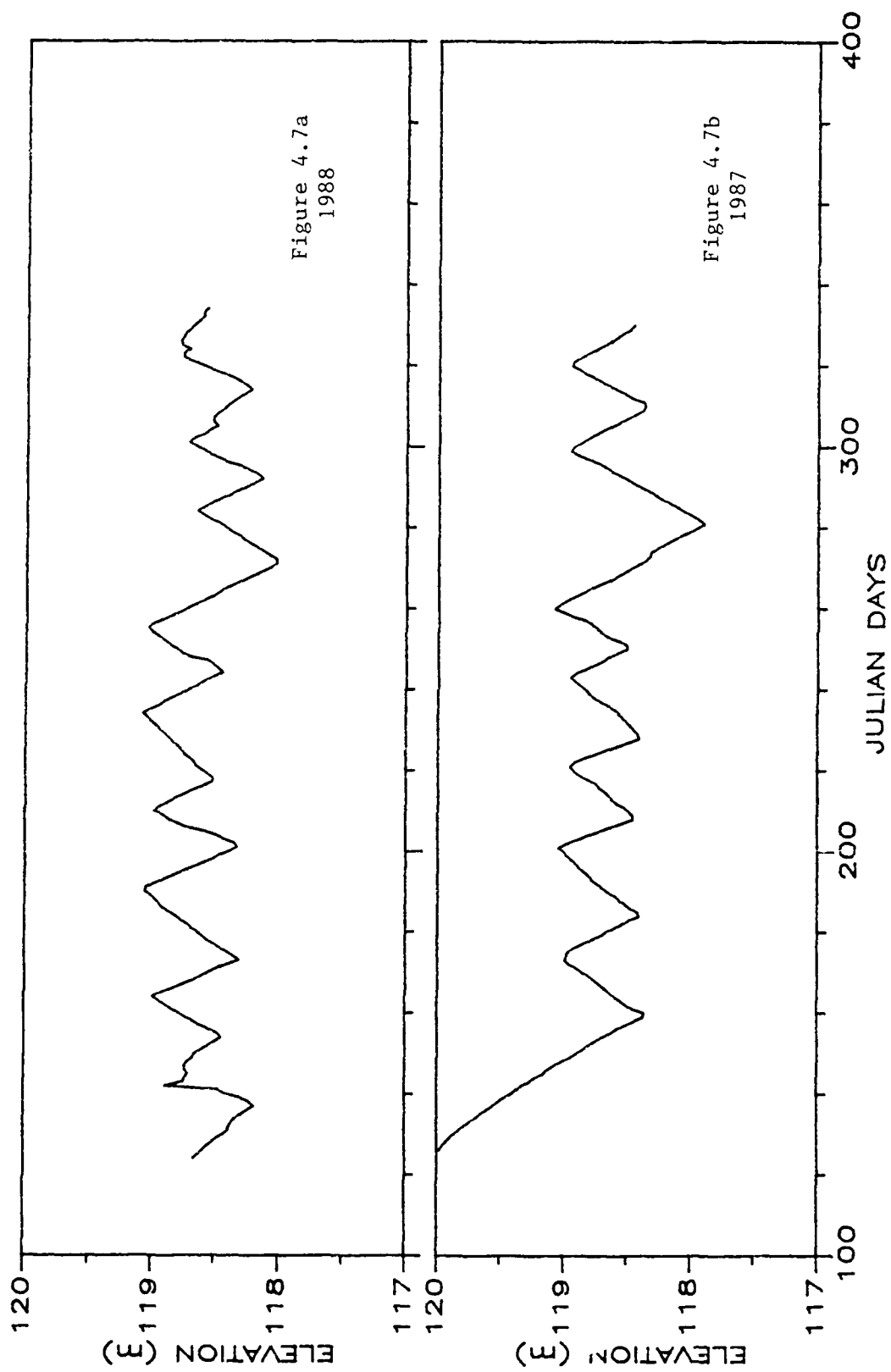


Figure 4.7 Surface elevations (measured).

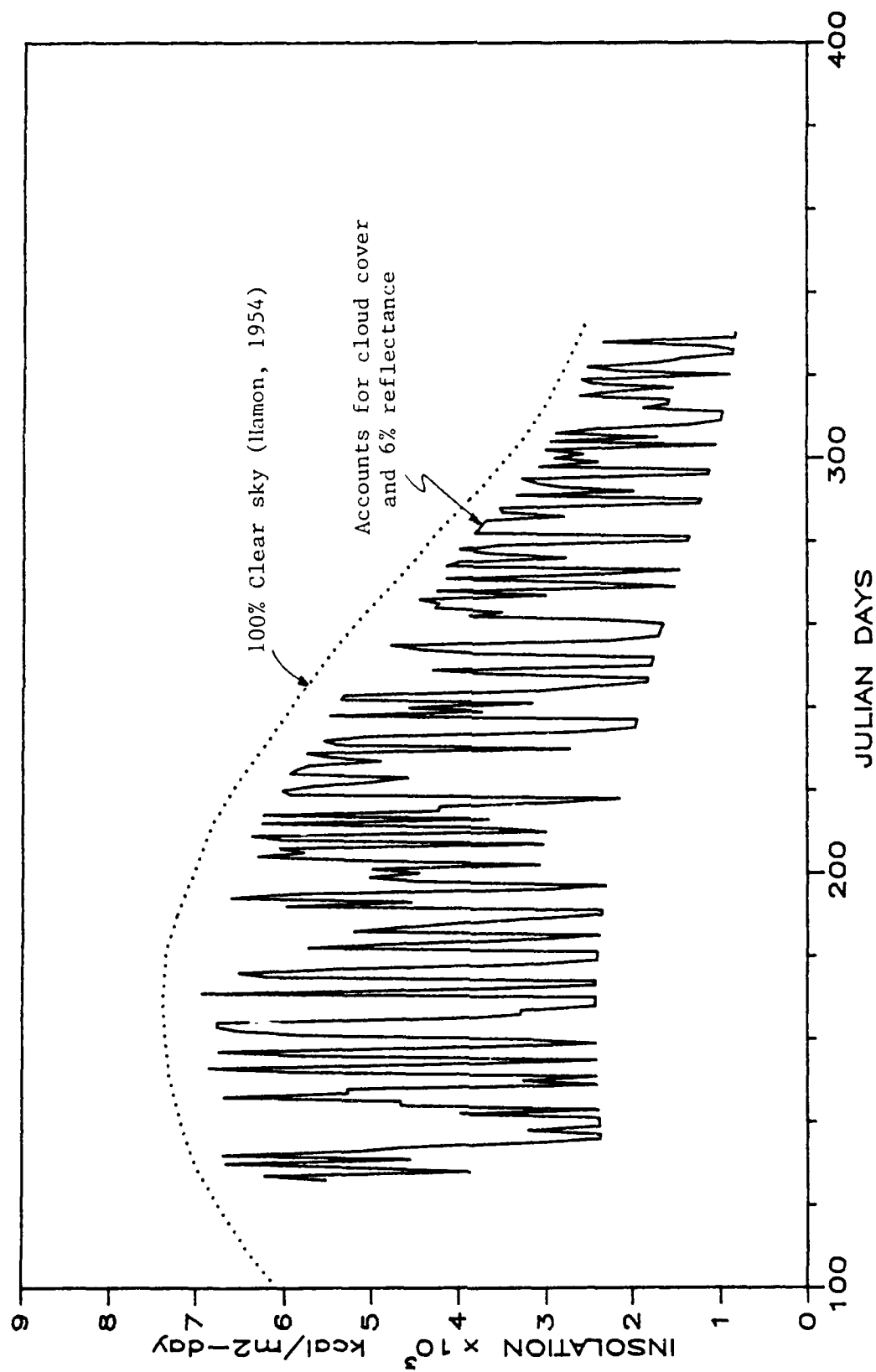


Figure 4.8 Short wave solar insolation 1987.

where

ϕ_{sn} = net solar radiation absorbed at water surface [Ryan and Harleman, 1973]

ϕ_{sc} = 100% clear sky solar radiation

CLC = cloud cover as a fraction of clear sky

RF = percent reflected at water surface

The clear sky radiation was interpolated from a 100% sunshine curve based on field measurements from 20 stations nationwide [Hamon et al., 1954]. This curve is shown as the dotted line in Figure 4.8 and represents daily averaged clear sky radiation for a latitude of 42° N. The lower curve is the net solar radiation entering the water after accounting for the amount reflected from the water surface and subtracting that lost due to the cloud cover.

Since the reflected solar radiation from the water surface is a function of the sun's angle in the sky, it not only changes throughout the day, but from month to month as well. Field studies on Lake Hefner have shown that 6% reflectance is a good annually averaged value [Ryan and Harleman, 1973]; therefore, it was used in this study as well. Thus, as Figure 4.8 illustrates, even with zero cloud cover the maximum energy available at the water surface is 94% of the incident clear sky value.

4.1.3 Inflow, Outflow, and Surface Elevations

A composite of major inflows to the Wachusett Reservoir is shown in Table 4.1. Since the three biggest sources comprise over 85% of the total inflow and they all enter the reservoir at the western end, it is appropriate to combine total inflows into one (with regard to volume and temperature of inflow). Similarly, the components of reservoir losses are shown in Table 4.2.

TABLE 4.1
 Annually Averaged Reservoir Inputs for 1987
 (taken from [CDM, 1989])

<u>Source</u>	<u>Rate (mgd)</u>	<u>Percent of total</u>
Quabbin Aqueduct (MDC meas.)	213	63
Quisapoxet River*	50	15
Stillwater River*	32	9
Other small tributaries*	32	9
Direct precipitation	<u>14</u>	<u>4</u>
TOTAL	341	100%

*from USGS runoff data

TABLE 4.2
 Annually Averaged Reservoir Losses for 1987
 (Compiled from records at MDC and CDM [1989])

<u>Outflow</u>	<u>Rate (mgd)</u>	<u>Percent of total</u>
Water supply (MDC meas.)	309	90
Dam outlet works/Spillway (MDC meas.)	27	8
Evaporation*	8	2
Groundwater (Est.)	<u><1</u>	<u><1</u>
TOTAL	345	100%

*CDM reported value of 8 mgd is estimated from regional weather data, US Weather Bureau, and evaporation data from Lake Massabesic, NH. MITEMP Model estimation of evaporative losses through calculation of evaporative heat flux as part of a total heat balance is 3.4 mgd for the period May 6 – Nov. 20, 1987.

Due to the high percent of outflow contained in the water supply (Cosgrove Aqueduct), all outflows were combined in order to simplify computations. Should other outflows become significant (such as periods of spillway flow), then the rate of outflow should be split and modeled at different levels. Multiple outflows at different elevations will have a significant impact on the hydrodynamics of the water column.

Evaporative water losses as estimated by CDM on Table 4.2 were extrapolated from field testing at Lake Massabesic in New Hampshire. More accuracy in the water balance would be obtained through calculations of a total heat balance with evaporative heat losses modelled. MITEMP calculates daily averaged evaporative heat flux through the water surface. Conversion of net evaporative heat flux ($\text{kcal/m}^2/\text{day}$) when multiplied by the latent heat of evaporation yielded a rate of water evaporation equal to 3.4 mgd for the 200 day simulation period. Since the simulated water temperatures are in close agreement with the measured values (see Figure 4.12), this would suggest accurate estimations of water loss through evaporation.

Inflow temperatures are needed as input data for the model, but measurements at the confluence of the Quabbin Aqueduct are not available. Hence, temperatures from Quabbin Reservoir were extrapolated to Wachusett Reservoir. Temperature measurements taken at intake depth in Quabbin for 1987 and 1988 are shown in Figure 4.9. Daily averaged inflow temperatures were interpolated from this data. These temperatures are assumed to be representative of the inflow temperatures at Wachusett due to the short residence time in the aqueduct. The aqueduct from the Quabbin reservoir is approximately 23 miles long and the residence time is calculated to be approximately 6 hours before discharge into the Wachusett Reservoir.

The inflow gates can remain closed for several days at a time should water not be needed from Quabbin. This would have the effect of increasing the residence time in the shaft and allowing the temperature to approach a mean subterranean

temperature, which is probably about 13°C (55°F). Corrections for this were not made. The sensitivity of up to several degrees for the inflow proved to be minor.

The spring of 1987 was extremely wet, with water surface elevations higher than normal, and water was discharged to the Nashua River via the spillway and dam control outlets for the period April 5-29, 1987. Field monitoring of the reservoir did not start until May 6, 1987, so that major effects of the high flows should have subsided by this time, with the onset of stratification developing normally. The year 1988, on the other hand, was generally warmer and drier; reflected in the slight drop of the surface elevation operating range and the greater outflows due to increased demand (see Figure 4.7.b). All surface elevation values used in the model are calculated by a mass balance of inflows and outflows. Actual measured values are used for comparison only. The comparison of calculated values and measured values for 1988 are shown in Figure 4.10.

For the calibration and verification of the model, an elevation of 111 meters (364 feet) was used for the level of the intake (see Figure 1.4). Currently, records are not maintained indicating which intake level is used and at what times they are switched. Intake usage is switched for maintenance, cleaning of the mesh screens, water quality considerations (high algal counts detected at intake depth), or the build-up of frazil ice on the mesh screens. The model sensitivity to changing the intake elevation is considerable and is discussed in Section 4.4.1, with the impact on temperature profiles illustrated in Figure 4.16 .

4.1.4 Diffusivity and Extinction Coefficient

A turbulent diffusivity, which is dependent on local stability was used in both the calibration and verification of the model (Option II, Section 3.4.3). The minimum value was specified at 10x molecular diffusion ($.124 \text{ m}^2/\text{day}$) while the maximum was

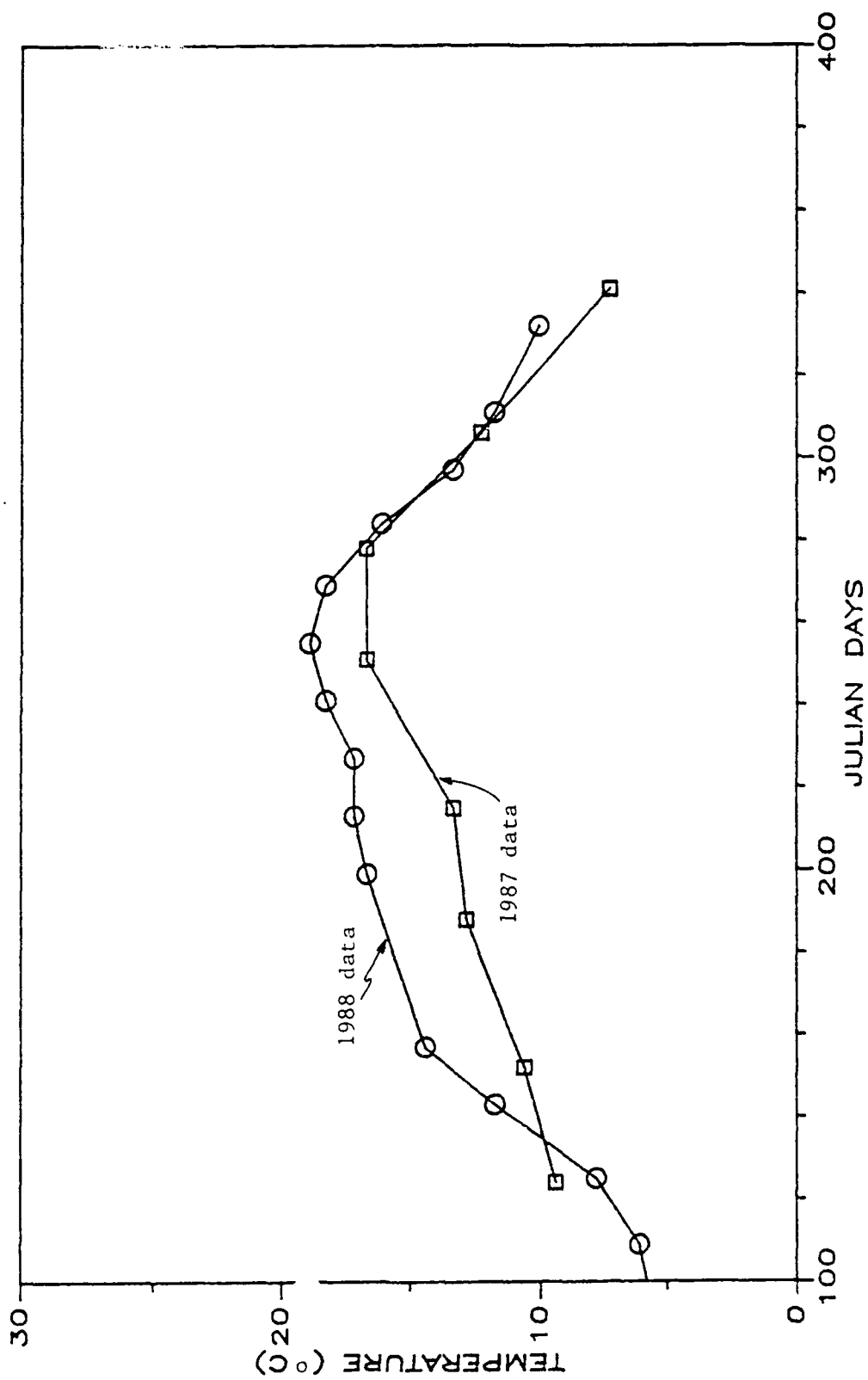


Figure 4.9 Water temperatures at intake depth at Quabbin Reservoir.

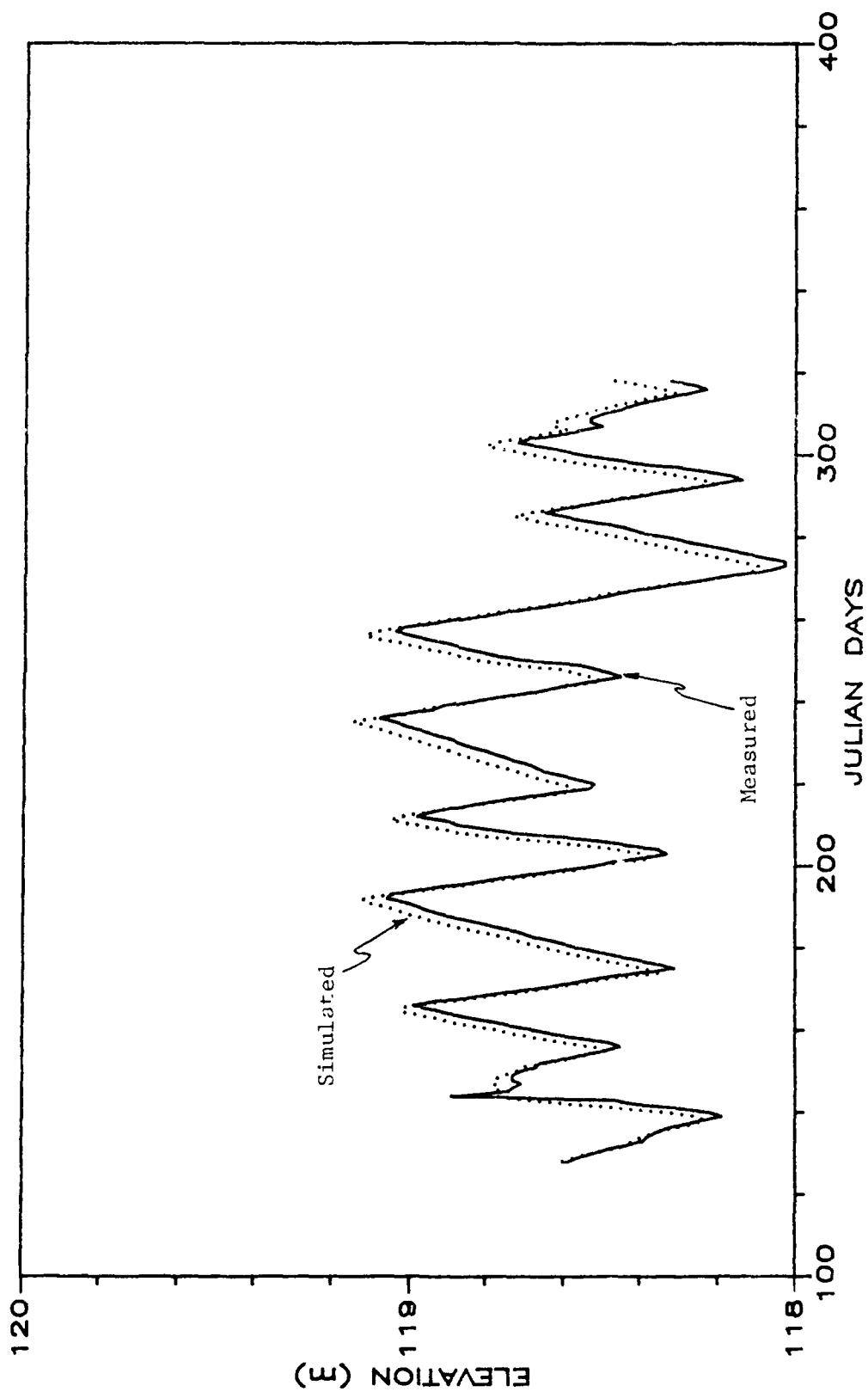


Figure 4.10 Water surface elevation; measured vs. calculated.

capped at 8.64 m²/day. This maximum diffusivity is consistent with field measurements by Imboden and Emerson (1978) using tracers. Other combinations of wind dependent and depth dependent diffusivities were tried and comparative results are described in Section 4.4.2. The depth dependent stability has the effect of increasing mixing when densities are uniform (e.g., in the mixed layer and hypolimnion) and inhibits the transport of heat when a strong density gradient exists, such as at the thermocline.

The extinction coefficient of solar radiation in water was calculated from measured Secchi disc readings throughout the reservoir. Generally, the Secchi readings ranged from 4 meters to 7 meters, which converts to an extinction coefficient of between .25 and .42 throughout the simulation period as given by:

$$\eta = \frac{1.7}{SD}$$

where SD = Secchi disc depth (m)

Vertical flow velocity data is not measured, thus values of velocity are not explicitly considered in the simulation results. Since the hydrothermal processes are coupled to the velocity velocity, an accurate simulation of the velocity is implied if the temperatures are accurately predicted.

4.2 Calibration of the Hydrothermal Model

The model was calibrated with 1987 data using the measured temperature profile on May 6 as an initial isothermal condition. The model was run through the end of November (200 time steps). The results are shown in Figure 4.11 . The values used for all model parameters are shown in Table 4.3, and those which were calibrated in Table 4.4 .

The dynamics of the hydrothermal processes are well represented in the results. Although the development of the upper mixed layer (epilimnion) was slightly behind the observed temperatures in May and June, by July the total heat content and the corresponding stratification were in agreement. In August and September erosion of the epilimnion began as a result of a net heat loss through the surface, causing instabilities of cooler, denser water on top of warmer, less dense water. These instabilities result in greater convective mixing in the epilimnion. The model overestimated the depth of the mixed layer in August and September but was on target by October, returning to isothermal conditions in November. Considering that the climatological data was not modified, these results are reasonable.

The reason for predicting too deep a mixed layer could be attributed to air temperatures measured at Worcester airport which may have been higher than were actually experienced at the reservoir, causing greater long wave radiation fluxes into the reservoir. However, the calibration procedure revealed that a variety of processes have similar effects on the thermal distribution in the reservoir. For example, a possible corrective measure to the problem just mentioned could be to increase wind velocities, inducing an increase in the evaporative cooling thereby reducing net heat content. Similarly, incident short wave insolation could be reduced during the summer months resulting in a shallower mixed layer. However, these thermal processes will have significantly different effects on the transport of matter and thus should not be arbitrarily adjusted only to achieve a model response which mimics field data.

A decision was made to leave the climatological data unchanged since it would be difficult to adjust when used in hypothetical years. If the model is not to be used as a predictive tool, the individual component fluxes could be back-calculated from the measured climatological data and the conservation of heat equation. To do so would

be to use the model strictly in an analytical sense. The value of the model as a predictive tool would be lost.

Besides comparing temperature profiles, a comparison of the temporal variation of surface and bottom temperatures can provide a check on the calibration. This comparison is shown in Figure 4.12 . The correlation shows that the assumptions in the model about the boundary fluxes are reasonable. Another check that should be made is comparison of the simulated versus actual temperatures of the outflow water. Due to a deficiency in monitoring, this check is questionable.

Outflow temperatures from Wachusett are not measured until the water reaches Shaft 4, some 13 miles away. At this location, temperatures are measured with uncalibrated dial-type thermometers from a faucet connection into the aqueduct. (See Figure 4.13 .) Considerable error can be introduced here when trying to make comparisons to actual outflow temperatures at the intake. The residence time through the aqueduct to Shaft 4 is approximately 6 hours, and some smoothing of the seasonal temperature variations could be expected since, like inflows, the temperatures will tend toward the almost constant subterranean temperature.

Another source of data to use for comparison of simulated versus actual outflow temperatures is the maintenance record for the two hydro-electric turbines. The main bearing shaft cooling water temperatures are recorded hourly. The cooling water comes directly from the intake and should be indicative of the water discharged to the aqueduct. However, these thermometers have never been calibrated and show a consistent discrepancy throughout the year. The three sources of temperature data along with simulated values are plotted in Figure 4.13 for comparison. Until confidence is achieved in the accuracy of measured temperatures, this check should not be conclusive.

TABLE 4.3

Calibrated Parameters for Option II

<u>Model name</u>	<u>Value</u>	<u>Description</u>
ELOUT*	111.0 m	intake elevation
E_z^*	min .124 m ² /day max 8.64 m ² /day	diffusion dependent on local stability
MIXED*	1.0	number of mixing layers
RMIX*	1.0	dilution factor of entrance mixing
SPREAD	1.96	number of outflow standard deviations

TABLE 4.4

Additional Input Parameters in the Model

<u>Model name</u>	<u>Value</u>	<u>Description</u>
CD	0.038	entrainment coefficient
CT	5.64	entrainment coefficient
CW	4.0	wind mixing efficiency
CCON	0.5	penetrative convection coefficient
DY	2.0	thickness of grip layer (m)
DT	1.0	time step (days)
Beta	0.5	fraction of heat absorbed at surface
DELCON	0.005	withdrawal layer thickness constant (for KAO eqn.)
SIGMAI	3.0	inflow standard deviation (m)
XTN	.30 - .46	extinction coefficient (m ⁻¹)
FACVI	(not used)	wind dependent diffusion coefficient (Option III, IV)

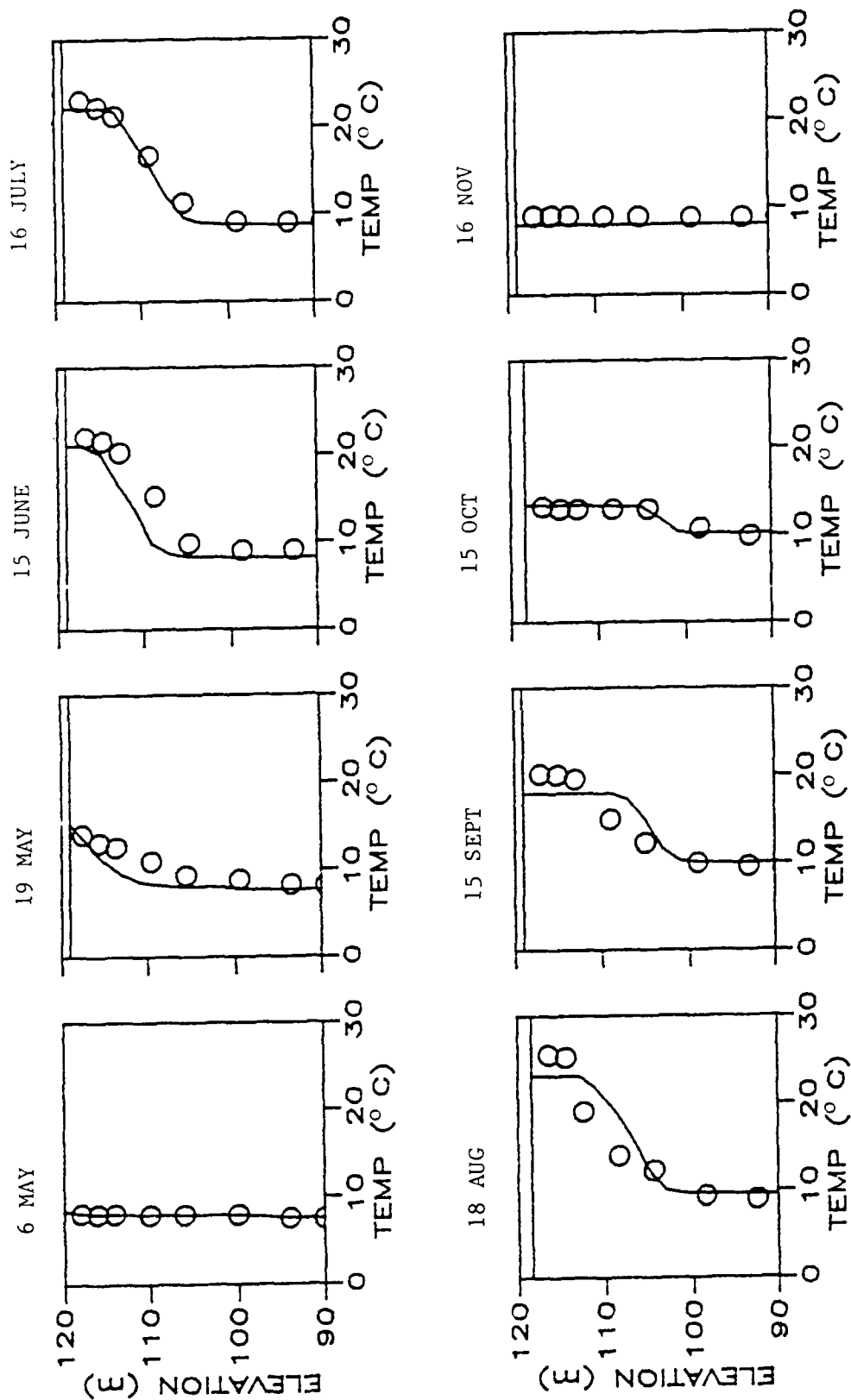


Figure 4.11 Model calibration of temperature profiles. 1987.
(Circles are measured values, solid line is simulated.)

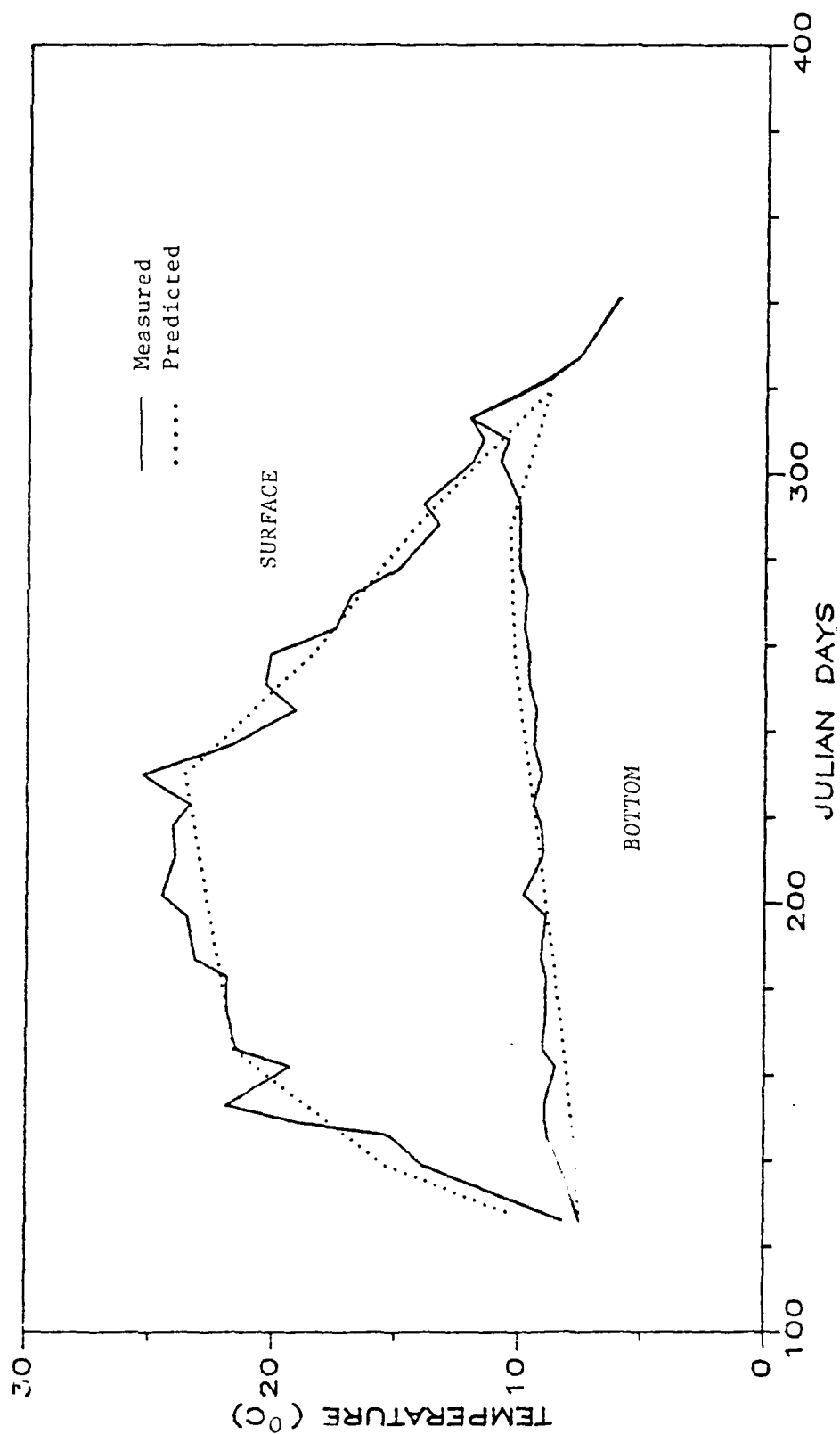


Figure 4.12 Model calibration bottom/surface temperature. 1987.

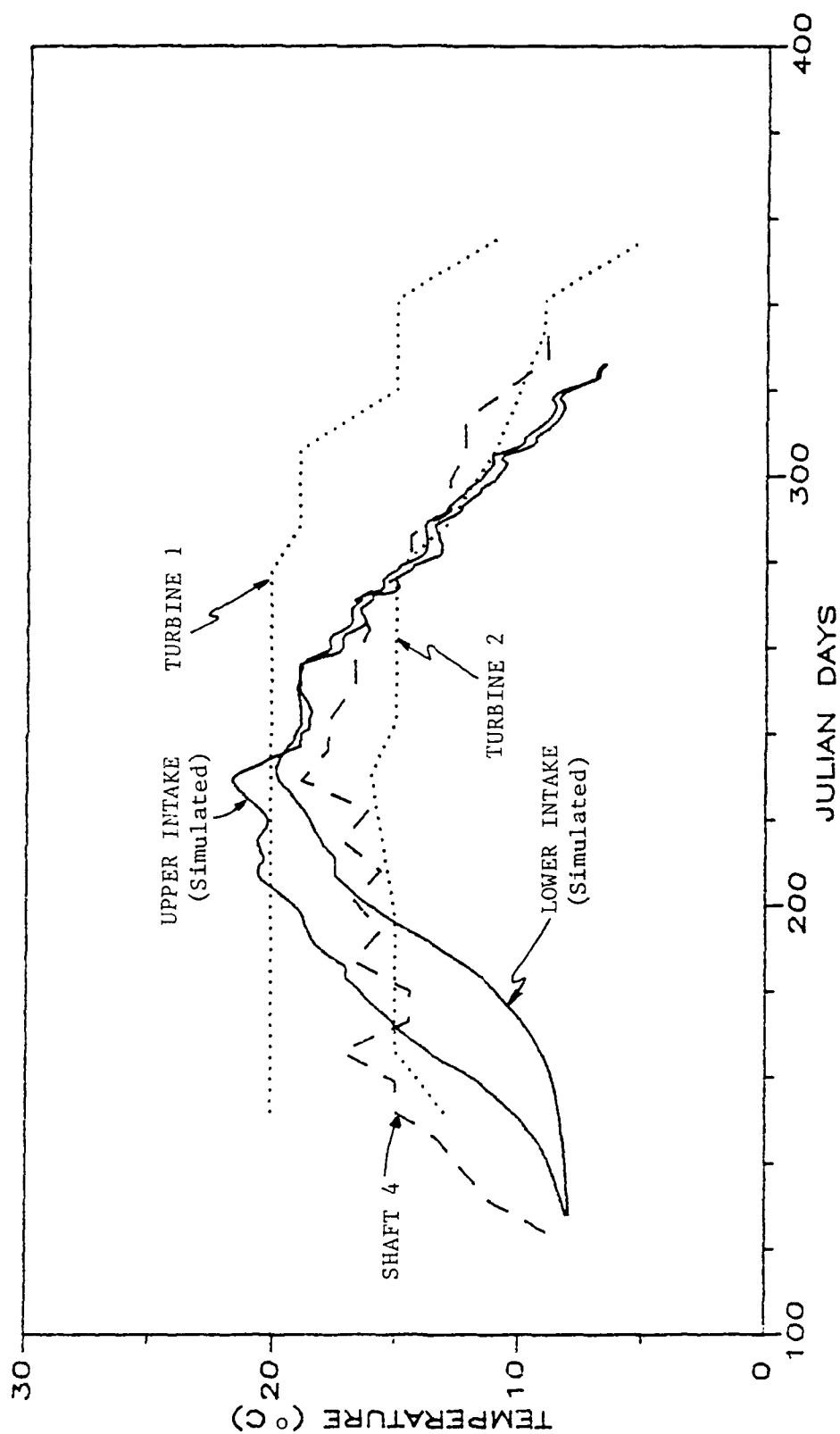


Figure 4.13 Model calibration, outflow temperature comparisons; measured vs. simulated. 1987.

4.3 Verification of the Hydrothermal Model

Calibrated parameters were not changed from the 1987 model runs and were subsequently applied to the 1988 data set. The results of the temperature profile simulation with respect to measured temperatures are shown in Figure 4.14 . Additionally, surface and bottom temperatures comparing simulated and measured values are shown in Figure 4.15 .

For 1988 data a well-defined mixed layer is evident in the spring months (probably due to the higher average wind velocities), and the verification results are better than for 1987. This is partly due to the wind mixing algorithm, described in Chapter 3, which will produce a well-defined mixed layer given sufficient wind. However, over-prediction of the mixed layer depth occurs in August and September, similar to 1987 results.

Again, the dynamics of the hydrothermal model are well represented with the development of a strong stratification by the end of July and its subsequent deterioration in late summer. Erosion of the thermocline is due to cool nights and reduced incoming short wave insolation during the day. The profile on October 11 is just before fall overturn and the temperature correlation is in agreement with the data.

4.4 Sensitivity of Parameters

In the course of model simulations, if an individual parameter is adjusted slightly (with respect to its magnitude) and produces a significant change in the results, this parameter is said to be *sensitive*. Sensitive parameters will exhibit a relatively narrow range of values that produce acceptable results. This section addresses the parameters that exhibit sensitivity. A list of the parameter values used in 1987 and 1988 is given in Table 4.3 and the sensitive parameters are identified with an asterisk.

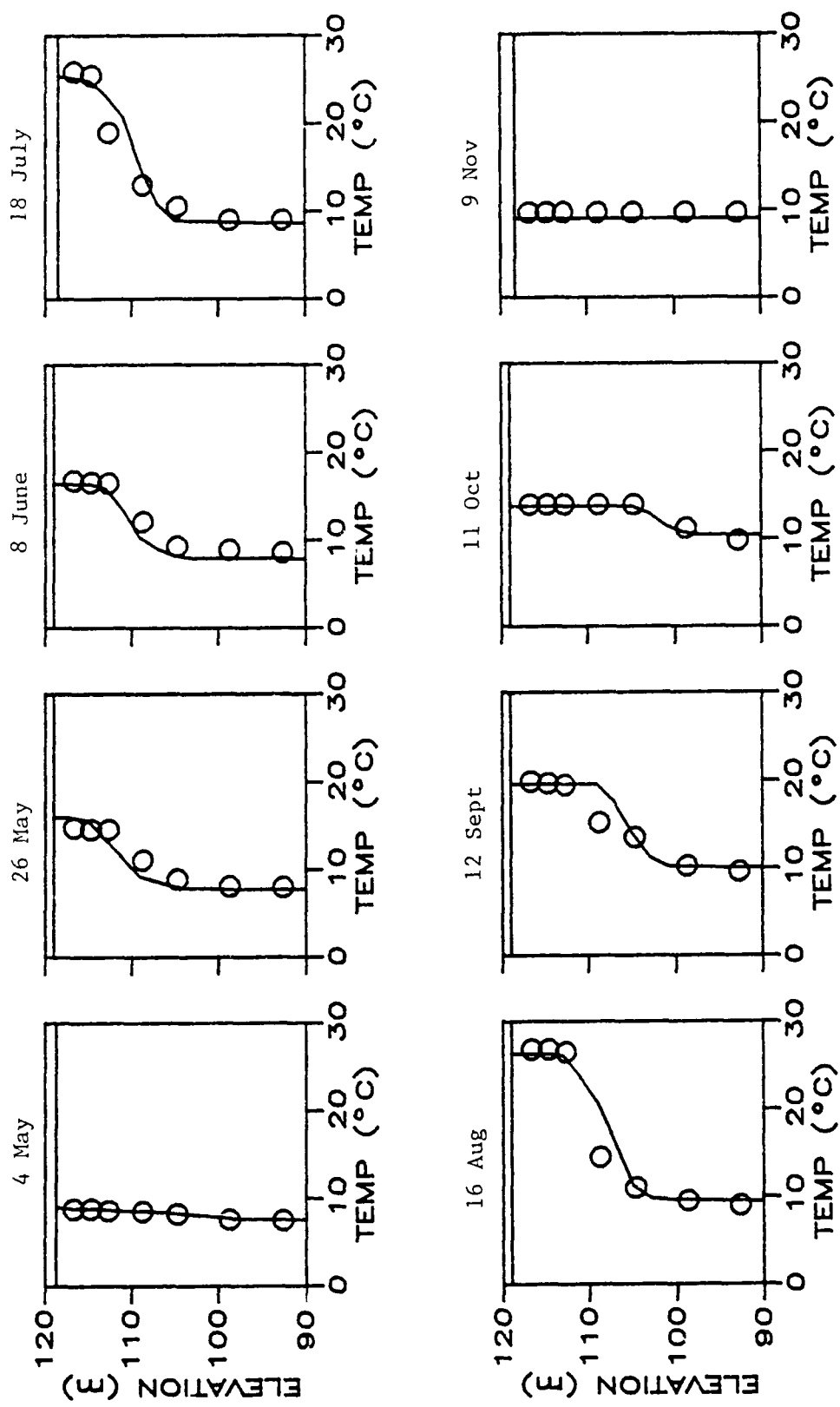


Figure 4.14 Model verification of temperature profile. 1988.
(Circles are measured values, solid line is simulated.)

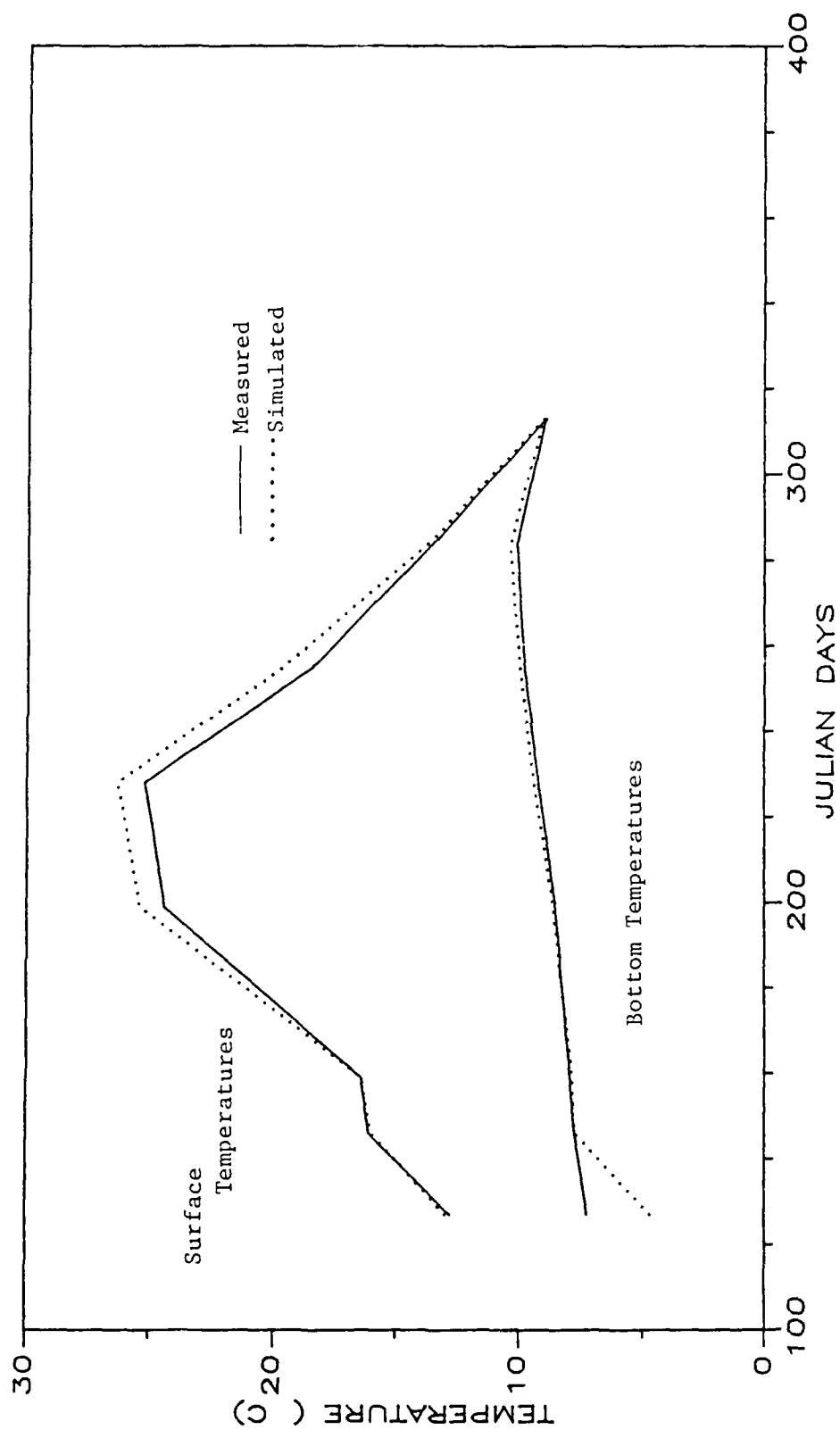


Figure 4.15 Model verification surface and bottom temperatures. 1988.

4.4.1 Intake Elevation

One of the major conclusions of this study is that the depth of withdrawal of the outflow can dramatically alter the thermal profile. Such change in withdrawal would have a similar effect on the chemical constituents in the outflow water.

To illustrate the impact of using different intake elevations, Figure 4.16 shows the resulting thermal profiles with intake level at 111 meters (upper shaft), 105 meters (lower shaft), and 95 meters (hypothetical case). By lowering the intake shaft elevation, considerable heat is retained in the reservoir water column. The entire thermal structure is altered and the displacement of the thermocline is significant. Because the intake lends itself to selective withdrawal experiments, as discussed in Section 5.6.1, alternate intake elevations provide simulations that later could be verified.

4.4.2 Sensitivity to Magnitude of Diffusion Term

The model has options for varying the diffusion from a constant molecular diffusion, to depth-dependent diffusivity (function of local diffusivity), to values which are dependent on wind shear and are both temporally and spatially variable (refer to Section 3.4.3). The maximum value of turbulent diffusivity in any one of these options is capped at $8.64 \text{ m}^2/\text{day}$ or almost three orders of magnitude larger than molecular diffusion. Three test cases shown in Figure 4.17 illustrate the variability and high degree of sensitivity experienced with each of the four options:

- I. molecular ($.0124 \text{ m}^2/\text{day}$)
- II depth dependent (min $.124 \text{ m}^2/\text{day}$; max $8.64 \text{ m}^2/\text{day}$)
- III. wind dependent only (min $.0124 \text{ m}^2/\text{day}$; max $8.64 \text{ m}^2/\text{day}$)

These cases coincide with Options I-IV described in Section 3.4.3 .

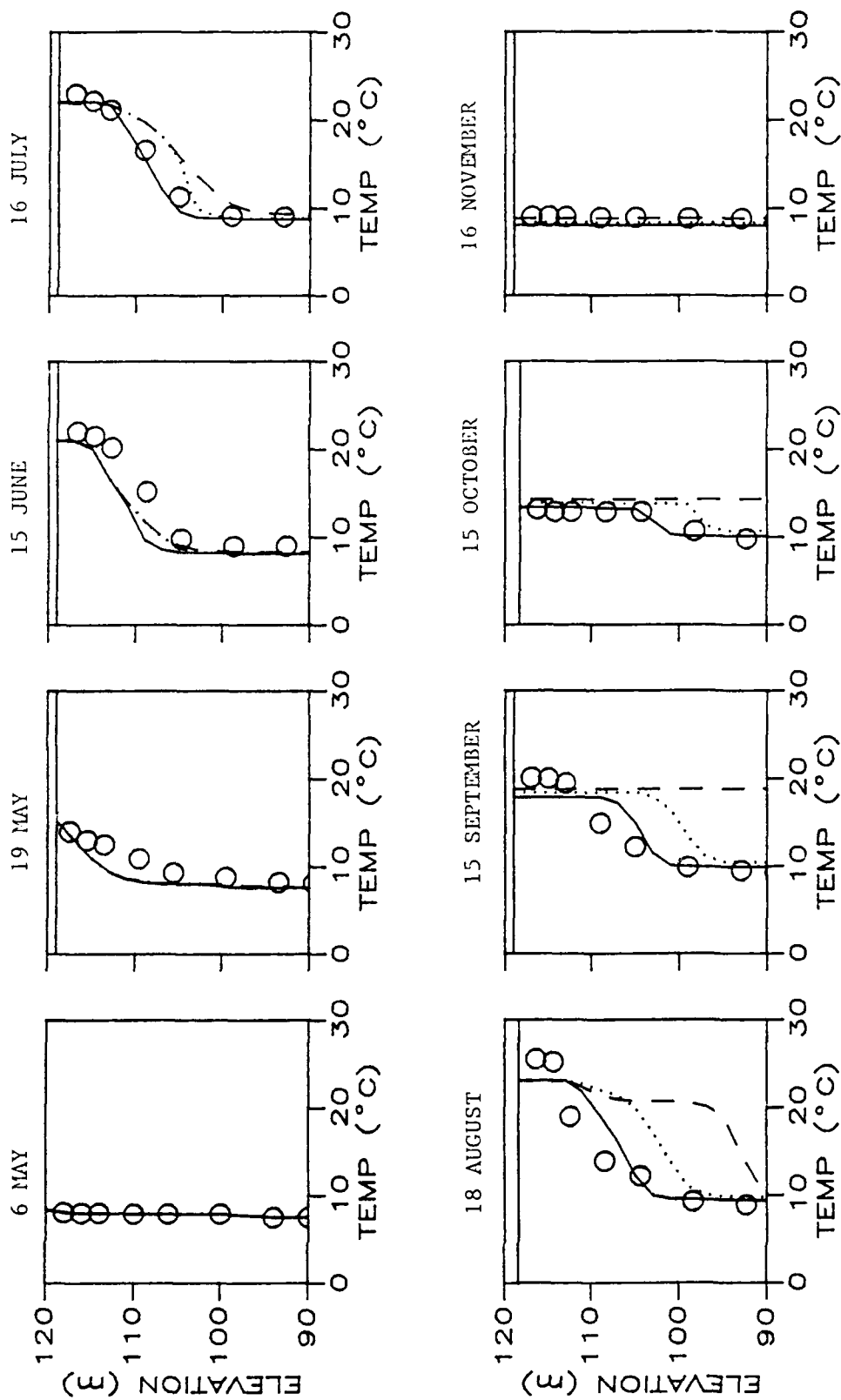


Figure 4.16 Effect of selective withdrawal on temperature, 1987.
(Solid line at 111 m, dotted line at 105 m, dashed line at 95 m.)

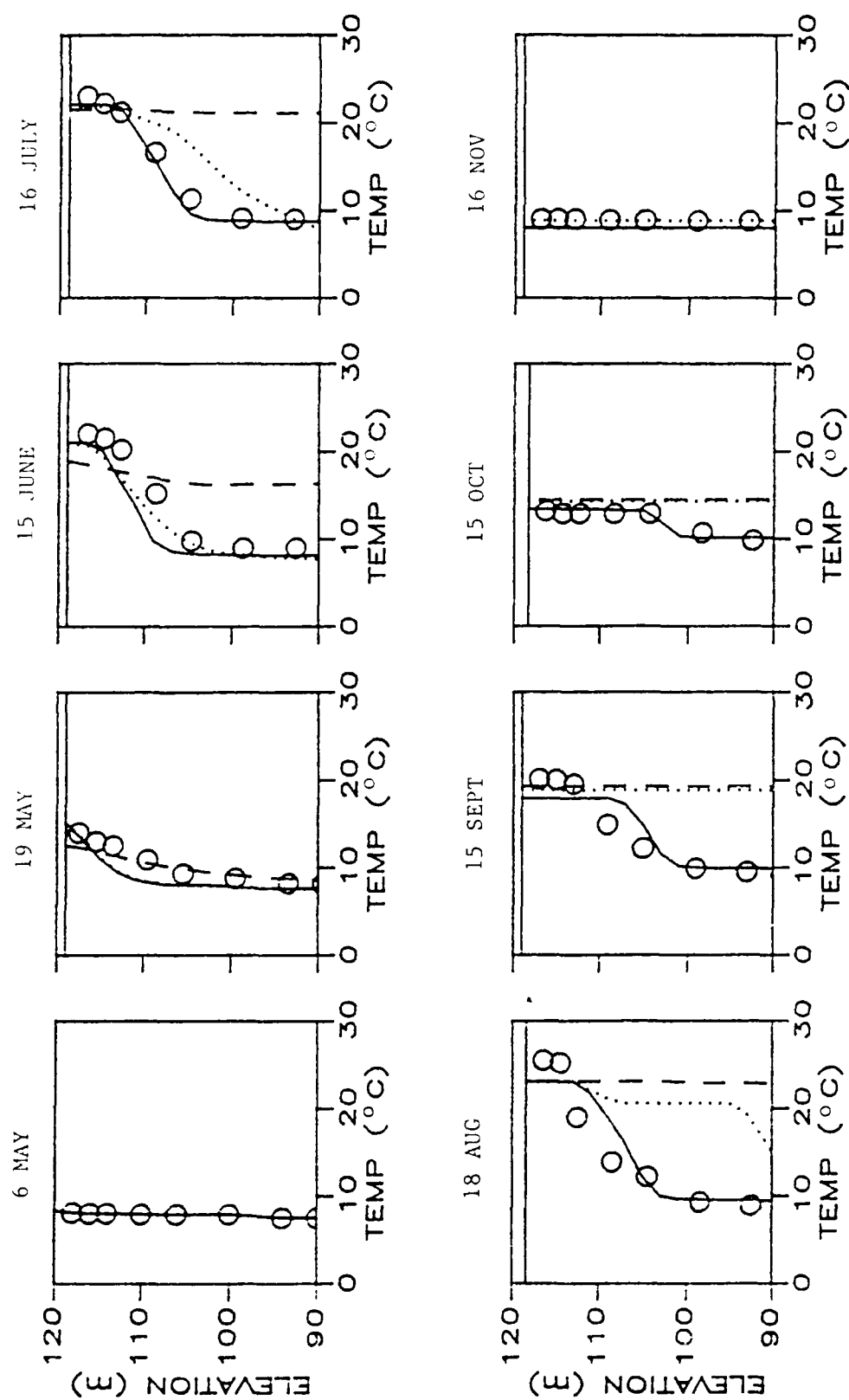


Figure 4.17 Effect of variable diffusion on temperature. (Solid line Option I, dotted line Option II, dashed line Option III.)

Since the mixed layer is characterized by fully mixed conditions due to the wind, it is not sensitive to variable diffusion rates. Local stability due to density gradients between adjacent layers determines the degree to which heat is transported through the hypolimnion as reflected by the case results. Using a turbulent depth dependent diffusivity with a minimum value specified at 10x molecular diffusion (Option II), results are much closer to measured temperatures than with molecular. When a turbulent diffusivity is used, which is a function of wind and the potential energy of the reservoir (Options III & IV), too much heat is transported to the lower levels causing isothermal conditions as early as August.

4.4.3 Sensitivity of Other Model Parameters

Model parameters which describe both the effective withdrawal layer and the degree of mixing and entrainment of inflows with surface layers (model names SPREAD, MIXED, RMIX), significantly affect the prediction of the temperature profile. The first of these parameters, SPREAD, dictates the number of standard deviations that will be contained in the withdrawal layer which is assumed to have a Gaussian velocity distribution. At the calibrated value of 1.96 (Table 4.3), 95% of the outflow water will come from the withdrawal layer. Sensitivity is slight in the range 1.0 (68%) to 1.96, however significant outflow of heat and a reduction in the mixed layer depth occur with values as low as .3 (23%) or .5 (38%). These values are felt to be unreasonably low since they imply that more than half of the outflowing water *does not* come from the withdrawal layer. Calibration of this parameter to other reservoirs (Sau Reservoir [Serrahima, 1987] and Fontana Reservoir [Markofsky and Harleman, 1971]), also used a value of 1.96 .

Two additional parameters, MIXED and RMIX, affect the degree of near field entrance mixing and dilution of inflowing water. MIXED describes the number of

layers involved in entrance mixing, and values greater than 2.0 resulted in an excessive depth of the mixed layer by mid-summer. Little sensitivity is experienced for values of MIXED less than 2.0, but values are slightly better using one layer of mixing. RMIX describes the entrainment of the reservoir water at the entrance and subsequent dilution of inflowing water. The sensitivity of this parameter is negligible for values greater than .2. Values of RMIX .2 or lower reflect a reduction of the mixed layer in August and September, but contribute adversely to results in June and July when temperatures tend to be under-predicted from the outset. Since trade-offs must be made, the best results overall were achieved with a value of 1.0, which infers the equal mixing of one part of inflow water with every one part of reservoir water (see Section 4.1).

4.5 Timing of the Spring Overturn

Throughout most of the winter months, the thermal processes are muted due to ice cover and the small amount of solar radiation that penetrates to the water column [Hutchinson, 1957]. During this period the temperatures will vary only about 3°C throughout the entire water column. However, following ice melt and the normally increased spring wind velocities, the distribution of heat in the water column is highly dynamic and unstable. In fact, the heat content of a lake or reservoir can change by as much as 10% in a couple days [Wetzel, 1983]. This highly variable condition underscores the importance of accurately measuring temperatures and capturing the timing of the initial isothermal conditions for the model. If these temperatures are not correct, errors will carry through subsequent heat balance simulations. Thus, modeling can only begin as early as the first field measurements are taken, which if not made early enough may miss significant spring turnover events. In this study modeling began on May 6, 1987 and May 4, 1988.

Chapter 5 Evaluation of Water Quality Management Techniques

The continuance of quality water from the Wachusett Reservoir is predicated on a comprehensive management plan which defines current problems and identifies short and long term actions needed to remediate existing problems, without posing additional threats to the ecological balance. Additionally, the plan should set up alternate contingencies in the event of worse case scenarios in the degradation of water quality. This is especially true for Wachusett Reservoir due to its status as the weak link in the water distribution system for the more than 2 million people of Boston who depend on it. This chapter identifies current practices employed to minimize taste and odor problems, reviews alternative practices that may effectively be used, and suggests possible short term objectives and long term goals to ensure the continued preservation of this resource. Despite the many "corrective" alternatives, the best long term solution is the curtailment of detrimental loadings into the reservoir.

5.1 Current Operational Management Techniques

The MDC/MWRA have employed various management practices as they pertain to the operation and treatment of the reservoir waters. A monitoring program with analysis of water biota and water quality parameters by laboratories of both agencies is ongoing with sampling generally from four in-reservoir stations; 3409, 3410, 3412, 3417 as well as several tributaries (see Figure 5.1). As outlined in a Memorandum of Understanding between the two agencies, the primary responsibility for monitoring the Wachusett Reservoir water quality constituents lies with the MDC. However, the MWRA augments this plan as needed and samples outside the Cosgrove intake (Station 3409) biweekly. The MDC often contracts for additional

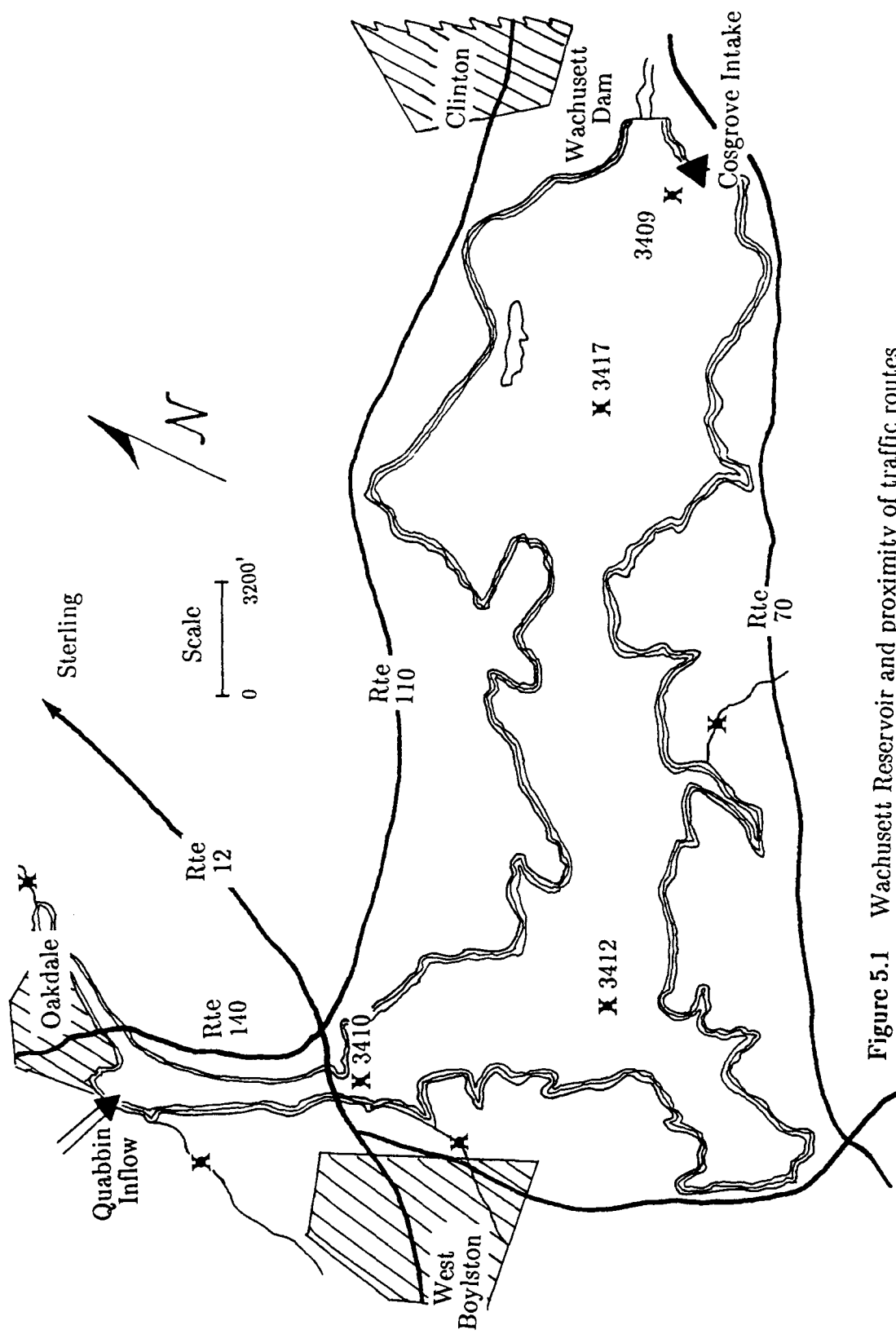


Figure 5.1 Wachusett Reservoir and proximity of traffic routes and towns. Monitoring stations shown by crossed circle.

services from private consultants for more extensive monitoring and/or analysis. Normally, parameters such as temperature, DO, pH, nutrients, Secchi disc, and phytoplankton/zooplankton species are measured in the reservoir every two weeks. Somewhat different parameters are monitored bi-weekly in the reservoir tributaries such as color, odor, turbidity, hardness, pH, temperature, and coliform.

Another management policy implemented at the reservoir is the application of copper sulfate to control objectionable algae growth. Based on algal counts in water samples and complaints from consumers as to objectionable taste and odor, copper sulfate (CuSO_4) is applied to the epilimnion of the reservoir. The method of treatment consists of dragging burlap sacks of the algicide crystal through the water near the intake, covering enough area to treat about one week's worth of water demand (approximately 100 acres) and achieve a residual concentration of .1 mgCu/l. When copper concentrations diminish to background levels, additional applications may be warranted should high algae counts persist. This treatment method has worked in prior years to a limited degree but has failed in recent spring and fall overturn periods [MWRA/MDC, 1988]. Figure 5.2 shows the application rate for the Fall of 1987 amounting to over 20 tons of algicide applied for the fall period.

In addition to a sampling program and copper sulfate application, the reservoir is monitored to ensure that a minimum surface level is maintained for water quality reasons. The normal operating range of the reservoir is at an elevation of 388-390 feet, but due to the large amount of shallow basin area, considerable bank exposure and resuspension of bottom sediments will result if surface elevations fall below 385 feet. With low water levels, water quality can be degraded by increased turbidity from wave action on sediments of fine, silty, particles. Alternately, resuspension of nutrients that had settled out encourage undesirable algal and bacterial growth. Odors from drying of the exposed sediments would be undesirable as well.

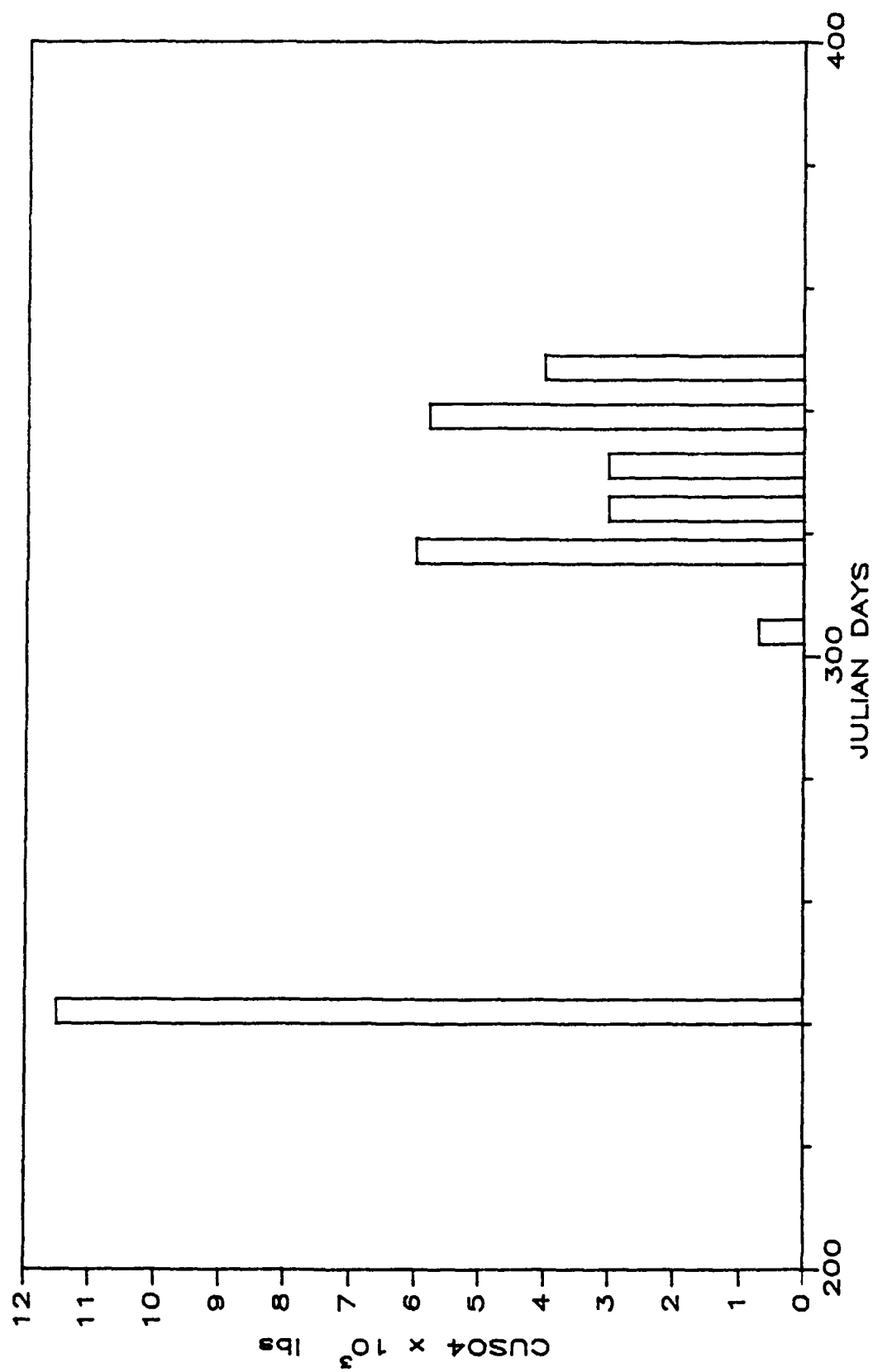


Figure 5.2 Application rates of copper sulfate for the fall of 1987.

Another practice employed to maintain good water quality is the use of mesh screens at the intake to preclude the entrainment of debris and fish into the water works. Additionally, minimal chemical treatment of the water has been adopted which includes the addition of chloramine, flouride, and sodium hydroxide to the water prior to distribution. Chloramine is a mixture of ammonia and chlorine (a ratio of 1:5 is used) and is a slower acting disinfectant than pure chlorine, thus maintaining its effectiveness for a longer periods. Greater duration of disinfection helps prevent the growth of microscopic organisms with long delivery times. Sodium hydroxide is added to the slightly acidic water thereby reducing the corrosiveness to the distribution pipes. Flouride is helpful in reducing dental caries in low concentrations ($\approx 1\text{mg/l}$).

5.2 Copper Toxicity and Considerations for Algicide Treatment

Currently, large volumes of copper sulfate crystals are applied to surface waters in the immediate vicinity of the intake. Effective toxicity to problem algae below the thermocline is unknown. *Synura*, one of the most potent of the problem algae, has been monitored at depths below the thermocline and can produce resting cysts that exist in the sediments [MWRA/MDC, 1988]. Because the intakes are also located at or below the thermocline, substantial numbers of algae may be entrained into intake waters without sufficient exposure to the algicide.

There are many factors involved in the effectiveness of the treatment which need to be considered in calculating the quantity of copper sulfate to be applied. Whipple (1948) suggests some of the considerations for effective application:

- * kind of algae to be destroyed
- * amount of organic matter present
- * hardness of the water

- * carbonic acid content
- * water temperature
- * quantity of water to be treated
- * species of fish present

In addition, the water circulation is important since lethal doses of chemical may not reach critical portions of the water column due to local hydrodynamics. Any one of these factors has the capability of rendering the treatment ineffective.

Copper is a trace element essential for metabolism in all living cells as well as the synthesis of chlorophyll in plants. Above a minimum threshold, however, copper is extremely toxic to many lower life forms. It is the cupric ion (Cu^{+}) ion which imparts toxicity to organisms. Studies with different algae have shown that the cupric ion is assimilated by living cells which effects the cells' collapse through lysis [McKnight, 1979]. Toxicity varies from among organisms thus it is important to identify target species accurately. For instance, *Anabaena* registers toxicity at concentrations of .12 mg/l while *Staurastrum* requires 1.5 mg/l to be controlled [Culp, 1986]. In the extreme case, some algae are known to be resistant to copper toxicity and have been observed in mining waste ponds containing high concentrations of copper (e.g., the green algae, *Chlorella*) [Owen, 1981]. Other species have been known to acquire a tolerance for increased concentrations [Mcknight, 1979]. Therefore, it is important to have positive identification of the problem algae before algicide treatment is considered.

Copper sulfate's effectiveness will be reduced with increased levels of organic matter, hardness, and carbonic acid [Chisholm, 1983]. This is due to a complexation with carbonate ions and organic molecules, thus tying up the cupric ion and reducing the effective concentration available to act on the algae. For instance, concentrations of 60 μ g/l copper sulfate are toxic to rainbow trout in soft waters (12 mg/l as $CaCO_3$)

whereas it takes up to 600 $\mu\text{g/l}$ to reach toxic levels in hard waters (320 mg/l as CaCO_3) [Train, 1979].

Warmer water temperatures have been shown to increase the toxicity of copper to organisms [Forstner, 1979]. This fact may be significant to Wachusett since substantial temperature variations can exist in the epilimnion from one month to the next. Thus, what were adequate doses during the summer months may be ineffective in the late fall or early spring due to colder waters.

A direct correlation exists between the amount of water to be treated and the application rate. The question which needs answering with each application is: to what depth should the algicide be effective to prevent subsequent blooms without over-dilution? Large doses of copper sulfate are applied at the surface with expectations of lethal concentrations reaching lower waters through turbulent mixing and diffusion. This higher-than-needed concentration at the surface can cause deleterious impacts on non-targeted surface biota which may be sensitive to this treatment dosage. In this way, copper sulfate treatment may actually contribute to the algae problem due to the reduction of other biota in the food chain, hence reducing the grazing pressures that normally exist.

Depending on the species, fish exhibit a range of copper concentrations to which they are sensitive. Bullhead, for example, exhibit sensitivity to .18 mg/l copper sulfate while Bass can withstand levels up to .62 mg/l [Train, 1979]. Additionally, younger fish are more sensitive, such as the Fathead Minnow tolerating maximum concentrations of only .084 mg/l. What constitutes a lethal dosage is dependent on both exposure time as well as concentration. If the length of exposure is kept to 48 hours or less, Bluegill can withstand concentrations of .67–.84 mg/l. However if the exposure is extended to 96 hours, 50% mortality is reached at concentrations of .24 mg/l [NAS, 1977]. Additionally, organisms rendered nonmotile (without capability

to move) by exposure to the cupric ion may be "revived" if exposure time was sufficiently short [Anderson, 1978].

5.3 Problems with Copper Sulfate Application

Chemically treating the entire reservoir is a prohibitive undertaking, but the localized dosing of intake waters will only be effective until the volume of treated water is replaced by untreated waters. Since algae productivity in untreated water has experienced no constraints, algicide application will be all the more necessary, however treatment of a full bloom may now be required.

The specific cause of the taste and odor originates from either the organic acids and fatty oils produced by the algae or alternately from actinonycetes ray fungi which decompose dead algae [Culp, 1986]. In either case, the magnitude of the problem is in direct proportion to the number of algae cells present. Copper sulfate is effective in killing targeted algae species, however it will not remove the organic chemical which is responsible for the taste and odor. Thus, treatment of a bloom may halt further growth, but objectionable taste and odor may persist until dead algae settle out or are removed mechanically. Subsequent chlorination does not usually help and, in fact, may make the problem worse by fragmenting algae cells into many parts, increasing unpalatability. The best solution for removal of organic compounds is through very strong oxidation (ozone) or filtering (activated carbon).

The application of copper sulfate is basically a "band-aide" solution to the taste and odor problem experienced in surface water impoundments. From an ecological standpoint, the toxicity of copper poses many uncertainties with regards to toxic side-effects on non-targeted biota populations. Evaluation of more rigorous management alternatives is warranted due to the concerns raised above and the fact that in spite of this, treatment has been largely ineffective.

5.4 Alternative Management Techniques

There are numerous techniques available today for improvement in the quality of water supplies [Lindeburg, 1986]. Naturally, the techniques that are the most effective and long lasting are the most difficult to implement and may require more far-reaching development of political policy aimed at the protection of the watershed and control of its use. This, in combination with treatment when problems do occur, is paramount to the prevention of significant water problems. It is the opinion of the author that while current strategies employed in the management of Wachusett Reservoir are fundamental in the development of any management plan, the methodology in the application of copper sulfate is perhaps not the best means of combating algae blooms and the subsequent taste and odor problems.

The taste and odor problem is essentially the result of a continuum of cause-and-effect relationships which interact at different tiers within the ecosystem. These relationships are depicted in Figure 5.3 beginning with the underlying activity of land disturbances/development and showing subsequent problems which build upon the initial disturbance. Evaluation of treatment methods should consider the targeted level in the hierarchy as it will shed light as to the likely permanence of the solution.

Many "corrective" solutions to water quality problems may focus on problems near the top of Figure 5.3 since they are easier to apply and manage. However these solutions will not have lasting effects since they are built upon broader problems which still exist. Although these broader problems are more difficult to identify (e.g., nonpoint pollution), their elimination offers the most permanent solution. It is important to keep in mind that as more frequent employment of short term solutions become necessary, it is indicative of a broader fundamental problem which could be best served by a long term solution.

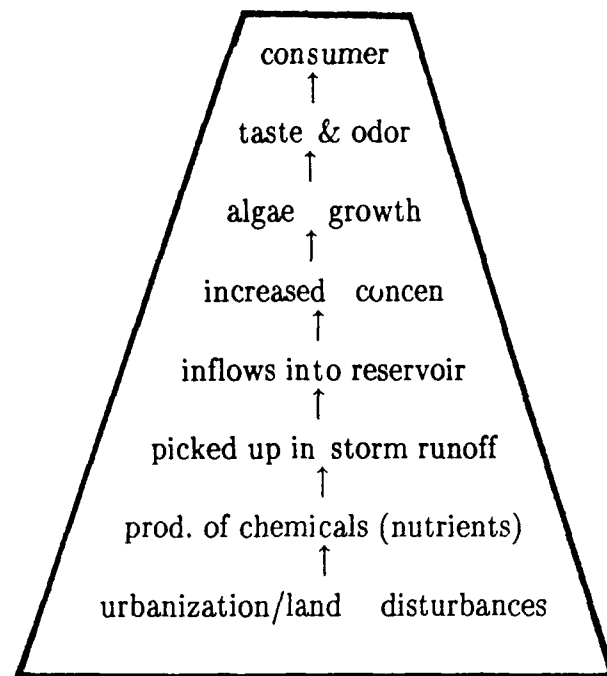


Figure 5.3 Hierarchy of Eutrophication Problems.

Since phosphorus is the limiting nutrient (the nutrient available in shortest supply) in most surface impoundments [Wetzel, 1983], corrective actions should focus on reducing these loadings. It is important to note that while there are many environmental sources for phosphorus into the reservoir, essentially the only removal mechanism from the reservoir is through the outflow or deposition to sediments by settling dead algae. Hence, phosphorus tends to accumulate in a water body and encourage the natural aging process which is represented by increased productivity.

Evaluation of the phosphorus budget for Wachusett [CDM, 1989] indicates that approximately 45% of the total phosphorus loading comes from the Quabbin Aqueduct. Since in-reservoir monitoring of the Quabbin Reservoir reveals very low phosphorus concentrations ($\approx .01$ mgP/l) [Tighe & Bond, 1988], other water sources such as the Ware River intake should be evaluated to determine the point of entry for sources of nutrient loading. Of the other small tributaries, Gates Brook and French

Brook show relatively high average loadings of .023 mgP/l and .020 mgP/l respectively. However their flows are small (<5 cfs) so their phosphorus contribution is not critical.

5.5 In-Reservoir Chemical Treatment Alternatives

Full scale treatment of reservoir water is the solution which is hoped can be avoided by alternative measures. Of course, a full range of "closed system" facilities are in use today which can virtually rejuvenate the most polluted of waters to drinkable standards. However the trade-off comes at a price which must be balanced against other alternatives. Since a treatment facility for Wachusett would be the last resort, alternatives which could be more easily adapted than a treatment plant are discussed here.

5.5.1 Deep Water Application of Copper Sulfate

Without changing the current strategy in the use of algicide, the application of copper sulfate could be improved most probably by deep water injection. More efficient use of the algicide would be achieved through a more uniform distribution of the chemical. Water samples taken by the MWRA outside the Cosgrove Intake (Station 3409) reveal the occurrence of *Synura* below the thermocline. Whether the algae typically reside at such depths or whether they are entrained by the intake waters and pulled down from the upper layers should be verified.

If in fact algae normally exist at depths below the thermocline, deep water application would more effectively control algae populations while smaller applications to the surface would target epilimnetic algae. Deep water application may lessen the impact on non-target species as well. Of at least equal importance,

the timing of the application is critical to achieve maximum effectiveness since copper sulfate is much better at preventing blooms than stopping one in full progress.

However, before a decision is made to continue the use of algicide, an assessment of the total environmental impact of copper sulfate should be made by looking at copper accumulations in the sediment, its impact on benthic organisms, and the effect on other zooplankton in the water body.

5.5.2 Alum Precipitation

Aluminum sulfate or Alum [$\text{Al}_2(\text{SO}_4)_3 \cdot \text{H}_2\text{O}$] is used to precipitate phosphorus which is normally available for use by phytoplankton. Due to continual loadings of phosphorus into the reservoir, this method would incur a large operating cost to the water supply works unless other actions are taken to reduce loadings. Additionally, vast quantities would be required for treatment of the sediments through the inactivation of phosphorus. A suggestion that might be investigated is the treatment of water entering the reservoir from the Quabbin Aqueduct to remove phosphorus since its contribution of phosphorus is considerable as mentioned earlier. The advantage of this is that the flow is contained at the west end of the reservoir which may be more easily treated by mechanical means than open water. Like copper, effects of accumulations of aluminum sulfate on the ecosystem are not well known.

5.5.3 Potassium Permanganate

Potassium Permanganate is an oxidizing agent and has been used as an algicide similar to copper sulfate. However, it is used more effectively in the destruction of the odor producing compounds than in killing the algae. Other uses include the removal of iron and manganese from solution, and use as a limited disinfectant.

Problems with its use is that it will nearly always require filtration to remove the flocculant manganese hydroxide hydrates (MnOH_2) before distribution to consumers. Furthermore, cases of overdosing often cause staining on clothing. Dosage rates of .5 to 2.5 mg/l are necessary for taste- and odor-causing chemicals and may have adverse effects on other biota. Due to its increased application rate and higher expense, the trade-offs are not so attractive for use at Wachusett.

5.5.4 Ozone

A very strong oxidant, the gas ozone (O_3) provides excellent water treatment for taste and odor by destroying the problematic organic substances. Injection of the gas into the intake waters would allow sufficient contact time with small molecular substances to breakdown their chemical composition (usually on the order of 15–30 minutes) while in the aqueduct. For larger molecular organics (e.g., algae), longer contact time or conjunctive use with filtering may be needed. The half-life of ozone is about 20–30 minutes (at 20°C) in water, and about 12 hours in air. Any "unused" ozone reverts to oxygen [Browning, 1981]. These characteristics of ozone enable it to be transported and handled after production but make it a fast reactant once introduced into the water.

Ozone is a toxic gas and explosive when in large enough concentrations (15–20% with air) however such concentrations are not reached through normal production. Ozone must be produced electrically and as such, has a power requirement. Although there are two 22 MW generators operated at the Cosgrove Intake, it probably would not be cost effective to produce ozone locally.

5.6 Physical Treatment Techniques

Since water from Wachusett Reservoir is normally of good quality, the use of corrective measures could be restricted to times when problems are experienced. For chemical treatment, periodic use will reduce operational expenses. It would stand to reason then, that treatment alternatives which can be stopped and started easily would be more advantageous than a continual year-round treatment process.

5.6.1 Selective Withdrawal

Some possibilities exist for physical manipulation of the water column to achieve better water quality at the intake. One which warrants consideration (and is possibly the least costly to implement) is selective withdrawal. This entails drawing water through the intake from variable elevations as dictated by analysis of water quality monitoring data.

As mentioned earlier, phosphorus sinks in the reservoir are only through the outflow and sedimentation. As seen by the hydrothermal model, significant alterations in the thermal structure of the water column can be achieved by altering withdrawal elevations by as little as 6–10 meters (see Figure 4.16). If withdrawals can be made at elevations containing the greatest concentration of phosphorus, maximum reductions of phosphorus and/or heat can be made, possibly preventing algal blooms. The quantitative implications for water quality constituents are not obvious at this time, however through coupling of the algae kinetics and the transformation processes of various chemical species in a water quality model, a more accurate assessment can be made.

A recent study of the Monksville reservoir in New Jersey by Huang (1988) reached a similar conclusion as to the positive effects of selective withdrawal. The

recommendation at Monksville was for the limited use of algicide, real time monitoring and selective withdrawal, to optimize the management practices.

The Cosgrove intake lends itself to experimenting with the selective withdrawal technique due to the current geometry of the intake and the method of water blockage used for maintenance purposes. Normally, twelve 6 ft mesh screens are placed end to end in front of the intake shaft. As shown in Figure 5.4, if blockage grates were installed at selected positions, water entry would essentially be restricted to pre-determined elevations.

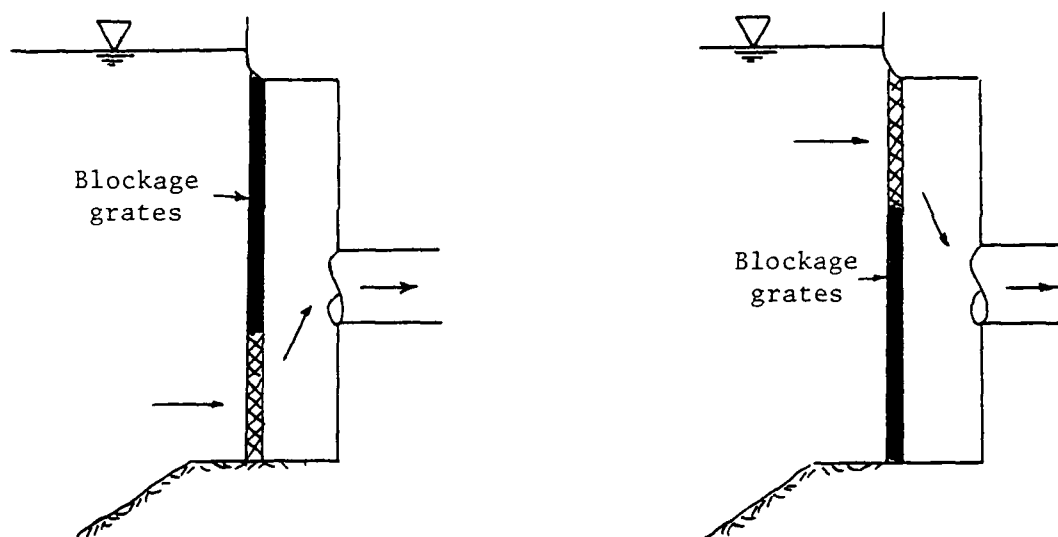


Figure 5.4 Method by which selective withdrawal can be achieved using blockage grates.

Rigorous monitoring of outflow water composition and temperature as well as in-reservoir changes in stratification can help determine the flow regime about the intake for various intake configurations. Correlation of results could be used to modify outflow water composition when taste and odor problems are reported.

Problems with frazil ice build-up on the mesh screens currently dictates that intake levels be changed at the Cosgrove Intake. Culp (1986) reports that the use of fiberglass reinforced plastic (FRP) for intake collars reduces the thermal conductivity and the capability of the ice to adhere to the surface. If the use of desired intakes is precluded by this icing problem, FRP may be a solution.

5.6.2 Activated Carbon Treatment

The use of activated carbon has been shown to be the most effective in the treatment of taste and odor problems than any other process [Culp, 1986]. Its effectiveness is derived from the principle of adsorption by which undesirable organic compounds adhere to the carbon granules. Because most all the taste and odor problems stem from the presence of organic compounds produced by algae, it is especially appropriate for the problems at Wachusett. Either water can be filtered through beds of granular activated carbon (GAC) or powdered activated carbon (PAC) can be added at the intake of the reservoir and later removed by filtration. Addition of PAC at the intake promotes thorough mixing, thus minimizing the necessary contact time (on the order of 20 minutes). Required concentration of PAC depends on the amount of organics to be removed, but a gross approximation would be on the order of 6.2 tons/day for Cosgrove intake (assuming 300 mgd flow rate).

Added benefits arise from PAC use in the removal of more harmful synthetic organic compounds. Further, rejuvenation plants for the reuse of activated carbon can be located near the treatment area to reduce transportation costs. The main drawback is that PAC represents a major investment so that further cost analysis would be necessary.

5.6.3 Destratification

Destratification is an in-reservoir technique involving the mechanical mixing either by powered equipment or through aeration strong enough to destratify the water column. Uniform distribution of both temperature and nutrient concentration result which may dilute high nutrient concentrations to levels which prevent an algae bloom. Alternately, Figure 5.5 shows how the algae which need light for energy may be carried out of the photic zone by this mixing, thereby reducing exposure time to light and reducing productivity.

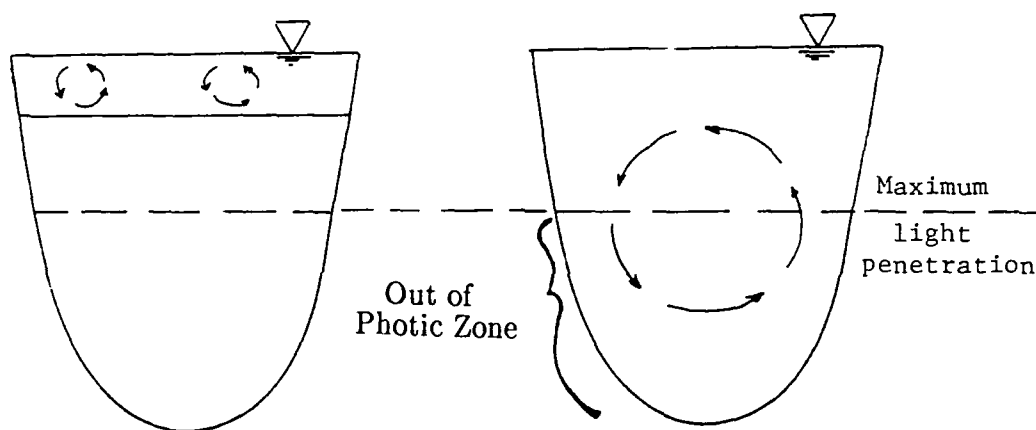


Figure 5.5 Effect of destratification on mixing algae out of the photic zone.

Destratification has an unproven track record for use in large reservoirs and indeed could foster greater problems by circulating needed nutrients that build up in the hypolimnion. In this way, it is key to note that *Synura* are heterotrophic algae, and if light is not available, chemical redox can be the source of energy. Hence, this method may not be effective in combating heterotrophic phytoplankton. Potentially negative effects on other ecosystem biota (esp. cold water fish) would need to be studied further.

5.7 Development of a Management Plan

5.7.1 Coordination Between MDC/MWRA

As of 1984, the responsibility for water quality has been shared between two agencies: the Massachusetts Water Resources Authority (MWRA), an independent authority, and the MDC's Division of Watershed Management (DWM), a state agency. A joint Memorandum of Understanding (1989, *rev.*), outlines this relationship which includes the sharing of operational data through the maintenance of a joint database and close communication between agency counterparts. Under the agreement, the MDC owns all the real property associated with water supply and distribution, while the MWRA has the right to use, maintain, and improve these facilities. The MDC is responsible for the structural integrity, maintenance and operational control of the dam and spillway as well as the user rights to the water supply and activities conducted within the watershed.

The MWRA was formed to achieve better operational maintenance of the water supply. As an independent agency, funds for operational expenses can be raised directly through customer rate charges. This source of funding is not possible for the MDC. Functions of the MWRA include supplementing the monitoring and treatment efforts of the DWM both in the reservoir and the watershed. All pumping, distribution functions, and day to day operations at man-made control points at the reservoir and aqueducts reside with the MWRA while regulatory responsibility is vested in the DWM. Under this umbrella of responsibility, the MWRA is financially responsible for long-range supply studies.

The working relationship between the MWRA and the MDC has direct bearing on the management of Wachusett Reservoir, as it is at the Cosgrove Intake that formal responsibility is separated. By design, accountability for clean water is shared by the two agencies. Although the delivery of water to Boston is the responsibility of

the MWRA, should treatment become mandatory due to activities permitted in the watershed, the MDC is mandated to do everything possible to mitigate the impact of these activities on the receiving waters [MWRA/MDC, 1989]. Furthermore, consultation between both agencies is necessary before imposition of any restrictions on flow allowances. Because of this interdependency, close communication between both agencies is essential.

5.7.2 Plan Objectives

To fully optimize limited resources between the MDC and the MWRA, a water quality management plan must be in place which ensures the communication of concerns and sharing of monitoring data. Additionally, long-range planning objectives need to be defined so that interim goals and research are more clearly focused. Finally, it is apparent that increased environmental stress in the Wachusett watershed is causing increased eutrophication of the reservoir. Attention must be given to land use planning and the adoption of guidelines for acceptable land practices on critical parcels. The implementation of actions of this type will go a long way toward preserving the high quality of water available in Wachusett Reservoir.

A management plan must include objectives to which interim efforts tend to gravitate. Plan objectives, at a minimum, should address the following issues:

- 1) contingency plan for catastrophic events — emergency actions that could be taken in the event of toxic contamination, flooding, or severe drought.

- 2) comprehensive reservoir monitoring plan — agency designation to conduct monitoring at particular stations, using standard techniques, and for specified parameters. (Author's recommendation given in Section 5.7.4).

3) algicide application criteria — designate responsibility for application, indicators of needed algicide application, maximum algicide dosages allowed, and emphasis toward the prevention of algae blooms as opposed to treatment of a full bloom.

4) documentation of customer feedback — recording of customer complaints on water quality, development of significant trends and statistical data for a database, list of questions for consumers reporting complaints.

5) land use objectives — prioritization of land use restrictions, mapping of watershed by activity, maintenance of current land use statistics, measures employed for enforcement of land use restrictions.

6) economic evaluations — inventory of economic resources within the watershed, comparative evaluations of treatment alternatives.

7) future research needed — questions needing answers to improve the management of water quality, comprehensive research needs including modeling and field studies, field testing of experimental equipment to assess impacts/results.

5.7.3 Land Use Planning

The most favorable situation in terms of arresting the growing influx of pollution is 100% ownership of the watershed by the regulating agency (MDC and MWRA). Total ownership is obviously not economically feasible and in truth, the MDC currently owns only 8.4% of the Wachusett watershed. Tight agency control is required over the remainder of the watershed to preclude further deterioration of surface water quality. As seen by the land use composite in Table 5.1, the major consideration in the Wachusett Watershed is nonpoint pollution sources. Point sources have been the focus of federal and state legislation over the past two decades,

and solutions are mainly engineered. Nonpoint sources are much more diffuse in nature, making identification of sources difficult.

TABLE 5.1

Land-use in Wachusett Watershed (compiled from CDM,1989)

<u>Land Use</u>	<u>Area</u>	<u>Percent</u>
Agricultural	5.4	4.4
Open Land	6.4	5.3
Forest	96.1	79.2
Open Water	1.4	1.2
Wetlands	1.2	0.9
Residential	8.6	7.1
Waste Disposal	0.2	0.1
Other*	<u>2.2</u>	<u>1.8</u>
TOTAL	121.4 mi ²	100%

* includes major highways, power lines, industrial & commercial areas, mining

The polluter involved with nonpoint sources consists mainly of private land owners and basically anyone who uses the land as compared to point sources which are mainly industry and commercial interests. Thus, pollution management must rely on different methodologies than for point sources. Management of nonpoint sources should focus on education, land use control, technical assistance, and incentives toward implementation of Best Management Practices (BMP). Examples of effective BMP's are grazing practices, crop management, tree/vegetation plantings, and practices to reduce erosion during construction.

Although there is also "natural pollution" from even untouched lands, major contributions of pollutants (nutrients, organic matter, and suspended solids) can be attributed to disturbances of the land. These disturbances are most notably devegetation, agriculture, and construction sites [Krenkel, 1985]. Since private land

owners often do not directly benefit from implementation of BMP's, economic incentives through various cost-share programs should be initiated. Funding for these types of incentive would necessarily come from the state or federal level.

Figure 5.1 shows the close proximity of several major transportation routes as well as encroaching urbanization to the reservoir. Some roads are within 100 feet of the reservoir and indeed, one state highway crosses the reservoir via causeway at the western end. Roads are impervious to rainwater, and the build-up of grease, oils, and dirt result in considerable loadings of pollutants into the surface water. A long-range plan should address the proximities of these facilities as well as other potential pollution sources and mandate future siting of similar facilities further inland.

Land use planning boards should be especially attentive to the shoreline region of the reservoir as it is this area which has the greatest direct impact on the quality of runoff that enters the reservoir. The more land surrounding the reservoir that the MDC can acquire the easier will be the task of control. In addition to land purchasing, regulating land use for activities such as landfilling, hazardous waste storage, and public recreation should receive top priority in any management plan.

5.7.4 Water Quality Monitoring Plan

A rigorous monitoring plan must be in place to track trends in water quality and capture the impacts of different management techniques employed. Such a plan should stress readability, standardized sampling procedures, and highlight key summary information to facilitate the transfer of information to managers making decisions on daily operations. This data collected needs to be mounted on a compatible computer database for easy access by consultants in addition to the responsible agency.

The time scale and spatial distribution of monitoring stations as well as the specific constituents which are tested warrant attention. A recommendation for such a plan is presented specifying what should be monitored, how often, and where the station should be located.

In-Reservoir (Routine) – For routine in-reservoir monitoring, data should be collected every two weeks. Every effort should be made to continue monitoring during the winter to fully understand the physical, bio-chemical processes that exist. Sampling stations should be located longitudinally along the reservoir centerline with full depth profiles for each constituent sampled in at least 5 meter intervals. Major inflows and outflows should be included in this routine monitoring plan. In this way, the relative contribution from inflow/outflow to the reservoir balance can be computed for any constituent. This infers the routine monitoring of the Quabbin inflow waters as well as the outflows in the Cosgrove Aqueduct.

The following are minimum water parameters to be sampled on a regular basis (not less than every two weeks) throughout the year in order to build a good database:

* temperature	* chlorophyll a	* Kjeldahl Nitrogen
* hardness	* Secchi disc	* pH
* dissolved oxygen	* ammonia	* NO ₃ /NO ₂
* PO ₄	* total phosphorus	* SiO ₃
* coliform	* BOD ₅	* color and turbidity
* zooplankton	* algae by major group & by problem species	

Silica is significant due to the large diatom populations measured in the reservoir. Population dynamics is often limited by the amount of silica available for use in cell construction. Additionally, the 5-day biological oxygen demand would

help ascertain the oxygen deficit during periods of stratification. Currently, neither of these constituents are monitored.

In-Reservoir (Special) -- As resources permit, a broader field of sampled constituents should be undertaken at intervals that can be afforded but at least every 6 months. The stations used for this category of monitoring should be in addition to the stations monitored routinely and provide data on cross-sectional variability as well as filling in the gaps on the longitudinal axis. These more thorough sampling runs would include all the constituents of the routine sample plus:

- | | | |
|-----------------------------|---------------|---------------------------|
| * heavy metals | * sediments | * total organic carbon |
| * BOD ₂₀ | * fish survey | * total suspended solids |
| * speciation of zooplankton | | * large organic compounds |

Local Weather Data/Intake Shaft Level -- Local meteorological data should be monitored at the reservoir to eliminate extrapolation errors from the Worcester airport due to significant topography differences. Additionally, record of the withdrawal level of each intake in use is important for model refinement and calculation of mass balance for the various constituents. As the shafts are opened and closed for servicing or seasonal considerations, the action merely needs to record shaft number and time of change. Minimum data to be recorded and the respective time interval include:

- | | | |
|-------------------------|-------------------------------------|---------------------|
| * air temperature (H) | * wind speeds (H) | * precipitation (D) |
| * relative humidity (H) | * intake shafts used
(as needed) | * cloud cover (H) |

(H) = hourly
(D) = daily

Tributary Monitoring – As many tributaries as possible should be monitored. However, prioritization should be made with respect to volume of inflow and/or unusually high concentrations of any particular constituent. An initial sampling of all tributaries is suggested to determine a priority list in the event of resource constraints. As mentioned earlier, the Quabbin Aqueduct would be included as part of the in-reservoir sampling and other tributaries should be sampled at least monthly for the following constituents:

- | | | |
|------------------------------------|--------------------|--------------------|
| * dissolved oxygen | * BOD ₅ | * PO ₄ |
| * NO ₂ /NO ₃ | * temperature | * pH |
| * volume of flow | * hardness | * SiO ₃ |
| * coliform | * chlorophyll a | |

A comprehensive database is essential to making intelligent management decisions. Data manipulation characterizing trends and summarizing sampling results should be standard procedure and provide a "quick glance" information to management. Assignment of monitoring stations to either agency (MDC or MWRA) should provide continuity and consistency in sampling methods and constituents. It is important to remember that any modeling can only be as good as the data collected. From inconsistent and spotty data, only very speculative results can be expected. On the other hand, a complete and sound database used in conjunction with other known activities within the watershed (e.g., statistics on land use), can provide the key to understanding the ecological interrelationships effecting water quality and the necessary steps to take toward the abatement of eutrophication.

Chapter 6 Conclusion and Recommendations

6.1 Reservoir Water Quality Status

Wachusett Reservoir is a typical northeastern reservoir exhibiting complete mixing of the water column twice a year (dimictic). During the summer months (June thru September) Wachusett develops a strong stratification with vertical temperature differences of 10° – 15° C . The water quality has been consistently in the oligotrophic/mesotrophic range but increased development in the vicinity of Wachusett is causing a degradation of inflow waters through increased nutrient transport (especially phosphorus).

Algae blooms due to increased nutrient loadings into the reservoir appear to be an annual event and actions currently employed to combat them are reporting limited success. Sound and aggressive management initiatives are vital to the preservation of water quality. The seasonal dynamics of algae populations, shown in Figure 6.1, illustrates the growth of diatoms and flagellates in reverse cycles. Algae are shown by major grouping as a percentage of the total algae present in the upper layers. As diatoms are a cooler water species, it is consistent for them to display peak growth rates in the spring and fall. The diatoms exhibit a relatively rapid die-off after spring, to return in the fall with cooler temperatures and recirculation of nutrients. diatoms may be sufficient to explain the resulting summer oxygen deficit.

In order to ascertain causal relationships in the aquatic environment, water quality monitoring must provide data which allows descriptive parameters to be quantified. In order to initiate water quality modeling, information on reservoir loading concentrations of nutrients (e.g., phosphate, nitrate, nitrite, ammonia, and silica), dissolved oxygen, and BOD should be available. In addition, the vertical

distribution of the aforementioned constituents and any algae species that is of particular interest, must be part of routine sampling.

Currently, measurements of total phosphorus, orthophosphate, nitrate/nitrite, ammonia, dissolved oxygen, and a preponderance of algal species are available, however further gains could be made with regard to the consistency of sampling at standard depths/times and additional water quality parameters. Future studies should include specific problematic algal species (e.g., *Synura*) and provide comparisons of productivity to one of the major algae groups for modeling purposes. This will provide information which will assist in developing indicators as to bloom arrival and aid in judging the optimal time for algicide application.

Modeling population dynamics of algae with consideration of algicide treatments poses an interesting question. Since treatment is currently localized within a short radius of the intake, the impact of this outflowing water is minimized with regard to the rest of the reservoir. Hence, modeling could be conducted without regard to copper toxicity to phytoplankton and be representative of mid-reservoir conditions. However, should treatments be implemented at various areas throughout the reservoir, new modeling challenges will arise.

The reservoir maintains dissolved oxygen concentrations indicative of a relatively unproductive reservoir. However, after the onset of summer stratification an oxygen deficit of 5 to 6 mg O₂/l develops in the hypolimnion as shown in Figures 6.2 and 6.3. The consumption of oxygen may be the result of detritus which has settled to the bottom. However, other causes such as nitrification could be significant and warrant further investigation. Additionally, nutrient concentrations of phosphorus (PO₄) and nitrogen (NO₂ / NO₃ combined, and NH₃) are shown in Figure 6.4 – 6.6 respectively for measurements both at the surface and at-depth. It is interesting to note that phosphorus does not show an appreciable difference between

surface and hypolimnetic concentrations, whereas nitrite and nitrate do seem to indicate an accumulation in the hypolimnion during the stratification period.

6.2 Conclusions of the Hydrothermal Study

The basic objective of this study was to evaluate the hydrothermal processes of Wachusett Reservoir through the use of a numerical model. This study is key to any subsequent study in water quality since bio-chemical processes are closely coupled to the physical processes which distribute heat throughout the water column.

A one-dimensional (vertical) hydrothermal model has been calibrated and verified. It simulates temperature profiles throughout the portion of the year when the reservoir is stratified. Effects of operational strategies on the reservoir heat balance (e.g., change in level of withdrawal) can predict the impact on long-term (seasonal) variability in the water column.

From this preliminary investigation of water quality problems experienced at Wachusett, four key areas warrant serious attention as part of a comprehensive management plan:

- 1) From results of a one-dimensional model, significant impacts on the reservoir heat balance arise from changing the elevation of the outflow. Selective withdrawal is an operational technique which shows considerable promise for the net loss (or retention) of heat in the reservoir which directly influences water quality. Coupled with a rigorous monitoring program, selected withdrawal elevations can maximize the removal of nutrients thus reducing serious algal blooms and associated taste and odor problems.
- 2) The key to any effective program of resource management is an effective sampling program with distribution (both temporally and spatially) which provides timely data on ever changing conditions. Current monitoring by the MDC and

MWRA provides a good foundation for future data collection policies, however some recommendations listed below will improve the identification of source nutrient loadings as well as verify results of management initiatives taken with regard to water quality.

* Monitoring must provide more definitive information on the constituents and temperature of major inflows (Quabbin Aqueduct and Stillwater River) and outflows. Measurements of the same constituents conducted at in-reservoir stations should also be made for outflow water in the Cosgrove Aqueduct. Additionally, records of withdrawal shafts operation need to be maintained for use in future modeling efforts.

* Constituents that should be measured on a bi-weekly basis are listed in Section 5.7.4 . The current monitoring should be expanded to include silica, BOD, as well as consistency of algae species. Silica is important due to the large diatom population which may play a significant part in reservoir dynamics.

* Basic meteorological data should be monitored at Wachusett Reservoir, thus should include wind velocity, air temperature, relative humidity, and cloud cover.

3) Land use planning plays a major role in water resource protection and necessitates having a long-term perspective on management priorities. Maximum energies should be focused on the sources of nonpoint pollution and investment of control strategies to abate nutrient loadings into the reservoir. Zoning and restricted use of vulnerable land parcels (such as the shoreline) should receive attention, including existing roadways which abut the reservoir.

4) Studies which couple a water quality model to the results of the hydrothermal model should be conducted. With a calibrated water quality model,

simulation of reservoir dynamics can illustrate the interrelationships of various water quality parameters and reveal the driving mechanism behind these dynamics.

Currently, a water quality model exists which couples to the MIT Temperature Model used in this study and would be appropriate for application to Wachusett.

The model tested by Serrahima (1987) simulates the cycling of phosphorus, nitrogen, and silica, and includes simulation of dissolved oxygen and BOD, and the kinetics of three types of algae.

Through real time monitoring, an understanding of the interrelationships of the dynamic reservoir processes can be established. This provides a basis for intelligent decisions with regard to strategies for the improvement of the quality of water.

Further, as positive results are attained by certain operational decisions, less reliance on chemical algicides will be necessary for algae control and the better chance there is of maintaining a "healthy" trophic state in the reservoir.

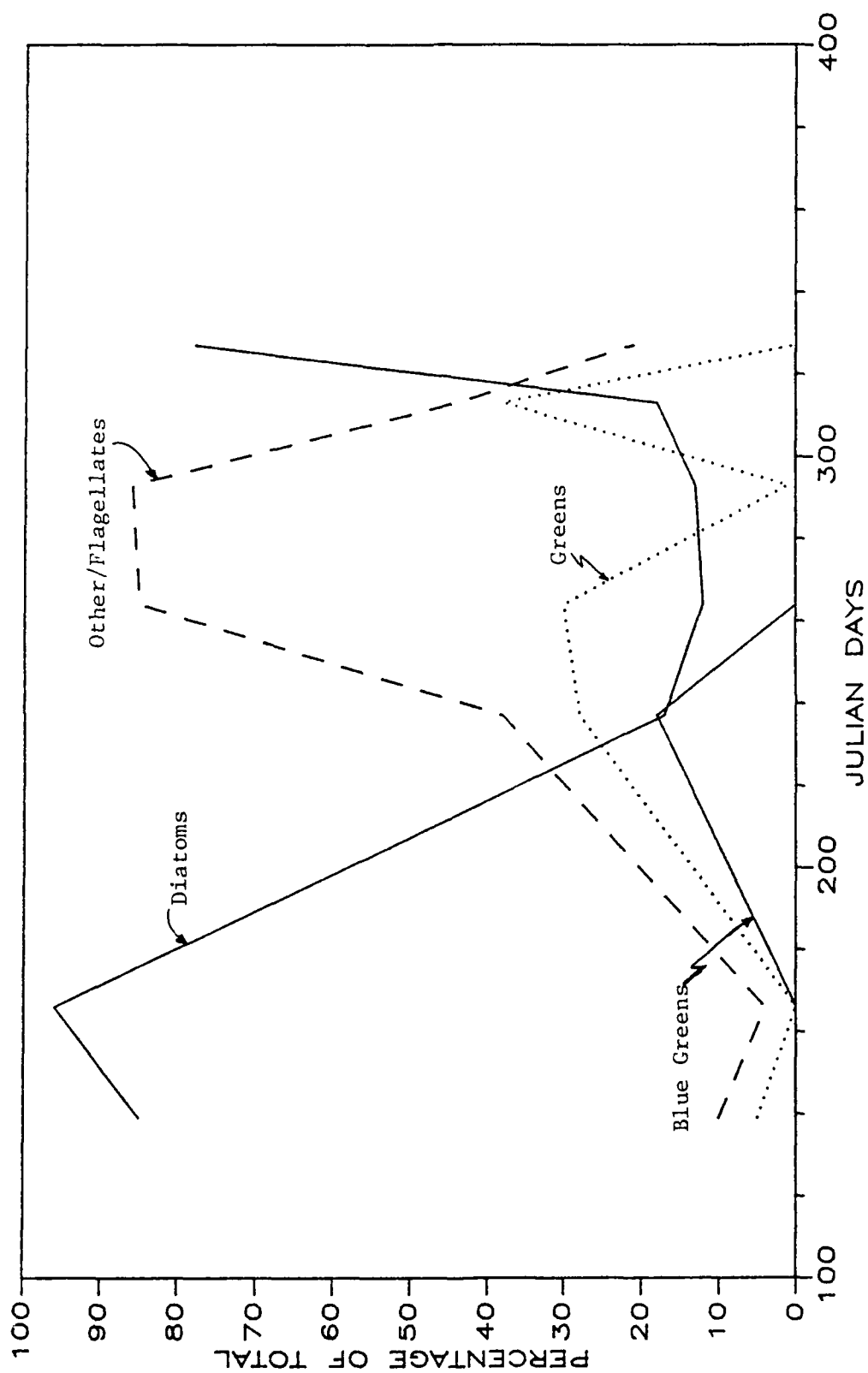


Figure 6.1 Relative percentage of algae in 10 ft. surface grab samples for 1987.

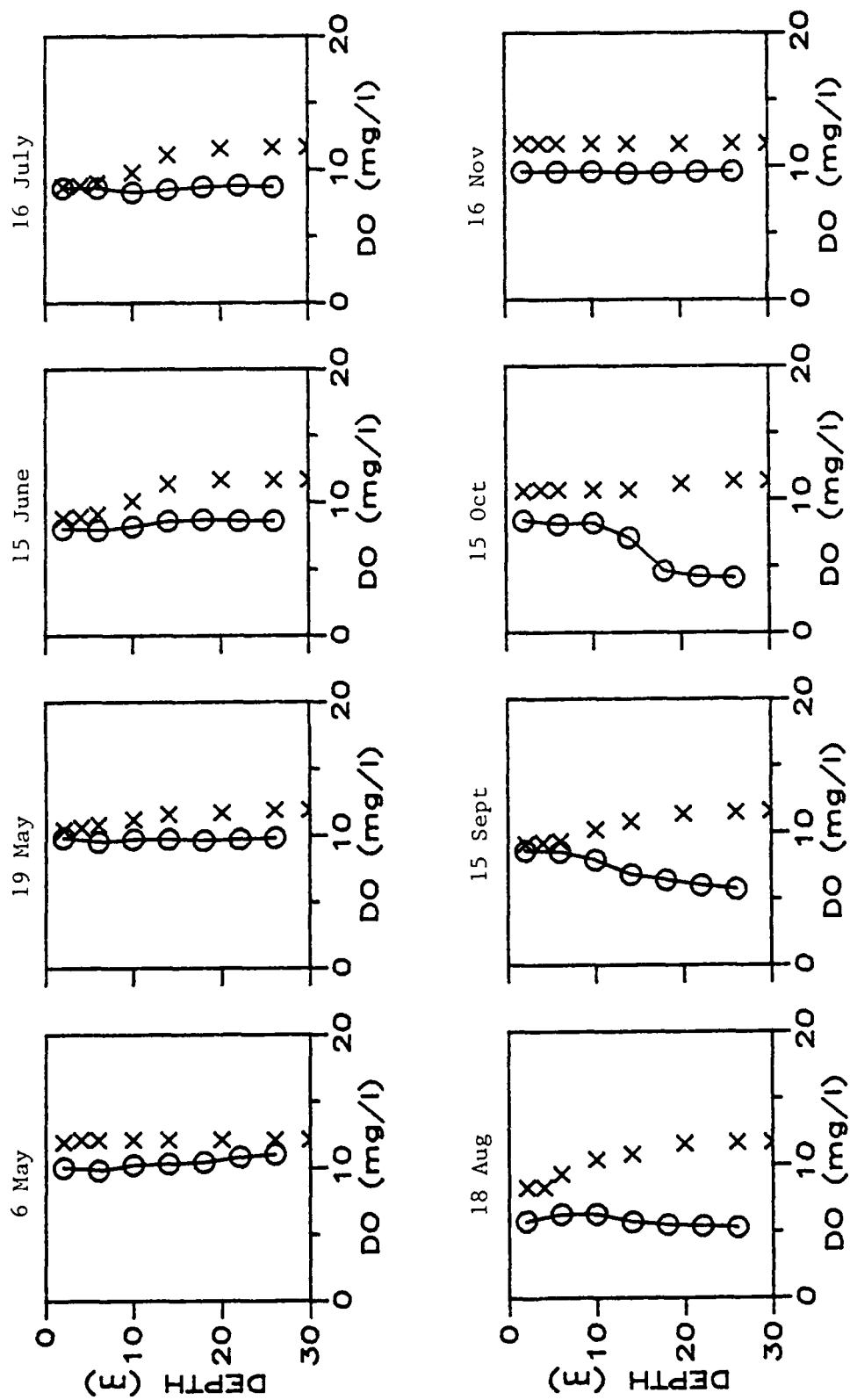


Figure 6.2 Dissolved oxygen profile for 1987. (Circles are measured, crosses are saturated values.)

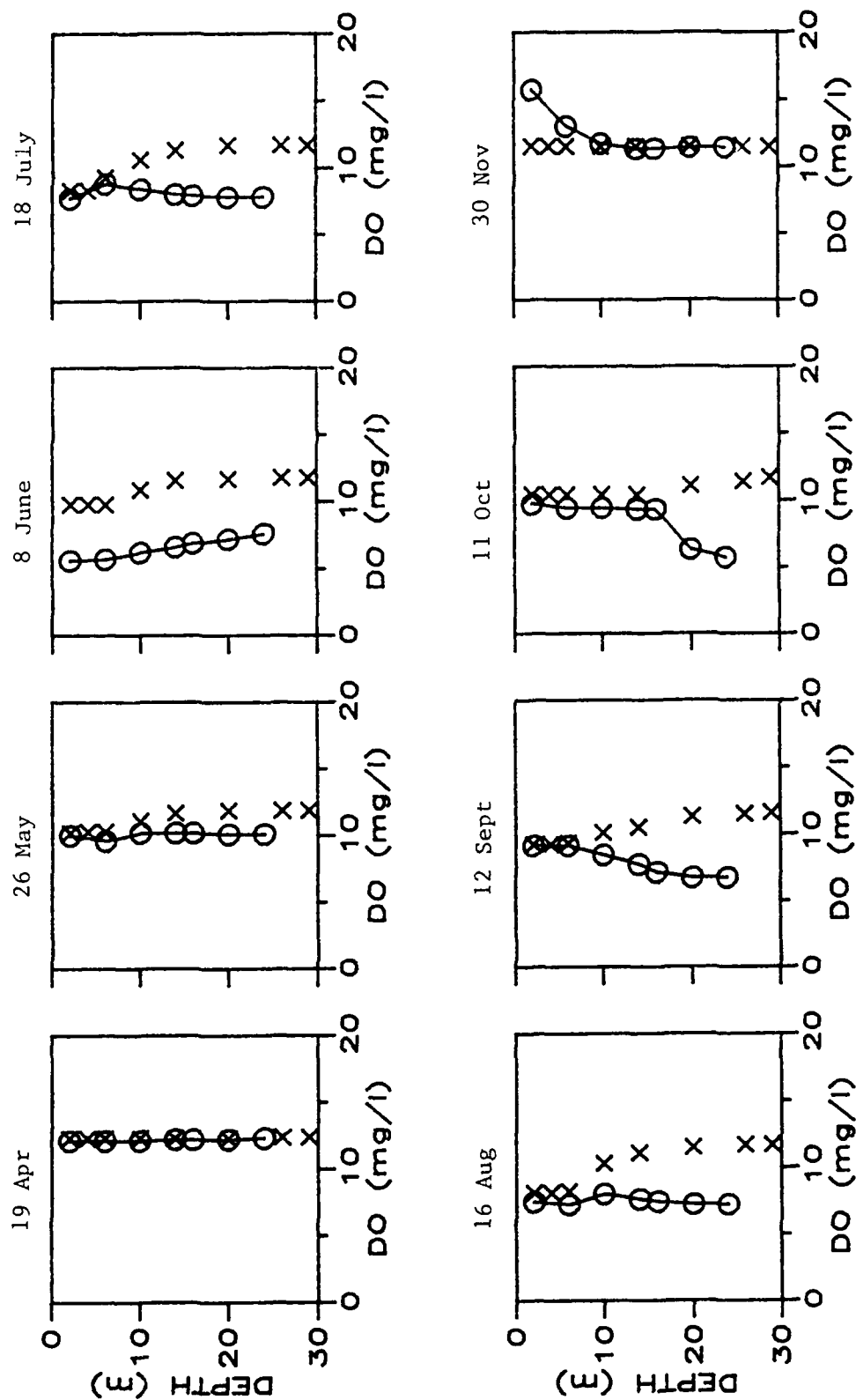


Figure 6.3 Dissolved oxygen profile for 1988. (Circles are measured, crosses are saturated values.)

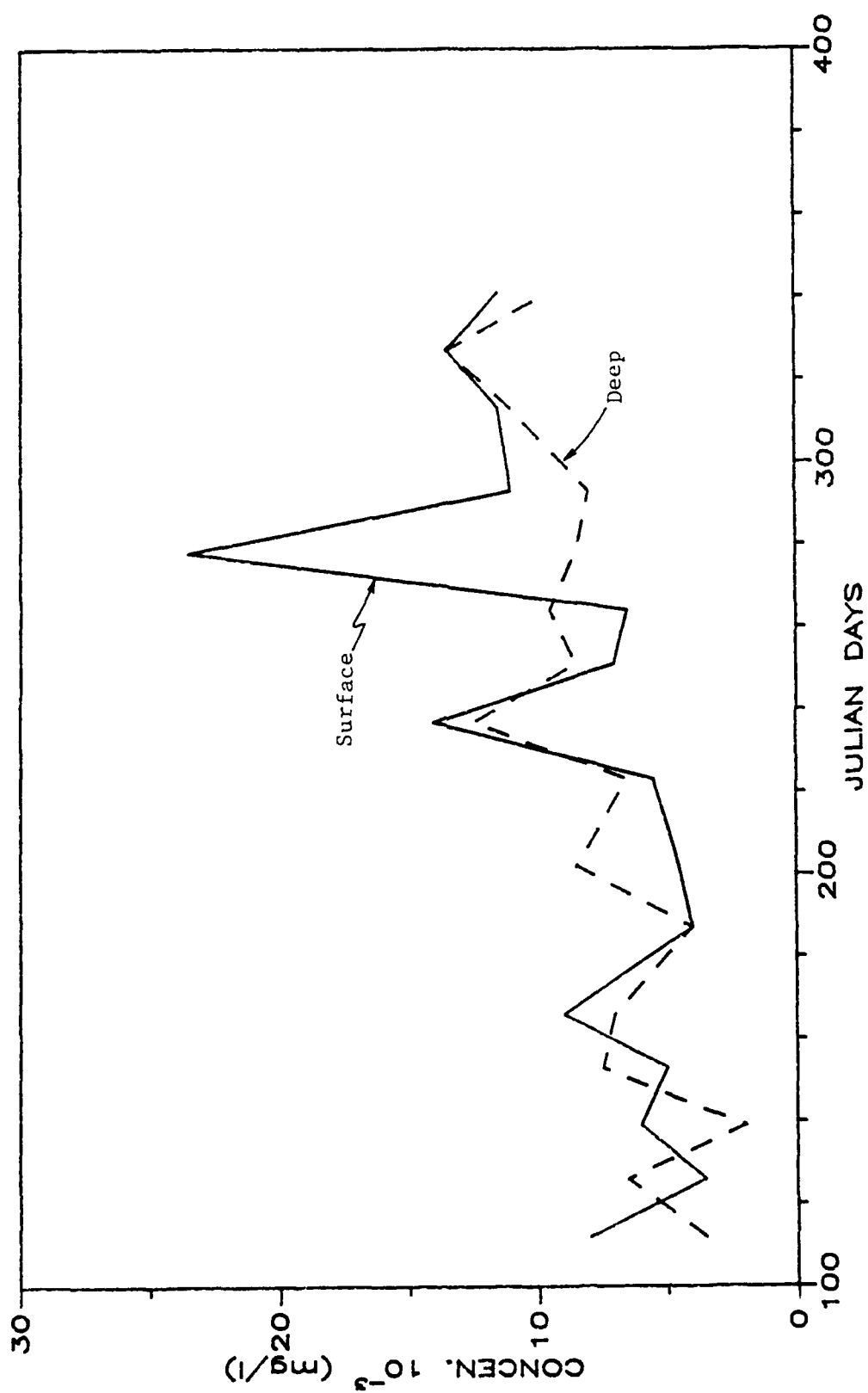


Figure 6.4 Phosphate (PO_4) concentration for 1987.

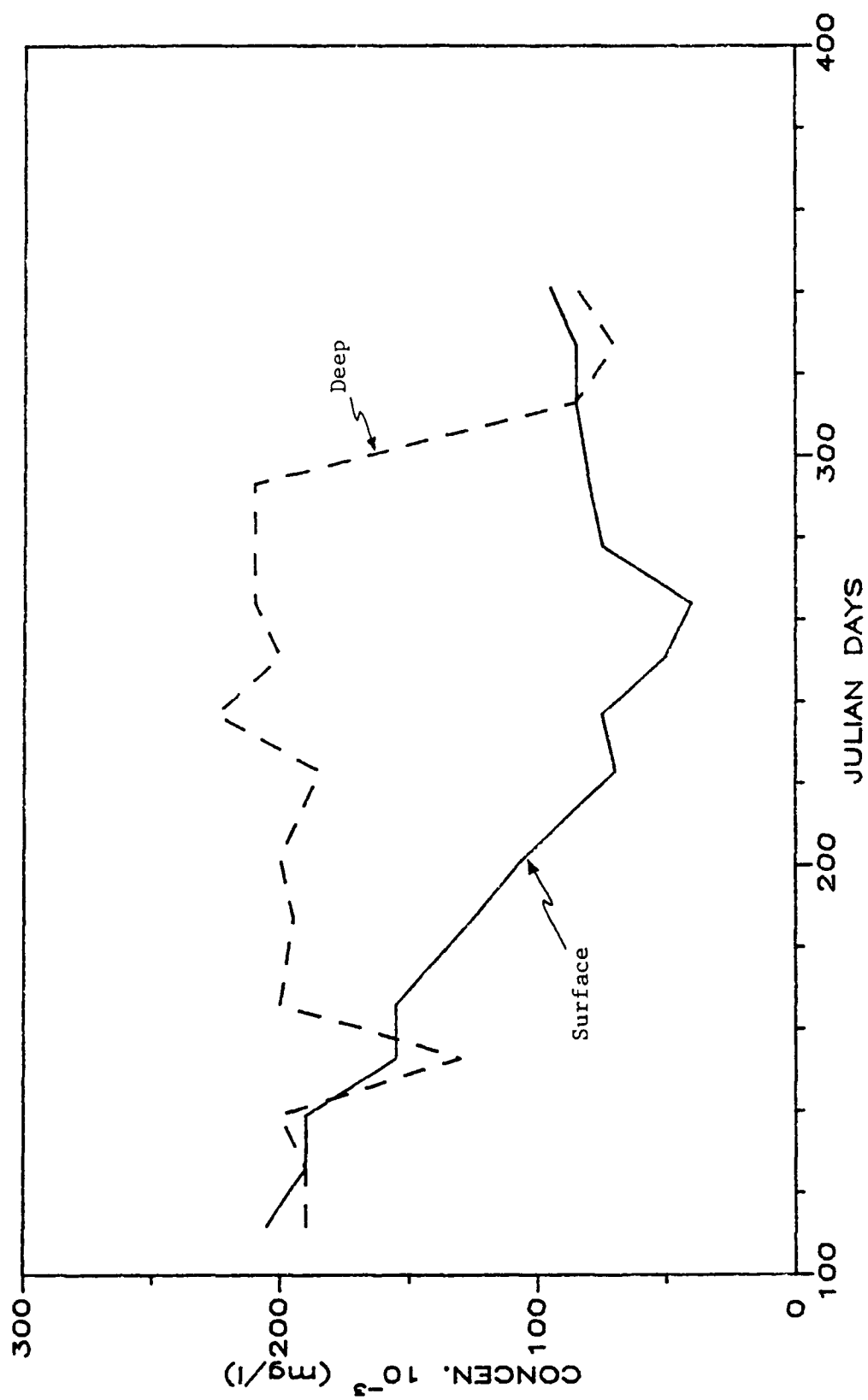


Figure 6.5 Nitrate/Nitrite concentrations for 1987.

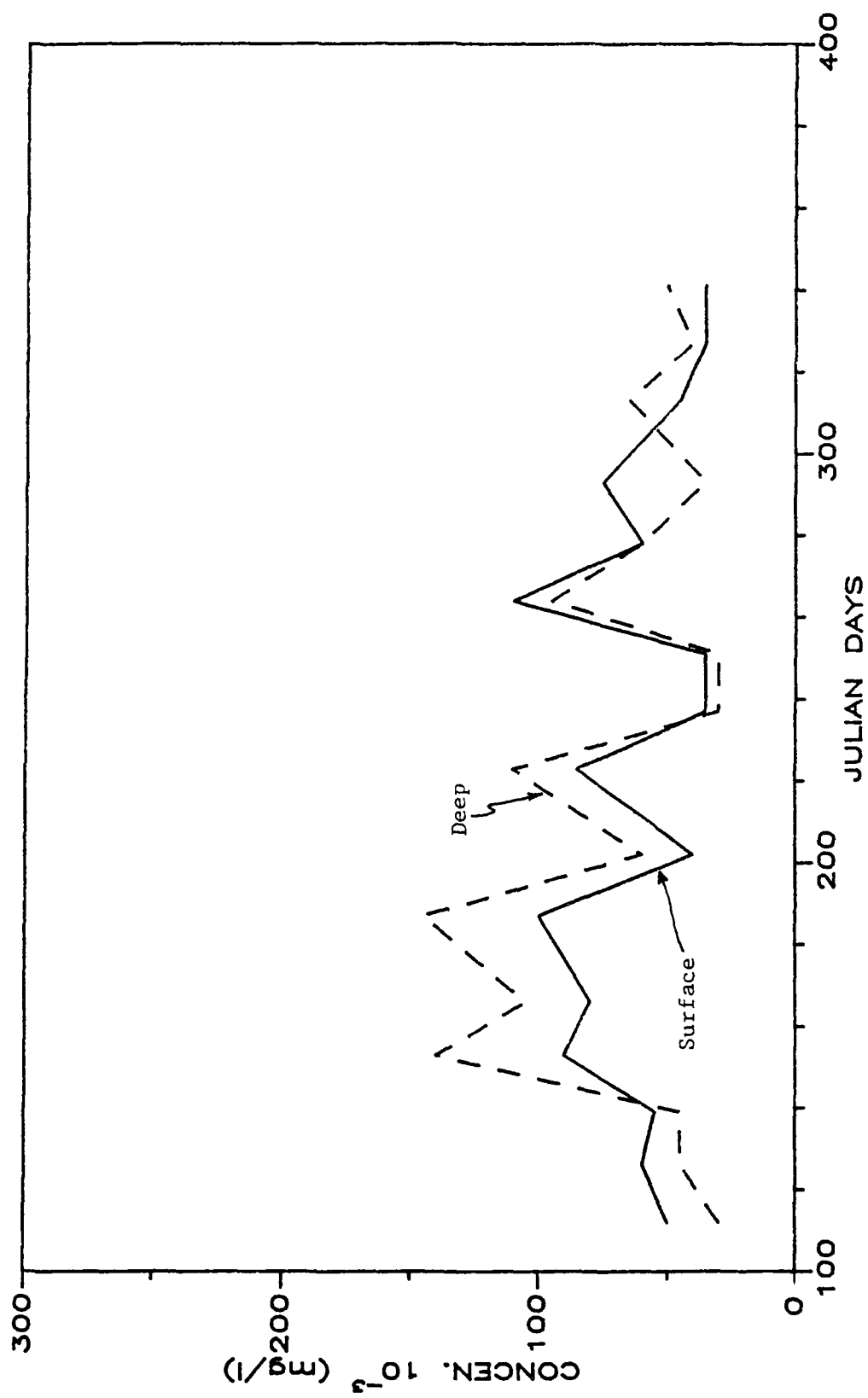


Figure 6.6 Ammonia concentration for 1987.

APPENDIX A

Day	Jan	Feb	Mar	Apr	May	June	July	Aug	Sep	Oct	Nov	Dec	Day
1	001	032	060	091	121	152	182	213	244	274	305	335	1
2	002	033	061	092	122	153	183	214	245	275	306	336	2
3	003	034	062	093	123	154	184	215	246	276	307	337	3
4	004	035	063	094	124	155	185	216	247	277	308	338	4
5	005	036	064	095	125	156	186	217	248	278	309	339	5
6	006	037	065	096	126	157	187	218	249	279	310	340	6
7	007	038	066	097	127	158	188	219	250	280	311	341	7
8	008	039	067	098	128	159	189	220	251	281	312	342	8
9	009	040	068	099	129	160	190	221	252	282	313	343	9
10	010	041	069	100	130	161	191	222	253	283	314	344	10
11	011	042	070	101	131	162	192	223	254	284	315	345	11
12	012	043	071	102	132	163	193	224	255	285	316	346	12
13	013	044	072	103	133	164	194	225	256	286	317	347	13
14	014	045	073	104	134	165	195	226	257	287	318	348	14
15	015	046	074	105	135	166	196	227	258	288	319	349	15
16	016	047	075	106	136	167	197	228	259	289	320	350	16
17	017	048	076	107	137	168	198	229	260	290	321	351	17
18	018	049	077	108	138	169	199	230	261	291	322	352	18
19	019	050	078	109	139	170	200	231	262	292	323	353	19
20	020	051	079	110	140	171	201	232	263	293	324	354	20
21	021	052	080	111	141	172	202	233	264	294	325	355	21
22	022	053	081	112	142	173	203	234	265	295	326	356	22
23	023	054	082	113	143	174	204	235	266	296	327	357	23
24	024	055	083	114	144	175	205	236	267	297	328	358	24
25	025	056	084	115	145	176	206	237	268	298	329	359	25
26	026	057	085	116	146	177	207	238	269	299	330	360	26
27	027	058	086	117	147	178	208	239	270	300	331	361	27
28	028	059	087	118	148	179	209	240	271	301	332	362	28
29	029		088	119	149	180	210	241	272	302	333	363	29
30	030		089	120	150	181	211	242	273	303	334	364	30
31	031		090		151		212	243		304		365	31

Julian Calendar (perpetual)

Appendix B

WACHUSETT RESERVOIR INPUT DATA FOR THE YEAR 1987 (MAY-NOV)

*VARIABLE NAMES COINCIDE WITH PROGRAM LISTING

*ALL UNITS IN METERS,DAYS,KILOCALORIES AND DEGREES CENTIGRADES

JM	KATRADKSUR	KOH	KQ	KLOSSNPRINT	KMIX	MIXED	KTRAVKSLRAD
18	2	2	2	1	2	1	1

XDAY
126

YSUR	DY	DT	STOP	EVAPCON
119.98	2.0	1.0	200.0	0.01

SPREAD	SIGMAI	BETA	RHO	HCAP	DELCON	RMIX	TEMPPDIF
1.96	3.0	0.5	997	0.998	.00461	1.0	0.0124

NTI	NTA	NSIGH	NTIN	NSURF	NQI	NQO	NOUT	NXTN	NTO
8.0	205	205	205	205	205	205	1	8	18

DTTI	DTTA	DTSIGH	DTFIN	DSURF	DTQI	DTQO	DTXTN
30.0	1.0	1.0	1.0	1.0	1.0	1.0	30.0

TI(I) INFLOW TEMPERATURES (TIME INTERVALS OF DTTI)

9.4	10.6	12.7	13.3	16.7	16.7	12.2	10.0
-----	------	------	------	------	------	------	------

TA(I) AIR TEMPERATURES (TIME INTERVALS OF DTTA)

20.6	18.3	16.1	11.1	12.7	13.3	11.1	20.0	15.0	12.7
11.1	13.9	18.3	14.4	8.9	11.1	16.1	12.7	19.4	25.0
25.6	26.7	24.4	18.3	16.1	13.9	18.9	15.0	13.9	18.9
17.8	16.1	16.7	16.7	23.3	21.7	25.0	22.2	18.3	19.4
22.8	23.9	21.7	20.6	15.0	18.3	16.1	13.9	17.2	17.8
20.0	23.9	21.1	17.8	16.1	22.8	21.1	20.6	17.2	19.4
23.9	27.2	25.0	25.0	25.6	22.8	19.4	17.2	19.4	22.8
21.7	20.6	23.3	23.9	24.4	26.7	26.1	22.8	20.6	20.0
18.3	18.9	15.6	20.0	18.3	21.7	24.4	22.8	20.0	20.0
22.8	19.4	15.6	18.9	18.9	18.9	19.4	21.7	24.4	26.1
25.6	22.8	21.1	20.0	18.9	16.7	14.4	15.6	18.3	13.3
12.7	12.2	16.1	17.2	16.1	13.3	15.0	15.0	17.2	18.3
18.9	21.7	22.2	22.2	17.2	16.1	16.7	18.3	16.7	17.2
18.3	12.2	11.1	11.1	13.9	15.6	15.0	14.4	8.9	10.6
12.2	17.2	20.6	16.1	10.6	11.7	14.4	5.0	8.9	14.4
15.6	8.9	6.1	12.2	5.0	4.4	6.7	8.9	11.1	12.2
12.7	13.9	11.7	12.2	10.0	5.5	7.7	11.1	8.3	6.7
7.2	10.6	5.5	5.5	8.3	7.2	6.7	10.0	17.2	10.0
0.0	0.0	6.7	11.7	2.8	-3.3	-6	3.3	7.2	4.4
5.5	9.4	12.7	5.0	1.7	-7.2	-6.1	-6	7.7	5.5
1.7	-1.7	0.0	1.1	8.9					

SIGH(I) RELATIVE HUMIDITY (TIME INTERVALS OF DTSIGH)

.455	.615	.720	.470	.550	.735	.410	.475	.605	.605
.530	.740	.750	.870	.865	.725	.700	.695	.810	.805
.750	.675	.720	.840	.810	.875	.740	.515	.530	.810
.670	.560	.465	.755	.775	.785	.640	.530	.485	.530
.590	.570	.650	.840	.875	.710	.840	.885	.950	.670
.635	.740	.600	.710	.865	.730	.695	.665	.665	.870
.810	.735	.810	.825	.855	.860	.635	.580	.510	.535
.605	.760	.765	.745	.680	.685	.695	.665	.510	.525
.565	.695	.540	.395	.605	.920	.715	.660	.685	.730
.645	.660	.935	.710	.590	.720	.705	.770	.750	.780
.695	.580	.635	.570	.800	.530	.450	.500	.535	.775
.880	.915	.690	.735	.740	.675	.625	.525	.615	.775
.905	.880	.880	.715	.905	.815	.965	.730	.615	.640
.740	.850	.880	.895	.890	.830	.730	.695	.555	.555
.530	.695	.660	.870	.700	.620	.805	.780	.640	.625
.770	.695	.580	.555	.755	.745	.600	.620	.610	.720
.720	.725	.680	.760	.855	.650	.650	.695	.725	.470
.735	.930	.660	.665	.680	.605	.635	.825	.705	.580
.465	.575	.585	.645	.905	.770	.665	.705	.660	.585
.715	.905	.710	.625	.750	.485	.415	.595	.730	.835
.910	.705	.660	.945	.965					

FIN(I) SHORT WAVE SOLAR INSOLATION (TIME INTERVALS OF DTFIN)

0.54452E+04	0.61459E+04	0.38275E+04	0.50403E+04	0.65960E+04
0.45061E+04	0.66279E+04	0.50892E+04	0.45387E+04	0.31610E+04
0.23422E+04	0.23477E+04	0.31837E+04	0.23589E+04	0.23625E+04
0.23665E+04	0.39553E+04	0.23741E+04	0.46303E+04	0.46381E+04
0.66387E+04	0.52296E+04	0.52382E+04	0.23971E+04	0.32483E+04
0.24050E+04	0.57587E+04	0.68370E+04	0.40216E+04	0.24122E+04
0.57761E+04	0.67230E+04	0.40338E+04	0.24195E+04	0.32759E+04
0.57965E+04	0.65189E+04	0.67468E+04	0.67495E+04	0.40486E+04
0.32839E+04	0.32852E+04	0.24293E+04	0.24304E+04	0.24313E+04
0.69438E+04	0.40535E+04	0.24283E+04	0.24277E+04	0.62124E+04
0.65252E+04	0.53066E+04	0.32795E+04	0.24231E+04	0.24221E+04
0.24214E+04	0.57815E+04	0.46944E+04	0.32550E+04	0.24007E+04
0.52434E+04	0.46547E+04	0.39805E+04	0.32202E+04	0.23754E+04
0.23691E+04	0.60489E+04	0.45887E+04	0.66718E+04	0.60009E+04
0.31629E+04	0.23316E+04	0.45278E+04	0.50756E+04	0.45035E+04
0.50481E+04	0.31125E+04	0.50223E+04	0.63686E+04	0.58434E+04
0.61242E+04	0.30716E+04	0.60915E+04	0.64531E+04	0.30471E+04
0.37484E+04	0.63598E+04	0.37230E+04	0.63487E+04	0.43087E+04
0.42908E+04	0.29692E+04	0.21855E+04	0.60563E+04	0.61515E+04
0.58057E+04	0.51377E+04	0.46745E+04	0.60705E+04	0.59993E+04
0.58504E+04	0.50038E+04	0.55950E+04	0.58723E+04	0.27836E+04
0.55048E+04	0.56646E+04	0.51840E+04	0.27248E+04	0.20036E+04
0.19927E+04	0.19822E+04	0.55959E+04	0.38180E+04	0.46661E+04
0.32362E+04	0.54745E+04	0.54447E+04	0.31801E+04	0.25619E+04
0.18819E+04	0.18697E+04	0.36168E+04	0.44166E+04	0.18335E+04
0.18213E+04	0.18095E+04	0.39321E+04	0.45665E+04	0.49285E+04
0.23786E+04	0.17453E+04	0.17325E+04	0.17197E+04	0.17068E+04
0.22917E+04	0.40228E+04	0.36455E+04	0.44401E+04	0.43985E+04

0.46286E+04	0.31250E+04	0.44231E+04	0.15743E+04	0.26015E+04
0.42957E+04	0.25505E+04	0.15134E+04	0.42873E+04	0.41402E+04
0.28719E+04	0.37430E+04	0.41407E+04	0.36772E+04	0.14236E+04
0.14108E+04	0.39950E+04	0.39508E+04	0.39065E+04	0.38626E+04
0.29248E+04	0.36760E+04	0.37057E+04	0.12900E+04	0.12745E+04
0.35038E+04	0.20751E+04	0.29427E+04	0.32710E+04	0.34357E+04
0.11887E+04	0.11749E+04	0.32319E+04	0.25115E+04	0.30497E+04
0.26805E+04	0.31407E+04	0.10926E+04	0.30632E+04	0.17830E+04
0.30043E+04	0.25082E+04	0.14043E+04	0.10278E+04	0.10176E+04
0.10074E+04	0.19418E+04	0.16469E+04	0.16332E+04	0.27009E+04
0.23027E+04	0.15920E+04	0.25445E+04	0.26789E+04	0.92943E+03
0.22043E+04	0.26085E+04	0.17617E+04	0.14970E+04	0.88962E+03
0.88205E+03	0.11835E+04	0.24135E+04	0.85968E+03	0.85211E+03

SURF(I) RESERVOIR SURFACE ELEVATIONS (MEASURED- TIME INTERVALS OF DSURF)

119.98	119.96	119.93	119.90	119.87	119.83	119.79	119.75	119.70	119.66
119.61	119.56	119.52	119.47	119.41	119.37	119.33	119.27	119.23	119.16
119.13	119.08	119.02	118.95	118.90	118.84	118.80	118.75	118.69	118.63
118.58	118.51	118.44	118.37	118.36	118.44	118.50	118.54	118.59	118.63
118.67	118.71	118.75	118.79	118.85	118.89	118.95	118.99	118.98	118.97
118.92	118.85	118.78	118.71	118.66	118.60	118.54	118.48	118.40	118.41
118.47	118.51	118.56	118.59	118.65	118.69	118.73	118.77	118.80	118.84
118.88	118.91	118.94	118.98	119.00	119.04	118.97	118.88	118.80	118.71
118.63	118.54	118.45	118.45	118.48	118.52	118.58	118.62	118.65	118.68
118.72	118.75	118.83	118.88	118.92	118.95	118.92	118.84	118.75	118.67
118.58	118.49	118.40	118.41	118.44	118.47	118.50	118.53	118.56	118.59
118.64	118.70	118.75	118.80	118.83	118.87	118.91	118.95	118.91	118.83
118.76	118.69	118.65	118.58	118.50	118.50	118.55	118.65	118.69	118.73
118.77	118.82	118.93	119.00	119.08	119.04	118.98	118.91	118.84	118.78
118.71	118.63	118.58	118.52	118.47	118.41	118.35	118.32	118.31	118.26
118.20	118.14	118.08	118.01	117.95	117.90	117.94	117.99	118.05	118.10
118.16	118.22	118.27	118.33	118.39	118.45	118.50	118.56	118.62	118.67
118.72	118.82	118.89	118.95	118.93	118.87	118.81	118.76	118.70	118.63
118.57	118.51	118.44	118.38	118.36	118.37	118.46	118.51	118.57	118.64
118.70	118.76	118.83	118.88	118.94	118.93	118.87	118.81	118.75	118.69
118.63	118.59	118.54	118.48	118.45					

QI(I) RESERVOIR INFLOW RATES (M3/SEC) (TIME INTERVALS OF DTQI)

8.81	8.21	6.91	6.90	6.76	6.29	5.84	5.84	5.85	4.69
4.60	4.57	4.61	4.02	4.69	4.43	4.86	4.89	4.34	9.51
4.03	5.22	3.57	4.65	3.95	6.50	5.22	4.12	4.20	5.00
2.28	3.09	2.92	14.44	29.11	24.99	24.40	24.27	23.74	23.62
24.70	24.27	23.74	27.24	23.90	24.31	23.44	12.15	14.69	5.60
3.62	2.74	3.48	5.81	4.12	2.77	3.56	1.91	19.33	25.73
25.23	24.50	23.74	26.51	24.01	24.01	23.68	22.82	23.79	23.59
23.19	23.16	23.63	23.66	23.12	5.57	1.78	1.76	0.79	1.34
1.74	1.08	19.32	23.16	24.72	25.14	22.34	22.13	22.47	23.06
21.22	28.47	23.40	22.49	21.73	4.95	0.82	0.25	1.02	0.74
1.11	0.57	17.67	22.59	21.95	20.89	21.30	21.13	21.58	23.90
25.46	24.44	22.82	21.84	22.45	21.31	22.32	7.25	0.17	0.27

1.57	6.06	2.67	0.97	15.58	22.48	31.74	23.08	22.15	23.10
23.65	33.80	28.16	28.56	6.24	3.13	2.06	1.69	1.63	1.24
1.33	2.12	2.97	4.51	2.38	2.16	8.75	12.67	5.07	4.10
4.66	4.29	2.05	2.43	3.90	20.32	23.94	23.89	23.96	23.56
23.40	23.19	23.31	23.29	24.18	19.90	23.08	24.54	22.33	22.07
31.01	26.26	26.67	9.88	1.96	2.09	2.94	2.40	2.47	2.45
0.67	1.08	1.76	9.50	15.78	29.00	23.93	24.45	25.06	24.50
25.08	25.71	22.91	24.61	10.72	0.88	2.26	2.23	3.40	2.68
4.87	3.95	2.69	6.65	8.39					

QO(I) RESERVOIR OUTFLOW RATES (M3/SEC)- (TIME INTERVALS AT DTQO)

13.40	13.40	13.25	13.25	13.70	13.85	13.95	13.95	13.95	13.95
13.85	13.80	13.85	13.80	13.30	12.45	15.20	14.75	15.20	14.65
14.85	16.20	16.80	14.85	14.70	14.40	14.25	14.85	14.85	15.10
15.15	15.35	15.70	15.10	14.60	15.20	16.00	15.80	15.85	16.25
17.35	17.50	16.35	15.95	15.45	14.60	14.90	15.05	15.25	15.20
16.05	16.85	16.15	15.00	14.25	14.80	15.05	15.90	16.55	15.65
16.80	17.25	16.45	16.15	16.70	16.70	16.30	16.05	16.45	17.35
17.45	16.90	17.35	17.35	17.35	17.90	18.10	17.05	17.15	17.60
17.90	17.85	17.60	16.65	16.50	15.05	15.55	15.90	16.25	16.30
15.55	14.35	13.80	14.90	14.90	14.95	15.45	15.95	16.10	16.90
17.25	17.15	16.90	16.85	15.65	15.15	15.75	15.95	15.30	14.80
14.05	14.15	14.80	14.90	14.95	14.95	14.80	14.50	14.15	14.15
13.75	14.45	14.80	15.35	14.95	13.95	13.70	15.00	14.65	14.75
15.05	13.85	13.60	13.60	14.60	14.30	13.80	14.00	13.95	13.50
13.00	13.75	14.15	13.40	13.45	13.80	14.25	14.30	14.45	14.60
14.50	14.15	13.70	13.40	12.60	13.65	13.95	13.85	13.90	13.50
12.75	12.55	12.60	12.60	12.90	12.95	12.95	13.25	12.70	13.00
12.95	12.60	13.15	12.70	13.20	13.25	13.65	13.60	13.55	13.50
12.95	12.75	12.85	13.35	13.50	13.30	13.25	13.20	13.20	13.20
13.15	13.15	13.15	13.15	13.00	12.75	12.95	13.45	13.45	13.25
13.15	12.75	12.70	12.20	12.25					

LOUT (GRID LEVEL OF OUTLET)

13

ELOUT (ELEVATION OF OUTLET)

111.0

XTN(I) EXTINCTION COEFFICIENTS- (TIME INTERVAL OF DTXTN)

.35 .46 .37 .30 .33 .35 .32 .32

GRAV (M/DAY2)

73156608000

VISCOS

0.0864

THICK1

.0001

THICK2

.0001

NAA

20

NXXL

20

NWIND

205

NATRAD

0

JMP

18

DAA	DXXL	DZTO	DTWIND	DATRAD	AAB	XXLB	DDZTO
1.829	1.829	2.0	1.0	1.0	86.9	86.9	87.0

AA(I) AREAS PER SCHEMATIZATION- (M2)

0.0	370284.	891303.	1467883.	2089166.	3079904.	3962954.	4837720.
5810234.	6657871.	7493081.	8100696.	8757599.	9574585.	10587897.	
11528104.	13007999.	14729573.	16057254.	16747292.			

XXL(I) LENGTHS PER SCHEMATIZATION- (M)

0.0	4743.	6665.	7884.	8250.	8656.	9469.	9591.	9631.	9672.
9712.	9733.	9753.	9786.	9814.	9819.	9826.	9831.	9835.	9844.

WIND(I) WIND SPEEDS (M/SEC)- (TIME INTERVAL OF NWIND)

5.50	4.30	3.70	3.58	4.23	6.30	4.60	4.55	2.35	2.15
2.85	3.44	6.80	4.15	2.80	1.45	2.40	3.40	5.45	3.25
4.60	4.25	3.35	3.09	2.95	2.00	3.05	4.80	3.85	4.10
5.90	5.65	4.75	6.05	3.65	4.10	4.25	3.70	3.85	2.55
4.15	2.35	1.45	1.95	3.65	3.30	4.30	2.30	1.55	4.35
5.20	4.65	2.35	2.90	2.10	4.35	3.05	3.25	3.18	2.85
2.80	1.55	1.95	2.55	2.60	4.11	4.92	2.54	2.54	4.56
2.99	3.93	3.63	1.83	2.46	4.20	3.30	5.14	4.11	2.91
2.45	3.49	3.08	2.90	3.13	4.15	2.63	2.68	2.68	2.41
4.10	2.50	2.90	4.38	2.19	2.05	3.08	4.02	4.02	4.02
3.97	2.68	4.11	3.35	5.00	5.23	4.33	4.33	3.12	2.23
2.50	3.26	2.77	4.65	3.71	3.12	2.72	2.27	3.21	3.76
3.62	2.99	3.71	2.68	2.59	2.95	2.86	4.11	3.22	4.20
2.50	4.82	5.63	5.72	2.73	1.43	3.35	4.07	4.38	4.91
2.86	5.05	4.60	3.89	5.54	5.45	3.40	8.04	3.53	3.67
3.75	4.82	4.52	4.34	3.44	2.59	3.80	2.19	1.97	2.59
2.55	3.21	3.04	2.95	3.98	5.10	3.89	4.16	6.26	3.44
4.07	4.29	5.19	4.47	4.52	2.77	2.90	7.24	5.05	6.48
8.99	6.75	5.59	4.87	4.11	7.24	8.54	4.07	3.76	2.23
2.37	4.20	7.55	4.16	3.76	8.14	6.67	4.42	3.80	2.59
3.67	2.86	1.34	2.86	3.49					

DCLOUD
1.0

NCLOUD
205

CLOUD(I) CLOUD COVER (FRACTION OF SKY)

0.50	0.30	0.80	0.60	0.00	0.70	0.00	0.60	0.70	0.90
1.00	1.00	0.90	1.00	1.00	1.00	0.80	1.00	0.70	0.70
0.20	0.60	0.60	1.00	0.90	1.00	0.50	0.10	0.80	1.00
0.50	0.20	0.80	1.00	0.90	0.50	0.30	0.20	0.20	0.80
0.90	0.90	1.00	1.00	1.00	0.00	0.80	1.00	1.00	0.40
0.30	0.60	0.90	1.00	1.00	1.00	0.50	0.70	0.90	1.00
0.60	0.70	0.80	0.90	1.00	1.00	0.40	0.70	0.10	0.40
0.90	1.00	0.70	0.60	0.70	0.60	0.90	0.60	0.20	0.40
0.30	0.90	0.30	0.00	0.90	0.80	0.10	0.80	0.00	0.70
0.70	0.90	1.00	0.20	0.10	0.30	0.50	0.60	0.00	0.10
0.20	0.50	0.30	0.10	0.90	0.30	0.20	0.40	0.90	1.00

1.00	1.00	0.10	0.70	0.50	0.80	0.10	0.10	0.80	0.90
1.00	1.00	0.70	0.50	1.00	1.00	1.00	0.60	0.40	0.20
0.90	1.00	1.00	1.00	1.00	0.90	0.50	0.60	0.30	0.30
0.00	0.70	0.20	1.00	0.80	0.20	0.80	1.00	0.00	0.20
0.70	0.40	0.00	0.40	1.00	1.00	0.00	0.00	0.00	0.00
0.60	0.20	0.10	1.00	1.00	0.20	0.80	0.50	0.30	0.00
1.00	1.00	0.20	0.60	0.30	0.50	0.10	1.00	0.10	0.80
0.10	0.50	0.90	1.00	1.00	1.00	0.70	0.80	0.80	0.20
0.50	0.80	0.30	0.00	1.00	0.50	0.00	0.70	0.80	1.00
1.00	0.90	0.20	1.00	1.00					

TT(I) INITIAL TEMPERATURE CONDITIONS (DATE= XDAY)

7.5	7.5	7.5	7.5	7.5	7.5	7.7	7.9	7.9	7.9
7.9	7.9	7.9	7.9	8.0	8.0	8.1	8.4		

WGHT (WIND HEIGHT M)

5.0

WIND MIXING PARAMETERS:

INDICE	IDFFLG	FACVI	CD	CT	CW	CCON
0	1	.5	.038	5.64	4.0	.5

NWRITE

2

PLOT

2

NNJUL (# OF DATES TO PRINT)

8

NJUL(I) (JULIAN DATES TO PRINT RESULTS)

128 139 166 197 230 258 288 320

NERROR

2

MMJUL

0

NPROF

0

Appendix C

```

C DATE: 5/19/89
C WATER QUALITY PROGRAM INACTIVE
C
C RESERVOIR STRATIFICATION PROGRAM (1971)
C REVISED (1986-1987)
C
C RESERVOIR TEMPERATURE AND WATER QUALITY MODEL
C STATE VARIABLES INCLUDED IN THE MODEL ARE :
C     1)TEMPERATURE
C     2)DISSOLVED OXYGEN
C     3)BIOCHEMICAL OXYGEN DEMAND
C     4)ALGAE      : ALGAE1
C                   ALGAE2
C                   ALGAE3
C                   TOTAL ALGAE (1+2+3)
C     5)NUTRIENTS : PHOSPHORUS (P-PO4)
C                   SILICA      (SiO3)
C                   NITROGEN  - NITRATE (N-NO3)
C                             - NITRITE (N-NO2)
C                             - AMONNIA (N-NH4)
C
C*****
C Input variables are defined here, grouped according to the read on which      *
C they appear. Where options are available asterisks indicate the option        *
C recommended for reservoirs.                                                    *
C*****
C Wherever PO4, NH4, NO2, and/or NO3 appear, they represent the element (P or N) *
C as either phosphate (P-PO4), ammonia (N-NH4), nitrite (N-NO2) or nitrate (N-NO3)*
C*****
C read # 1 :
C     WH  = alphanumeric var. used to print the title at the beginning
C           of the output.
C read # 2 :
C     WH  = alphanumeric variable used to list the units used in the model
C read # 3 :
C     JM  = initial number of layers (or grid points)
C     KATRAD = 1 atmospheric radiation is read in                                (**)
C           = 2 atmospheric radiation is calculated with Swinsbank's eqn.
C           = 3 " " " " " " " " Brutsaerts' "
C     KSUR = 1 for a constant surface elevation
C           = 2 for a variable surface elevation                                (**)
C     KOH  = 1 for use of Koh's eqn. for computing withdrawal thickness
C           = 2 for use of Kao's eqn. " " " " " " " " " " (**)
C     KQ   = 1 for computations with inflow and outflow                        (**)
C           = 2 for computations w/o inflow and outflow
C     KLOSS = 1 for Kohler field evaporation formula
C           = 2 for Rowher " " " " " " " " " " (**)
C           = 3 for Lake Hefner " " " " " " " " " "
C     NPRINT = number of time steps between prints out of daily calculations
C              used only when NWRITE = 1 (read #56), else set to 1

```



```

C    KMIX  = 1 for no entrance mixing
C          = 2 for entrance mixing                                (**)
C    MIXED = number of grid espases in surface layer for entrance mixing
C    KTRAV = 1 travel time within reservoir is neglected          (**)
C          = 2 " " " " " is accounted for
C    KSLRAD = 1 solar radiation is read in                        (**)
C          = 2 solar radiation is calculated in the program
C    XDAY  = Julian day corresponding to the initial day used
C read # 4 :
C    YSUR  = initial surface elevation (m)
C    DY    = vertical increment (m)
C    DT    = time step (days)
C    TSTOP = time stepchl at which program ceases calculation
C    EVPCON = constant in evaporation formula for KLOSS=2 (EVPCON=0.01)
C read # 5 :
C    SPREAD = number of outflow standard deviations, equal to half the
C            withdrawal thickness (SPREAD=1.96)
C    SIGMAI = inflow standard deviation
C    BETA   = fraction of solar radiation absorbed at the surface
C    RHO    = water density (RHO= 997.0 kg/m3)
C    HCAP   = water specific heat (HCAP= 0.998 kcal/kg)
C    DELCON = half the value of the constant used to predict the withdrawal
C            thickness (DELCON= 0.00461 for KOH=2)
C    RMIX   = mixing ratio (RMIX= 1.0)
C    TEMDIF = molecular heat diffusion coefficient (TEMDIF= 0.0125 m2/day)
C read # 6 :
C    NTI    = number of inflow temperatures to be read in
C    NTA    = "      air      temperatures      "
C    NSIGH  = "      relative humidities      "
C    NFIN   = "      insolation values      "
C    NSURF  = "      surface elevations      "
C    NQI    = "      inflow rates      "
C    NQO    = "      outflow rates      "
C    NOUT   = "      outlets      "
C    NXTN   = "      extinction coefficients      "
C    NTO    = "      initial temperatures      "
C read # 7 :
C    DTTI   = time interval between input values of TI (days)
C    DTTA   = "      "      "      "      "      "      TA (days)
C    DTSIGH = "      "      "      "      "      "      SIGH (days)
C    DTFIN  = "      "      "      "      "      "      FIN (days)
C    DSURF  = "      "      "      "      "      "      SURF (days)
C    DTQI   = "      "      "      "      "      "      QI (days)
C    DTQO   = "      "      "      "      "      "      QO (days)
C    DTXTN  = "      "      "      "      "      "      XTN (days)
C read # 8 :
C    TI     = values of inflow temperature (C)
C read # 9 :
C    TA     = values of air temperature (C)
C read #10 :
C    SIGH   = values of relative humidities (0 to 1)

```

```

C read #11 : (if KSLRAD=2,omit)
C   FIN   = values of insolation (kcal/m2-day)
C read #12 : (if KSLRAD=1,omit)
C   XLAT  = reservoir latitude
C   ELMAX = reservoir maximum elevation
C   RG    = ground reflectivity
C   DDPL  = dust depletion factor
C read #13 :
C   SURF  = values of surface elevations (m)
C read #14 :
C   QI    = values of inflow rates (m3/sec)
C read #15 :
C   QO    = values of outflow rates (m3/sec)
C read #16 :
C   LOUT  = number of grid points corresponding to outlet elevations
C read #17 :
C   ELOUT = outlet elevations (m)
C read #18 :
C   XTN   = values of extinction coefficient (1/m)
C read #19 :
C   GRAV  = acceleration due to gravity (GRAV=7.315E10 m/day2)
C   VISCOS = kinematic viscosity of water (0.0864 m2/day)
C read #20 : (set both to 0.0 if KTRAV=1)
C   THICK1 = observed thickness of inflow layer when traveling along the
C           reservoir bottom
C   THICK2 = observed thickness of inflow layer when traveling horizontally
C read #21 :
C   NAA    = number of areas to be read in
C   NXXL   = number of lengths to be read in
C   NWIND  = number of wind values to be read in
C   NATRAD = number of atmospheric radiation values to be read in
C   JMP    = number of grid points for which the program should be initialized
C           (maximum value of JM expected to occur in the calculations)
C read #22 :
C   DAA    = vertical distance interval between input values of AA (m)
C   DXXL   = " " " " " " " of XXL (m)
C   DZTO   = " " " " " " " of TO (m)
C   DTWIND = time interval between input values of WIND (days)
C   DATRAD = " " " " " " of ATRAD (days)
C   AAB    = elevation of first (lowest) value of AA (m)
C   XXLB   = " " " " " of XXL (m)
C   DDZTO  = " " " " " of TO (m)
C read #23 :
C   AA     = values of horizontal cross-sectional areas (m2)
C read #24 :
C   XXL    = values of reservoir lengths (m)
C read #25 :
C   WIND   = values of wind speed (m/s)
C read #26 : (if KATRAD=2, omit)
C   ATRAD  = values of atmospheric radiation (kcal/m2-day)
C read #27 : (if both KATRAD =1 and KSLRAD=1, omit)

```

C DCLOUD = time interval between input values of CLOUD (days)
 C NCLLOUD = number of sky cover values to be read in
 C read #28 : (only if read #27 holds)
 C CLOUD = values of sky covered by clouds
 C read #29 :
 C TO = initial temperature values (C)
 C read #30 :
 C WGHT = wind measurement height above reservoir level (m)
 C read #31 :
 C NDISSO = number of inflow DO values to be read in
 C NBOD = " " " BOD " " " " "
 C NSIL = " " " SiO3 " " " " "
 C NPHOS = " " " PO4 " " " " "
 C NNIT = " " " NO3 " " " " "
 C NAMON = " " " NH4 " " " " "
 C NNO2 = " " " NO2 " " " " "
 C read #32 :
 C DDOC = time interval between read in values of DO (days)
 C DBOD = " " " " " " " BOD (days)
 C DSIL = " " " " " " " SiO3 (days)
 C DPHOS = " " " " " " " PO4 (days)
 C DNIT = " " " " " " " NO3 (days)
 C DAMON = " " " " " " " NH4 (days)
 C DNO2 = " " " " " " " NO2 (days)
 C read #33 :
 C DO = values of inflow DO (mg/l)
 C read #34 :
 C BOD = " " " BOD (mg/l)
 C read #35 :
 C SIL = " " " SiO3 (mg/l)
 C read #36 :
 C PHOS = " " " PO4 (mg/l)
 C read #37 :
 C ANIT = " " " NO3 (mg/l)
 C read #38 :
 C AMON = " " " NH4 (mg/l)
 C read #39 :
 C ANO2 = " " " NO2 (mg/l)
 C read #40 :
 C ZKBOD = BOD first order decay rate (1/day)
 C BENTHC = benthic uptake coefficient (g O2/m2-day)
 C TBASE = temperature at which rate constants are specified (C)
 C SPEDIF = mass diffusion coefficient (m2/day)
 C XAIR = reaeration coefficient weighting factor
 C read #41 :
 C GROW1 = maximum growth rate for algae #1 (1/day)
 C SINKV1 = sinking velocity for algae #1 (m/day)
 C PHOTO1 = photosynthetic DO production rate for algae #1 (mg O2/ug chl-a)
 C RESP1 = respiration rate for algae #1 (1/day)
 C HALFL1 = light half saturation constant for algae #1 (kcal/m2-day)
 C DEATH1 = death rate coefficient for algae #1 (1/day)
 C DECA1 = decay coefficient for algae #1 (1/day)
 C CORES1 = respiration DO consumption rate for algae #1 (mg O2/ug chl-a)

C read #42 :
 C GROW2 = maximum growth rate for algae #2 (1/day)
 C SINKV2 = sinking velocity for algae #2 (m/day)
 C PHOTO2 = photosynthetic DO production rate for algae #2 (mg O2/ug chl-a)
 C RESP2 = respiration rate for algae #2 (1/day)
 C HALFL2 = light half saturation constant for algae #2 (kcal/m2-day)
 C DEATH2 = death rate coefficient for algae #2 (1/day)
 C DECA2 = decay coefficient for algae #2 (1/day)
 C CORES2 = respiration DO consumption rate for algae #2 (mg O2/ug chl-a)
 C read #43 :
 C GROW3 = maximum growth rate for algae #3 (1/day)
 C SINKV3 = sinking velocity for algae #3 (m/day)
 C PHOTO3 = photosynthetic DO production rate for algae #3 (mg O2/ug chl-a)
 C RESP3 = respiration rate for algae #3 (1/day)
 C HALFL3 = light half saturation constant for algae #3 (kcal/m2-day)
 C DEATH3 = death rate coefficient for algae #3 (1/day)
 C DECA3 = respiration DO consumption rate for algae #3 (mg O2/ug chl-a)
 C read #44 :
 C MM = number of water quality state variables, excluding temperature
 C read #45 :
 C DT1 = T value where algae #1 start growing (C)
 C DT2 = T " " " reach maximum growth (C)
 C DT3 = T " " " leave " " (C)
 C DT4 = T " " " do not grow anymore (C)
 C DK1 = f(T) value at DT1
 C DK4 = f(T) value at DT4
 C read #46 :
 C GT1 = T value where algae #2 start growing (C)
 C GT2 = T " " " reach maximum growth (C)
 C GT3 = T " " " leave " " (C)
 C GT4 = T " " " do not grow anymore (C)
 C GK1 = f(T) value at GT1
 C GK4 = f(T) value at GT4
 C read #47 :
 C FT1 = T value where algae #3 start growing (C)
 C FT2 = T " " " reach maximum growth (C)
 C FT3 = T " " " leave " " (C)
 C FT4 = T " " " do not grow anymore (C)
 C FK1 = f(T) value at FT1
 C FK4 = f(T) value at FT4
 C read #48 :
 C STO1 = stoichiometric coefficient relating silica uptake and alg#1 (mg SiO3/ug chl-a)
 C HALF1 = Monod half saturation constant relating silica and alg#1 (mg SiO3/l)
 C HALF4 = Monod half saturation constant relating phosphorus and alg#1 (mg PO4/l)
 C SINKSI = silica settling velocity (m/s)
 C REL7 = silica release from dead alg#1 (mg SiO3/ug chl-a)
 C read #49 :
 C STO2 = stoichiometric coefficient relating phosphates uptake and alg#1 (mg PO4/ug chl-a)

C STO3 = " " " " " and
 alg#2 (mg PO4/ug chl-a)
 C HALF2 = Monod half saturation constant relating phosphates and alg#2 (mg
 PO4/l)
 C REL1 = coefficient relating dead alg#1 and phosphate release (mg PO4/ug
 chl-a)
 C REL2 = " " " alg#2 " " " (mg
 PO4/ug chl-a)
 C SED1 = phosphate release from sediments (g PO4/m2-day)
 C SED2 = phosphate uptake by sediments (m/day)
 C read #50 :
 C STO4 = stoichiometric coefficient relating nitrate uptake and alg#1 (mg NO3/ug
 chl-a)
 C STO5 = " " " " " and alg#2
 (mg NO3/ug chl-a)
 C HALF3 = Monod half saturation constant relating nitrogen and alg#2 (mg N/ug
 chl-a)
 C SED3 = nitrate uptake rate by sediments (m/day)
 C DENIT = denitrification rate (1/day)
 C OXNO2 = NO2 oxidation rate (1/day)
 C OCON1 = oxygen consumption by NO2 oxidation (mg O2/mg NO2)
 C read #51 :
 C STO6 = stoichiometric coefficient relating ammonia uptake and alg#1 (mg
 NH4/ug chl-a)
 C STO7 = " " " " " "
 alg#2 (mg NH4/ug chl-a)
 C REL3 = coefficient relating ammonia release and dead alg#1 (mg NH4/ug chl-a)
 C REL4 = " " " " " " alg#2 (mg
 NH4/ug chl-a)
 C SED4 = ammonia release from sediments (g NH4/m2-day)
 C OXNH4 = ammonia oxidation rate (1/day)
 C OCON2 = oxygen consumption by ammonia oxidation (mg O2/mg NH4)
 C read #52 :
 C HALF5 = Monod half saturation constant relating phosphorus and alg#3 (mg
 PO4/l)
 C HALF6 = " " " " " nitrogen and alg#3
 (mg N/l)
 C STO8 = stoichiometric coefficient relating phosphate uptake and alg#3 (mg PO4/ug
 chl-a)
 C STO9 = " " " nitrate " " alg#3
 (mg NO3/ug chl-a)
 C STO10 = " " " ammonia " "
 alg#3 (mg NH4/ug chl-a)
 C REL5 = coefficient relating phosphate release and dead alg#3 (mg PO4/ug chl-a)
 C REL6 = " " ammonia " " " alg#3 (mg
 NH4/ug chl-a)
 C read #53 :
 C DZSPEC(M)= vertical distance interval between input values of SPECIN(M) (m)
 C NSPEC = number of SPECIN(M) values to be read in
 C read #54 :
 C SPECIN(M)= values of initial state variable M concentrations

```

C      note that in the input file "reads #53 & #54" have to be repeated
C      for every state variable (M of them) where:
C          M=1 : DO (mg/l)
C          M=2 : BOD (mg/l)
C          M=3 : ALGAE #1 (ug/l)
C          M=4 : ALGAE #2 (ug/l)
C          M=5 : TOTAL ALGAE (1+2+3) (ug/l)
C          M=6 : SiO3 (mg/l)
C          M=7 : PO4 (mg/l)
C          M=8 : NO3 (mg/l)
C          M=9 : NH4 (mg/l)
C          M=10 : NO2 (mg/l)
C          M=11 : ALGAE #3 (ug/l)
C read #55 :
C  INDICE  = 0 if molecular diffusion is to be used
C           = 1 if variable diffusion is to be used                      (**)
C  IDFFLG  = 0 if depth-independent diffusion is to be used
C           = 1 if depth-dependent diffusion is to be used              (**)
C  FACVI   = multiplier to be used in computing diffusivities
C    CD     = coefficient in entrainment equation (0.038)
C    CT     = " " " " " (5.64)
C    CW     = wind mixing coefficient
C    CCON   = penetrative convection mixing coefficient (0.5)
C read #56 :
C  NWRITE  = 1 prints results every NPRINT days
C           = 2 prints results every specified date
C read #57 :
C  NNJUL   = number of days to print if NPRINT=2
C read #58 :
C  NJUL    = julian dates to be printed
C read #59 :
C  NERROR  = 1 data profiles are read to evaluate errors
C           = 2 no error evaluation
C  MMJUL   = number of days with profiles to be read
C  NPROF   = number of variables to be read each day
C read #60 :
C  MJUL    = julian dates to be read
C read #61 :
C  MJM     = number of data values to be read (equal to number of layers),
C            one value per day,since probably number of layers differ
C read #62 :
C    Y     = data values; there must be as many groups of values per day
C            as variables, and as many days as MMJUL.
C

```

```

C *****
C                                     MAIN PROGRAM
C *****
C
COMMON /PARAM/  JM,DT,DY,DTT,TSTOP,ET,T(102,2)
COMMON /CONST/  RHO,HCAP,GRAV,VISCOS,TEMDIF,ZIB
COMMON /SWITCH/  KSUR,KOH,KQ,KLOSS,KMIX,KATRAD
COMMON /EXTIN/  ETA,BETA,XTN(366),DTXTN
COMMON /SURS/   DYSUR,AYSUR,SURF(366),YSUR,SAREA,TS
COMMON /GEOM/   XL(102),A(102),EL(102),S(102),B(102),YBOT
COMMON /MET/    TAIR,PSI,CLC,W,WINDY
COMMON/METEOA/  TA(400),SIGH(400),CLOUD(400),WIND(400),TI(400)
COMMON /METEOB/  FIN(400),ATRAD(400)
COMMON /TIMES/  DTTA,DTSIGN,DCLOUD,DTWIND,DTTI,DTFIN,DATRAD
COMMON /FLUXES/  EVAP,RAD,AR,EVPCON
COMMON /OUTLET/  NOUT,LOUT(5),ELOUT(5),QIN(400),TIN(400)
COMMON /OUTB/   YOUT,JOUT,JIN,TOUTC(5)
COMMON /FLOWS/  QI(400),QO(400,5),DTQI,DTQO
COMMON /MIX/    QQMIX(102),RMIX,JMIXB,MIXED,QMIX
COMMON /VELA/   UI(102,1),UOT(102,5),V(102,1),UO(102,1),III
COMMON /VELB/   UOMAX(5),UIMAX(1),EX(102),EXO(102),OX(102),EXI(102)
COMMON /VELC/   SIGMAI,SIGMAO,SPREAD,HAFDEL,EPSIL,DERIV,DELCON
COMMON /METWD/  WHGT,TAU
COMMON /ENERGY/  EO,E1,E2,E3
COMMON /MIXA/   DMIX,MIXH
COMMON /SUNFX/  ELMAX,DDPL,XLAT,RG,KSLRAD,IDAY
COMMON /WQPARM/ JEUP,MM
COMMON/WQCONC/  CC(11,105,2),CCC(11,400),COUT(11,5),CCT(11,5)
COMMON/WQCONT/  ZKBOD,BENTHC,TBASE,SPEDIF,XAIR
COMMON/DIATOM/  GROW1,SINKV1,PHOTO1,RESP1,HALFL1,DEATH1,DECA1
COMMON/GREENS/  GROW2,SINKV2,PHOTO2,RESP2,HALFL2,DEATH2,DECA2
COMMON/DOBOD/   DO(400),BOD(400),DDOC,DBOD
COMMON/WQMIX/   LAGTIM(400),NTRAC(20),NLEVE(400),ITR
COMMON/SURSB/   CUMQIN,CUMQOT,JM1,DYSUR1,DSUPF,SAREA1,SURMES
COMMON/TEMP/    DELTF,FLUXOT,TSAVE
COMMON /WDM86/  DIFU,FCTR(102),BRUNT(102),D(102),USTR,VSTR,WSTR,
$FACVI,IDFFFLG,CD,CT,INDICE,CW,CCON
COMMON/ERRORS/  AVE(11),ADEV(11),SDEV(11),Y(102,11,30)
COMMON/NUTRI/   SIL(400),DSIL,PHOS(400),DPHOS,ANIT(400),DNIT,
$AMON(400),DAMON,ANO2(400),DNO2
COMMON/STOCHI/  STO1,STO2,STO3,STO4,STO5,STO6,STO7,DENIT
COMMON/SEDIM/   SED1,SED2,SED3,SED4
COMMON/HALFL/   HALF1,HALF2,HALF3,HALF4
COMMON/OXID/    OXNH4,OXNO2,OCON1,OCON2
COMMON/RECY/    REL1,REL2,REL3,REL4,CORES1,CORES2,CORES3
COMMON/TEMCON/  DT1,DT2,DT3,DT4,DK1,DK4,GT1,GT2,GT3,GT4,GK1,GK4
COMMON/FLAGEL/  GROW3,SINKV3,PHOTO3,RESP3,HALFL3,DEATH3,DECA3
COMMON/FLACOM/  FT1,FT2,FT3,FT4,FK1,FK4,SINKSI
COMMON/FLAG/    HALF5,HALF6,STO8,STO9,STO10,REL5,REL6
COMMON/HORAD/TP
DIMENSION WH(20),AA(102),XXL(102),TT(102)

```

```

    DIMENSION DZSPEC(10),SPECIN(102)
    DIMENSION DELTT(10),FLX(10),DELTO2(10)
    DIMENSION NJUL(102)
    DIMENSION MJUL(102),MJM(102)
    DIMENSION C(11,105,2),SATRAT(102),DOSAT(102),ELE(102),TW(102),
$RATSAT(102)
    OPEN (5,FILE='DATA.IN',STATUS='OLD')
    OPEN (6,FILE='SOLU.OUT',STATUS='NEW')
    OPEN (8,FILE='SPLOT.MAY',STATUS='NEW')
    OPEN (9,FILE='SPLOT.JUN',STATUS='NEW')
    OPEN (10,FILE='SPLOT.JUL',STATUS='NEW')
    OPEN (11,FILE='SPLOT.AUG',STATUS='NEW')
    OPEN (12,FILE='SPLOT.SEP',STATUS='NEW')
    OPEN (13,FILE='SPLOT.OCT',STATUS='NEW')
    OPEN (14,FILE='SPLOT.NOV',STATUS='NEW')
    OPEN (15,FILE='OUTLETEMP.SIM',STATUS='NEW')
    IOU TL=15
    INPUT= 5
    IOUT= 6
    IOU TP=7
C
C READ IN ALL DATA FOR PROGRAM.
C
    READ (INPUT,900) (WH(I),I=1,20)
    WRITE (IOUT,1000) (WH(I),I=1,20)
    READ (INPUT,900) (WH(I),I=1,20)

```



```

      READ (INPUT,*)   JM,KATRAD,KSUR,KOH ,KQ,KLOSS,NPRINT,KMIX,
1MIXED,KTRAV,KSLRAD,XDAY
      READ (INPUT,*)   YSUR,DY,DT,TSTOP,EVPCON
      READ(INPUT,*)    SPREAD,SIGMAI,BETA,RHO,HCAP,DELCON,RMIX,TEMDIF
      READ(INPUT,*)    NTI,NTA,NSIGH,NFIN,NSURF,NQI,NQO,NOUT,NXTN,
$NTO
      READ(INPUT,*)    DTTI,DTTA,DTSIGH,DTFIN,DSURF,DTQI,DTQO,DTXTN
      READ (INPUT,*)    (TI(I),I=1,NTI)
      READ (INPUT,*)    (TA(I),I=1,NTA)
      READ (INPUT,*)    (SIGH(I),I=1,NSIGH)
      GO TO(3000,3010), KSLRAD
3000 CONTINUE
      READ (INPUT,*)    (FIN(I),I=1,NFIN)
      GO TO 3020
3010 CONTINUE
      READ(INPUT,*)    XLAT,ELMAX,RG,DDPL
      IDAY=XDAY
3020 READ(INPUT,*)    (SURF(I),I=1,NSURF)
      READ (INPUT,*)    (QI(I),I=1,NQI)
      DO 3001 I=1,NOUT
3001 READ(INPUT,*)    (QO(N,I),N=1,NQO)
      READ(INPUT,*)    (LOUT(I),I=1,NOUT)
      READ(INPUT,*)    (ELOUT(I),I=1,NOUT)
      READ (INPUT,*)    (XTN(I),I=1,NXTN)
      READ(INPUT,*)    GRAV,VISCOS
      READ (INPUT,*)    THICK1,THICK2
      YBOT=ELOUT(1)-DY*FLOAT(LOUT(1)-1)
2 READ(INPUT,*)    NAA,NXXL,NWIND,NATRAD,JMP
      READ (INPUT,*)    DAA,DXXL,DZTO,DTWIND,DATRAD,AAB,XXLB,DDZTO
      READ (INPUT,*)    (AA(I), I=1,NAA)
      READ(INPUT,*)    (XXL(I),I=1,NXXL)
      READ (INPUT,*)    (WIND(I),I=1,NWIND)
      GO TO (9,10,10), KATRAD
9 READ (INPUT,*)    (ATRAD(I),I=1,NATRAD)
      GO TO (11,10),KSLRAD
10 READ(INPUT,*)    DCLOUD,NCLOUD
      READ(INPUT,*)    (CLOUD(I),I=1,NCLOUD)
11 DO 3 I=1,JMP
      EL(I) = YBOT+DY*FLOAT(I-1)
      RA=(EL(I)-AAB)/DAA +1.0
      IF (I-JMP) 6664,6666,6666
6664 L=RA
      GO TO 6665
6666 L=RA-0.001
6665 A(I)=AA(L)+(RA-FLOAT(L))*(AA(L+1)-AA(L))
      RA = (EL(I)-XXLB)/DXXL +1.0
      IF (I-JMP) 7774,7777,7777
7774 L=RA
      GO TO 7775
7777 L=RA-0.001
7775 XL(I) = XXL(L)+(RA-FLOAT(L))*(XXL(L+1)-XXL(L))

```

```

3 B(I)=A(I)/XL(I)
  READ (INPUT,*) (TT(J),J=1,NT0)
  DO 6661 I=1,JM-1
    RA=(EL(I)-DDZTO)/DZTO+1.0
    IF (I-JMP) 6662,6663,6663
6662 L=RA
    GO TO 6661
6663 L=RA-0.001
6661 T(I,1)=TT(L)+(RA-FLOAT(L))*(TT(L+1)-TT(L))
    T(JM,1)=TT(NT0)
    JMAS=JM+1
    IF(JMAS.LT.JMP) GO TO 2345
    DO 1234 I=JMAS,JMP
    T(I,1)=0.0
1234 CONTINUE
2345 CONTINUE
    TZERO=T(JM,1)
    READ(INPUT,*) WHGT
C
C WRITE ALL GENERAL INFORMATION CONCERNING THE PRESENT RUN, THAT
IS,
C MODES CHOSEN, PARAMETERS AND CONSTANTS THAT DO NOT VARY
THROUGH THE RUN
C
  WRITE (IOUT,900) (WH(I),I=1,20)
  WRITE (IOUT,904) JM,YSUR,RHO
  WRITE (IOUT,905) (LOUT(I),ELOUT(I),I=1,NOUT)
  WRITE (IOUT,906) DY,YBOT
  WRITE (IOUT,907) DT, TZERO,BETA
  WRITE (IOUT,908) KTRAV,SIGMAI,HCAP
  WRITE (IOUT,909) TSTOP,SPREAD,TEMDIF
  WRITE (IOUT,910) KATRAD,KSUR,KOH,KQ, KLOSS,XDAY, EVPCON,DELCON,
    KMIX
  WRITE (IOUT,923) MIXED,RMIX
C
C READ PARAMETERS AND DATA FOR DO CALCULATIONS
C READ DATA FOR DO, BOD, SILICA, PHOSPHORUS, NITROGEN
C
C
C ALL ALGAE RELATED PARAMETERS ARE READ HERE; # 1 STANDS FOR
DIATOMS,
C # 2 STANDS FOR GREENS (kind of algae included february 1987)
C
C
C INITIALIZE MANY VARIABLES.
C
  KH=0
  ST1=0.0
  ST2=0.0
C

```

```

C READ DATA FOR INITIAL CONDITION OF ALL WATER QUALITY
PARAMETERS:
C DO,BOD,ALGAE #1,ALGAE #2,TOTAL ALGAE,SILICA,PHOSPHORUS AND
C NITROGEN. UNITS ARE (mg/l) EVERYWHERE EXCEPT ALGAE (ug/l)
C
C READ DATA FOR NEW WIND MIXING AND DIFFUSION ROUTINES
C
C READ (INPUT,*) INDICE,IDFFLG,FACVI,CD,CT,CW,CCON
C READ (INPUT,*) PLOT
C
C READ DATA TO PRINT ONLY SOME SPECIFIC DATES
C IF NWRITE=1,THE PROGRAM WILL PRINT RESULTS EVERY "NPRINT"
C DAYS; IF NWRITE=2, ONLY THE SPECIFIED DATES WILL BE PRINTED
C
C READ (INPUT,*) NWRITE
C IF (NWRITE.EQ.2) THEN
C READ (INPUT,*) NNJUL
C READ (INPUT,*) (NJUL(I),I=1,NNJUL)
C ELSE
C CONTINUE
C ENDIF
C
C DATA PROFILES ARE READ HERE TO CALCULATE SIMULATION ERRORS
C IF NERROR=1,PROFILES ARE READ
C IF NERROR=2,NO DATA READING AND NO ERROR CALCULATION
C MMJUL =NUMBER OF DAYS WITH PROFILES TO BE READ
C MJUL(I) = DATES (JULIAN DAYS)
C MJM(I) = NUMBER OF DATA VALUES TO BE READ (= # OF LAYERS),
C ONE VALUE PER DAY
C NPROF = NUMBER OF VARIABLES TO BE READ (=7, DO,BOD,TOTAL ALGAE,
C SiO3,NO3,NH4,NO2)
C
C READ(INPUT,*) NERROR,MMJUL,NPROF
C IF (NERROR.EQ.1)THEN
C READ(INPUT,*) (MJUL(I),I=1,MMJUL)
C READ(INPUT,*) (MJM(I),I=1,MMJUL)
C DO 5003 K=1,MMJUL
C MJ=MJM(K)
C DO 5004 J=1,NPROF
C READ(INPUT,*) (Y(I,J,K),I=1,MJ)
5004 CONTINUE
5003 CONTINUE
C ELSE
C GO TO 5005
C ENDIF
5005 CONTINUE
C K=0
C DTT=DT
C NPR=0
C NSP=0
C JXM=JM

```

```

      N=1
      JMXB = JM-MIXED
      QMIX = 0.0
      ET=1.0
      RAD = 0.0
      EVAP = 0.0
      TAIR = 0.0
      EPSIL = 0.0
      HAFDEL = 0.0
      JIN = JM
      CUMQIN=0.0
      CUMQOT=0.0
      DYSUR=YSUR-EL(JM)+DY/2.0
      IF(YSUR-EL(JM)) 858,858,859
858  AYSUR=A(JM)-(DY/2.0-DYSUR)*(A(JM)-A(JM-1))/DY
      GO TO 860
859  AYSUR=A(JM)+(DYSUR-DY/2.0)*(A(JM+1)-A(JM))/DY
860  SAREA=(AYSUR+(A(JM)+A(JM-1))/2.0)/2.0
      SAREA1=SAREA
      DYSUR1=DYSUR
      SAREA2=SAREA
      DYSUR2=DYSUR
      JM1=JM
C
C  INITIALIZE VARIABLES USED IN ENERGY CHECK
C
      E2=0.0
      E3=0.0
      RHOE0=1000.-0.00663*(T(1,1)-4.)*(T(1,1)-4.)
      E0=A(1)*DY/2.*T(1,1)*RHOE0*HCAP
      RHOS=1000.-0.00663*(T(JM,1)-4.)*(T(JM,1)-4.)
      E0=E0+SAREA*DYSUR*T(JM,1)*RHOS*HCAP
      JMM=JM-1
      DO 13 I=2,JMM
      RHO0=1000.-0.00663*(T(I,1)-4.)*(T(I,1)-4.)
13  E0=E0+A(I)*DY*T(I,1)*RHO0*HCAP
17  GO TO (20,18), KQ
18  UIMAX(1)=0.0
      UOMAX(1) = 0.0
      TS=0.0
      DO 19 J=1,JM
      UI(J,1) = 0.0
      UO(J,1)=0.0
19  V(J,1) = 0.0
      SIGMAO = 1.0
C
C  STATEMENT 20 IS BEGINNING OF MAIN ITERATION LOOP OF PROGRAM.
C
      20 N=N+1
C
C  CALCULATE ELAPSED TIME (ET) AND JULIAN DAY (DAY)

```

```

C
    ET=ET+DT
    DAY=XDAY+ET
C
C EVALUATE EXTINCTION COEFFICIENT
C
C EXTINCTION COEFFICIENT IS EVALUATED AS A FUNCTION OF TOTAL
CHLOROPHYLL.A
C CONCENTRATION; IF INTERPOLATION IS TO BE USED, THE CALCULATION IS
GIVEN HERE
C AND THE READ IN VALUES WILL BE USED. IT IS STRONGLY
RECOMMENDED TO USE THE
C FUNCTION INSTEAD OF THE INTERPOLATION
    R=ET/DTXTN+1.0
    L=R
    RR=R-FLOAT (L)
    ETA=XTN(L)+RR*(XTN(L+1)-XTN(L))
C    CHL=(CC(5,JM,1)+CC(5,JM-1,1))*0.5
C    SC=3.705*EXP(-0.0169*CHL)
C    ETA=1.7/SC
    GO TO (21,503),KQ
21 GO TO (24,22), KMIX
C
C MIX INFLOW WATER IF INDICATED.
C
22 TP=0.0
    DO 23 J=JMIXB,JM
    TP = TP+T(J,1)
23 CONTINUE
    TP = TP/FLOAT(MIXED+1)
    TS=(TTIN(N)+TP*RMIX)/(1.0+RMIX)
    TMIT=TS
    GO TO 25
24 TS=TTIN(N)
    TMIT= TS
25 CONTINUE
C
C LOCATE ACTUAL LEVEL OF DAYS INPUT
C
C INFLOW DENSITY
C
    DS=1000.-0.00663*(TS-4.)*(TS-4.)
C
C RESERVOIR DENSITY
C
    DO 27 I=1,JM
    J = JM+1-I
    DJ=1000.-0.00663*(T(J,1)-4.)*(T(J,1)-4.)
    IF (DJ-DS) 27,30,30
27 CONTINUE
30 JIN=J+1

```

```

      IF(JIN-JM) 32,32,33
33  JIN=JM
32  CONTINUE
      IF (JIN.EQ.2) JIN=3
      JEUP=JM-4.6/ETA/DY
      IF(JIN-JEUP) 570,580,580
580  NLEVE(N)=1
      GO TO 550
570  NLEVE(N)=2
550  CONTINUE
      JXM=JM
      GO TO (46,47),KTRAV
47  IF(QQIN(N).LE.0.0) GO TO 46
C
C  CALCULATION OF TRAVEL TIME
C  VELF=DOWNSLOPE VELOCITY,HVELF=HORIZONTAL VELOCITY
C
      QLIT=QQIN(N)*(1.0+RMIX)/B(JM)
      IF(JM-2-JIN) 870,870,871
870  VELF=QLIT/THICK1
      JIN=JM
      XLAG=XL(JM)/VELF
      GO TO 872
871  DELRHO=6.6E-06*((T(JM,1)-4.0)**2-(TS-4.0)**2)/2.0
      GPRIME=GRAV*DELRHO
      SLOPE=(EL(JM)-EL(JIN))/(XL(JM)-XL(JIN))
      DFLOW=1.92*(QLIT*VISCOS/GPRIME/SLOPE)**0.33
      VELF=QLIT/DFLOW
      HVELF=QLIT/THICK2
      SLDIST=FLOAT(JM-JIN)*DY/SLOPE
      XLAG=SLDIST/VELF+XL(JIN)/HVELF
872  LAGTIM(N)=XLAG/DT
      ML=N+LAGTIM(N)
      IF(ML.GT.IFIX(TSTOP)) GO TO 48
      QIN(ML)=QIN(ML)+QQIN(N)
      TIN(ML)=(TIN(ML)*(QIN(ML)-QQIN(N))+TTIN(N)*QQIN(N))/QIN(ML)
      TP=0.0
      DO 1023 J=JMIXB,JM
1023  TP=TP+T(J,1)
      TP=TP/FLOAT(MIXED+1)
      TS=(TIN(N)+TP*RMIX)/(1.0+RMIX)
      TMIT=TS
C
C  RELOCATE LEVEL OF INFLOW WATER.
C
      DO 4745 I=1,JM
      J=JM+1-I
      IF(TS-T(J,1)) 4745,4746,4746
4745  CONTINUE
4746  JIN=J+1
      IF(JIN-JM) 4747,4747,4748

```

```

4748 JIN=JM
4747 CONTINUE
      GO TO 48
      46 QIN(N)=QQIN(N)
         TIN(N)=TTIN(N)
      48 GO TO (45,31),KSUR
C
C SUBROUTINE SURFEL PERFORMS COMPUTATIONS WHEN SURFACE
ELEVATION
C VARIES WITH TIME
C
      31 CALL SURFEL(N)
      45 CONTINUE
         JMIXB=JM-MIXED
C
C NEW SURFACE CONCENTRATIONS DUE TO CHANGES IN SURFACE
ELEVATION
C
C
C IF SURFACE ELEVATION DECREASES TO A DIFFERENT LAYER LEVEL
C
C
C IF SURFACE ELEVATION INCREASES TO A DIFFERENT LAYER LEVEL
C
C
C IF SURFACE DOES NOT VARY OR VARIES WITHIN THE SAME LAYER
C
      SAREA2=SAREA
      DYSUR2=DYSUR
C
C SUB SPEED COMPUTES WITHDRAWAL THICKNESS AND VELOCITIES AT
EACH TIME STEP
C
      CALL SPEED(N)
C
C SUBROUTINE XMIX CALCULATES COMPOSITION OF INFLOWS
C
C
C COMPUTE VERTICAL DIFFUSIVITIES
C
C COMPUTE DENMED - VOLUME-WEIGHTED AVERAGE DENSITY
C
      SUMV=0.
      SUMD=0.
      DO 2000 J=1,JM
        D(J)=1000.-.00663*(T(J,1)-4.)*(T(J,1)-4.)
        SUMV=SUMV+A(J)*DY
      2000 SUMD=SUMD+D(J)*A(J)*DY
      DENMED=SUMD/SUMV
C
C COMPUTE POTEN - TOTAL POTENTIAL ENERGY OF STRATIFICATION
C

```

```

      POTEN=0.5*(DENMED-D(1))*0.5*DY*DY*9.8*A(1)
      POTEN=POTEN+0.5*(DENMED-D(JM))*0.5*DY*DYSUR*9.8*A(JM)
      DO 2010 J=2,JM-1
2010  POTEN=POTEN+(DENMED-D(J))*(J-0.5)*DY*DY*9.8*A(J)
      POTEN=ABS(POTEN)
C
C  COMPUTE SHEAR STRESS AND SHEAR VELOCITY OF WIND
C
      PAIR=1.18
      VKARMN=0.41
      IF(N.EQ.2) THEN
      W=WIND(2)
      ELSE
      W=WINDY
      ENDIF
      KT=0
      GRAV=73150000000.
2030  RHS=(ALOG(GRAV*2./86400./86400./0.011/W/W))/VKARMN
      IF(W.LE.1.) GO TO 2070
      IF(W.LT.3.) GO TO 2040
      IF(W.GT.12.) GO TO 2050
      C1=0.0016
      GO TO 2060
2040  C1=0.00125
      GO TO 2060
2050  C1=0.0026
2060  OS=1./((C1**.5)+ALOG(C1)/VKARMN
      IF(ABS(OS-RHS).LE.0.5) GO TO 2080
      C1=C1+(OS-RHS)/20000.
      KT=KT+1
      IF(KT.GT.10) GO TO 2080
      GO TO 2060
2070  C1=0.0005
2080  C0=C1
      TAU=C0*W*W*PAIR
      USTR=(TAU/1000.)**.5
C
C  COMPUTE DIFFUSIVITIES (DIFFUSION=MOLECULAR + EDDY)
C  IN THIS VERSION OF THE MODEL ALL UNIT CHANGES HAVE BEEN
C  INCLUDED EXPLICITLY IN THE FORMULATION AND THUS, THE VALUE
C  OF Calfa (FACVI) IS EQUIVALENT TO 1/86400 OF THE VALUE OF
C  Calfa IN PREVIOUS VERSIONS
C
      PROF=(JM-1)*DY
      DIFU=8.64
      IF(POTEN.NE.0.) DIFU=.0124+1000.*86400*FACVI*PROF*PROF*USTR*
      USTR*USTR*A(JM)/POTEN
      IF(DIFU.GT.8.64) DIFU=8.64
      IF(INDICE.EQ.0) DIFU=.124
      XFACT1=DIFU/8.64
      XFACT2=DIFU/.124

```



```

      DDENSE=D(1)-D(JM)
C
C IDFFLG=1 - USE DEPTH DEPENDENT DIFFUSIVITY
C   WRITE(IOUTF,994) (N+126),DIFU,DDENSE
C
      DO 2100 J=2,JM
      IF(IDFFLG.EQ.1) THEN
      IF(DDENSE.LE.0.) THEN
      FCTR(J)=8.64/DIFU
      ELSE
      FCTR(J)=PROF/(D(1)-D(JM))*(D(J-1)-D(J))/DY
      ENDIF
      IF(FCTR(J).LT.XFACT1) FCTR(J)=XFACT1
      IF(FCTR(J).GT.XFACT2) FCTR(J)=XFACT2
C
C IDFFLG<>1 - USE DEPTH-INDEPENDENT DIFFUSIVITY
C
      ELSE
      FCTR(J)=1.
      ENDIF
C   WRITE(IOUTF,993) J,D(J),FCTR(J)
2100 CONTINUE
      WRITE(IOUTEZ,991) (N+126),DIFU/FCTR(12),DIFU/FCTR(9)
C
C STABILITY CHECK V*DT IS LESS THAN DY
C
      VVV=ABS(V(2,1))
      DO 501 J=3,JM
      IF(VVV-ABS(V(J,1)))502,501,501
502 VVV=ABS(V(J,1))
501 CONTINUE
      VM=DY/DTT
      IF(VVV-VM) 503,504,504
504 DT=DY/VVV
      IDT=DTT/DT+1
      DT=DTT/IDT
      GO TO 2200
503 IDT=1
2200 DIFMAX=.0124
      DO 2210 J=2,JM
2210 DIFMAX=AMAX1(DIFMAX,(DIFU/FCTR(J)))
      DELTAZ=AMAX1(DY,DYSUR)
      DIMAX=0.5*DELTAZ*DELTAZ/DTT
      IF(DIFMAX.LE.DIMAX) GO TO 2220
      DT1=0.5*DY*DY/DIFMAX
      IDT1=DTT/DT1+1
      DT1=DTT/IDT1
      GO TO 2230
2220 IDT1=1
      GO TO 2240
2230 IF(DT1.LT.DT) DT=DT1

```

```

        IF(IDT1.GT.IDT) IDT=IDT1
        IF(DT.EQ.0.) DT=DTT
        IF(IDT.EQ.0.) IDT=1
2240 CONTINUE
C
C BEGIN LOOP FOR SUBDIVIDED TIME STEP
C
        DO 79 KM=1,IDT
C
C HEAT TRANSPORT CALCULATIONS
C
        FLUXOT=FLXOUT(N)
C
C SUBROUTINE TEMDIS CALCULATES THE VERTICALDISTRIBUTION
C OF TEMPERATURES
C
        CALL TEMDIS(N)
C
C SUB SPECIAL CALCULATES THE DISTRIBUTION OF THE SPECIFIED
C CONSTITUENTS
C
1150 CONTINUE
C
C CHECK REASONABLENESS OF RESULTS.
C
        IF (ABS(T(JM,2))-100.0) 60,57,57
57 TSTOP = ET
        GO TO 80
C
C SUB AVER MIXES LAYERS IN THE EVENT OF AN INSTABILITY
C
60 CONTINUE
        CALL AVER(N)
        DELTT(1)=DELTF
        KK=1
        DO 2009 KK=2,10
            FLAX=FLXOUT(N)
            DELTT(KK)=-FLAX*AYSUR/RHO/HCAP/DYSUR/SAREA*DT
            DELTS=(DELTT(1)+DELTT(KK))/2.
            T(JM,1)=TSAVE+DELTS
            DO 2001 J=1,JMM
2001 T(J,1)=T(J,2)
            CALL AVER(N)
            IF (ABS(DELTT(KK)-DELTT(KK-1)).LE.0.004) GO TO 2002
2009 CONTINUE
2002 DOSA=14.4776-0.3579*T(JM,1)+0.0043*(T(JM,1)*T(JM,1))
C
C SUBROUTINE SPECAL MIXES SPECIFIED MATERIAL
C
        79 CONTINUE
        DT=DTT

```

```

DO 78 I=1,NOUT
  III=I
  GO TO (115,116),KQ
116 TOUTC(I)=0.0
  GO TO 78
C
C COMPUTE WEIGHTED AVERAGE OF OUTFLOW TEMPERATURES
C
115 CALL TOUT(HEATOT,FLOWOT)
  TOUTC(I)=HEATOT/FLOWOT
  IF (QOUT(N,I).EQ.0.0) TOUTC(I)=0.0
78 CONTINUE

C
C ENERGY CHECK
C
  RHOE1=1000.-0.00663*(T(1,1)-4.)*(T(1,1)-4.)
  E1=A(1)*DY/2.0*T(1,1)*RHOE1*HCAP
  JMM=JM-1
  DO 111 J=2,JMM
    RHOJ=1000.-0.00663*(T(J,1)-4.)*(T(J,1)-4.)
111 E1=E1+A(J)*DY*T(J,1)*RHOJ*HCAP
    RHOJM=1000.-0.00663*(T(JM,1)-4.)*(T(JM,1)-4.)
    E1=E1+SAREA*DYSUR*T(JM,1)*RHOJM*HCAP
    RHOE2=1000.-0.00663*(TIN(N)-4.)*(TIN(N)-4.)
    E2=E2+FLXIN(N)*AYSUR*DT+QIN(N)*DT*TIN(N)*RHOE2*HCAP
    E3=E3+FLAX*AYSUR*DT
  DO 112 I=1,NOUT
    RHOE3=1000.-0.00663*(TOUTC(I)-4.)*(TOUTC(I)-4.)
112 E3=E3+QOUT(N,I)*DT*TOUTC(I)*RHOE3*HCAP
    ENRAT=(E1-E0)/(E2-E3)
    TENRAT=(E1+E3)/(E2+E0)
    DT=DTT
C
C SUB SPECOT CALCULATES COMPOSITION OF OUTFLOWS
  FLXN=FLXIN(N)
C
C SUB DATE CALCULATES DAY AND MONTH OF THE JULIAN DAY
C
  CALL XDATE(DAY,LDAY,NMONTH)
  IF (NWRITE.EQ.1) THEN
5002 IF (N-NPR) 100,100,80
  80 NPR = NPR+NPRINT
  WRITE (IOUT,1012)NMONTH,LDAY
  WRITE (IOUT,912) DAY,SURMES,TIN(N)
  WRITE (IOUT,913) N,YSUR,TAIR
  WRITE (IOUT,914) JM,EL(JIN),PSI
  FLXN=FLXIN(N)
  WRITE (IOUT,915) JIN,EVAP,FLXN
  DMIX=FLOAT(MIXH-1)*DY+DYSUR
  WRITE(IOUT,925) DMIX,AR,WINDY
  QITN=QIN(N)*DTT/86400.

```

```

      WRITE (IOUT,916) FLUXOT,RAD,QITN
      GO TO (85,89), KQ
85    F = 2.0*HAFDEL
      WRITE (IOUT,918) ETA,F,SIGMAO
      DO 88 I=1,NOUT
C
C THE ADIMENSIONAL PARAMETER (A*E)/(Q*D) IS EVALUATED HERE; IF
C PARAM >>1 THEN DIFFUSION DOMINATES ADVECTION;
C PARAM = 1 THEN THERE IS COMPETITION;
C PARAM <<1 THEN ADVECTION DOMINATES DIFFUSION
C
      IF(QOUT(N,I).EQ.0.0)THEN
      PARAM=100.00
      ELSE
      PARAM=(A(LOUT(I))*DIFU)/(QOUT(N,I)*(YSUR-ELOUT(I)))
      ENDIF
      WRITE (IOUT,1002) DIFU,PARAM
      QOTN=QOUT(N,I)*DTT/86400.
      WRITE(IOUT,917) ELOUT(I),QOTN,TOUTC(I)
88    WRITE (IOUT,926) ENRAT,E1,E2,E3
86    WRITE (IOUT,924) TMIT,TS,TENRAT
C
C EVALUATE THE RATIO DO VS DOSAT
C
      DO 332 J=1,JM
      I=JM+1-J
      ELE(I)=EL(J)
332  CONTINUE
      DO 334 J=1,JM
      I=JM+1-J
      TW(I)=T(J,1)
334  CONTINUE
89    JI=1
90    IF(JM-JI) 100,91,91

```

```

91  WRITE(IOUT,920)
C   PLOTTING FILES TO LINE 1705
    IF(IOUTP.EQ.7)THEN
      GO TO 1705
    ELSE
      CONTINUE
    ENDIF
    WRITE(IOUTP,1601)
    WRITE(IOUTP,1602)
    WRITE(IOUTP,1603)
    WRITE(IOUTP,1604)
    WRITE(IOUTP,1603)
    WRITE(IOUTP,1604)
    DO 1705 J=1,JM
      I=JM+1-J
      L=2*(J-1)
      WRITE(IOUTP,1605) ELE(J),TW(J),ELE(1),L
1705 CONTINUE
      IOUTP=IOUTP+1
      DO 95 J=1,JM
        I=JM+1-J
        L=2*(J-1)
95    WRITE(IOUT,921) I,ELE(J),TW(J)
C
C
      JI=JI+45
      GO TO 90
    ELSE
      DO 5000 I=1,NNJUL
        NDAY=DAY
        IF(NDAY.LT.NJUL(I))THEN
          GO TO 100
        ELSE IF (NDAY.EQ.NJUL(I)) THEN
          GO TO 5002
        ELSE
          GO TO 5000
        ENDIF
5000 CONTINUE
      ENDIF
      100 IF(NERROR.EQ.1)THEN
        DO 5010 I=1,MMJUL
          MDAY=DAY
          IF(MDAY.LT.MJUL(I)) THEN
            GO TO 101
          ELSE IF (MDAY.EQ.MJUL(I))THEN
C
C SUBROUTINE ERROR EVALUATES THE ERROR MADE WHILE CALCULATING
RESULTS
C COMPARING SIMULATION RESULTS AND FIELD DATA. VALUES GIVEN IN %
C
      CALL ERROR (N)

```

```

        GO TO 5011
      ELSE
        GO TO 5010
      ENDIF
5010 CONTINUE
      ENDIF
      GO TO 101
5011 WRITE(IOUT,1004) AVE(1),SDEV(1),ADEV(1)
      WRITE(IOUT,1005) AVE(2),SDEV(2),ADEV(2)
      WRITE(IOUT,1006) AVE(3),SDEV(3),ADEV(3)
      WRITE(IOUT,1007) AVE(6),SDEV(6),ADEV(6)
      WRITE(IOUT,1008) AVE(7),SDEV(7),ADEV(7)
      WRITE(IOUT,1009) AVE(8),SDEV(8),ADEV(8)
      WRITE(IOUT,1010) AVE(9),SDEV(9),ADEV(9)
      WRITE(IOUT,1011) AVE(10),SDEV(10),ADEV(10)
101 IF (ET-TSTOP) 20,1,1
    1 CONTINUE
C
C ALL FORMATS GIVEN HERE
C
1601 FORMAT (' TEMP PROFILE—SIMULATED')
1602 FORMAT (' 4')
1603 FORMAT (' DEPTH')
1604 FORMAT (' TEMP')
1605 FORMAT (F6.2,5X,F5.1,3X,F6.2,3X,I2)
1606 FORMAT (F7.0,E12.5)
1607 FORMAT (I3,3X,F6.2,3X,F6.2)
  930 FORMAT (10X,'ONSET OF STRATIFICATION',F7.2,'END OF STRATIFICATION'
    .,F7.2)
1003 FORMAT (' TEMPERATURE OF THE TOP LAYER',/,(1X,I4,5X,F5.1
    .,10X,I4,5X,F5.1,10X,I4,5X,F5.1,10X,I4,5X,F5.1,10X,I4,5X,F5.1,/))
  900 FORMAT (20A4)
  908 FORMAT (' KTRAV=',I5,31X,'INFLOW STD. DEV.=',F6.2,21X,
    .HEAT CAPACITY=',F8.5)
  909 FORMAT (' STOP AT TIME=',F7.2,22X,'OUTFLOW SPREAD CONST.=',F8.5,
    $10X,'MOLEC HEAT DIFF.=',F8.4,'MM/DAY')
  910 FORMAT (' KATRAD=',I2,10X,'KSUR=',I2,10X,'KOH=',I2,10X,'KQ=',I2,
    $10X,'KLOSS=',I2,10X,'INITIAL JUL DAY=',F6.2/' EVAPORATION CONSTANT
    $=',E11.4,10X,'CONST IN EQN FOR OUTFLOW DELTA=',F9.6,7X,
    $'KMIX=',I2)
  912 FORMAT (' JULIAN DAY=',F7.2,24X,'ACTUAL SURFACE
    $ ELEVATION =',F7.2,10X,'INFLOW TEMPERATURE=',F6.2)
  913 FORMAT (' NO. OF TIME STEPS=',I4,20X,'SURFACE ELEVATION USED=',
    $F9.2,11X,'AIR TEMPERATURE=',F6.2)

```

```

914 FORMAT (' NO. OF GRID POINTS=',I3,20X,'ELEVATION OF INFLOW=',F7.2,
$16X,'RELATIVE HUMIDITY=',F5.2)
915 FORMAT (' LEVEL OF INFLOW=',I3,23X,'EVAPORATION FLUX=',E12.5,14X,
$'INSOLATION FLUX=',E12.5)
916 FORMAT (' HEAT LOSS FLUX=',E12.5,15X,'RADIATION FLUX=',E12.5,
$16X,'INFLOW RATE=',F11.1)
918 FORMAT (' EXTINCTION COEFFICIENT=',F7.2,1X,'1/M',8X,
$'WITHDRAWAL THICKNESS=',F7.2,15X,'OUTFLOW STD. DEV.',F6.2)
923 FORMAT (' NO. GRID SPACES IN MIXED LAYER=',I3,8X,'MIXING RATIO=',
$F5.2)
924 FORMAT (' MIXED INFLOW TEMP=',F6.2,15X,'MIXED LAYER TEMP=',
$F6.2,19X,'TOTAL ENERGY RATIO=',F9.5)
925 FORMAT (' MIXING DEPTH=',F5.2,24X,'ATMOSPHERIC RADIATION=',E12.5,
$9X,'WIND SPEED=',F5.2)
926 FORMAT(' ENERGY RATIO=',F7.3,4X,'ENERGY STORED=',E12.5,4X,
$'ENERGY INFLOW=',E12.5,3X,'ENERGY OUTFLOW=',E12.5)
927 FORMAT (8F10.2)
928 FORMAT(F10.5,I5)
932 FORMAT(' BOD DECAY=',F6.4,' (1/DAY)',4X,'BENTHIC UPTAKE=',
$F6.4,' (GR/DAY-M2)',4X,'TEMP BASE=',F6.2,' C',4X,
$'MOLEC MASS DIFFUSIVITY=',F10.6,' (M2/DAY)')
933 FORMAT(' ALGAE #1 :',2X,'GROWTH=',F6.3,' (1/DAY)',4X,
$'SINKING VEL.',F6.2,' (M/DAY)',4X,'DEATH=',F6.3,' 1/DAY',
$4X,'DECAY=',F6.3,' 1/DAY')
970 FORMAT(' ALGAE #3 :',2X,'GROWTH=',F6.3,' (1/DAY)',4X,
$'SINKING VEL.',F6.2,' (M/DAY)',4X,'DEATH=',F6.3,' 1/DAY',
$4X,'DECAY=',F6.3,' 1/DAY')
934 FORMAT(11X,'PHOTOSYNTHESIS=',F8.5,' (mgO2/ugChl)',4X,
$'RESPIRATION=',F8.5,' (1/DAY)',4X,'LIGHT HALF=',F8.2,
$' (KCAL/M2-DAY)',4X)
973 FORMAT(11X,'RESP.COEF=',F8.2,' (mgO2/ugChl)')
942 FORMAT(12X,'T1=',F5.2,5X,'T2=',F5.2,5X,'T3=',F5.2,5X,'T4=',
$F5.2,5X,'K1=',F5.3,5X,'K4=',F5.3)
935 FORMAT(' ALGAE #2 :',2X,'GROWTH=',F6.3,' (1/DAY)',4X,
$'SINKING VEL.',F6.2,' (M/DAY)',4X,'DEATH=',F6.3,' 1/DAY',
$4X,'DECAY=',F6.3,' 1/DAY')
936 FORMAT(' MIXED INFLOW DO =',F7.2,' mg/l',14X,'MIXED INFLOW BOD=',
$F7.2,' mg/l')
937 FORMAT(' MIXED INFLOW SiO3=',F7.2,' mg/l',5X,'MIXED INFLOW',
$' PO4=',F8.4,' mg/l',5X,'MIXED INFLOW NO3=',F8.4,' mg/l')
938 FORMAT(' MIXED INFLOW NH4=',F8.4,' mg/l',5X,'MIXED INFLOW',
$' NO2=',F8.4,' mg/l')
1000 FORMAT(/////,15X,20A4,/,30X,70('*'),/////////)
917 FORMAT(' OUTLET ELEV=',F6.1,4X,'OUTFLOW=',F6.1,4X,'TEMP=',
$F6.2,' C')
920 FORMAT(/(' J ELEV TEMP '))
921 FORMAT(I3,1X,F7.2,1X,F7.1)
940 FORMAT('TOPT=',F7.2,' C',20X,'LIGHT HALF=',F8.2,'KCAL/MM/DAY',
$17X,'RESPIRATION=',F8.5,' 1/DAY')
941 FORMAT(' Calfa=',F6.3,3X,'(Coefficient used in diffusion eqn.)')
1002 FORMAT(' DIFFUSION COEFFICIENT=',F9.5,1X,'M2/DAY',4X,'PARAM',
$'(DIF/ADV)=',F7.3)

```

```

1004 FORMAT(' TEMPERATURE:',2X,'MEAN ERROR=',F9.3,'% ',4X,'STANDARD ',
$'DEVIATION=',F9.3,4X,'AVER.STANDARD DEV.=',F9.3)
1005 FORMAT(' DO :',2X,'MEAN ERROR=',F9.3,'% ',4X,'STANDARD ',
$'DEVIATION=',F9.3,4X,'AVER.STANDARD DEV.=',F9.3)
1006 FORMAT(' TOT. ALGAE :',2X,'MEAN ERROR=',F9.3,'% ',4X,'STANDARD ',
$'DEVIATION=',F9.3,4X,'AVER.STANDARD DEV.=',F9.3)
1007 FORMAT(' SILICA :',2X,'MEAN ERROR=',F9.3,'% ',4X,'STANDARD ',
$'DEVIATION=',F9.3,4X,'AVER.STANDARD DEV.=',F9.3)
1008 FORMAT(' PHOSPHORUS :',2X,'MEAN ERROR=',F9.3,'% ',4X,'STANDARD ',
$'DEVIATION=',F9.3,4X,'AVER.STANDARD DEV.=',F9.3)
1009 FORMAT(' NO3 :',2X,'MEAN ERROR=',F9.3,'% ',4X,'STANDARD ',
$'DEVIATION=',F9.3,4X,'AVER.STANDARD DEV.=',F9.3)
1010 FORMAT(' NH4 :',2X,'MEAN ERROR=',F9.3,'% ',4X,'STANDARD ',
$'DEVIATION=',F9.3,4X,'AVER.STANDARD DEV.=',F9.3)
1011 FORMAT(' NO2 :',2X,'MEAN ERROR=',F9.3,'% ',4X,'STANDARD ',
$'DEVIATION=',F9.3,4X,'AVER.STANDARD DEV.=',F9.3)
919 FORMAT (23X,'ALGAE1=',F7.2,4X,'ALGAE2=',F7.2,3X,'ALGAE3=',F7.2,
$3X,'TOTALG=',F7.2,3X,'SiO3=',F8.2)
922 FORMAT (23X,'PO4 =',F7.4,3X,'NO3 =',F8.4,2X,'NH4 =',F8.4,2X,
$'NO2=',F8.4)
943 FORMAT (' STO1=',F6.4,5X,'HALF1=',F6.4,5X,'HALF4=',F6.4)
944 FORMAT (' STO2=',F6.4,5X,'STO3 =',F6.4,5X,'HALF2=',F6.4,5X,
$'REL2 =',F6.4,5X,'SED1 =',F6.4,5X,'SED2 =',F6.4)
945 FORMAT (' STO4=',F6.4,5X,'STO5 =',F6.4,5X,'HALF3=',F6.4,5X,
$'SED3=',F6.4,5X,'DENIT=',F6.4,5X,'OXNO2=',F6.4,5X,'OCON1=',F6.4)
946 FORMAT (' STO6=',F6.4,5X,'STO7 =',F6.4,5X,'REL3=',F6.4,5X,
$'REL4=',F6.4,5X,'SED4=',F6.4,5X,'OXNH4=',F6.4,5X,'OCON2=',F6.4)
971 FORMAT (' STO8=',F6.4,5X,'STO9 =',F6.4,5X,'STO10=',F6.4,5X,
$'HALF5=',F6.4,5X,'HALF6=',F6.4)
972 FORMAT (' REL5=',F6.4,5X,'REL6=',F6.4,5X,'REL7=',F6.4,5X,
$'REL1=',F6.4)
1012 FORMAT ('1',//,' MONTH=',I5,5X,'DAY=',I5)
STOP
END

```



```

C*****
SUBROUTINE AVER(N)
C*****
C
C PERFORMS CONVECTIVE MIXING OF SURFACE LAYERS.
C
COMMON /PARAM/ JM,DT,DY,DTT,TSTOP,ET,T(102,2)
COMMON /GEOM/ XL(102),A(102),EL(102),S(102),B(102),YBOT
COMMON /SURS/ DYSUR,AYSUR,SURF(366),YSUR,SAREA,TS
COMMON /MIXA/ DMIX,MIXH
COMMON/WQCONC/ CC(11,105,2),CCC(11,400),COUT(11,5),CCT(11,5)
DIMENSION D(102)
DO 100 J=1,JM
100 D(J)=1000.-0.00663*(T(J,1)-4.)*(T(J,1)-4.)
    AV1=0.0
    AV2=0.0
    JMM=JM-1
    DO 5 I=1,JMM
        J=JM-I+1
        JJ=J-1
        IF (D(JJ)-D(J)) 6,7,7
    6 CONTINUE
        IF(J-2) 8,8,9
    8 T(2,1)=(T(2,1)*A(2)+T(1,1)*A(1)/2.0)/(A(2)+A(1)/2.0)
        T(1,1)=T(2,1)
        GO TO 7
    9 DO 10 K=1,JJ
        KJ=J+1-K
        KJJ=KJ-1
        IF(JM-KJ) 2,2,3
    2 AREA=(AYSUR+(A(JM)+A(JM-1))/2.0)/2.0*DYSUR/DY
        GO TO 4
    3 AREA=A(KJ)
    4 AV1=AV1+T(KJ,1)*AREA
        AV2=AV2+AREA
        TAV=AV1/AV2
        DAV=1000.-0.00663*(TAV-4.)*(TAV-4.)
        IF (D(KJJ)-DAV) 10,20,20
    10 CONTINUE
    20 IF (J.LT.JM) GO TO 25
        MIXH=K
    25 CONTINUE
        DO 30 L=KJ,J
    30 T(L,1)=TAV
    7 AV1=0.0
        AV2=0.0
    5 CONTINUE
    RETURN
    END

```

```

C*****
C*****
      SUBROUTINE WDMIX(N)
C*****
C
C Evaluates wind effects on water mixing
C
      COMMON /PARAM/ JM,DT,DY,DTT,TSTOP,ET,T(102,2)
      COMMON /CONST/ RHO,HCAP,GRAV,VISCOS,TEMDIF
      COMMON /GEOM/ XL(102),A(102),EL(102),S(102),B(102),YBOT
      COMMON /SURS/ DYSUR,AYSUR,SURF(366),YSUR,SAREA,TS
      COMMON /MET/ TAIR,PSI,CLC,W,WINDY
      COMMON /METWD/ WHGT,TAU
      COMMON /MIXA/ DMIX,MIXH
      COMMON /WDM86/ DIFU,FCTR(102),BRUNT(102),D(102),USTR,VSTR,WSTR,
      FACVI,IDFFLG,CD,CT,INDICE,CW,CCON
      COMMON/DENS/TDEN
      DO 100 J=1,JM
100 D(J)=1000.-0.00663*(T(J,1)-4.)*(T(J,1)-4.)
C
C COMPUTE BRUNT-VAISALA FREQUENCY WITH DEPTH
C
      DO 110 J=1,JM-1
      BRUNT(J)=0.
      DRO=(D(J-1)-D(J))
      IF(DRO.LE.0.) GO TO 110
      BRUNT(J)=SQRT(9.8*DRO/1000./DY)
110 CONTINUE
C
C COMPUTE ESPESO - EXISTING MIXED LAYER DEPTH
C
      ESPESO=DYSUR
      DMEZ=D(JM)
      DO 120 J=1,JM
      KK=JM-J+1
      IF(D(KK).EQ.DMFZ) ESPESO=ESPEO+DY
120 CONTINUE
C
C ENTRAINMENT VELOCITY APPROACH
C
      TMIX=T(JM,1)
      DMIX=D(JM)
      VMIX=DYSUR*A(JM)
      JMM=JM-1
C
C COMPUTE TOTAL ENERGY AVAILABLE FOR MIXING - WIND AND
CONVECTION
C
      WSTR=0.
      BEXPAN=0.00028
      CALOR=(-FLUXOT+(1.-BETA)*FLXIN(N))*(1.-EXP(-ETA*DYSUR))*

```

```

      .(A(JM)+A(JM-1))/2./AYSUR))/86400.
      IF(CALOR.LT.0.) WSTR=(BEXPAN*9.8*ESPESO*CALOR/HCAP/1000.):**0.3333
      VSTR=(CW*USTR**3.+CCON*WSTR**3.):**0.3333
      ENGY=1000.*VSTR**3.*DTT*86400.
C
C BEGIN MAIN LOOP FOR DETERMINATION OF MIXED LAYER DEPTH
C
      DO 200 K1=1,JMM
      J=JM-K1
      H2=DYSUR/2.+(K1-1)*DY/2.
      PE1=(D(J)-DMIX)*DY*9.8*H2
      IF(VSTR) 210,210,220
220 RICH=((D(J)-DMIX)*9.8*H2*2.)/(1000.*VSTR*VSTR)
      IF(RICH.LT.0.0) RICH=0.0
C
C LEAKAGE PARAMETER ESTIMATION
C
      IF(BRUNT(J).NE.0.) THEN
      GPR=9.8*(D(J)-DMIX)/1000.
      A2=VSTR/BRUNT(J)
      ELSE
      A2=0.
      ENDIF
C
C COMPUTE EFFICIENCY IN MIXING
C
      RS=2.*H2*(A2*A2)*BRUNT(J)*BRUNT(J)*BRUNT(J)/VSTR/VSTR/VSTR
      IF(RICH.NE.0.) CWIND=0.5*RICH*(1.-CD*RS)/(CT+RICH)
      IF(RICH.EQ.0.) CWIND=0.
      IF(CWIND.LE.0.) CWIND=0.
      GO TO 230
210 CWIND=0.0
230 IF(PE1-CWIND*ENGY) 250,250,300
C
C MIX ENTIRE LAYER WITH MIXED LAYER
C
250 TMIX=(TMIX*VMIX+T(J,1)*A(J)*DY)/(VMIX+A(J)*DY)
      VMIX=VMIX+A(J)*DY
      DMIX=1000.-0.00663*(TMIX-4)*(TMIX-4.)
      K2=K1+1
      DO 260 JJ=1,K2
      I=JM+1-JJ
      T(I,1)=TMIX
260 D(I)=DMIX
      IF(PE1.LE.0.0) GO TO 200
      ENGY=ENGY-PE1/CWIND
200 CONTINUE
      GO TO 350
C
C MIX FRACTION OF A LAYER
C

```

```

300  X=CWIND*ENGY
      DELTAY=X/((D(J)-DMIX)*9.8*H2)
      DELY=DELTAY/DY
      TMIX=(TMIX*VMIX+T(J,1)*A(J)*DELTAY)/(VMIX+A(J)*DELTAY)
      T(J,1)=T(J,1)*(1.-DELY)+TMIX*DELY
      DO 330 JJ=1,K1
        I=JM+1-JJ
330  T(I,1)=TMIX
350  CONTINUE
      MIXH=K1
      RETURN
      END

```

```

C*****
C*****
      SUBROUTINE SPECAV(N)
C*****
C
C  AVERAGING OF SPECIFIED MATERIAL IN MIXED LAYERS
C
      COMMON /PARAM/ JM,DT,DY,DTT,TSTOP,ET,T(102,2)
      COMMON /GEOM/ XL(102),A(102),EL(102),S(102),B(102),YBOT
      COMMON /SURS/ DYSUR,AYSUR,SURF(366),YSUR,SAREA,TS
      COMMON/WQCONC/ CC(11,105,2),CCC(11,400),COUT(11,5),CCT(11,5)
      COMMON /MIXA/ DMIX,MIXH
      COMMON /WQPARM/ JEUP,MM
      JMIXH=JM-MIXH+1
      IF(MM)120,120,10
10    CONTINUE
      DO 40 M=1,MM
      XCC=0.0
      XA=0.0
      JMM=JM-1
      DO 20 J=JMIXH,JMM
      XCC=CC(M,J,1)*(A(J)+A(J-1))*5*DY+XCC
20    XA=XA+(A(J)+A(J-1))*5*DY
      XCC=XCC+CC(M,JM,1)*SAREA*DYSUR
      XA=XA+SAREA*DYSUR
      DO 30 I=JMIXH,JM
30    CC(M,I,2)= XCC/XA
      IF(CC(M,I,2).LE.0.0) CC(M,I,2)=0.0
40    CONTINUE
      DO 50 I=1,JM
      CC(5,I,2)=CC(3,I,2)+CC(4,I,2)+CC(11,I,2)
50    CONTINUE
120   CONTINUE
      RETURN
      END
C*****

```

```

C*****
      SUBROUTINE TOUT(HEATOT,FLOWOT)
C*****
C
C COMPUTE WEIGHTED AVERAGE OF OUTFLOW TEMPERATURE.
C
      COMMON /PARAM/ JM,DT,DY,DTT,TSTOP,ET,T(102,2)
      COMMON /GEOM/ XL(102),A(102),EL(102),S(102),B(102),YBOT
      COMMON /SURS/ DYSUR,AYSUR,SURF(366),YSUR,SAREA,TS
      COMMON /VELA/ UI(102,1),UOT(102,5),V(102,1),UO(102,1),III
      I=III
      HEATOT=T(JM,1)*B(JM)*UOT(JM,I)*DYSUR+T(1,1)*B(1)*UOT(1,I)*DY/2.0
      FLOWOT=B(JM)*UOT(JM,I)*DYSUR+B(1)*UOT(1,I)*DY/2.0
      JMM=JM-1
      DO 2 J=2,JMM
      HEATOT=HEATOT+UOT(J,I)*B(J)*DY*T(J,1)
2 FLOWOT=FLOWOT+UOT(J,I)*B(J)*DY
      IF(FLOWOT.EQ.0.0) FLOWOT=1.0
      CONTINUE
      RETURN
      END

```

```

C*****
      SUBROUTINE SPECOT(N)
C*****
C
C PROPORTION OF SPECIFIED CONSTITUENTS IN OUTFLOW
C
      COMMON /PARAM/ JM,DT,DY,DTT,TSTOP,ET,T(102,2)
      COMMON /GEOM/ XL(102),A(102),EL(102),S(102),B(102),YBOT
      COMMON /WQCONC/ CC(11,105,2),CCC(11,400),COUT(11,5),CCT(11,5)
      COMMON /VELA/ UI(102,1),UOT(102,5),V(102,1),UO(102,1),III
      I=III
      IF (QOUT(N,I).EQ.0.0) GO TO 10
      DOT=CC(1,JM,1)*B(JM)*UOT(JM,I)*DYSUR+CC(1,1,1)*B(1)*UOT(1,I)/2.
      $*DY
      BODOT=CC(2,JM,1)*B(JM)*UOT(JM,I)*DYSUR+CC(2,1,1)*B(1)*UOT(1,I)*
      $DY/2.0
      ALG1T=CC(3,JM,1)*B(JM)*UOT(JM,I)*DYSUR+CC(3,1,1)*B(1)*UOT(1,I)
      $/2.*DY
      ALG2T=CC(4,JM,1)*B(JM)*UOT(JM,I)*DYSUR+CC(4,1,1)*B(1)*UOT(1,I)
      $/2.*DY
      ALG3T=CC(11,JM,1)*B(JM)*UOT(JM,I)*DYSUR+CC(11,1,1)*B(1)*UOT(1,I)
      ALGTT=ALG1T+ALG2T+ALG3T
      SILT=CC(6,JM,1)*B(JM)*UOT(JM,I)*DYSUR+CC(6,1,1)*B(1)*UOT(1,I)
      $/2.*DY
      PHOST=CC(7,JM,1)*B(JM)*UOT(JM,I)*DYSUR+CC(7,1,1)*B(1)*UOT(1,I)
      $/2.*DY

```

```

      ANITT=CC(8,JN,1)*B(JM)*UOT(JM,I)*DYSUR+CC(8,1,1)*B(1)*UOT(1,I)
      $/2.*DY
      AMONT=CC(9,JM,1)*B(JM)*UOT(JM,I)*DYSUR+CC(9,1,1)*B(1)*UOT(1,I)
      $/2.*DY
      ANT=CC(10,JM,1)*B(JM)*UOT(JM,I)*DYSUR+CC(10,1,1)*B(1)*UOT(1,I)
      $/2.*DY
      FLOWOT=B(JM)*UOT(JM,I)*DYSUR+B(1)*UOT(1,I)*DY/2.0
      JMM=JM-1
      DO 2 J=2,JMM
      DOT=DOT+UOT(J,I)*CC(1,J,1)*DY*B(J)
      BODOT=BODOT+UOT(J,I)*CC(2,J,1)*DY*B(J)
      ALG1T=ALG1T+UOT(J,I)*CC(3,J,1)*DY*B(J)
      ALG2T=ALG2T+UOT(J,I)*CC(4,J,1)*DY*B(J)
      ALG3T=ALG3T+UOT(J,I)*CC(11,J,1)*DY*B(J)
      ALGTT=ALG1T+ALG2T+ALG3T
      SILT=SILT+UOT(J,I)*CC(6,J,1)*DY*B(J)
      PHOST=PHOST+UOT(J,I)*CC(7,J,1)*DY*B(J)
      ANITT=ANITT+UOT(J,I)*CC(8,J,1)*DY*B(J)
      AMONT=AMONT+UOT(J,I)*CC(9,J,1)*DY*B(J)
      ANT=ANT+UOT(J,I)*CC(10,J,1)*DY*B(J)
2  FLOWOT=FLOWOT+UOT(J,I)*DY*B(J)
      IF(FLOWOT.LE.0.0) FLOWOT=1.0
      COUT(1,I)=DOT/FLOWOT
      COUT(2,I)=BODOT/FLOWOT
      COUT(3,I)=ALG1T/FLOWOT
      COUT(4,I)=ALG2T/FLOWOT
      COUT(5,I)=ALGTT/FLOWOT
      COUT(6,I)=SILT/FLOWOT
      COUT(7,I)=PHOST/FLOWOT
      COUT(8,I)=ANITT/FLOWOT
      COUT(9,I)=AMONT/FLOWOT
      COUT(10,I)=ANT/FLOWOT
      COUT(11,I)=ALG3T/FLOWOT
      GO TO 11
10 COUT(1,I)=0.0
      COUT(2,I)=0.0
      COUT(3,I)=0.0
      COUT(4,I)=0.0
      COUT(5,I)=0.0
      COUT(6,I)=0.0
      COUT(7,I)=0.0
      COUT(8,I)=0.0
      COUT(9,I)=0.0
      COUT(10,I)=0.0
      COUT(11,I)=0.0
11 RETURN
      END

```

```

C*****
SUBROUTINE XDATE(DAY,LDAY,NMONTH)
C*****
INTEGER MONTH(12)/31,28,31,30,31,30,31,31,30,31,30,31/
LDAY=DAY
IF(LDAY.LE.MONTH(1)) GO TO 30
DO 10 I=1,12
IF(I.EQ.12) GO TO 20
LDAY=LDAY-MONTH(I)
IF(LDAY.LE.MONTH(I+1))GO TO 20
10 CONTINUE
20 NMONTH=I+1
IF(NMONTH.EQ.13)NMONTH=1
RETURN
30 NMONTH=1
RETURN
END

C*****
FUNCTION FLXOUT(N)
C*****
C
C CALCULATION OF SURFACE LOSSES DUE TO EVAPORATION, CONDUCTION,
C AND RADIATION
C
COMMON /PARAM/ JM,DT,DY,DTT,TSTOP,ET,T(102,2)
COMMON /CONST/ RHO,HCAP,GRAV,VISCOS,TEMDIF,ZIB
COMMON /METWD/ WHGT,TAU
COMMON /SWITCH/ KSUR,KOH,KQ,KLOSS,KMIX,KATRAD
COMMON /GEOM/ XL(102),A(102),EL(102),S(102),B(102),YBOT
COMMON /SURS/ DYSUR,AYSUR,SURF(366),YSUR,SAREA,TS
COMMON /MET/ TAIR,PSI,CLC,W,WINDY
COMMON/METEOA/ TA(400),SIGH(400),CLOUD(400),WIND(400),TI(400)
COMMON /METEOB/ FIN(400),ATRAD(400)
COMMON /TIMES/ DTTA,DTSIGH,DCLOUD,DTWIND,DTTI,DTFIN,DATRAD
COMMON /FLUXES/ EVAP,RAD,AR,EVPCON
C
C KLOSS=1 FOR FIELD USING KOHLER FORMULA.
C 2 FOR FIELD USING ROHWER FORMULA.
C 3 FOR FIELD USING LAKE HEFNER FORMULA
C KATRAD = 1 MEASURED ATMOSPHERIC RADIATION
C 2 ATMOS. RAD. CALCULATED WITH SWINBANK'S FORMULA.
C 3 ATMOS. RAD. CALCULATED WITH BRUTSAERT'S FORMULA.
C
OPEN (20,FILE='EVAP.OUT',STATUS='OLD')
IOUTEVP=20
ET=DTT*FLOAT(N)
R=ET/DTTA +1.0

```



```

      L=R
      RR = R-FLOAT(L)
      TAIR=TA(L)+RR*(TA(L+1)-TA(L))
      R=ET/DTSIGH +1.0
      L=R
      RR = R-FLOAT(L)
      PSI=SIGH(L)+RR*(SIGH(L+1)-SIGH(L))
      TS = T(JM,1)
      H = 597.3-0.56*TS
C
C   EXPONENTIAL APPROX. FOR VAPOR PRESS.
C
      TSF=TS*9./5.+32.
      ES=25.4*EXP(17.62-9500.8/(TSF+460.))
      TAIRF=TAIR*9./5.+32.
      EA=PSI*25.4*EXP(17.62-9500.8/(TAIRF+460.))
      DE=(ES-EA)*10.304/ALOG(WHGT/0.000067)
C
C   FOR FIELD DATA, WIND SPEED IS IN M/SEC.
C
      20 R=ET/DTWIND +1.0
      L=R
      W=WIND(L)+(R-FLOAT(L))*(WIND(L+1)-WIND(L))
      WINDY=W
      WO=W*7.6/ALOG(WHGT*1000.)
C
C   CALCULATION OF ATMOSPHERIC RADIATION
C   UNITS OF RADIATION ARE KCAL/M-M-DAY.
C
      GO TO (7,11,11), KATRAD
      7 R=ET/DATRAD +1.0
      L=R
      AR=ATRAD(L)+(R-FLOAT(L))*(ATRAD(L+1)-ATRAD(L))
      RAD = 1.13587E-6*(TS+273.16)**4-AR
      GO TO 9
      11 R=ET/DCLOUD+1.0
      L=R
      CLC=CLOUD(L)+(R-FLOAT(L))*(CLOUD(L+1)-CLOUD(L))
      GO TO (7,8,10), KATRAD
      8 AR=1.0643102E-11*(TAIR+273.16)**6*(1.0+0.17*CLC**2)
      RAD=1.13587E-6*(TS+273.16)**4-AR
      GO TO 9
C
C   VAPOR PRESSURE IN MILLIBARS
C
      10 EA=EA/0.750062
      AR=1.24*(EA/(TAIR+273.16))**(1./7.)*1.13587E-6*(TAIR+273.16)**4
      $(1.0+0.17*CLC**2)
      RAD=1.13587E-6*(TS+273.16)**4-AR
      9 GO TO (25,30,50), KLOSS
C

```

C CALCULATION OF FIELD EVAPORATION USING KOHLER FORMULA.
 C VAPOR PRESSURES IN MB.

C
 25 DE = DE/0.750062
 EVAP = H*DE+HCAP*DE*TS
 EVAP=.000135*RHO*WO*EVAP
 CONDUCT=RHO*.000135*WO*372.0*(TS-TAIR)
 IF(EVAP)3,3,4
 3 EVAP=0.0
 4 EVAP=EVAP+CONDUCT
 FLXOUT=EVAP+RAD
 RETURN

C
 C CALCULATION OF FIELD EVAPORATION USING ROHWER FORMULA.
 C ADJUSTMENTS TO REDUCE DATA HEIGHT FROM 2 M TO 6 INCHES

C
 30 CONTINUE
 IF(WO-1.76) 61,61,62
 61 WW=WO*0.66
 GO TO 31
 62 WW=WO*0.57
 31 CHI=RHO*(H*DE+TS*HCAP*DE)
 FW=0.0308+0.0185*WW
 EVAP = CHI*FW*EVPCON
 IF(ZIB.EQ.2.0) THEN
 WRITE (IOUTEVP,1700) EVAP
 ELSE
 CONTINUE
 ENDIF
 1700 FORMAT(F6.1)
 CONDUCT=RHO*EVPCON*269.1*(TS-TAIR)*FW
 IF(EVAP)5,5,6
 5 EVAP=0.0
 6 EVAP=EVAP+CONDUCT
 FLXOUT =EVAP+RAD
 RETURN

C
 C CALCULATION OF FIELD EVAPORATION USING LAKE HEFNER FORMULA.
 C WIND IN MPH

C
 50 W2=WO/.447
 EVAP=17*W2*DE*2.7126
 CONDUCT=.255*((TS-TAIR)*1.8/DE)*EVAP
 IF (EVAP) 51,51,52
 51 EVAP=0.0
 52 EVAP=EVAP+CONDUCT
 FLXOUT=EVAP+RAD
 RETURN
 END

```

C*****
FUNCTION FLXIN(N)
C*****
C
C COMPUTE INCOMING SOLAR RADIATION FROM READ IN VALUES.
C READ IN VALUES TREATED AS A STEP FUNCTION.
C
COMMON /PARAM/ JM,DT,DY,DTT,TSTOP,ET,T(102,2)
COMMON /MET/ TAIR,PSI,CLC,W,WINDY
COMMON /METEOA/ TA(400),SIGH(400),CLOUD(400),WIND(400),TI(400)
COMMON /METEOB/ FIN(400),ATRAD(400)
COMMON /TIMES/ DTTA,DTSIGN,DCLOUD,DTWIND,DTTI,DTFIN,DATRAD
COMMON /SUNFX/ ELMAX,DDPL,XLAT,RG,KSLRAD,IDAY
DIMENSION DPT(400)
IF(KSLRAD.EQ.2) GO TO 10
ET=DTT*FLOAT(N)
R=ET/DTFIN+1.0
L = R
FLXIN=FIN(L)
RETURN
10 CONTINUE
C
C COMPUTE DEW POINT FROM RELATIVE HUMIDITY,AIR TEMPERATURE
C
J=N+IDAY
ET=DTT*FLOAT(N)
R=ET/DCLOUD+1.0
L=R
CLC=CLOUD(L)+(R-FLOAT(L))*(CLOUD(L+1)-CLOUD(L))
IF(TAIR.LT.0.)GO TO 20
EA=PSI* EXP(2.3026*((7.5*TAIR)/(TAIR+273.3)+0.7858))
DPT(J)=(237.3*(ALOG10(EA)-0.7858))/(7.5+0.7858-ALOG10(EA))
GO TO 30
20 EA=PSI* EXP(2.3026*((9.5*TAIR)/(TAIR+265.5)+0.7858))
DPT(J)=(265.5*(ALOG10(EA)-0.7858))/(9.5+0.7858-ALOG10(EA))
30 CONTINUE
C
C COMPUTE SOLAR RADIATION
C
X12=XLAT*3.14159/180.
X1= SIN(X12)
X2= COS(X12)
X3=((288.-6.5E-3*ELMAX)/288.)**5.256
C
C ENTER DAY LOOP
C
SSOL=.
C
C ATMOSPHERIC WATER CONTENT
C
XW=0.85* EXP(0.11+6.14E-2*DPT(J))

```

```

      X186MN=186-J
C
C DISTANCE EARTH-SUN
C
      R=1.+1.7E-2* COS(3.14159*X186MN/182.5)
      X172MN=172-J
      CO=0.40928* COS(3.14159*X172MN/182.5)
      C9=1164./R**2
C
C COMPUTE HOUR ANGLE OF SUNSET
C
      XJ1=-X1* SIN(CO)/(X2* COS(CO))
      IF(XJ1.EQ..0)GO TO 40
      XJ2= SQRT(1.-XJ1**2)
      XJ3= ATAN2(XJ2,XJ1)*180./3.14159
      IF(XJ3.GT.0.)GO TO 50
      TO=180.+XJ3
      GO TO 60
40    TO=90
      GO TO 60
50    TO=XJ3
60    TO=TO*4./60.
      NTO=TO
C
C ENTER HOUR LOOP TO INTEGRATE SOLAR RADIATION OVER SUNSHINE
DURATION
C
      DO 120 I=1,NTO
      XIMOP5=I-0.5
C
C SINUS OF SOLAR ALTITUDE
C
      SINA=X1* SIN(CO)+X2* COS(CO)* COS(XIMOP5*3.14159/12.)
      A7= ATAN2(SINA, SQRT(1.-SINA**2))*180./3.14159
C
C OPTICAL AIR MASS AFTER KASTEN
C
      XM7=X3/(CINA+0.15*(1./(A7+3.885)**1.253))
C
C ATMOSPHERIC TRANSMISSION AFTER KIMBALL USING ORLOB-SELNA
FORMULAS
C
      A1= EXP(-(.465+.134*XW)*(.129+.171* EXP(-.88*XM7))*XM7)
      A2= EXP(-(.465+.134*XW)*(.179+.421* EXP(-.721*XM7))*XM7)
      A3=A2+(1.-A1-DDPL)/2
      A0=A3/(1.-RG*.5*(1.-A1+DDPL))
C
C SOLAR RADIATION REACHING THE SURFACE
C
      X=C9*SINA*A0
C

```

```

      IF(CLC.EQ.0.)GO TO 70
      IF(CLC.LT.0.5)GO TO 80
      IF(CLC.LT.0.9)GO TO 90
      IF(CLC.EQ.1.)GO TO 100

C
C TOTAL SOLAR RADIATION REFLECTIVITY AFTER ANDERSON
C
70    RO=1.-1.18*(1./A7**(0.77))
      GO TO 110
80    RO=1.-2.2*(1./A7**(0.97))
      GO TO 110
90    RO=1.-0.95*(1./A7**(0.75))
      GO TO 110
100   RO=1.-0.33*(1./A7**(0.45))
110   SOL=X*RO
      SSOL=SSOL+SOL
120   CONTINUE
      RSOL=0.5*(TO-NTO)*SOL
      SSOL=SSOL+RSOL

C
C DAILY TOTAL SOLAR RADIATION ENTERING THE WATER SURFACE IN
KCAL/M**2-DA
C
      FIN(N)=SSOL*(1.-0.65*(CLC)**2)*2.
      FLXIN=FIN(N)
      RETURN
      END

C*****
      FUNCTION TTIN(N)
C*****
C
      COMPUTE INFLOW TEMPERATURE FROM READ IN VALUES.
C LINEAR INTERPOLATION BETWEEN READ IN VALUES.
C
      COMMON /PARAM/ JM,DT,DY,DTT,TSTOP,ET,T(102,2)
      COMMON/METEOA/ TA(400),SIGH(400),CLOUD(400),WIND(400),TI(400)
      COMMON /TIMES/ DTTA,DTSIGH,DCLOUD,DTWIND,DTTI,DTFIN,DATRAD
      ET=DTT*FLOAT(N)
      R=ET/DTTI +1.0
      L=R
      RR = R-FLOAT(L)
      TTIN=TI(L)+RR*(TI(L+1)-TI(L))
      RETURN
      END

```

```

C*****
      FUNCTION QOUT(N,I)
C*****
C
C COMPUTE OUTFLOW RATE FROM READ IN VALUES.
C READ IN VALUES TREATED AS A STEP FUNCTION.
C
      COMMON /PARAM/ JM,DT,DY,DTT,TSTOP,ET,T(102,2)
      COMMON /FLOWS/ QI(400),QO(400,5),DTQI,DTQO
      ET=DTT*FLOAT(N)
      R=ET/DTQO +1.0
      L=R
      QOUT=QO(L,I)*86400.
      RETURN
      END

```

```

C*****
      FUNCTION QQIN(N)
C*****
C
C COMPUTE INFLOW RATE FROM READ IN VALUES.
C READ IN VALUES TREATED AS A STEP FUNCTION.
C
      COMMON /PARAM/ JM,DT,DY,DTT,TSTOP,ET,T(102,2)
      COMMON /FLOWS/ QI(400),QO(400,5),DTQI,DTQO
      ET=DTT*FLOAT(N)
      R=ET/DTQI +1.0
      L=R
      QQIN=QI(L)*86400.
      RETURN
      END

```

```

C*****
      FUNCTION DDO(N)
C*****
C
C COMPUTE INPUT DO FROM READ IN VALUES
C
      COMMON /PARAM/ JM,DT,DY,DTT,TSTOP,ET,T(102,2)
      COMMON/DOBOD/ DO(400),BOD(400),DDOC,DBOD
      COMMON/WQMIX/LAGTIM(400),NTRAC(20),NLEVE(400),ITR
      COMMON/WQCONT/ZKBOD,BENTHC,TBASE,SPEDIF,XAIR
      Z=ZKBOD
      ET=DTT*FLOAT(N)
      R=ET/DDOC+1.0

```

```

      L=R
      NGOT=NLEVE(N)
      DDO=DO(L)
      IF(LAGTIM(N))30,30,10
10    GO TO (30,20),NGOT
C
C  SUBSURFACE ENTRANCE
C
20    DDO=DO(L)-BBOD(N)*(1.-EXP(LAGTIM(N)*DTT*(-Z)))/(EXP(LAGTIM(N)
      1*DTT*(-Z)))
30    CONTINUE
      RETURN
      END

```

```

C*****
      FUNCTION BBOD(N)
C*****
C
C  CALCULATES INPUT BOD FROM READ IN VALUES
C
      COMMON/WQCONT/ZKBOD,BENTHC,TBASE,SPEDIF,XAIR
      COMMON/WQMIX/LAGTIM(400),NTRAC(20),NLEVE(400),ITR
      COMMON/DOBOD/ DO(400),BOD(400),DDOC,DBOD
      COMMON /PARAM/ JM,DT,DY,DTT,TSTOP,ET,T(102,2)
      RBOD=ET/DBOD+1.0
      LBOD=RBOD
      RRBOD=-RBOD-FLOAT(LBOD)
      BBOD=BOD(LBOD)*QQIN(LBOD)+RRBOD*(BOD(LBOD+1)*QQIN(LBOD+1)
      3-BOD(LBOD)*QQIN(LBOD))
      BBOD=BBOD/QQIN(N)
      NGOT=NLEVE(N)
      GO TO (10,20),NGOT
10    BBOD=BBOD
      GO TO 30
C
C  SUBSURFACE ENTRANCE
C
20    BBOD=BBOD*(EXP(LAGTIM(N)*DTT*(-ZKBOD)))
30    CONTINUE
      RETURN
      END

```

```

C*****
      FUNCTION SSIL(N)
C*****
C
C EVALUATES SiO3 CONCENTRATION IN INFLOW WATERS
C
      COMMON/PARAM/JM,DT,DY,DTT,TSTOP,ET,T(102,2)
      COMMON/NUTRI/SIL(400),DSIL,PHOS(400),DPHOS,ANIT(400),DNIT,
      $AMON(400),DAMON,ANO2(400),DNO2
      RSIL=ET/DSIL+1.0
      LSIL=RSIL
      RRSIL=RSIL-FLOAT(LSIL)
      SSIL=SIL(LSIL)*QQIN(LSIL)+RRSIL*(SIL(LSIL+1)*QQIN(LSIL+1)
      $-SIL(LSIL)*QQIN(LSIL))
      SSIL=SSIL/QQIN(N)
      RETURN
      END

```

```

C*****
      FUNCTION PPHOS(N)
C*****
C
C EVALUATES PO4 CONCENTRATION IN INFLOW WATERS
C
      COMMON/PARAM/JM,DT,DY,DTT,TSTOP,ET,T(102,2)
      COMMON/NUTRI/SIL(400),DSIL,PHOS(400),DPHOS,ANIT(400),DNIT,
      $AMON(400),DAMON,ANO2(400),DNO2
      RPHOS=ET/DPHOS+1.0
      LPHOS=RPHOS
      RRPPOS=RPHOS-FLOAT(LPHOS)

      PPHOS=PHOS(LPHOS)*QQIN(LPHOS)+RRPHOS*(PHOS(LPHOS+1)*QQIN(LPHOS+1)
      $-PHOS(LPHOS)*QQIN(LPHOS))
      PPHOS=PPHOS/QQIN(N)
      RETURN
      END

```


C*****

FUNCTION AANIT(N)

C*****

C

C EVALUATES NO3 CONCENTRATION IN INFLOW WATERS

C

```
COMMON/PARAM/JM,DT,DY,DTT,TSTOP,ET,T(102,2)
COMMON/NUTRI/SIL(400),DSIL,PHOS(400),DPHOS,ANIT(400),DNIT,
$AMON(400),DAMON,ANO2(400),DNO2
RNIT=ET/DNIT+1.0
LNIT=RNIT
RRNIT=RNIT-FLOAT(LNIT)
AANIT=ANIT(LNIT)*QQIN(LNIT)+RRNIT*(ANIT(LNIT+1)*QQIN(LNIT+1)
$-ANIT(LNIT)*QQIN(LNIT))
AANIT=AANIT/QQIN(N)
RETURN
END
```

C*****

FUNCTION AAMON(N)

C*****

C

C EVALUATES NH4 CONCENTRATION IN INFLOW WATERS

C

```
COMMON/PARAM/JM,DT,DY,DTT,TSTOP,ET,T(102,2)
COMMON/NUTRI/SIL(400),DSIL,PHOS(400),DPHOS,ANIT(400),DNIT,
$AMON(400),DAMON,ANO2(400),DNO2
RAMON=ET/DAMON+1.0
LAMON=RAMON
RRAMON=RAMON-FLOAT(LAMON)
```

```
AAMON=AMON(LAMON)*QQIN(LAMON)+RRAMON*(AMON(LAMON+1)*QQIN(LAMON
+1)
```

```
$-AMON(LAMON)*QQIN(LAMON))
AAMON=AAMON/QQIN(N)
RETURN
END
```

```

C*****
      FUNCTION AANO2(N)
C*****
C
C EVALUATES NO2 CONCENTRATION IN THE INFLOW
C
      COMMON/PARAM/JM,DT,DY,DTT,TSTOP,ET,T(102,2)
      COMMON/NUTRI/SIL(400),DSIL,PHOS(400),DPHOS,ANIT(400),DNIT,
      $AMON(400),DAMON,ANO2(400),DNO2
      RNO2=ET/DNO2+1.0
      LNO2=RNO2
      RRNO2=RNO2-FLOAT(LNO2)
      AANO2=ANO2(LNO2)*QQIN(LNO2)+RRNO2*(ANO2(LNO2+1)*QQIN(LNO2+1)
      $-ANO2(LNO2)*QQIN(LNO2))
      AANO2=AANO2/QQIN(N)
      RETURN
      END

```

```

C*****
      FUNCTION REAR(N)
C*****
C
C EVALUATES REAERATION COEFFICIENT
C
      COMMON /PARAM/ JM,DT,DY,DTT,TSTOP,ET,T(102,2)
      COMMON /MET/ TAIR,PSI,CLC,W,WINDY
      COMMON /WQCONT/ZKBOD,BENTHC,TBASE,SPEDIF,XAIR
      AKL=86400.*(1.0E-6+(W*7.99E-6))
      TFAC=1.025**(T(JM-1,1)-20.0)
      REAR=AKL*TFAC
      RETURN
      END

```

```

C*****
C
      SUBROUTINE XMIX(N)
C
C*****
C  CALCULATION OF COMPOSITION OF INFLOW
      COMMON /PARAM/ JM,DT,DY,DTT,TSTOP,ET,T(102,2)
      COMMON /OUTLET/ NOUT,LOUT(5),ELOUT(5),QIN(400),TIN(400)
      COMMON /MIX/ QQMIX(102),RMIX,JMIXB,MIXED,QMIX
      COMMON/WQCONC/ CC(11,105,2),CCC(11,400),COUT(11,5),CCT(11,5)
      COMMON/NUTRI/SIL(400),DSIL,PHOS(400),DPHOS,ANIT(400),DNIT,
      $AMON(400),DAMON,ANO2(400),DNO2
      COMMON/WQMIX/LAGTIM(400),NTRAC(20),NLEVE(400),ITR
      COMMON /SWITCH/ KSUR,KOH,KQ,KLOSS,KMIX,KATRAD
      COMMON/WQPARM/JEUP,MM
      GO TO (10,20),KMIX
C
C IF NO ENTRANCE MIXING ALLOWED
C
      10 IF (QIN(N).EQ.0.0)THEN
          DO 213 I=1,MM
              CCC(I,N)=0.0
      213 CONTINUE
          ELSE
              CCC(1,N)=DDO(N)
              CCC(2,N)=BBOD(N)
              CCC(6,N)=SSIL(N)
              CCC(7,N)=PPHOS(N)
              CCC(8,N)=AANIT(N)
              CCC(9,N)=AAMON(N)
              CCC(10,N)=AANO2(N)
          ENDIF
          RETURN
C
C IF ENTRANCE MIXING ALLOWED (RECOMMENDED CASE)
C
      20 CONTINUE
          XQ=QIN(N)*(1.0+RMIX)
          IF(XQ.EQ.0.0) THEN
              DO 212 I=1,MM
                  CCC(I,N)=0.0
      212 CONTINUE
          ELSE
              JMIXB=JM-MIXED
              JMM=JM-1
              YQ1=QQMIX(JM)*CC(1,JM,1)
              YQ2=QQMIX(JM)*CC(2,JM,1)
              YQ6=QQMIX(JM)*CC(6,JM,1)
              YQ7=QQMIX(JM)*CC(7,JM,1)
              YQ8=QQMIX(JM)*CC(8,JM,1)
              YQ9=QQMIX(JM)*CC(9,JM,1)

```

```

YQ10=QQMIX(JM)*CC(10,JM,1)
DO 160 J=JMIXB,JMM
YQ1=YQ1+QQMIX(J)*CC(1,J,1)
YQ2=YQ2+QQMIX(J)*CC(2,J,1)
YQ6=YQ6+QQMIX(J)*CC(6,J,1)
YQ7=YQ7+QQMIX(J)*CC(7,J,1)
YQ8=YQ8+QQMIX(J)*CC(8,J,1)
YQ9=YQ9+QQMIX(J)*CC(9,J,1)
160 YQ10=YQ10+QQMIX(J)*CC(10,J,1)
CCC(1,N)=YQ1/XQ
CCC(2,N)=YQ2/XQ
CCC(6,N)=YQ6/XQ
CCC(7,N)=YQ7/XQ
CCC(8,N)=YQ8/XQ
CCC(9,N)=YQ9/XQ
CCC(10,N)=YQ10/XQ
IF(N-60)180,180,170
170 NX=60
GO TO 190
180 NX=N
190 CONTINUE
DO 210 I=1,NX
NLM=N+1-I
IF(N-(NLM+LAGTIM(NLM)))209,200,209
200 CCC(1,N)=CCC(1,N)+QQIN(NLM)*DDO(NLM)/XQ
CCC(2,N)=CCC(2,N)+QQIN(NLM)*BBOD(NLM)/XQ
CCC(6,N)=CCC(6,N)+QQIN(NLM)*SSIL(NLM)/XQ
CCC(7,N)=CCC(7,N)+QQIN(NLM)*PPHOS(NLM)/XQ
CCC(8,N)=CCC(8,N)+QQIN(NLM)*AANIT(NLM)/XQ
CCC(9,N)=CCC(9,N)+QQIN(NLM)*AAMON(NLM)/XQ
CCC(10,N)=CCC(10,N)+QQIN(NLM)*AANO2(NLM)/XQ
209 CONTINUE
210 CONTINUE
ENDIF
RETURN
END

```

```

C*****
C
  SUBROUTINE TEMDIS(N)
C
C*****
C
C
C CALCULATES THE VERTICAL DISTRIBUTION OF TEMPERATURES
C
  COMMON /PARAM/ JM,DT,DY,DTT,TSTOP,ET,T(102,2)
  COMMON /CONST/ RHO,HCAP,GRAV,VISCOS,TEMDF
  COMMON /SWITCH/ KSUR,KOH,KQ,KLOSS,KMIX,KATRAD
  COMMON /EXTIN/ ETA,BETA,XTN(366),DTXTN
  COMMON /GEOM/ XL(102),A(102),EL(102),S(102),B(102),YBOT
  COMMON /SURS/ DYSUR,AYSUR,SURF(366),YSUR,SAREA,TS
  COMMON /VELA/ UI(102,1),UOT(102,5) V(102,1),UO(102,1),III
  COMMON/TEMP/ DELTF,FLUXOT,TSAVE
  COMMON /WDM86/ DIFU,FCTR(102),BRUNT(102),D(102),USTR,VSTR,WSTR,
  .FACVI,IDFFLG,CD,CT,INDICE,CW,CCON
  JMM=JM-1
C
C CALCULATIONS FOR INTERMEDIATE LAYERS
C
  DO 1114 J=2,JMM
C
C DIRECT ABSORPTION TERM - MODIFIED 10/29/86 EMO
C
  ARJ1=(A(J)+A(J+1))/2.0
  ARJ2=(A(J)+A(J-1))/2.0
  ARG1=ETA*(YSUR-EL(J))
  IF(ARG1.GT.20.0) THEN
    DELTA=0.0
  ELSE
    DELTA=(1.0-BETA)*FLXIN(N)*(EXP(-ETA*(YSUR-EL(J)-DY/2.0))*ARJ1-
    $EXP(-ETA*(YSUR-EL(J)+DY/2.0))*ARJ2)/A(J)/DY/HCAP/RHO
  ENDIF
C
C VERTICAL ADVECTION TERM
C
  IF(V(J,1)) 1160,1160,1161
1160 IF(V(J+1,1))1170,1170,1171
1170 DELTB=(V(J,1)*T(J,1)*(A(J)+A(J-1))/2.0-V(J+1,1)*T(J+1,1)*(A(J+1)+
  $A(J))/2.0)/A(J)/DY
  GO TO 1162
1171 DELTB=(V(J,1)*T(J,1)*(A(J)+A(J-1))/2.0-V(J+1,1)*T(J,1)*(A(J+1)+
  $A(J))/2.0)/A(J)/DY
  GO TO 1162
1161 IF(V(J+1,1))1172,1172,1173
1173 DELTB=(V(J,1)*T(J-1,1)*(A(J)+A(J-1))/2.0-V(J+1,1)*T(J,1)*(A(J+1)+
  $A(J))/2.0)/A(J)/DY
  GO TO 1162

```

```

1172 DELTB=(V(J,1)*T(J-1,1)*(A(J)+A(J-1))/2.0-V(J+1,1)*T(J+1,1)*(A(J+1)
    $+A(J))/2.0)/A(J)/DY
C
C HORIZONTAL ADVECTION TERM
C
1162 DELTC=(UI(J,1)*TS-UO(J,1)*T(J,1))*B(J)*DY/A(J)/DY
C
C DIFFUSION TERM - MODIFIED 10/29/86 EMO
C
    DELTD=DIFU*((T(J+1,1)-T(J,1))/DY/FCTR(J+1)*ARJ1-(T(J,1)-T(J-1,1))
    $/DY/FCTR(J)*ARJ2)/A(J)/DY
    DELT=(DELTA+DELTB+DELTG+DELTD)*DT
1114 T(J,2)=T(J,1)+DELT
C
C CALCULATIONS FOR SURFACE LAYER
C
    FLXN=FLXIN(N)

DELTA=DT*((1.0-BETA)*FLXIN(N)*(AYSUR-EXP(-ETA*DYSUR)*(A(JM)+A(JM-1
    $))/2.0)/SAREA/DYSUR/HCAP/RHO)
    DELTD=-DIFU/FCTR(JM)*(T(JM,1)-T(JM-1,1))/DY*(A(JM)+A(JM-1))
    $/2.0/SAREA/DYSUR*DT
    DELTE=BETA*FLXIN(N)*AYSUR/RHO/HCAP/DYSUR/SAREA*DT
    DELTF=-FLUXOT*AYSUR/RHO/HCAP/DYSUR/SAREA*DT
    IF (V(JM,1))1163,1164,1164
1164 DELTI=DT*(V(JM,1)*(T(JM-1,1)-T(JM,1))*(A(JM)+A(JM-1))/2.0/SAREA
    $/DYSUR+UI(JM,1)*(TS-T(JM,1))*B(JM)/SAREA)
    GO TO 1165
1163 DELTI=DT*(UI(JM,1)*(TS-T(JM,1))*B(JM)/SAREA)
1165 T(JM,2)=T(JM,1)+DELTA+DELTD+DELTE+DELTG+DELTJ
C
C CALCULATIONS FOR BOTTOM HALF LAYER
C DIFFUSION TERMS MODIFIED 10/29/86 EMO
C
    ARG2=ETA*(YSUR-EL(1))
    IF(V(2,1)) 1166,1167,1167
1167 IF(ARG2.GT.20.0)THEN
    DELT11=0.0
    ELSE
    DELT11=DT*(1.0-BETA)*FLXIN(N)*EXP(-ETA*(YSUR-EL(1)-DY/2.0))*
    $(A(2)+A(1))/2.0/(A(1)*DY/2.0)/RHO/HCAP
    ENDIF
    DELT1=DELT11+DT*(UI(1,1)*B(1)*DY/2.0*(TS-T(1,1))
    $+DIFU/FCTR(2)*(T(2,1)-T(1,1))*(A(2)+A(1))/2.0/DY)/A(1)/DY*2.0
    GO TO 1168
1166 IF(ARG2.GT.20.0)THEN
    DELT11=0.0
    ELSE
    DELT11=DT*(1.0-BETA)*FLXIN(N)*EXP(-ETA*(YSUR-EL(1)-DY/2.0))*
    $(A(2)+A(1))/2.0/(A(1)*DY/2.0)/RHO/HCAP
    ENDIF

```

```

      DELT1=DELT11+DT*(UI(1,1)*B(1)*DY/2.0*(TS-T(1,1))-V(2,1)*(A(2)+
      $A(1))/2.0*(T(2,1)-T(1,1)) +DIFU/FCTR(2)*(T(2,1)-T(1,1))*
      $(A(2)+A(1))/2.0/DY)/A(1)/DY*2.0
1168 T(1,2)=T(1,1)+DELT1
      TSAVE=T(JM,1)+DELTA+DELTD+DELTE+DELTI
      DO 1118 J=1,JM
1118 T(J,1)=T(J,2)
      RETURN
      END

```

```

C*****
C
      SUBROUTINE SPECAL(N)
C
C*****
C
C      CALCULATION OF DISTRIBUTION OF SPECIFIED INPUTS
C
      COMMON /PARAM/ JM,DT,DY,DTT,TSTOP,ET,T(102,2)
      COMMON /EXTIN/ ETA,BETA,XTN(366),DTXTN
      COMMON /SURS/ DYSUR,AYSUR,SURF(366),YSUR,SAREA,TS
      COMMON /GEOM/ XL(102),A(102),EL(102),S(102),B(102),YBOT
      COMMON /VELA/ UI(102,1),UOT(102,5),V(102,1),UO(102,1),III
      COMMON /WQPARM/ JEUP,MM
      COMMON/WQCONC/ CC(11,105,2),CCC(11,400),COUT(11,5),CCT(11,5)
      COMMON/WQCONT/ZKBOD,BENTHC,TBASE,SPEDIF,XAIR
      COMMON/DIATOM/GROW1,SINKV1,PHOTO1,RESP1,HALFL1,DEATH1,DECA1
      COMMON/GREENS/GROW2,SINKV2,PHOTO2,RESP2,HALFL2,DEATH2,DECA2
      COMMON/FLAGEL/GROW3,SINKV3,PHOTO3,RESP3,HALFL3,DEATH3,DECA3
      COMMON/WDM86/ DIFU,FCTR(102),BRUNT(102),D(102),USTR,VSTR,WSTR,
      $FACVI,IDFFFLG,CD,CT,INDICE,CW,CCON
      COMMON/STOCHI/STO1,STO2,STO3,STO4,STO5,STO6,STO7,DENIT
      COMMON/HALFL/HALF1,HALF2,HALF3,HALF4
      COMMON/OXID/OXNH4,OXNO2,OCON1,OCON2
      COMMON/RECY/REL1,REL2,REL3,REL4,CORES1,CORES2,CORES3
      COMMON/TEMCON/DT1,DT2,DT3,DT4,DK1,DK4,GT1,GT2,GT3,GT4,GK1,GK4
      COMMON/FLACOM/FT1,FT2,FT3,FT4,FK1,FK4,SINKSI
      COMMON/FLAG/HALF5,HALF6,STO8,STO9,STO10,REL5,REL6
      COMMON/SEDIM/SED1,SED2,SED3,SED4
      DIMENSION XINF(102),OUTF(102),PROD(102),ZLIGHT(102)
      DIMENSION SETL1(102),SETL2(102),PROD1(102),PROD2(102)
      DIMENSION DEAD1(102),DEAD2(102),ZKBO(102)
      DIMENSION TVAR(102),TBOD(102),BENTH(102),RES1(102),RES2(102)
      DIMENSION PHOT1(102),PHOT2(102),SE1(102),SE2(102),SE3(102),
      $SE4(102)
      DIMENSION DECAY1(102),DECAY2(102),DECAY3(102)
      DIMENSION SETL3(102),PROD3(102),DEAD3(102),RES3(102)
      DIMENSION PHOT3(102),SETSIL(102)

```

```

        DIMENSION OXNH(102),OXNO(102),DENI(102)
        DIMENSION AL(102)
        JMM=JM-1
        FLUX=FLXIN(N)
C
C  EVALUATE COEFFICIENTS FOR THE TEMPERATURE MODULATION
C  FACTORS CALCULATION. NOTICE THAT DK1,DK4,GK1,GK4,FK1,FK4
C  HAVE TO BE LESS THAN 1.0 AND MORE THAN 0.0; FOR THE SAME
C  REASON, DK IS FIXED AT 0.98 INSTEAD OF 1.0
C
      if(et.gt.220.) then
        gt1=14.
        gt2=16.
      else
        continue
      endif
      DK=0.98
      IF ((DT2-DT1).LE.0.0) THEN
        DL1=0.0
      ELSE IF (DK1.LE.0.0) THEN
        DL1=0.0
      ELSE
        DL1=(1./(DT2-DT1))*LOG((DK*(1.-DK1))/(DK1*(1.-DK)))
      ENDIF
      IF ((DT4-DT3).LE.0.0) THEN
        DL2=0.0
      ELSE IF (DK4.LE.0.0) THEN
        DL2=0.0
      ELSE
        DL2=(1./(DT4-DT3))*LOG((DK*(1.-DK4))/(DK4*(1.-DK)))
      ENDIF
      IF ((GT2-GT1).LE.0.0) THEN
        GL1=0.0
      ELSE IF (GK1.LE.0.0) THEN
        GL1=0.0
      ELSE
        GL1=(1./(GT2-GT1))*LOG((DK*(1.-GK1))/(GK1*(1.-DK)))
      ENDIF
      IF ((GT4-GT3).LE.0.0) THEN
        GL2=0.0
      ELSE IF (GK4.LE.0.0) THEN
        GL2=0.0
      ELSE
        GL2=(1./(GT4-GT3))*LOG((DK*(1.-GK4))/(GK4*(1.-DK)))
      ENDIF
      IF ((FT2-FT1).LE.0.0) THEN
        FL1=0.0
      ELSE IF (FK1.LE.0.0) THEN
        FL1=0.0
      ELSE
        FL1=(1./(FT2-FT1))*LOG((DK*(1.-FK1))/(FK1*(1.-DK)))

```



```

ENDIF
IF ((FT4-FT3).LE.0.0) THEN
  FL2=0.0
ELSE IF (FK4.LE.0.0) THEN
  FL2=0.0
ELSE
  FL2=(1./(FT4-FT3))*LOG((DK*(1.-FK4))/(FK4*(1.-DK)))
ENDIF
C
C START EVALUATION OF ALL DEPTH DEPENDENT PARAMETERS
C
  DO 6 I=1,JM
    DENSE=1000.-0.00663*(T(I,1)-4.)*(T(I,1)-4.)
  C
  C VISCOSITY CALCULATION MODIFIED JAN-87
  C AFTER SWINDELLS,NATIONAL BUREAU OF STANDARDS
  C
    IF (T(I,1).LE.20.0)THEN
      CPOISE=10**((1301./(998.333+8.1855*(T(I,1)-20.))+
      $0.00585*(T(I,1)-20.）**2))-1.30233)
    ELSE
      CPOISE=10**(((1.3272*(20.-T(I,1))-0.001053*(T(I,1)-
      $20.）**2)/(T(I,1)+105.))+1.002)
    ENDIF
    POISE=CPOISE/100.
  C
  C SETTLING VELOCITY CALCULATED WITH STOKES LAW;
  C THE INPUT VALUE OF SETTLING VELOCITY AT 20 C (SINKV) IS
  C MODIFIED BY THE RATIO OF STOKES SET.VEL AT TEMPERATURE T
  C TO STOKES SET.VEL.AT 20 C.
  C SETL1 STANDS FOR ALGAE #1
  C SETL2 STANDS FOR ALGAE #2
  C SETL3 STANDS FOR ALGAE #3
  C SETSIL STANDS FOR SILICA
  C
    IF (SINKV1.EQ.0.0)THEN
      SETL1(I)=0.0
    ELSE
      SETL1(I)=SINKV1*(1000.-DENSE)/POISE/179.59
    ENDIF
    IF (SINKV2.EQ.0.0) THEN
      SETL2(I)=0.0
    ELSE
      SETL2(I)=SINKV2*(1000.-DENSE)/POISE/179.59
    ENDIF
    IF (SINKV3.EQ.0.0) THEN
      SETL3(I)=0.0
    ELSE
      SETL3(I)=SINKV3*(1000.-DENSE)/POISE/179.59
    ENDIF
    IF (SINKSI.EQ.0.0) THEN

```

```

      SETSIL(I)=0.0
      ELSE
      SETSIL(I)=SINKSI*(1000.-DENSE)/POISE/179.59
      ENDIF

C
C CALCULATION OF THE TEMPERATURE MODULATION FACTORS, FOR GROWTH
C AND DEATH RATES AFTER THORNTON AND LESSEM (1978)
C
C TEMPERATURE FACTOR FOR ALGAE # 1
C
      Z=EXP(DL1*(T(I,1)-DT1))
      ZZ=EXP(DL2*(DT4-T(I,1)))
      TLIM1=(DK1*Z)*(DK4*ZZ)/((1.+DK1*(Z-1.))*(1.+DK4*(ZZ-1.)))
      TDEAD1=DK4*ZZ/(1.+DK4*(ZZ-1.))

C
C TEMPERATURE FACTOR FOR ALGAE # 2
C
      Z=EXP(GL1*(T(I,1)-GT1))
      ZZ=EXP(GL2*(GT4-T(I,1)))
      TLIM2=(GK1*Z)*(GK4*ZZ)/((1.+GK1*(Z-1.))*(1.+GK4*(ZZ-1.)))
      TDEAD2=GK4*ZZ/(1.+GK4*(ZZ-1.))

C
C TEMPERATURE FACTOR FOR ALGAE # 3
C
      Z=EXP(FL1*(T(I,1)-FT1))
      ZZ=EXP(FL2*(FT4-T(I,1)))
      TLIM3=(FK1*Z)*(FK4*ZZ)/((1.+FK1*(Z-1.))*(1.+FK4*(ZZ-1.)))
      TDEAD3=FK4*ZZ/(1.+FK4*(ZZ-1.))

C
C ALGAE LIGHT MODULATION FACTORS
C
      XETA=ETA
      ARG=XETA*(YSUR-EL(I))
      IF(ARG.LE.15.) THEN
      ZLIGHT(I)=(1.-BETA)*FLUX*EXP(- ARG)
      XLIGH1=ZLIGHT(I)/(ZLIGHT(I)+HALFL1)
      XLIGH2=ZLIGHT(I)/(ZLIGHT(I)+HALFL2)
      XLIGH3=ZLIGHT(I)/(ZLIGHT(I)+HALFL3)
      ELSE
      ZLIGHT(I)=0.0
      XLIGH1=0.0
      XLIGH2=0.0
      XLIGH3=0.0
      ENDIF

C
C CALCULATION OF NUTRIENT GROWTH LIMITATION FACTORS
C
C SILICA AND ALGAE #1
C
      IF (CC(6,I,1).LE.0.0) THEN
      DIASIL=0.0

```

```

ELSE
DIASIL=CC(6,I,1)/(HALF1+CC(6,I,1))
ENDIF
C
C PHOSPHORUS AND ALGAE #1
C
IF (CC(7,I,1).LE.0.0) THEN
DIAPHO=0.0
ELSE
DIAPHO=CC(7,I,1)/(HALF4+CC(7,I,1))
ENDIF
C
C PHOSPHORUS AND ALGAE #2
C
IF (CC(7,I,1).LE.0.0) THEN
GREPHO=0.0
ELSE
GREPHO=CC(7,I,1)/(HALF2+CC(7,I,1))
ENDIF
C
C NITROGEN AND ALGAE #2
C
IF (CC(8,I,1).LE.0.0) THEN
IF (CC(9,I,1).LE.0.0) GRENIT=0.0
ELSE
GRENIT=(CC(8,I,1)+CC(9,I,1))/(HALF3+CC(8,I,1)+CC(9,I,1))
ENDIF
C
C PHOSPHORUS AND ALGAE #3
C
IF (CC(7,I,1).LE.0.0) THEN
FLAPHO=0.0
ELSE
FLAPHO=CC(7,I,1)/(HALF5+CC(7,I,1))
ENDIF
C
C NITROGEN AND ALGAE #3
C
IF (CC(8,I,1).LE.0.0) THEN
IF (CC(9,I,1).LE.0.0) FLANIT=0.0
ELSE
FLANIT=(CC(8,I,1)+CC(9,I,1))/(HALF6+CC(8,I,1)+CC(9,I,1))
ENDIF
C
C ALGAE PRODUCTION RATES; ALGAE #1 ARE LIGHT AND SILICA
DEPENDENT
C (USUALLY DIATOMS), WHILE ALGAE #2 ARE LIGHT, PHOSPHORUS AND
C NITROGEN DEPENDENT (USUALLY GREENS AND BLUE-GREENS)
C ALGAE #3 ARE LIGHT,PHOSPHORUS AND NITROGEN DEPENDENT
C ALSO ALGAE DEATH RATES ARE EVALUATED
C

```

```

      IF (GROW1.LE.0.0) THEN
      PROD1(I) = 0.0
      ELSE
      XMIN1=MIN(DIASIL,DIAPHO)
      PROD1(I)=GROW1*TLIM1*XLIGH1*XMIN1*CC(3,I,1)
      ENDIF
C
      IF (GROW2.LE.0.0) THEN
      PROD2(I)=0.0
      ELSE
      XMIN2=MIN(GREPHO,GRENIT)
      PROD2(I)=GROW2*TLIM2*XLIGH2*CC(4,I,1)*XMIN2
      ENDIF
C
      IF (GROW3.LE.0.0) THEN
      PROD3(I)=0.0
      ELSE
      XMIN3=MIN(FLAPHO,FLANIT)
      PROD3(I)=GROW3*TLIM3*XLIGH3*XMIN3*CC(11,I,1)
      ENDIF
C
      IF (DEATH1.LE.0.0) THEN
      DEAD1(I)=0.0
      ELSE
      DEAD1(I)=DEATH1*(1.-TDEAD1)*CC(3,I,1)
      ENDIF
C
      IF (DEATH2.LE.0.0) THEN
      DEAD2(I)=0.0
      ELSE
      DEAD2(I)=DEATH2*(1.-TDEAD2)*CC(4,I,1)
      ENDIF
C
      IF (DEATH3.LE.0.0) THEN
      DEAD3(I)=0.0
      ELSE
      DEAD3(I)=DEATH3*(1.-TDEAD3)*CC(11,I,1)
      ENDIF

      EVALUATION OF ALL TEMPERATURE DEPENDENT WATER QUALITY
      CONSTANTS
C
      TVAR(I)=1.02**(T(I,1)-TBASE)
      TBOD(I)=1.08**(T(I,1)-TBASE)
      ZKBOD(I)=ZKBOD*TBOD(I)
      DENI(I)=DENIT*TVAR(I)
      BENTH(I)=BENTHC*TVAR(I)
      RES1(I)=RESP1*TVAR(I)
      RES2(I)=RESP2*TVAR(I)
      RES3(I)=RESP3*TVAR(I)
      PHOT1(I)=PHOTO1*TVAR(I)

```

```

    PHOT2(I)=PHOTO2*TVAR(I)
    PHOT3(I)=PHOTO3*TVAR(I)
    SE1(I)=SED1*TVAR(I)
    SE2(I)=SED2*TVAR(I)
    SE3(I)=SED3*TVAR(I)
    SE4(I)=SED4*TVAR(I)
C
C EVALUATION OF ALGAE DECAY WHEN THEY REACH THE APHOTIC ZONE
C
    IF (CC(1,I,1).LE.0.1.OR.ARG.GT.15.0) THEN
        DECAY1(I)=DECA1*TVAR(I)
        DECAY2(I)=DECA2*TVAR(I)
        DECAY3(I)=DECA3*TVAR(I)
    ELSE
        DECAY1(I)=0.0
        DECAY2(I)=0.0
        DECAY3(I)=0.0
    ENDIF
C
C DEPENDING ON THE AVAILABILITY OF DO, SOME OF THE PARAMETERS
C WILL TAKE DIFFERENT VALUES;I.E., IF DO IS NOT PRESENT,PROCESSES
C THAT REQUIRE DO WILL NOT OCCUR
C
    IF (CC(1,I,1).LE.0.01) CC(1,I,1)=0.0
    IF (CC(1,I,1).LE.0.0) THEN
        ZKBO(I)=0.0
        BENTH(I)=0.0
        SE2(I)=0.0
        RES1(I)=0.0
        RES2(I)=0.0
        RES3(I)=0.0
    ELSE
        SE1(I)=0.0
        SE3(I)=0.0
        SE4(I)=0.0
        DENI(I)=0.0
    ENDIF
    IF (CC(1,I,1).LE.0.5) THEN
        OXNH(I)=0.0
        OXNO(I)=0.0
    ELSE
        OXNH(I)=OXNH4*CC(1,I,1)/(CC(1,I,1)+OCON2)
        OXNO(I)=OXNO2*CC(1,I,1)/(CC(1,I,1)+OCON1)
    ENDIF
6 CONTINUE
C
C EVALUATE ALL LATERAL AREAS TO ACCOUNT FOR SEDIMENT
INTERACTIONS. THE
C BASIN IS ASSUMED TO BE RECTANGULAR AND THE LATERAL AREAS ARE
CALCULATED
C AS IF THEY WERE TRAPEZOIDS

```

```

C AS PER CONVERSATION WITH FELIP SERRAHIMA 5/12/88, THE FOLLOWING
C RECOMMENDATIONS ON AREA CALCULATIONS WERE MADE:
C ALL(1)=((XL(2)+2*XL(1))/2)*SQRT((XL(2)/4)**2+(DY/2)**2)
C ALB(1)=((B(2)+2*B(1))/2)*SQRT((B(2)/4)**2+(DY/2)**2)
C AL(1)=(ALL(1)+ALB(1)+S(1))/A(1)*DY*0.5
C DO 500 J=2,JMM
C AXL=ABS(XL(J+1)-XL(J-1))
C ALL(J)=((XL(J+1)+2*XL(J)+XL(J-1))/2)*SQRT(((AXL/4)**2)+DY**2)
C AXB=ABS(B(J+1)-B(J))
C ALB(J)=((B(J+1)+2*B(J)+B(J-1))/2)*SQRT(((AXB/4)**2)+DY**2)
C AL(J)=(ALL(J)+ALB(J))/(A(J)*DY)
C THESE SUBSTITUTIONS WERE TO BE REPLACED FOR THE FOLLOWING
C LINES UP TO LINE [500 CONTINUE] IN ADDITION, DIMENSION AL(102)
C ALL(102),AND ALB(102)
  AL(1)= (S(1)+((XL(1)**2+(DY*0.5)**2)**0.5)*XL(1)*0.5
  $+((B(1)**2+DY**2)**0.5)*B(1)*0.5)/(A(1)*DY*0.5)
  DO 500 J=2,JMM
  AL(J)= (((XL(J)-XL(J-1))**2+DY**2)**0.5)*(XL(J)+XL(J-1))
  $+(((B(J)-B(J-1))**2+DY**2)**0.5)*(B(J)+B(J-1)))/(A(J)*DY)
500 CONTINUE
  DO 30 I=2,JMM
  IF(V(I,1))10,10,20
10  OUTF(I)=(UO(I,1)*B(I)*DY-V(I,1)*(A(I)+A(I-1))/2.0)*DT
  XINF(I)=-V(I+1,1)*(A(I)+A(I+1))/2.0*DT
  CONTINUE
  GO TO 30
20  OUTF(I)=(UO(I,1)*B(I)*DY+V(I+1,1)*(A(I)+A(I+1))/2.0)*DT
  XINF(I)=V(I,1)*(A(I)+A(I-1))/2.0*DT
  CONTINUE
30  CONTINUE
  DO 210 I=2,JMM
  DO 195 M=1,MM
  IF(V(I,1))130,130,160
130 IF(V(I+1,1))140,140,150
140 CC(M,I,2)=(CC(M,I,1)*A(I)*DY
  $-OUTF(I)*CC(M,I,1)
  $+CCC(M,N)*UI(I,1)*DT*B(I)*DY
  $+XINF(I)*CC(M,I+1,1)
  $)/A(I)/DY
  GO TO 190
150 CC(M,I,2)=(CC(M,I,1)*A(I)*DY
  $-OUTF(I)*CC(M,I,1)
  $+CCC(M,N)*UI(I,1)*DT*B(I)*DY
  $+XINF(I)*CC(M,I,1)
  $)/A(I)/DY
  GO TO 190
160 IF(V(I+1,1))180,180,170
170 CC(M,I,2)=(CC(M,I,1)*A(I)*DY
  $-OUTF(I)*CC(M,I,1)
  $+CCC(M,N)*UI(I,1)*DT*B(I)*DY
  $+XINF(I)*CC(M,I-1,1)

```

```

    $)/A(I)/DY
    GO TO 190
180  CC(M,I,2)=(CC(M,I,1)*A(I)*DY
    $-UO(I,1)*B(I)*DY*DT*CC(M,I,1)
    $-V(I+1,1)*(A(I)+A(I+1))/2.0*DT*CC(M,I+1,1)
    $+CCC(M,N)*UI(I,1)*DT*B(I)*DY
    $+XINF(I)*CC(M,I-1,1)
    $)/A(I)/DY
C
C  DIFFUSION CALCULATION - USE TURBULENT DIFFUSIVITIES IF REQUIRED
C
190  IF(INDICE.EQ.0.OR.(DIFU/FCTR(I+1)).LT.SPEDIF) THEN
    COEFD=DT*SPEDIF/DY/DY
    COEFD1=COEFD
    ELSE
    COEFD=0.1*DT*(DIFU/FCTR(I+1))/DY/DY
    COEFD1=0.1*DT*(DIFU/FCTR(I))/DY/DY
    ENDIF
    CC(M,I,2)=CC(M,I,2)+(COEFD*(CC(M,I+1,1)-CC(M,I,1))*(A(I+1)
    $+A(I))/2.0-COEFD*(CC(M,I,1)-CC(M,I-1,1))*(A(I)+A(I-1))/2.0)/A(I)
195  CONTINUE
C  BOD
    CC(2,I,2)=CC(2,I,2)
    $-ZKBO(I)*CC(2,I,1)*DT
    $+(DECAY1(I)*CC(3,I,1)+DECAY2(I)*CC(4,I,1)+DECAY3(I)*CC(11,I,1))
    $*DT*0.025
    $+(DEAD1(I)+DEAD2(I)+DEAD3(I))*DT*0.025
    $+(RES1(I)*CC(3,I,1)+RES2(I)*CC(4,I,1)+RES3(I)*CC(11,I,1))
    $*DT*0.025
C  DO
    CC(1,I,2)=CC(1,I,2)
    $+PROD1(I)*DT*PHOT1(I)
    $+PROD2(I)*DT*PHOT2(I)
    $+PROD3(I)*DT*PHOT3(I)
    $-ZKBO(I)*DT*CC(2,I,1)
    $-BENTH(I)*DT*AL(I)
    $-RES1(I)*CORES1*CC(3,I,1)*DT
    $-RES2(I)*CORES2*CC(4,I,1)*DT
    $-RES3(I)*CORES3*CC(11,I,1)*DT
    $-OCON1*DT*CC(10,I,1)*OXNO(I)
    $-OCON2*DT*CC(9,I,1)*OXNH(I)
C  ALGAE # 1
    CC(3,I,2)=CC(3,I,2)
    $+PROD1(I)*DT
    $-RES1(I)*DT*CC(3,I,1)
    $+SETL1(I+1)*(A(I+1)+A(I))/2.0*DT*CC(3,I+1,1)/A(I)/DY
    $-SETL1(I)*(A(I+1)+A(I))/2.0*DT*CC(3,I,1)/A(I)/DY
    $-DEAD1(I)*DT
    $-DECAY1(I)*CC(3,I,1)*DT
C  ALGAE # 2
    CC(4,I,2)=CC(4,I,2)

```

```

$+PROD2(I)*DT
$-RES2(I)*DT*CC(4,I,1)
$+SETL2(I+1)*(A(I+1)+A(I))/2.0*DT*CC(4,I+1,1)/A(I)/DY
$-SETL2(I)*(A(I+1)+A(I))/2.0*DT*CC(4,I,1)/A(I)/DY
$-DEAD2(I)*DT
$-DECAY2(I)*CC(4,I,1)*DT
C  ALGAE # 3
    CC(11,I,2)=CC(11,I,2)
    $+PROD3(I)*DT
    $-RES3(I)*DT*CC(11,I,1)
    $+SETL3(I+1)*(A(I+1)+A(I))/2.0*DT*CC(11,I+1,1)/A(I)/DY
    $-SETL3(I)*(A(I+1)+A(I))/2.0*DT*CC(11,I,1)/A(I)/DY
    $-DEAD3(I)*DT
    $-DECAY3(I)*CC(11,I,1)*DT
    IF(CC(3,I,2).LT.1.0)CC(3,I,2)=1.0
    IF(CC(4,I,2).LT.1.0)CC(4,I,2)=1.0
    IF(CC(11,I,2).LT.1.0)CC(11,I,2)=1.0
C  TOTAL ALGAE
    CC(5,I,2)=CC(3,I,2)+CC(4,I,2)+CC(11,I,2)
C  SILICA
    CC(6,I,2)=CC(6,I,2)
    $-STO1*PROD1(I)*DT
    $+SETSIL(I+1)*(A(I+1)+A(I))/2.0*DT*CC(6,I+1,1)/A(I)/DY
    $-SETSIL(I)*(A(I+1)+A(I))/2.0*DT*CC(6,I,1)/A(I)/DY
    $+REL7*(RES1(I)*CC(3,I,1)+DEAD1(I)+DECAY1(I)*CC(3,I,1))*DT
C  PHOSPHATES
    CC(7,I,2)=CC(7,I,2)
    $-STO2*PROD1(I)*DT
    $-STO3*PROD2(I)*DT
    $-STO8*PROD3(I)*DT
    $+REL1*(RES1(I)*CC(3,I,1)+DEAD1(I)+DECAY1(I)*CC(3,I,1))*DT
    $+REL2*(RES2(I)*CC(4,I,1)+DEAD2(I)+DECAY2(I)*CC(4,I,1))*DT
    $+REL5*(RES3(I)*CC(11,I,1)+DEAD3(I)+DECAY3(I)*CC(11,I,1))*DT
    $+SE1(I)*AL(I)*DT
    $-SE2(I)*CC(7,I,1)*AL(I)*DT
C  NITRATES
    IF (CC(8,I,1).LE.0.0) THEN
        TN1=0.0
        TN2=0.0
        TN5=0.0
    ELSE
        TN1=-STO4*PROD1(I)*DT
        TN2=-STO5*PROD2(I)*DT
        TN5=-STO9*PROD3(I)*DT
    ENDIF
    TN3=+OXNO(I)*CC(10,I,1)*DT
    TN4=-DENI(I)*CC(8,I,1)*DT
    TN6=-SE3(I)*CC(8,I,1)*DT*AL(I)
    CC(8,I,2)=CC(8,I,2)+TN1+TN2+TN3+TN4+TN5+TN6
C  AMMONIA
    IF (CC(9,I,1).LE.0.0) THEN

```



```

VN1=0.0
ELSE
VN1=-(STO6*PROD1(I)*DT+STO7*PROD2(I)*DT+STO10*PROD3(I)*DT)
ENDIF
VN2=-OXNH(I)*CC(9,I,1)*DT
VN3=+REL3*(RES1(I)*CC(3,I,1)+DEAD1(I)+DECAY1(I)*CC(3,I,1))*DT
VN4=+REL4*(RES2(I)*CC(4,I,1)+DEAD2(I)+DECAY2(I)*CC(4,I,1))*DT
VN5=+REL6*(RES3(I)*CC(11,I,1)+DEAD3(I)+DECAY3(I)*CC(11,I,1))*DT
VN6=+SE4(I)*DT*AL(I)
CC(9,I,2)=CC(9,I,2)+VN1+VN2+VN3+VN4+VN5+VN6
C  NITRITES
  CC(10,I,2)=CC(10,I,2)
  $+OXNH(I)*CC(9,I,1)*DT
  $-OXNO(I)*CC(10,I,1)*DT
210 CONTINUE
C
C  CALCULATION FOR SURFACE LAYER
C
  AREA=SAREA*DYSUR
C
C  DIFFUSION TERM
C
  IF(INDICE.EQ.0.OR.(DIFU/FCTR(JM)).LT.SPEDIF) THEN
    COEFD=DT*SPEDIF/DY/DY
  ELSE
    COEFD=0.1*DT*(DIFU/FCTR(JM))/DY/DY
  ENDIF
  DO 300 M=1,MM
    IF(V(JM,1))280,280,290
280  CC(M,JM,2)=(CC(M,JM,1)*AREA
    $-UO(JM,1)*B(JM)*DYSUR*CC(M,JM,1)*DT
    $+CCC(M,N)*UI(JM,1)*B(JM)*DYSUR*DT
    $+V(JM,1)*(A(JM)+A(JM-1))/2.0*CC(M,JM,1)*DT
    $)/AREA-COEFD*(CC(M,JM,1)-CC(M,JM-1,1))*DY*
    $(A(JM)+A(JM-1))/2.0/AREA
    GO TO 300
290  CC(M,JM,2)=(CC(M,JM,1)*AREA
    $-UO(JM,1)*B(JM)*DYSUR*CC(M,JM,1)*DT
    $+CCC(M,N)*UI(JM,1)*B(JM)*DYSUR*DT
    $+V(JM,1)*(A(JM)+A(JM-1))/2.0*CC(M,JM-1,1)*DT
    $)/AREA-COEFD*(CC(M,JM,1)-CC(M,JM-1,1))*DY*
    $(A(JM)+A(JM-1))/2.0/AREA
300  CONTINUE
C  BOD
  CC(2,JM,2)=CC(2,JM,2)
  $-ZKBO(JM)*CC(2,JM,1)*DT
  $+(DEAD1(JM)+DEAD2(JM)+DEAD3(JM))*DT*0.025
  $+(RES1(JM)*CC(3,JM,1)+RES2(JM)*CC(4,JM,1)+RES3(JM)*CC(11,JM,1))
  $*DT*0.025
C  DO
  CC(1,JM,2)=CC(1,JM,2)

```

```

$+PROD1(JM)*DT*PHOT1(JM)
$+PROD2(JM)*DT*PHOT2(JM)
$+PROD3(JM)*DT*PHOT3(JM)
$-ZKBO(JM)*DT*CC(2,JM,1)
$-BENTH(JM)*DT*(AYSUR-(A(JM)+A(JM-1))/2.0)/AREA
$-RES1(JM)*CORES1*CC(3,JM,1)*DT
$-RES2(JM)*CORES2*CC(4,JM,1)*DT
$-RES3(JM)*CORES3*CC(11,JM,1)*DT
$-OCON1*DT*CC(10,JM,1)*OXNO(JM)
$-OCON2*DT*CC(9,JM,1)*OXNH(JM)
C  ALGAE # 1
    CC(3,JM,2)=CC(3,JM,2)
    $+PROD1(JM)*DT
    $-RES1(JM)*DT*CC(3,JM,1)
    $-SETL1(JM)*DT*AYSUR*CC(3,JM,1)/AREA
    $-DEAD1(JM)*DT
C  ALGAE # 2
    CC(4,JM,2)=CC(4,JM,2)
    $+PROD2(JM)*DT
    $-RES2(JM)*DT*CC(4,JM,1)
    $-SETL2(JM)*DT*AYSUR*CC(4,JM,1)/AREA
    $-DEAD2(JM)*DT
C  ALGAE # 3
    CC(11,JM,2)=CC(11,JM,2)
    $+PROD3(JM)*DT
    $-RES3(JM)*DT*CC(11,JM,1)
    $-SETL3(JM)*DT*CC(11,JM,1)*AYSUR*CC(11,JM,1)/AREA
    $-DEAD3(JM)*DT
    IF(CC(3,JM,2).LT.1.0)CC(3,JM,2)=1.0
    IF(CC(4,JM,2).LT.1.0)CC(4,JM,2)=1.0
    IF(CC(11,JM,2).LT.1.0)CC(11,JM,2)=1.0
C  TOTAL ALGAE
    CC(5,JM,2)=CC(3,JM,2)+CC(4,JM,2)+CC(11,JM,2)
C  SILICA
    CC(6,JM,2)=CC(6,JM,2)
    $-STO1*PROD1(JM)*DT
    $-SETL1(JM)*AYSUR*DT*CC(6,JM,1)/AREA
C  PHOSPHATES
    CC(7,JM,2)=CC(7,JM,2)
    $-(STO2*PROD1(JM)*DT)
    $-(STO3*PROD2(JM)*DT)
    $-(STO8*PROD3(JM)*DT)
    $+REL1*(RES1(JM)*DT*CC(3,JM,1)+DEAD1(JM)*DT)
    $+REL2*(RES2(JM)*DT*CC(4,JM,1)+DEAD2(JM)*DT)
    $+REL5*(RES3(JM)*DT*CC(11,JM,1)+DEAD3(JM)*DT)
C  NITRATES
    IF (CC(8,JM,1).LE.0.0) THEN
        XN1=0.0
        XN2=0.0
        XN5=0.0
    ELSE

```

```

      XN1=-STO4*PROD1(JM)*DT
      XN2=-STO5*PROD2(JM)*DT
      XN5=-STO9*PROD3(JM)*DT
      ENDIF
      XN3=+OXNO(JM)*CC(10,JM,1)*DT
      XN4=-DENI(JM)*CC(8,JM,1)*DT
      CC(8,JM,2)=CC(8,JM,2)+XN1+XN2+XN3+XN4+XN5
C   AMMONIA
      IF (CC(9,JM,1).LE.0.0) THEN
        YN1=0.0
        YN2=0.0
        YN6=0.0
      ELSE
        YN1=-STO6*PROD1(JM)*DT
        YN2=-STO7*PROD2(JM)*DT
        YN6=-STO10*PROD3(JM)*DT
      ENDIF
      YN3=-OXNH(JM)*CC(9,JM,1)*DT
      YN4=+REL3*(RES1(JM)*DT*CC(3,JM,1)+DEAD1(JM)*DT)
      YN5=+REL4*(RES2(JM)*DT*CC(4,JM,1)+DEAD2(JM)*DT)
      YN7=+REL6*(RES3(JM)*DT*CC(11,JM,1)+DEAD3(JM)*DT)
      CC(9,JM,2)=CC(9,JM,2)+YN1+YN2+YN3+YN4+YN5+YN6+YN7
C   NITRITES
      CC(10,JM,2)=CC(10,JM,2)
      $+OXNH(JM)*CC(9,JM,1)*DT
      $-OXNO(JM)*CC(10,JM,1)*DT
C
C   CALCULATION FOR BOTTOM LAYER
C
C   DIFFUSION TERM
C
      IF(INDICE.EQ.0.OR.(DIFU/FCTR(2)).LT.SPEDIF) THEN
        COEFD=DT*SPEDIF/DY/DY
      ELSE
        COEFD=0.1*DT*(DIFU/FCTR(2))/DY/DY
      ENDIF
      DO 370 M=1,MM
340    IF(V(2,1))350,350,360
350    CC(M,1,2)=(CC(M,1,1)*A(1)*DY/2.0
      $-UO(1,1)*B(1)*DY/2.0*CC(M,1,1)*DT
      $+CCC(M,N)*UI(1,1)*B(1)*DY/2.0*DT
      $-V(2,1)*(A(1)+A(2))/2.0*CC(M,2,1)*DT
      $)/A(1)/DY/0.5
      $+COEFD*(CC(M,2,1)-CC(M,1,1))*(A(2)+A(1))/2./A(1)
      GO TO 370
360    CC(M,1,2)=(CC(M,1,1)*A(1)*DY/2.0
      $-UO(1,1)*B(1)*DY/2.0*CC(M,1,1)*DT
      $+CCC(M,N)*UI(1,1)*B(1)*DY/2.0*DT
      $-V(2,1)*(A(1)+A(2))/2.0*CC(M,1,1)*DT
      $)/A(1)/DY/0.5
      $+COEFD*(CC(M,2,1)-CC(M,1,1))*(A(2)+A(1))/2./A(1)

```

370 CONTINUE

C BOD

CC(2,1,2)=CC(2,1,2)
\$-ZKBO(1)*DT*CC(2,1,1)
\$+(DECAY1(1)*CC(3,1,1)+DECAY2(1)*CC(4,1,1)+DECAY3(1)*CC(11,1,1))
\$*DT*0.025
\$+(DEAD1(1)+DEAD2(1)+DEAD3(1))*DT*0.025
\$+(RES1(1)*CC(3,1,1)+RES2(1)*CC(4,1,1)+RES3(1)*CC(11,1,1))
\$*DT*0.025

C DO

CC(1,1,2)=CC(1,1,2)
\$+PROD1(1)*DT*PHOT1(1)
\$+PROD2(1)*DT*PHOT2(1)
\$+PROD3(1)*DT*PHOT3(1)
\$-ZKBO(1)*DT*CC(2,1,1)
\$-BENTH(1)*DT/DY
\$-RES1(1)*CORES1*CC(3,1,1)*DT
\$-RES2(1)*CORES2*CC(4,1,1)*DT
\$-RES3(1)*CORES3*CC(11,1,1)*DT
\$-OCON1*DT*CC(10,1,1)*OXNO(1)
\$-OCON2*DT*CC(9,1,1)*OXNH(1)
\$-(DEAD1(1)+DEAD2(1)+DEAD3(1))*DT*ZKBO(1)*0.1
\$-(DECAY1(1)*CC(3,1,1)+DECAY2(1)*CC(4,1,1)+DECAY3(1)*CC(11,1,1))*DT

C ALGAE # 1

CC(3,1,2)=CC(3,1,2)
\$+PROD1(1)*DT
\$-RES1(1)*DT*CC(3,1,1)
\$-(A(2)+A(1))/A(1)*CC(3,1,1)*SETL1(1)*DT/DY
\$+SETL1(2)*DT*(A(2)+A(1))*CC(3,2,1)/A(1)/DY
\$-DEAD1(1)*DT
\$-DECAY1(1)*DT*CC(3,1,1)

C ALGAE # 2

CC(4,1,2)=CC(4,1,2)
\$+PROD2(1)*DT
\$-RES2(1)*DT*CC(4,1,1)
\$-(A(2)+A(1))/A(1)*CC(4,1,1)*SETL2(1)*DT/DY
\$+SETL2(2)*DT*(A(2)+A(1))*CC(3,2,1)/A(1)/DY
\$-DEAD2(1)*DT
\$-DECAY2(1)*DT*CC(4,1,1)

C ALGAE # 3

CC(11,1,2)=CC(11,1,2)
\$+PROD3(1)*DT
\$-RES3(1)*DT*CC(11,1,1)
\$-(A(2)+A(1))/A(1)*CC(11,1,1)*SETL3(1)*DT/DY
\$+SETL3(2)*DT*(A(2)+A(1))*CC(11,2,1)/A(1)/DY
\$-DEAD3(1)*DT
\$-DECAY3(1)*CC(11,1,1)*DT
IF(CC(3,1,2).LT.1.0) CC(3,1,2)=1.0
IF(CC(4,1,2).LT.1.0) CC(4,1,2)=1.0
IF(CC(11,1,2).LT.1.0) CC(11,1,2)=1.0

C TOTAL ALGAE

```

      CC(5,1,2)=CC(3,1,2)+CC(4,1,2)+CC(11,1,2)
C  SILICA
      CC(6,1,2)=CC(6,1,2)
      $-(STO1*PROD1(1)*DT)
      $-(A(2)+A(1))/A(1)*CC(6,1,1)*SETSIL(1)*DT/DY
      $+SETSIL(2)*DT*(A(2)+A(1))*CC(6,2,1)/A(1)/DY
      $+REL7*(RES1(1)*CC(3,1,1)+DEAD1(1)+DECAY1(1)*CC(11,1,1))*DT
C  PHOSPHATES
      CC(7,1,2)=CC(7,1,2)
      $-(STO2*PROD1(1)*DT)
      $-(STO3*PROD2(1)*DT)
      $-(STO8*PROD3(1)*DT)
      $+REL1*(RES1(1)*CC(3,1,1)+DEAD1(1)+DECAY1(1)*CC(3,1,1))*DT
      $+REL2*(RES2(1)*CC(4,1,1)+DEAD2(1)+DECAY2(1)*CC(4,1,1))*DT
      $+REL3*(RES3(1)*CC(11,1,1)+DEAD3(1)+DECAY3(1)*CC(11,1,1))*DT
      $+(SE1(1)*DT-SE2(1)*CC(7,1,1)*DT)*AL(1)
C  NITRATES
      CC(8,1,2)=CC(8,1,2)
      IF (CC(8,1,1).LE.0.0) THEN
        ZN1=0.0
      ELSE
        ZN1=-(STO4*PROD1(1)*DT+STO5*DT*PROD2(1)+STO9*DT*PROD3(1))
      ENDIF
      ZN2=+OXNO(1)*CC(10,1,1)*DT
      ZN3=-DENI(1)*CC(8,1,1)*DT
      ZN4=-SE3(1)*CC(8,1,1)*DT*AL(1)
      CC(8,1,2)=CC(8,1,2)+ZN1+ZN2+ZN3+ZN4
C  AMMONIA
      CC(9,1,2)=CC(9,1,2)
      IF (CC(9,1,1).LE.0.0) THEN
        WN1=0.0
      ELSE
        WN1=-(STO6*PROD1(1)*DT+STO7*PROD2(1)*DT+STO10*PROD3(1)*DT)
      ENDIF
      WN2=-OXNH(1)*CC(9,1,1)*DT
      WN3=+REL3*(RES1(1)*CC(3,1,1)+DEAD1(1)+DECAY1(1)*CC(3,1,1))*DT
      WN4=+REL4*(RES2(1)*CC(4,1,1)+DEAD2(1)+DECAY2(1)*CC(4,1,1))*DT
      WN5=+SE4(1)*DT*AL(1)
      WN6=+REL6*(RES3(1)*CC(11,1,1)+DEAD3(1)+DECAY3(1)*CC(11,1,1))*DT
      CC(9,1,2)=CC(9,1,2)+WN1+WN2+WN3+WN4+WN5+WN6
C  NITRITES
      CC(10,1,2)=CC(10,1,2)
      $+OXNH(1)*CC(9,1,1)*DT
      $-OXNO(1)*CC(10,1,1)*DT
375 DO 410 M=1,MM
      DO 400 L=1,JM
400 IF(CC(M,L,2).LE.0.1E-30) CC(M,L,2)=0.0
410 CONTINUE
      RETURN
      END

```

```

C*****
SUBROUTINE SPEED(N)
C*****
C
C COMPUTATION OF VERTICAL AND SOURCE AND SINK VELOCITIES.
C ALSO, COMPUTATION OF WITHDRAWAL THICKNESS.
C SOURCE AND SINK VELOCITIES ARE ASSUMED TO HAVE GAUSSIAN
DISTRIBUTION.
C
COMMON /PARAM/ JM,DT,DY,DTT,TSTOP,ET,T(102,2)
COMMON /SWITCH/ KSUR,KOH,KQ,KLOSS,KMIX,KATRAD
COMMON /GEOM/ XL(102),A(102),EL(102),S(102),B(102),YBOT
COMMON /SURS/ DYSUR,AYSUR,SURF(366),YSUR,SAREA,TS
COMMON /OUTLET/ NOUT,LOUT(5),ELOUT(5),QIN(400),TIN(400)
COMMON /OUTB/ YOUT,JOUT,JIN,TOUTC(5)
COMMON /FLOWS/ QI(400),QO(400,5),DTQI,DTQO
COMMON /MIX/ QQMIX(102),RMIX,JMIXB,MIXED,QMIX
COMMON /VELA/ UI(102,1),UOT(102,5),V(102,1),UO(102,1),III
COMMON /VELB/ UOMAX(5),UIMAX(1),EX(102),EXO(102),OX(102),EXI(102)
COMMON /VELC/ SIGMAI,SIGMAO,SPREAD,HAFDEL,EPSIL,DERIV,DELCON
C
C COMPUTE INFLOW VELOCITY
C COMPUTE EXPONENTIAL FACTOR
C
1000 DO 1 I=1,JM
      S(I)=(DY*FLOAT(I-1))**2
      ARG1=S(I)/2.0/SIGMAI/SIGMAI
      IF(ARG1-20.0)4,4,5
4     EX(I)=EXP(-ARG1)
      GO TO 1
5     EX(I)=0.0
1     CONTINUE
      DO 2 J=1,JM
        II=IABS(J-JIN)+1
2     EXI(J)=EX(II)
C
C COMPUTE MAX INFLOW VEL.
C
VOLIN=EXI(1)*B(1)*DY/2.0+EXI(JM)*B(JM)*DYSUR
JMM=JM-1
DO 3 J=2,JMM
3 VOLIN=VOLIN+EXI(J)*B(J)*DY
  UIMAX(1)=QIN(N)/VOLIN
  GO TO (8,7),KMIX
7 UIMAX(1)=UIMAX(1)*(1.0+RMIX)
8 DO 6 J=1,JM
6 UI(J,1)=UIMAX(1)*EXI(J)
C
C COMPUTE OUTFLOW VELOCITIES
C
DO 10 LT=1,NOUT

```

```

      JOUT=LOUT(LT)
C
C COMPUTE WITHDRAWAL THICKNESS.
C NOTE THAT ONLY HALF THE WITHDRAWAL THICKNESS IS COMPUTED.
C
      IF(JOUT.LE.JM) GO TO 200
      DO 210 J=1,JM
210   UOT(J,LT)=0.0
      GO TO 10
200   IF(JOUT.EQ.1) GO TO 40
      IF (JOUT.EQ.JM) GO TO 45
      DERIV = (T(JOUT+1,1)-T(JOUT-1,1))/2.0/DY
      GO TO 49
40   DERIV=(T(JOUT+1,1)-T(JOUT,1))/DY
      GO TO 49
45   DERIV=(T(JOUT,1)-T(JOUT-1,1))/DY
49   IF (DERIV-0.010) 11,11,15
      11 JOUT1=JOUT+2
C
C CUTOFF DUE TO SHARP CHANGE IN DENSITY GRADIENT
C
      IF (JOUT1-JMM) 50,51,51
50   DO 12 J=JOUT1,JMM
      IF((T(J+1,1)-T(J,1))/DY-.05)12,13,13
12   CONTINUE
51   SIGMAO=30.0*DY
      HAFDEL= 15.0*DY
      GO TO 19
13   HAFDEL=FLOAT(J-JOUT)*DY
      IF(HAFDEL.LT.2.0) HAFDEL=2.0
      SIGMAO=HAFDEL/SPREAD
19   JOUT2=JOUT-2
      IF (JOUT2) 14,14,53
53   DO 21 I=1,JOUT2
      J=JOUT2+2-I
      IF((T(J,1)-T(J-1,1))/DY-0.05) 21,21,22
21   CONTINUE
      GO TO 14
22   HAFD1=FLOAT(JOUT-J)*DY
      SIGM1=HAFD1/SPREAD
      IF(SIGM1.LT.SIGMAO) SIGMAO=SIGM1
      GO TO 14
C
C APPROXIMATING FORMULA USED FOR DENSITY IS
RHO=1.0-0.00000663*(T-4.0)**2
C
      15 EPSIL=2.0*ABS(T(JOUT,1)-4.0)/((151000.0-(T(JOUT,1)-4.0)**2)*DERIV
      GO TO (17,16),KOH
C
C CALCULATION OF WITHDRAWAL THICKNESS USING KAO FORMULA.
C

```

```

16 QPUW=QOUT(N,LT)/B(JOUT)
   HAFDEL = DELCON*SQRT(QPUW)/EPSIL**0.25
   IF (HAFDEL.LT.2.0) HAFDEL=2.0
   GO TO 18
C
C CALCULATION OF WITHDRAWAL THICKNESS USING KOH FORMULA.
C
17 HAFDEL = DELCON/EPSIL**0.1666667
   IF (HAFDEL.LT.2.0) HAFDEL=2.0
18 SIGMAO = HAFDEL/SPREAD
   IF(SIGMAO) 20,20,14
20 SIGMAO=1.0
14 CONTINUE
   IF(QOUT(N,LT).EQ.0.0) THEN
     HAFDEL=0.0
     SIGMAO=0.0
     GO TO 10
   ELSE
     CONTINUE
   ENDIF
C
C COMPUTE EXP. FACTOR
C
   DO 100 I=1,JM
     S(I)=(DY*FLOAT(I-1))**2
     ARGO=S(I)/2.0/SIGMAO/SIGMAO
     IF(ARGO-20.0) 104,105,105
104 OX(I)=EXP(-ARGO)
     GO TO 100
105 OX(I)=0.0
100 CONTINUE
     DO 110 J=1,JM
       IO=IABS(J-JOUT)+1
110 EXO(J)=OX(IO)
C
C FIRST COMPUTE MAXIMUM VELOCITIES, THEN OTHERS.
C
   VOLOUT=EXO(1)*B(1)*DY/2.0+EXO(JM)*B(JM)*DYSUR
   JMM=JM-1
   DO 120 J=2,JMM
120 VOLOUT=VOLOUT+EXO(J)*B(J)*DY
     UOMAX(LT)=QOUT(N,LT)/VOLOUT
     DO 130 J=1,JM
130 UOT(J,LT)=UOMAX(LT)*EXO(J)
10 CONTINUE
C
C COMPUTE VELOCITIES CAUSED BY ENTRAINMENT
C
   DO 36 J=1,JM
     GO TO (31,32),KMIX
32 IF(J-JMIXB) 31,33,33

```



```

33 QQMIX(J)=QIN(N)*RMIX/(MIXED+1)
   UO(J,1)=QQMIX(J)/B(J)/DY
   IF(J.EQ.JM) UO(JM,1)=UO(J,1)*DY/DYSUR
   GO TO 37
31 UO(J,1)=0.0
37 DO 35 LT=1,NOOUT
   IF (QOUT(N,LT).EQ.0.0) THEN
     UOT(J,LT)=0.0
   ELSE
     CONTINUE
   ENDIF
35 UO(J,1)=UO(J,1)+UOT(J,LT)
36 CONTINUE
C
C COMPUTE VERTICAL ADVECTIVE VELOCITY
C
   V(1,1)=0.0
   V(2,1)=(UI(1,1)-UO(1,1))*B(1)*DY/(A(1)+A(2))
   JMX=JM+1
   DO 500 J=3,JMX
     V(J,1)=(V(J-1,1)*(A(J-2)+A(J-1))/2.0+(UI(J-1,1)-UO(J-1,1))*B(J-1)
1*DY)/(A(J)+A(J-1))*2.0
500 CONTINUE
   RETURN
   END
C*****

```

```

C*****
SUBROUTINE SURFEL(N)
C*****
COMMON /PARAM/ JM,DT,DY,DTT,TSTOP,ET,T(102,2)
COMMON /GEOM/ XL(102),A(102),EL(102),S(102),B(102),YBOT
COMMON /SURS/ DYSUR,AYSUR,SURF(366),YSUR,SAREA,TS
COMMON /OUTLET/ NOUT,LOUT(5),ELOUT(5),QIN(400),TIN(400)
COMMON/SURSB/CUMQIN,CUMQOT,JM1,DYSUR1,DSURF,SAREA1,SURMES
31 JJM=JM
CUMQIN=CUMQIN+QIN(N)*DT
DO 332 I=1,NOUT
332 CUMQOT=CUMQOT+QOUT(N,I)*DT
QIO=CUMQIN-CUMQOT
IF(QIO) 34,34,35
35 SUM=-SAREA1*DYSUR1
DO 36 M=1,JM
SUM=SUM+A(JM1+M-1)*DY
IF (ABS(QIO)-SUM) 37,37,36
36 CONTINUE
34 SUM=DYSUR1*SAREA1
DO 38 M=1,JM
IF(ABS(QIO)-SUM) 39,39,38
38 SUM=SUM+A(JM1-M)*DY
37 YSUR=EL(JM1)+(M-0.5)*DY+(QIO-SUM)/A(JM1+M-1)
GO TO 40
39 YSUR=EL(JM1)-(M-0.5)*DY+(QIO+SUM)/A(JM1-M+1)
40 DYS=YSUR-EL(JM1)+DY/2.0
IF(DYS) 41,42,42
42 M=IFIX(DYS/DY)
GO TO 43
41 M=IFIX(DYS/DY)-1
43 JM=JM1+M
DYSUR=YSUR-EL(JM)+DY/2.0
C
C CALCULATE MEASURED SURFACE LEVEL
C
R=ET/DSURF +1.0
L=R-0.001
RR=R-FLOAT(L)
SURMES=SURF(L)+RR*(SURF(L+1)-SURF(L))
C
C CALCULATE SURFACE AREA
C
IF(YSUR-EL(JM)) 58,58,59
58 AYSUR=A(JM)-(DY/2.0-DYSUR)*(A(JM)-A(JM-1))/DY
GO TO 61
59 AYSUR=A(JM)+(DYSUR-DY/2.0)*(A(JM+1)-A(JM))/DY
61 SAREA=(AYSUR+(A(JM)+A(JM-1))/2.0)/2.0
C
C CHECK ACCURACY OF SURFACE LEVEL
C

```

```

SUMV=0.0
JMM=JM-1
IF(JM-JM1) 510,511,512
512 DO 513 J=JM1,JMM
513 SUMV=SUMV+A(J)*DY
511 SUMV=SUMV+SAREA*DYSUR-SAREA1*DYSUR1
GO TO 515
510 JMM1=JM1-1
DO 514 J=JM,JMM1
514 SUMV=SUMV+A(J)*DY
SUMV=-(SUMV+SAREA1*DYSUR1-SAREA*DYSUR)
515 ERROR=SUMV-QIO
DYCOR=ERROR/SAREA
DYSUR=DYSUR-DYCOR
IF(DYSUR-0.25*DY) 506,506,507
506 DYSUR=DYSUR+DY
JM=JM-1
507 MN=JM-JJM
IF(MN) 44,44,50
50 DO 51 I=1,MN
J=JM+1-I
51 T(J,1)=T(JJM,1)
44 T(JM,1)=T(JJM,1)
RETURN
END
C*****

```

```

C*****
      SUBROUTINE ERROR(N)
C*****
C
C THIS SUBROUTINE EVALUATES THE ERROR RESULTING FROM THE
SIMULATION
C IT RETURNS THE AVERAGE ABSOLUTE ERROR (AVER), THE STANDARD
DEVIATION (SDEV)
C AND THE AVERAGE STANDARD DEVIATION (ADEV). ERROR CALCULATED IN
%
C
      COMMON/PARAM/JM,DT,DY,DTT,TSTOP,ET,T(102,2)
      COMMON/WQCONC/CC(11,105,2),CCC(11,400),COUT(11,5),CCT(11,5)
      COMMON/ERRORS/AVE(11),ADEV(11),SDEV(11),Y(102,11,30)
      DIMENSION A(50,11),XT(11),VAR(11),P(11),X(102,11)
      DO 1 I=1,JM
          X(I,1)=T(I,1)
          X(I,2)=CC(1,I,1)
          X(I,3)=CC(5,I,1)
          X(I,4)=CC(6,I,1)
          X(I,5)=CC(7,I,1)
          X(I,6)=CC(8,I,1)
          X(I,7)=CC(9,I,1)
          X(I,8)=CC(10,I,1)
1      CONTINUE
          K=K+1
          DO 2 J=1,8
              XT(J)=0.
              DO 3 I=1,JM
                  IF(X(I,J).LT.0.001)THEN
                      X(I,J)=0.001
                  ELSE
                      CONTINUE
                  ENDIF
                  IF(Y(I,J,K).LT.0.001)THEN
                      Y(I,J,K)=0.001
                  ELSE
                      GO TO 13
                  ENDIF
              3      CONTINUE
          2      CONTINUE
          DO 4 J=1,8
              13      A(I,J)=((X(I,J)-Y(I,J,K))/X(I,J))*100.
                     XT(J)=XT(J)+ABS(A(I,J))
          4      CONTINUE
      C
      C CALCULATE THE MEAN ABSOLUTE ERROR VALUE
      C
      C CALCULATE OTHER PARAMETERS
      C NOTE THAT WHEN THE ERROR IS TOO LARGE, LARGER THAN 999.,
      C THE SUBROUTINE RETURNS THE VALUE 999. FOR ALL THE PARAMETERS

```

```

    AVE(J)=XT(J)/JM
    ADEV(J)=0.
    VAR(J)=0.
    DO 5 I=1,JM
        IF(ABS(AVE(J)).GT.999.)THEN
            GO TO 5
        ELSE
            XT(J)=ABS(A(I,J))-AVE(J)
            ADEV(J)=ADEV(J)+ABS(XT(J))
            P(J)=XT(J)*XT(J)
            VAR(J)=VAR(J)+P(J)
        ENDIF
5    CONTINUE
4    CONTINUE
    DO 6 J=1,8
        IF(ABS(AVE(J)).GT.999.)THEN
            ADEV(J)=999.
            AVE(J)=999.
            SDEV(J)=999.
        ELSE
            ADEV(J)=ADEV(J)/JM
            VAR(J)=VAR(J)/(JM-1)
            SDEV(J)=SQRT(VAR(J))
        ENDIF
6    CONTINUE
    RETURN
    END
C*****
C THIS IS THE LAST SUBROUTINE OF THE MODEL
C*****

```

BIBLIOGRAPHY

- Adams, E., et al. 1987. Performance evaluation of surface water transport and dispersion models. *Journal of Hydraulic Engineering* 113:(8).
- Aldama, A., Harleman, D. R. F., and Adams, E. E. 1988. Hypolimnetic mixing in a weakly stratified lake. *Water Resources Research*, in press.
- Ambrose, R., et al. 1988. *WASP4, A Hydrodynamic and Water Quality Model*. Athens, GA. Environmental Research Laboratory, EPA/600/3-87/039.
- Anderson, D. M. and Morel, F.M.M. March 1978. Copper sensitivity of *Gonyaulax tamarensis*. *Limnology and Oceanography*, 283-295.
- Beck, M. B. 1978. Mathematical modeling of water quality. *Summary Report IIASA Workshop*, October 1978, Laxenburg, Austria. International Institute for Applied Systems Analysis. CP-78-10.
- Bloss, S. and Harleman, D. R. F. 1979. *Effect of Wind Mixing on the Thermocline Formation in Lakes and Reservoirs*. Technical Report No. 249. Cambridge, MA. Ralph M. Parsons Laboratory, Massachusetts Institute of Technology.
- Browning, M. E. and Rice, R. B. 1981. *Ozone Treatment of Industrial Wastewater*. Noyes Data Corp. Park Ridge, NJ.
- Burby, R. J., et al. 1983. *Drinking Water Supplies: Protection through Watershed Management*. Michigan. Ann Arbor Science Publishers.
- Calcagno, A. 1979. A wind mixing dissolved oxygen model for reservoirs. SM degree thesis, Ralph M. Parsons Laboratory, Massachusetts Institute of Technology.
- Camp, Dresser & McKee Inc. January 1989. *Wachusett Reservoir Taste and Odor Study*. Boston, MA.
- Chisholm, Sallie W., et al. 1983. CuSO_4 treatment of nuisance algal blooms in drinking water reservoirs. *Environmental Management* 7(4):311-320.
- Corps of Engineers (U. S. Army). 1986. *An Assessment of Reservoir Mixing Processes*. Vicksburg, MS. Waterways Experiment Station.
- Corps of Engineers (U. S. Army). July 1986. CE-QUAL-R1: *A Numerical One-dimensional Model of Reservoir Water Quality*. MS39180-0631. Vicksburg, MS. Waterways Experiment Station.
- Culp, G. L. and Williams, R. B. 1986. *Handbook of Public Water Systems*. New York. Van Nostrand Reinhold Co.
- Dake, J. and D. R. F. Harleman. 1966. *An Analytical and Experimental Investigation on Thermal Stratification in Lakes and Ponds*. Technical Report No. 93. Cambridge, MA. Ralph M. Parsons Laboratory, Massachusetts Institute of Technology.

- EPA (Environmental Protection Agency). March 1977. *Legal and Institutional Approaches to Water Quality Management Planning and Implementation*. Washington, DC. EPA.
- EPA. June 1975. *Evaluation of Mathematical Models for Temperature Prediction in Deep Reservoirs*. Report No. EPA-660-3-75-038. National Environmental Research.
- Forstner, U. and Wittman, G. J. 1979. *Metal Pollution in the Aquatic Environment*. Springer-Verlag. New York.
- French, Jonathan A. 1986. Boston's water resource development: Past, present, and future. *Proceedings of a session sponsored by the Boston Society of Civil Engineers Section in conjunction with the ASCE National Convention in Boston, MA*.
- Grimsrud, P., et al. 1976. *Evaluating Water Quality Models: A Management Guide for Planners*. Washington, DC. EPA-600/5-76-004.
- Harleman, D. R. F. 1982. Hydrothermal analysis of lakes and reservoirs. *Proceedings of the American Society of Civil Engineers*. ASCE. March. 108(HY3):302-325.
- Harleman, D. R. F. 1988. Molecular mass transport in binary system. Class notes from Civil Engineering course, Water Quality Control. Ralph M. Parsons Laboratory, Massachusetts Institute of Technology.
- Hamon, R. W., Weiss, L. L., Wilson, W. T. June 1954. Insolation as an empirical function of daily sunshine duration. *Monthly Weather Review* 82(6).
- Hocking, Graeme C., et al. 1988. Algorithm for selective withdrawal from stratified reservoir. *Journal of Hydraulic Engineering*. ASCE. July. 114(7).
- Huang, Po-Shu. March 1988. *Influence of Wanaque South Diversion: South Dimension of the Trophic Level of Wanaque Reservoir and its Water Quality Management Program*. Eatontown, NJ. Najarian & Associates.
- Huber, W. and D. R. F. Harleman. 1968. *Laboratory and Analytical Studies of the Thermal Stratification of Reservoirs*. Technical Report No. 112. Cambridge, MA. Ralph M. Parsons Laboratory, Massachusetts Institute of Technology.
- Hutchinson, G. E. 1957. *A Treatise on Limnology*. volume 1:466. New York. John Wiley Publisher.
- Imboden, D. M. and Emerson, S. 1978. Natural radon and phosphorus as limnologic tracers: Horizontal and vertical eddy diffusion in Griefensee. *Limnology and Oceanography* 23(1):77-90.
- Imboden, D. M. and Gachter, R. 1978. A dynamic lake model for trophic state prediction. *Ecological Modelling*. 4:77-98.

- Krenkel, P. A. April 1985. Impact of non-point pollution in receiving waters. *Proceedings, Non-point Pollution Abatement Symposium*, Division of Continuing Education, Marquette University. Milwaukee, Wisconsin.
- Lerman, A. 1978. *Lakes: Chemistry, Geology, Physics*. New York. Springer-Verlag.
- Lindeburg, M. R. 1986. *Civil Engineering Reference Manual*. San Carlos, CA. Professional Publications Inc.
- Maine Department of Environmental Protection, Bureau of Water Quality Control. April 1976. *Guidelines for Lake Watershed Management Planning*. Prepared by Edward C. Jordan Company, Inc. Portland, Maine.
- Markofsky, M. and D. R. F. Harleman. 1971. *A Predictive Model for Thermal Stratification and Water Quality in Reservoirs*. Technical Report No. 134. Cambridge, MA. Ralph M. Parsons Laboratory for Water Resources and Hydrodynamics, Massachusetts Institute of Technology.
- MWRA (Massachusetts Water Resources Authority). 1986. Annual Report.
- MWRA. 1988. Annual Report.
- MWRA/MDC. 1985. *Memorandum of Understanding: Division of Properties, Personnel, Policy and Joint Functions Between MDC and the MWRA*, revised January 1989. Boston, MA.
- MWRA/MDC Taste and Odor Task Force. February 1988. *Algal Taste and Odor Problems: Interim Report, Finding and Recommendations*. Boston, MA.
- McKnight, Diane M. 1979. Interactions between freshwater plankton and copper speciation. Ph.D. thesis. Cambridge, MA. Ralph M. Parsons Laboratory for Water Resources and Hydrodynamics, Massachusetts Institute of Technology.
- National Academy of Sciences. 1977. *Copper, Medical & Biological Effects of Environmental Pollutants*. Committee on Medical & Biological Effects of Environmental Pollutants.
- Nesson, Fern L. 1983. *Great Waters*. Published for Brandeis University by University Press of New England.
- Nix, J., et al. 1987. *Symposium on Monitoring, Modeling, and Mediating Water Quality*. Bethesda, MD. American Water Resources Association.
- Octavio, K. and D. R. F. Harleman. 1977. *Vertical Heat Transport Mechanisms in Lakes and Reservoirs*. Technical Report No. 227. Cambridge, MA. Ralph M. Parsons Laboratory, Massachusetts Institute of Technology.
- Orlob, G. T. 1983. *Mathematical Modeling of Water Quality: Streams, Lakes and Reservoirs*. International Institute for Applied Systems Analysis. Bath, England. Petman Press.
- Owen, C. A. 1981. *Copper Deficiency and Toxicity*. Noyes Publications, NJ.

- Ryan, Patrick L. and D. R. F. Harleman. 1973. *An Analytical and Experimental Study of Transient Cooling Pond Behavior*. Technical Report No. 161. Cambridge, MA. Ralph M. Parsons Laboratory for Water Resources and Hydrodynamics, Massachusetts Institute of Technology.
- Serrahima, F. 1987. Modeling for control of eutrophication in Sau Reservoir. E.E. Thesis. Cambridge, MA. Ralph M. Parsons Laboratory, Massachusetts Institute of Technology.
- Tighe and Bond Inc. November 1988. *Water Quality Monitoring at Quabbin Wachusett and Northfield Reservoir, the Swift and Ware Rivers*. Final Report May 1987 - April 1988. Easthampton, MA.
- Train, Russell E. 1979. *Quality Criteria for Water*. U.S. Environmental Protection Agency. Washington DC. Castle House Publications, Ltd.
- Vogel, Richard M. and David I. Hellstrom. 1988. Long-range surface water supply planning. *Civil Engineering Practice*, Spring, pp. 7-25.
- Vollenweider, R. A. 1968. *Water Management Research*. OECD Paris. Report No. DAS/CSI/68.27.
- Volz, Ulrike Eva. March 17, 1982. *Boston's Water Supply System*. Boston, MA. Franklin Institute of Boston. AEIV.
- Waite, T. D. 1984. *Principles of Water Quality*. New York. Academic Press, Inc.
- Walters, Roy A. 1980. A time- and depth-dependent model for physical, chemical and biological cycles in temperature lakes. *Ecological Modelling* 8:79-86.
- Wetzel, R. G. 1983. *Limnology*. Philadelphia, PA. Saunders Company Publication.
- Whipple, G. C. 1948. *The Microscopy of Drinking Water*. New York. John Wiley & Sons.
- Zeman, O., Tennekes, H. 1977. Parameterization of the turbulent energy budget at the top of the day time atmospheric boundary layer. *Journal of Atmospheric Sciences* 34:111-123.

DATA SOURCES

- MDC. 1987. *Wachusett Yield Report. Monthly Summaries*. Boston, MA. Massachusetts District Commission.
- MDC. 1988. *Wachusett Yield Report. Monthly Summaries*.
- MDC. 1988. Wachusett Reservoir stage-storage table. Elev. 285'-297'. 1903.
- MDC. 1988. Oakdale 72 Bypass valve openings and closings. June 16, 1987 - August 27, 1988.

MDC. Maps of MDC land ownership.

National Oceanic and Atmospheric Administration. 1987/1988. Local climatological data. Monthly summaries. Worcester Municipal Airport, MA.

Tighe and Bond Inc. December 1987. *Water quality monitoring at Quabbin Wachusett and Northfield reservoir, the Swift and Ware rivers*. Quarterly Report May - July 1987. Easthampton, MA.

_____. January 1988. *Water quality monitoring at Quabbin Wachusett and Northfield reservoir, the Swift and Ware rivers*. Quarterly Report August - October, 1987. Easthampton, MA.

_____. March 1988. *Water quality monitoring at Quabbin Wachusett and Northfield reservoir, the Swift and Ware rivers*. Quarterly Report November 1987 - January 1988. Easthampton, MA.

_____. January 1988. *Water quality monitoring at Quabbin Wachusett and Northfield reservoir, the Swift and Ware rivers*. Final Report May 1986 - April 1987. Easthampton, MA.